

*Akademiya Nauk Latviiiskoi SSR*

NASA  
TT  
F-565  
c.1

**E. Kh. Khermanis, Editor**

# **AUTOMATIC CONTROL**

LOAN COPY: RETURN  
AFWL (WLOL)  
KIRTLAND AFB, N M



**TRANSLATED FROM RUSSIAN**

Published for the National Aeronautics and Space Administration  
and the National Science Foundation, Washington, D.C.  
by the Israel Program for Scientific Translations



AKADEMIYA NAUK LATVIISKOI SSR  
INSTITUT ELEKTRONIKI I VYCHISLITEL'NOI TEKHNIKI  
Academy of Sciences of the Latvian SSR  
Institute of Electronics and Computer Technology

E. Kh. Khermanis, Editor

# AUTOMATIC CONTROL

(Avtomaticheskoe upravlenie)

Editorial Board

E. Kh. Khermanis,  
G. F. Fritsnovich and M. P. Svilans

Izdatel'stvo "Zinatne"  
Riga 1967

*Automatic  
Control*

Translated from Russian

Israel Program for Scientific Translations  
Jerusalem 1969

NASA TT F-565  
TT 69-55028

Published Pursuant to an Agreement with  
THE NATIONAL AERONAUTICS AND SPACE ADMINISTRATION  
and  
THE NATIONAL SCIENCE FOUNDATION, WASHINGTON, D. C.

Copyright © 1969  
Israel Program for Scientific Translations Ltd.  
IPST Cat. No. 5445

Translated by D. Louvish and IPST Staff

Printed in Jerusalem by Keter Press  
Binding: Wiener Bindery Ltd., Jerusalem

Available from the  
U. S. DEPARTMENT OF COMMERCE  
Clearinghouse for Federal Scientific and Technical Information  
Springfield, Va. 22151

## Table of Contents

THEORY OF DISCRETE AUTOMATA .....	1
E. A. YAKUBAITIS. Time-dependent asynchronous logical automata .....	1
E. A. YAKUBAITIS, V. G. GOROBETS. Synthesis of sequential asynchronous logical automata using three types of modules .....	16
A. A. KURMIT. Determining the initial and compatible internal states of the inverse automaton of Class II by analyzing the operation of the original automaton .....	26
A. A. KURMIT. Finding the initial internal states of the inverse automaton by examining the operation of the original automaton .....	32
T. A. FRANTSIS, G. F. YANBYKH. Automatic error correcting in discrete automata .....	36
T. A. FRANTSIS. Error correcting in asynchronous automata .....	63
G. F. FRITSNOVICH. Extending the field of application of the method of inertial subcircuits .....	72
THEORY OF AUTOMATIC CONTROL .....	78
A. K. ZUEV, L. A. RASTRIGIN. Estimating the parameters of the object of optimization .....	78
L. K. LAPKOVSKII, L. A. RASTRIGIN. Diagnosis by completion .....	86
Ya. A. GEL' FANDBEIN, L. V. KOLOSOV. Determination of internal disturbance in multivariable dynamic systems during performance .....	92
Ya. A. GEL' FANDBEIN, L. V. KOLOSOV. Determination of the statistical characteristics of disturbance in a sampled-data system during operation .....	101
L. A. GIPSH, V. P. PEKA. Determination of optimal stock level for random demand .....	108
L. A. GIPSH, V. P. PEKA. Determination of optimal stock level for a group of customers under conditions of random demand .....	111
S. G. ZVONOV. Application of the two-dimensional Z-transform in determining the autocorrelation function of the input signal in a linear sampled-data system .....	118
Ya. Ya. OSIS. Minimization of the number of check points .....	131



L. N. VOLKOV. An engineering method for analytic least-squares optimization of realizable systems . . . . .	138
RELIABILITY OF SYSTEMS . . . . .	145
A. N. SKLYAREVICH. Initial data for the organization of preventive maintenance in a system with a possible structural fault . . . . .	145
L. P. LEONT'EV. Evaluating the reliability of a system with aftereffects under incomplete preventive maintenance—a special case . . . . .	152
V. I. LEVIN. A method for analysis of random processes with independent increments and discrete states . . . . .	158
A. M. MARGULIS. Standby redundancy system as a particular case of systems with possible structural faults . . . . .	168
V. P. CHAPENKO. Applications of structural redundancy to increase the reliability of analogue-digital functional converters . . . . .	173
L. P. LEONT'EV, B. M. KOPELEVICH. Theoretical gain in reliability by means of series-parallel and parallel-series standby redundancy . . . .	186
V. F. YADINA. Failure intensity of a system allowing for structural faults . . . .	191
G. A. VOLOVNIK. Experimental determination of the parameters of the reliability function for a system with possible faults . . . . .	196
AUTOMATION UNITS AND DEVICES . . . . .	199
I. Ya. BILINSKII, E. K. GULEVSKII. Tunnel diode switching delay . . . . .	199
M. F. GRINKHOF. Design of a two-cycle shift ferrite-diode register with allowance for component tolerances . . . . .	210
A. Ya. KHESIN. A TV method for automatic control of TV distortions . . . . .	220
A. Ya. KHESIN, T. A. GRENDZE. The use of photoelectric sensors for automatic control of geometrical TV distortions . . . . .	230
L. Yu. VEITSMAN, V. L. SREBNYI. Thyristor switching circuit for a pulsed control system of d.c. electric motors . . . . .	241
E. Kh. KHERMANIS, Yu. Ya. KOKT, V. A. ZALITIS, V. G. KARKLIN'SH, G. P. TARASOV. Automatic compensation circuit for slow-sweep control of a stroboscopic oscillograph . . . . .	252
D. K. ZIBIN'. Synthesis of multistage triggers . . . . .	256
G. S. GOLTVINSKAYA, D. K. ZIBIN'. An assembly of transistorized multivibrator circuits . . . . .	259
E. M. ANDRIANOV. A universal multistable device . . . . .	263

## EXPLANATORY LIST OF ABBREVIATIONS IN THIS BOOK

Abbreviation	Full name (transliterated)	Translation
AN	Akademiya Nauk	Academy of Sciences
DAN	Doklady Akademii Nauk	Reports of the Academy of Sciences
GEI	Gidroenergeticheskii Institut	Hydropower Institute
GOST	Gosudarstvennyi Obshche- soyuznyi Standart	All-Union State Standard
GVF	Grazhdanskii Vozdushnyi Flot	Civil Aviation
LGU	Leningradskii Gosudar- stvennyi Universitet	Leningrad State University
MFAU	Mezhdunarodnaya Federatsiya Spetsialistov po Avtomatike Upravleniya	International Federa- tion of Automatic Control

*E.A. Yakubaitis*

**TIME-DEPENDENT ASYNCHRONOUS  
LOGICAL AUTOMATA**

The structure of time-dependent asynchronous logical automata is considered, and methods given for their synthesis using concrete logic elements.

Consider an asynchronous logical automaton /1/, which we shall henceforth call an automaton. Suppose that steady signals  $A_1, A_2, \dots, A_n$  are applied to the inputs of the automaton. To simplify the exposition we assume that the automaton has one input  $Z$ .

Any finite sequence of consecutive input signals will be called an input sequence. An automaton in which the output signal is a function of a finite number of input sequences will be called time-independent. If the output signal also depends on the time, the automaton will be time-dependent.

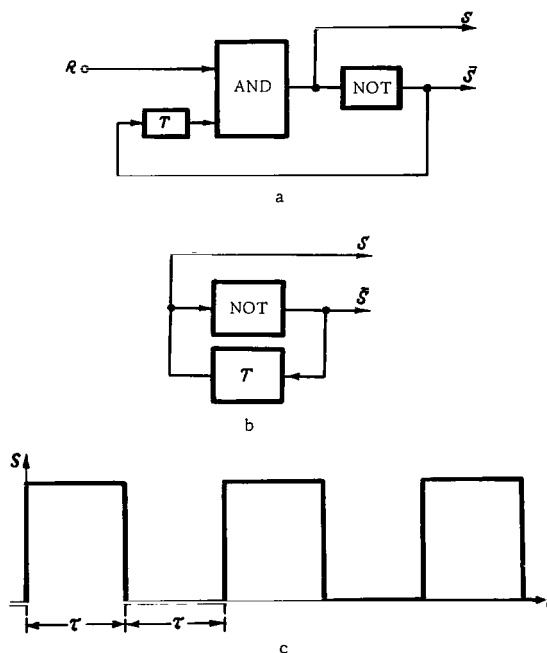


FIGURE 1. Rectangular-pulse generator.

The signal emitted by the automaton for constant input signals  $A_1, A_2, \dots, A_n$  forms a time sequence. Later we shall consider the case when any time sequence has finite length  $l$ , and the time between two changes in the values of the input signals  $A_1, A_2, \dots, A_n$  exceeds the time required for the emission of a given time sequence.

We shall consider methods for the synthesis of time-dependent automata using concrete logic elements (elements whose operation involves a finite time lag). This will be done for logic elements of types AND, OR, NOT, though our methods are easily extended to any other set of logic elements. In all cases the automata contain no delay elements. We employ the terminology of [1].

A time-dependent automaton must produce at least one time sequence. It turns out that this may be achieved either by using delay elements or by supplementing the given input signals  $A_1, A_2, \dots, A_n$  with a signal from a rectangular-pulse generator (Figure 1c). The signal  $S$  is a pulse. However, any pulse-type signal may be regarded as a particular kind of steady signal, and so, for convenience, we shall always assume that  $S$  is a steady signal.

Methods for the synthesis of time-dependent automata using delay elements were described in [2]. Here we shall study methods which utilize rectangular-pulse generators.

The duration  $\tau$  of the pulse emitted by the generator must be sufficient to allow for the transition processes involved in the change of any of the input signals  $A_1, A_2, \dots, A_n, S$ .

## 1. TIME-DEPENDENT AUTOMATON WITH UNCONTROLLED RECTANGULAR-PULSE GENERATOR

The time sequences emitted by an automaton must often be synchronized with the performance of some external device. In this case the time-dependent automaton must employ an external uncontrolled generator which emits an unlimited sequence of rectangular pulses (Figure 1b).

When the signal  $S$  appears at one of the inputs of the automaton, the required time sequences can be produced. Synthesis of a time-dependent automaton with  $n$  input signals  $A_1, A_2, \dots, A_n$  thus reduces to synthesis of a time-independent automaton with  $n+1$  input signals  $A_1, A_2, \dots, A_n, S$ .

In this connection it must be borne in mind that the input signals  $A_1, A_2, \dots, A_n$  may change at any instant of time. At these instants the signal  $S$  may either remain constant or change

- 1)  $S: 0 \rightarrow 1$ ;
  - 2)  $S = 1$ ;
  - 3)  $S: 1 \rightarrow 0$ ;
  - 4)  $S = 0$ .
- (1)

In most cases the time sequence must not depend on the signal  $S$  at the instant the signals  $A_1, A_2, \dots, A_n$  change, when the sequence is to be emitted.

In this case an input signal may change only when  $S: 1 \rightarrow 0$  or  $S: 0 \rightarrow 1$ . When  $S=0$  or  $S=1$  the automaton must postpone the change until the appropriate change  $S: 1 \rightarrow 0$  or  $S: 0 \rightarrow 1$  occurs.

Analysis shows that the synthesized automaton is simpler if the emission of a time sequence can coincide only with one of these changes (either  $S: 1 \rightarrow 0$  or  $S: 0 \rightarrow 1$ ).

Accordingly, we shall confine ourselves to automata in which time sequences are emitted after  $S: 0 \rightarrow 1$ . Our method is easily extended to the case when the change  $S: 1 \rightarrow 0$  or both changes  $S: 0 \rightarrow 1$  and  $S: 1 \rightarrow 0$  are permitted.

If a generator is available, any time-dependent automaton can be constructed without delay elements. As for the generator itself, its circuit (Figure 1) must contain a delay element  $T$ .

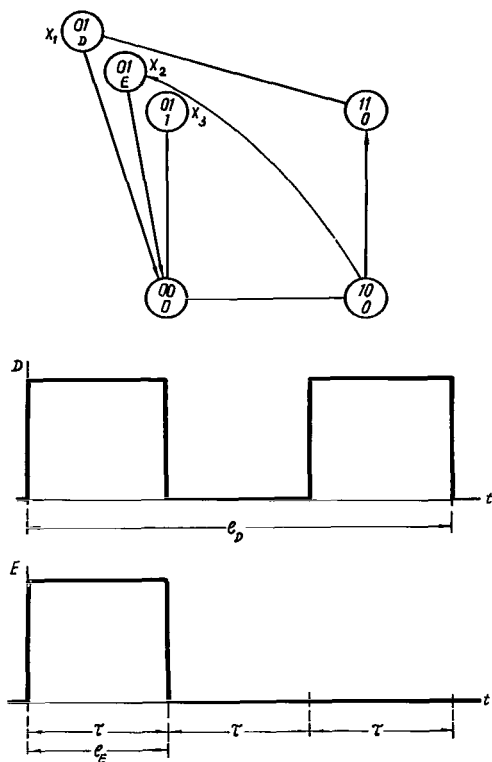


FIGURE 2. Graph of finite automaton and time sequence.

Consequently, any time-dependent automaton can be constructed on the basis of a circuit containing a single delay element.

Just as in the time-independent case, a time-dependent automaton can be defined by the state graph or table of a finite automaton, involving  $n$  input signals  $A_1, A_2, \dots, A_n$ . In this case, however, certain nodes of the graph

will contain not the value of an output signal but signals designating time sequences. The latter are represented as (separate) functions of time.

The graph and time sequences illustrated in Figure 2 provide an example of the definition of a time-dependent automaton. Let us call the nodes at which  $Z=0$  or  $Z=1$  time-independent; nodes at which time sequences are produced will be called time-dependent.

The parameter  $l_i$  defines the **length** of the  $i$ -th time sequence. The length of a sequence is measured in terms of the number of durations  $\tau$ . Accordingly, in this example  $l_D=3$  and  $l_E=1$ .

The initial point ( $t=0$ ) for each time sequence is preassigned as the first instant after a change in the signals  $A_1, A_2, \dots, A_n$  when the change  $S:0 \rightarrow 1$  occurs.

Table 1 is the table of the finite automaton whose graph is given in Figure 2.

TABLE 1.

$A$	$B$	$Z$	$X_1$	$X_2$	$X_3$
0	0	0	0	0	1
0	1	$X_1(D), X_2(E), X_3(1)$	$X_1$	$X_2$	$X_3$
1	0	0	0	1	0
1	1	0	1	0	0

A time-dependent automaton is uniquely determined by the graph (or table) of a finite automaton together with diagrams of time sequences, but this method is not convenient for synthesis. We therefore adopt a different mode of representation.

Every time sequence can be represented by a subgraph involving  $n+1$  input signals ( $A_1, A_2, \dots, A_n, S$ ). Thus, the sequence  $D$  (Figure 2) is represented by the subgraph of Figure 3.

The time subgraph contains  $l$  working nodes (cycles), which represent the time sequence. In addition, since the sequence can begin only when  $S:0 \rightarrow 1$ , each subgraph contains two additional preparatory nodes (cycles).

The time-dependent automaton operates as follows. If the given change of one or several (simultaneous) signals  $A_1, A_2, \dots, A_n$  occurs when  $S=1$ , the automaton proceeds to the first preparatory node ( $\pi_1$ ). If  $S:1 \rightarrow 0$  or  $S=0$  at this instant, it proceeds to the second preparatory node ( $\pi_2$ ). But if the change of  $A_1, A_2, \dots, A_n$  occurs at the same time as  $S:0 \rightarrow 1$ , the automaton proceeds directly to the first working node ( $\rho_1$ ).

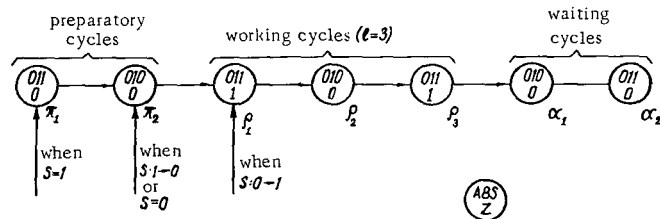


FIGURE 3. Subgraph.

When the time sequence (working node) is completed, the signals  $A_1, A_2, \dots, A_n$  may remain constant for some time. Each working node is therefore provided with two waiting nodes ( $\alpha_1, \alpha_2$ ).

In synthesizing an automaton each node of the subgraph must be assigned an intermediate signal. However, the number of intermediate signals may be reduced by transferring the transition which occurs when  $S:0 \rightarrow 1$  at the node  $\rho_1$  to the node  $\pi_1$ . Both multiple-valued nodes, from which there are transitions to the nodes  $\pi_1$  and  $\pi_2$ , may then be assigned the same intermediate signal. The speed of the automaton is then somewhat lower, but this will be apparent only on the rare occasions when changes in the input signals  $A_1, A_2, \dots, A_n$  coincide in time with  $S:0 \rightarrow 1$ .

The number of intermediate signals may also be reduced by adding a transition from the node  $\rho_3$  to the node  $\alpha_2$ . The waiting nodes may then be assigned the same intermediate signal.

To coordinate the subgraph of Figure 3 with that of Figure 2 we must replace the node  $A=1, B=1$  by two nodes, at which  $A=1, B=1, S=0$  and  $A=1, B=1, S=1$ . The subgraph of Figure 3 is linked to this pair of nodes in Figure 4. In accordance with the above reasoning, Figure 4 differs from Figure 3 in that the transition  $\gamma \rightarrow \rho_1$  has been replaced by  $\gamma \rightarrow \pi_1$ , and a transition  $\rho_3 \rightarrow \alpha_2$  has been added.

Construction of the subgraph representing the time sequence E is analogous (Figure 5). Comparison of the subgraphs of Figures 4 and 5 shows the nodes  $\rho_3, \alpha_1, \alpha_2$  are common to both. This enables us to construct a subgraph representing both time sequences (Figure 6).

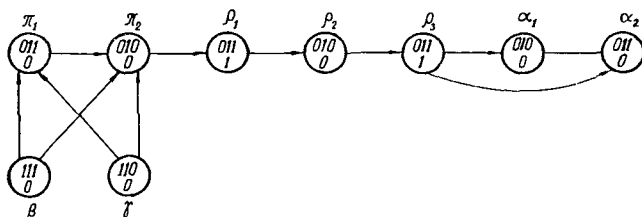


FIGURE 4. Subgraph D in transformed form.

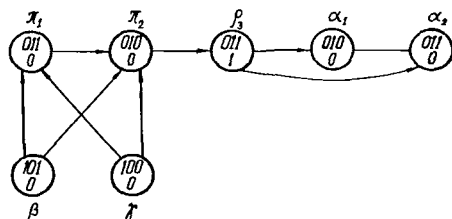


FIGURE 5. Subgraph E.

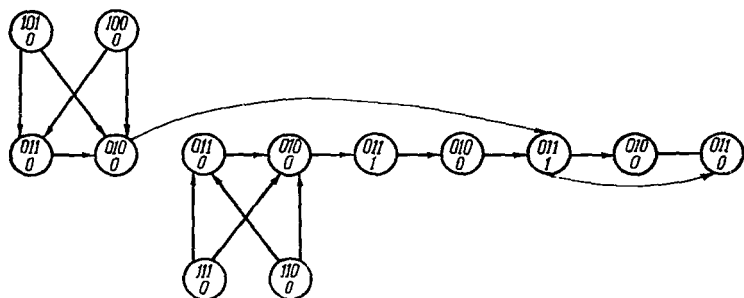


FIGURE 6. Combination of subgraphs *D* and *E*.

In general, several time subgraphs can be combined in such a way that they share the waiting nodes. If the time sequences represented by the subgraphs in one or more intervals  $\tau$ , beginning from the end of the sequences, coincide, the corresponding working nodes are also common to all the subgraphs. On the other hand, the preparatory nodes can never be shared by several time sequences.

Note that combination of several subgraphs into one is not essential. If the combination is not carried out, it will occur during the synthesis process, when equivalent nodes are combined.

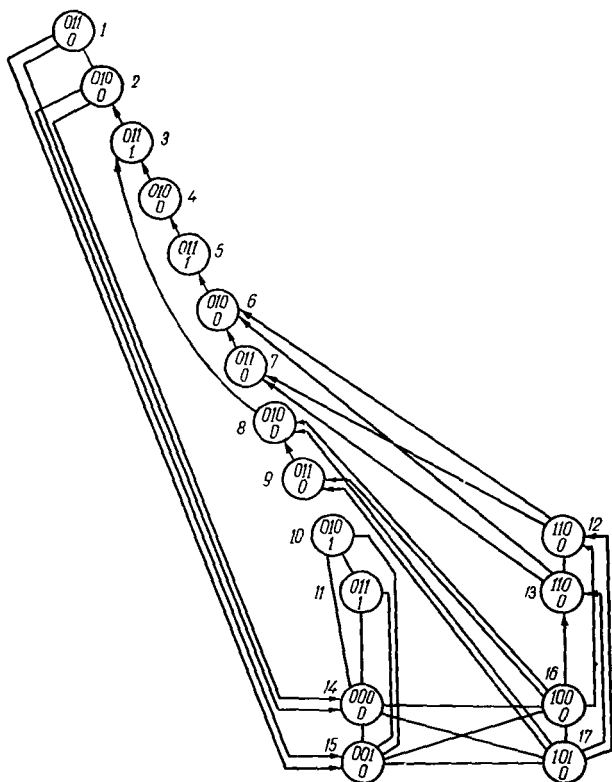


FIGURE 7. Graph of a finite automaton.



The signal  $S$  appears in the time subgraphs. It must therefore be introduced in the remaining part of the graph of the finite automaton. To this end, every time-dependent node of the graph with the  $n$  signals  $A_1, A_2, \dots, A_n$  is replaced by two nodes, one with  $S=0$  and the other with  $S=1$ . Each time-dependent node is replaced by the corresponding time subgraph.

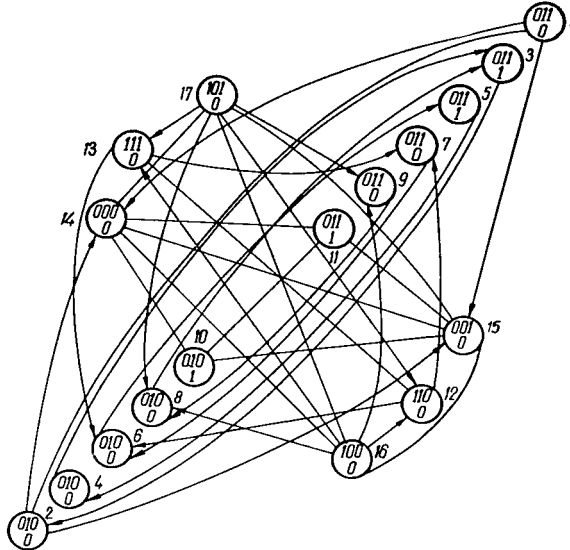


FIGURE 8. Graph of finite automaton — second form.

The result is a graph with  $n+1$  input signals, whose nodes, if it is completely defined, are marked  $Z=0$  or  $Z=1$ . Thus the distinction between time-dependent and time-independent nodes disappears, and the graph is in no way different from that of a time-independent automaton.

Figure 7 illustrates the graph for  $n+1$  input signals based on the graph of Figure 2 and the subgraph of Figure 6. A different form of this graph is obtained by grouping together nodes with the same input signals, as in the case of time-independent automata (see Figure 8). To clarify the correspondence between the two forms of the graph the nodes have been numbered.

Construction of the graph for  $n+1$  input signals is considerably simplified by adopting the following convention. Besides nodes corresponding to  $n+1$  input signals, we shall admit nodes corresponding to  $n$  signals (where  $S$  may have any value).

In this way, using a given graph for  $n$  input signals and given time sequences, one constructs the simplified graph.

Thus, for example, Figure 9 illustrates the simplified graph based on the example of Figure 2. It is evident that the simplified graph is much simpler than those of Figures 7 and 8.

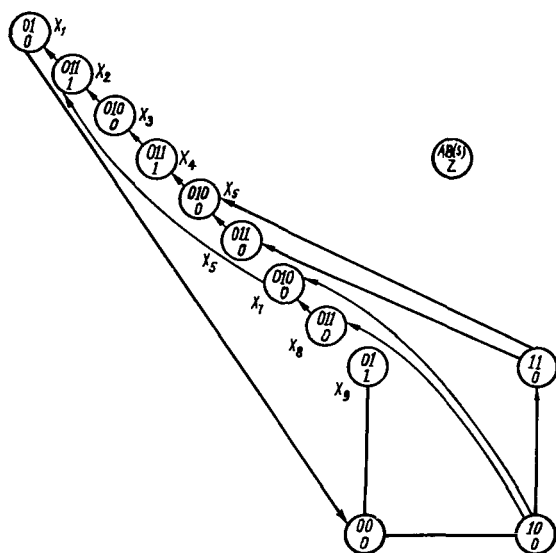


FIGURE 9. Simplified graph.

Any of the graphs constructed above (Figures 7—9) may be used to set up the table of the corresponding finite automaton. In our example (Figure 9), assigning signals  $X_1, X_2, \dots, X_9$  to the multiple-valued vertices, we obtain Table 2.

TABLE 2.

A	B	S	Z	$X_1$	$X_2$	$X_3$	$X_4$	$X_5$	$X_6$	$X_7$	$X_8$	$X_9$
0	0	0	0	0	0	0	0	0	0	0	0	1
0	0	1	0	0	0	0	0	0	0	0	0	1
0	1	0	$X_1(0), X_2(0), X_3(0), X_7(0), X_9(1)$	$X_1$	$X_3, X_7$	$X_3$	$X_5$	$X_5$	0	$X_7$	0	$X_9$
0	1	1	$X_1(0), X_2(1), X_4(1), X_6(0), X_8(0), X_9(1)$	$X_1, X_2$	$X_2$	$X_4$	$X_4$	$X_6$	$X_6$	$X_8$	$X_8$	$X_9$
1	0	0	0	0	0	0	0	0	0	1	1	0
1	0	1	0	0	0	0	0	0	0	1	1	0
1	1	0	0	0	0	0	0	1	1	0	0	0
1	1	1	0	0	0	0	0	1	1	0	0	0

TABLE 3.

A	B	S	Z	$X_1$	$X_2$	$X_3$	$X_4$	$X_5$	$X_6$	$X_7$	$X_8$	$X_9$
0	0	—	0	0	0	0	0	0	0	0	0	1
0	1	0	$X_1(0), X_3(0), X_5(0), X_7(0), X_9(1)$	$X_1$	$X_3, X_7$	$X_5$	$X_6$	$X_8$	0	$X_7$	0	$X_9$
0	1	1	$X_1(0), X_2(1), X_4(1), X_6(0), X_8(0), X_9(1)$	$X_1, X_2$	$X_2$	$X_4$	$X_4$	$X_6$	$X_6$	$X_8$	$X_8$	$X_9$
1	0	—	0	0	0	0	0	0	0	1	1	0
1	1	—	0	0	0	0	0	1	1	0	0	0

TABLE 4.

A	B	S	Z	$X_1$	$X_2$	$X_3$	$X_4$	$X_5$	$X_6$	$X_7$	$X_8$	$X_9$	$X_{10}$
0	0	—	0	1	0	0	0	0	0	0	0	1	0
0	1	—	1	0	1	1	0	0	0	0	0	1	0
1	0	—	$X_9(0), X_{10}(1)$	$X_9, X_{10}$	0	0	0	0	0	0	0	$X_9$	$X_{10}$
1	1	0	$X_1(0), X_3(0), X_6(1), X_7(1), X_8(0)$	$X_1$	0	$X_3$	$X_3$	$X_5$	$X_5$	$X_7$	$X_7, X_8$	$X_1$	$X_8$
1	1	1	$X_1(0), X_2(0), X_4(1), X_6(0), X_8(0)$	$X_1$	$X_2$	$X_2$	$X_4$	$X_4$	$X_6$	$X_6$	$X_8$	$X_1$	$X_8$

In most cases, the resulting table may be simplified by using the row-combination rule:

Any two rows in the table of a finite automaton which differ only in the value of one input signal may be combined.

Using this rule, we may replace Table 2 by Table 3. The dashes in the S-column signify that the corresponding entry in the table may be either  $S=0$  or  $S=1$ .

As indicated, the signal S is only needed in time-dependent automata, and not in time-independent automata. If for some reason the signal S is introduced in the specification of a time-independent automaton, it takes no part in the synthesis process and does not figure in the resulting equation system.

We now consider an example of the synthesis of a time-dependent automaton with uncontrolled rectangular-pulse generator.

Example 1. Let us construct the time-dependent automaton represented by the finite-automaton graph and time sequence given in Figure 10. Undesirable competition is avoided by using filters. We assume the presence of an uncontrolled generator emitting the unlimited sequence of pulses illustrated in Figure 1c.

We construct the subgraph for the given time sequence (signal D), illustrated in Figure 11. Combining this subgraph with the graph of Figure 10, we get the simplified graph of Figure 12.

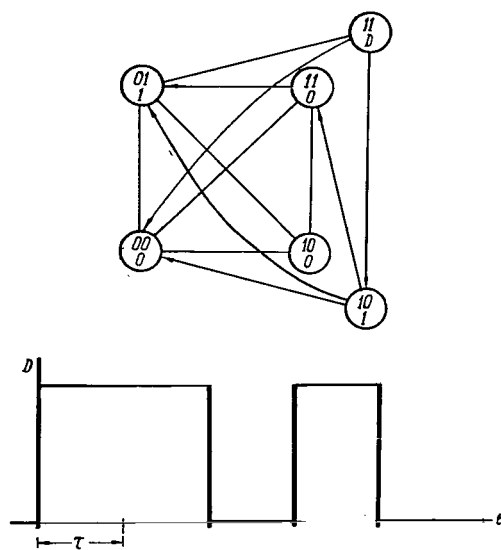


FIGURE 10. Graph and time sequence for Example 1.

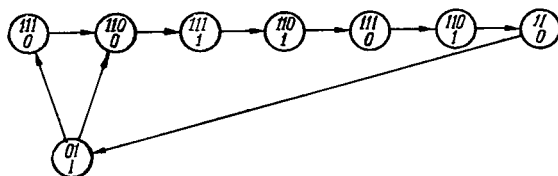


FIGURE 11. Subgraph.

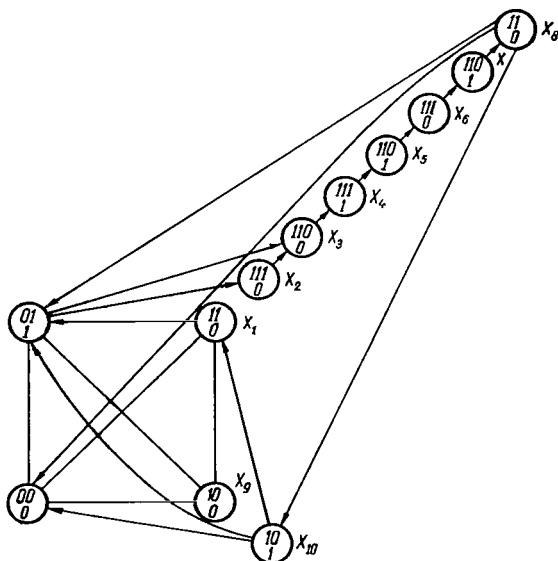


FIGURE 12. Simplified graph.

Using the simplified graph, we construct the finite-automaton table (Table 4). This table shows that the signals  $X_1$  and  $X_9$  are superfluous. With this in mind, easy computations yield the equation system for the given time-dependent automaton:

$$\left. \begin{aligned} Z &= \overline{A}B + A\overline{B}X_{10} + AB\overline{S}X_5 + AB\overline{S}X_7 + ABSX_4; \\ X_2 &= \overline{A}B + ABSX_2; \\ X_3 &= \overline{A}B + AB\overline{S}X_3 + ABSX_2; \\ X_4 &= AB\overline{S}X_3 + ABSX_4; \\ X_5 &= AB\overline{S}X_5 + ABSX_4; \\ X_6 &= AB\overline{S}X_5 + ABSX_6; \\ X_7 &= AB\overline{S}X_7 + ABSX_6; \\ X_8 &= AB\overline{S}X_7 + ABX_8; \\ X_{10} &= A\overline{B}X_{10} + ABX_8. \end{aligned} \right\} \quad (2)$$

On the basis of equations (2) we construct the circuit illustrated in Figure 13. Any undesirable competition is eliminated by filters.

## 2. TIME-DEPENDENT AUTOMATON WITH CONTROLLED RECTANGULAR-PULSE GENERATOR

The use of an uncontrolled rectangular-pulse generator, which produces an unlimited sequence of pulses, requires the construction of  $q$  inertial subautomata, which govern the performance of the automaton at the preparatory nodes.

$$q = 2v, \quad (3)$$

where  $v$  is the given number of time sequences.

When there is no need to synchronize the time sequences produced by the automaton with an external device, a controlled generator of rectangular pulses can be used.

By a controlled generator we mean a generator which produces a sequence of rectangular pulses only on application of a control signal  $R=1$ . The circuit of such a generator is illustrated in Figure 1a.

The control signal is described by the following Boolean function:

$$R = \sum_{i=1}^d (\tilde{A}_1 \tilde{A}_2 \dots \tilde{A}_n)_i (X_{a_i} + X_{b_i} + \dots + X_{e_i}), \quad (4)$$

where  $(\tilde{A}_1 \tilde{A}_2 \dots \tilde{A}_n)_i$  is a conjunction determining a set of nodes at least one of which must produce a time sequence;  $X_{a_i}, X_{b_i}, \dots, X_{e_i}$  are the intermediate signals assigned to the working nodes of the subgraph representing the time

sequence;  $d$  is the number of conjunctions  $(\hat{A}_1 \hat{A}_2 \dots \hat{A}_n)_i$ .

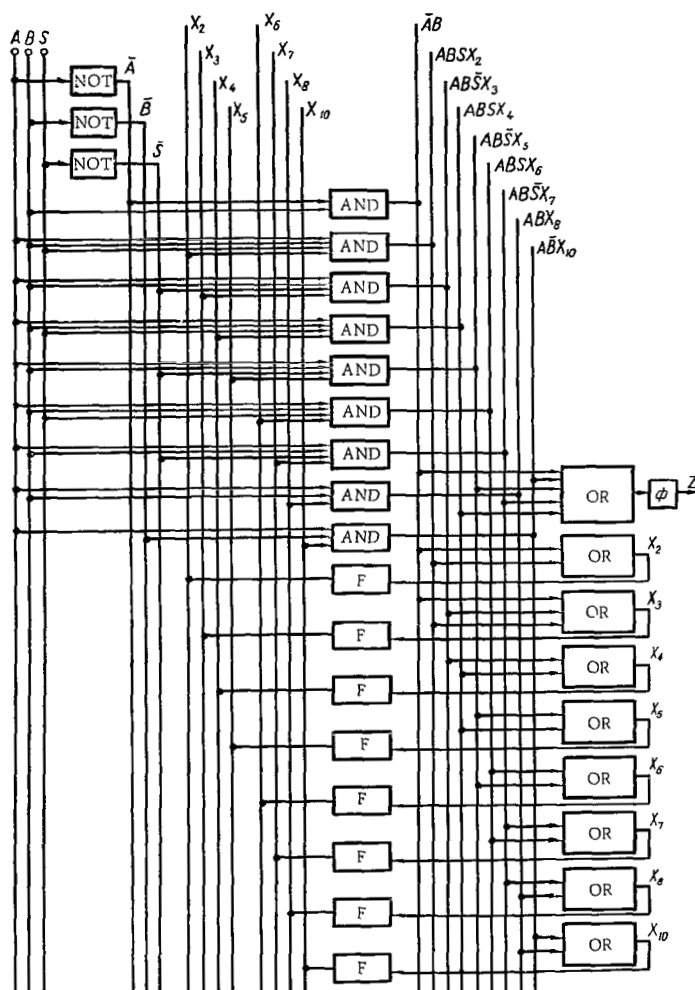


FIGURE 13. Circuit of automaton.

To form the two inertial subautomata characterizing the waiting nodes (e.g., subautomata  $X_2, X_3$  in equations (2)) one needs at least two AND-elements, two OR-elements, and two filters. When a controlled generator is used there is no need for preliminary nodes; consequently, the above elements become superfluous.

On the other hand, the controlled generator (Figure 1a) contains one more AND-element than the uncontrolled generator (Figure 1b). In addition, to produce the signal  $R(4)$  one needs at most one AND-element, two OR-elements, and one filter, for each time sequence.

These results are compared in Table 5.

TABLE 5.

Subcircuit	Type of element			
	AND	OR	NOT	F
Inertial subautomata characterizing the waiting nodes	$2v$	$2v$	$2v$	$2v$
Components added in controlled generator	1	0	0	0
Production of signal $R$	$v$	$v+1$	0	1

It is clear from this table that when  $v \geq 1$  a controlled generator should always be used, as far as the simplicity of the circuit of the time-dependent automaton is concerned. The resulting simplification is greater, the greater  $v$ .

We now consider an example of synthesis of a time-dependent automaton containing a controlled generator.

Example 2. We construct the time-dependent automaton whose graph and diagrams are given in Figure 2. As before, undesirable competition is eliminated by filters.

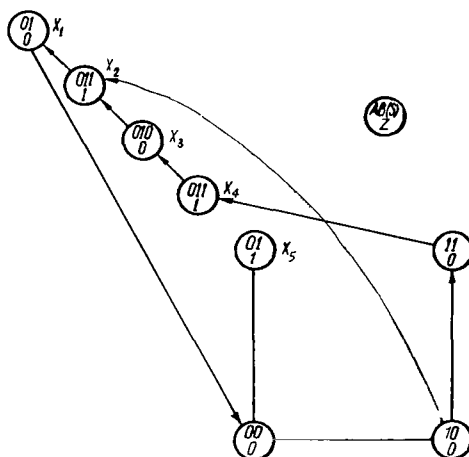
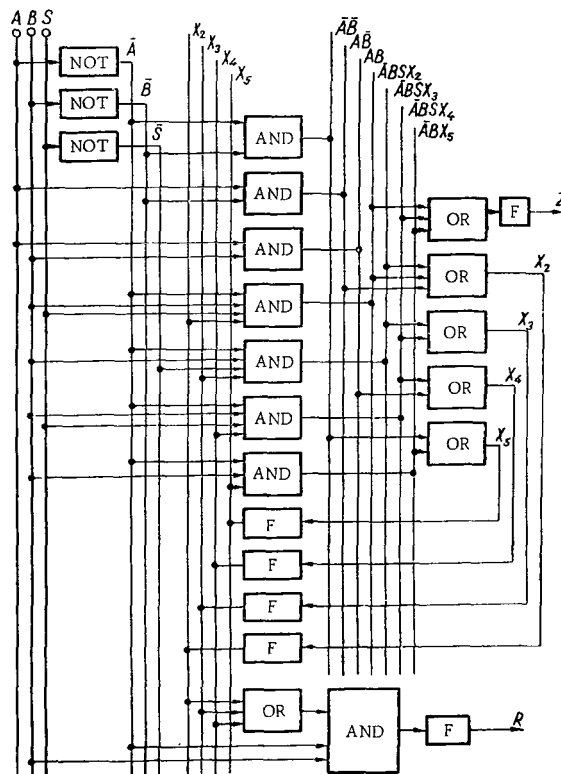


FIGURE 14. Simplified graph.

On the basis of Figure 2 we construct the simplified graph illustrated in Figure 14. A comparison of this graph with that of Figure 9 shows that with the incorporation of a controlled generator the four waiting nodes are dropped.

Using the graph of Figure 14 we set up the finite-automaton table (Table 6).

$A$	$B$	$S$	$Z$	$X_1$	$X_2$	$X_3$	$X_4$	$X_5$
0	0	—	0	0	0	0	0	1
0	1	0	$X_1(0), X_3(0), X_5(1)$	$X_1$	$X_3$	$X_5$	0	$X_5$
0	1	1	$X_1(0), X_2(1), X_4(1), X_5(1)$	$X_1, X_2$	$X_2$	$X_4$	$X_4$	$X_5$
1	0	—	0	0	1	0	0	0
1	1	—	0	0	0	0	1	0

$$\left. \begin{aligned} Z &= \bar{A} B S X_2 + \bar{A} B S X_4 + \bar{A} B X_5; \\ X_2 &= \bar{A} B \bar{S} X_3 + \bar{A} B S X_2 + A \bar{B}; \\ X_3 &= \bar{A} B \bar{S} X_3 + \bar{A} B S X_4; \\ X_4 &= \bar{A} B S X_4 + A B; \\ X_5 &= \bar{A} \bar{B} + \bar{A} B X_5. \end{aligned} \right\} \quad (5)$$
$$R = \overline{A} B (X_2 + X_3 + X_4). \quad (6)$$


14



The circuit based on equations (5) and (6) is illustrated in Figure 15. Undesirable competition in the circuit is eliminated by filters.

### Bibliography

1. Yakubaitis, E. A. Asinkhronnyi logicheskii avtomat (An Asynchronous Logical Automaton). Avtomatika i vychislitel'naya tekhnika, Vol.1. 1967.
2. Yakubaitis, E. A. Asinkhronnye logicheskie avtomaty (Asynchronous Logical Automata). Riga, "Zinatne," 1966.

*E. A. Yakubaitis, V. G. Gorobets*

**SYNTHESIS OF SEQUENTIAL ASYNCHRONOUS LOGICAL AUTOMATA USING THREE TYPES OF MODULES**

A method is given for synthesizing sequential asynchronous logical automata using a minimum number of modules of three types, allowing for two restrictions.

**1. INTRODUCTION**

Microminiaturization of semiconductor elements and the developing technology of integrated circuits raises the problem of constructing automata based on modules.

This paper considers methods for the synthesis of time-independent sequential asynchronous logical automata (briefly — automata) based on three types of modules.\*

In the general case /1/ an automaton is specified by a state graph, a state table, or a numerical expression, and described by a system of  $k+m$  equations which define the inertial and primitive subautomata:

$$\left\{ \begin{array}{l} X_j = \bigvee_{i=0}^{2^n-1} \alpha_{ij} (\tilde{A}_n \tilde{A}_{n-1} \dots \tilde{A}_1)_i (\beta_{ij} + X_{ij}), (j=1, 2, \dots, k); \\ Z_t = \bigvee_{i=0}^{2^n-1} \gamma_{it} (\tilde{A}_n \tilde{A}_{n-1} \dots \tilde{A}_1)_i (\delta_{it} + X_{it}), (t=1, 2, \dots, m), \end{array} \right. \quad (1)$$

$$\left\{ \begin{array}{l} X_j = \bigvee_{i=0}^{2^n-1} \alpha_{ij} (\tilde{A}_n \tilde{A}_{n-1} \dots \tilde{A}_1)_i (\beta_{ij} + X_{ij}), (j=1, 2, \dots, k); \\ Z_t = \bigvee_{i=0}^{2^n-1} \gamma_{it} (\tilde{A}_n \tilde{A}_{n-1} \dots \tilde{A}_1)_i (\delta_{it} + X_{it}), (t=1, 2, \dots, m), \end{array} \right. \quad (2)$$

where  $n$  is the number of inputs,  $k$  the number of inertial subautomata,  $m$  the number of outputs,  $(\tilde{A}_n \tilde{A}_{n-1} \dots \tilde{A}_1)_i$  the elementary conjunction of  $n$  input variables defined by the  $i$ -th row of the table,  $\alpha_{ij}, \beta_{ij}, \gamma_{it}, \delta_{it}$  coefficients defined by the table, with values zero or one,  $X_1, X_2, \dots, X_k$  intermediate variables,  $X_{ij}$  and  $X_{it}$  variables from the set  $X_1, X_2, \dots, X_k$ , and  $Z_1, Z_2, \dots, Z_m$  output variables.

\* We employ the terminology of /1/.

## 2. DESCRIPTION OF THE MODULES

We assume that the modules are based on elements of type AND, NOT, and F (filter). The circuits of these elements are illustrated in Figures 1, 2, and 3. It is assumed that the outputs of these elements can be connected at  $q_{AND}$ ,  $q_{NOT}$ ,  $q_F$ , respectively, to the inputs of other elements.

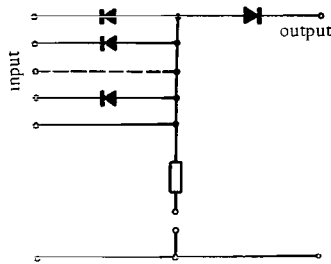


FIGURE 1. AND circuit.

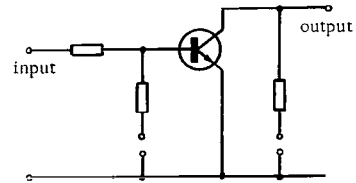


FIGURE 2. NOT circuit.

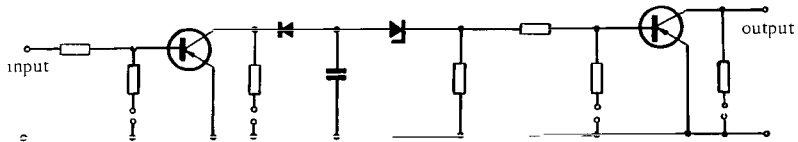


FIGURE 3. Filter circuit.

### a. A-module

This type of module involves  $l_A$  NOT elements, used to produce the negations of input or intermediate signals.

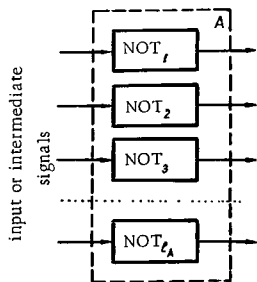


FIGURE 4. Circuit of A-module.

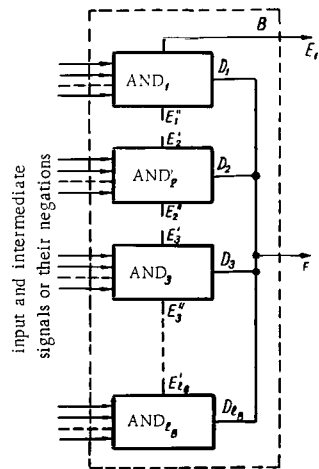


FIGURE 5. Circuit of B-module.

### b. *B* -module

The circuit of this module is given in Figure 5. It consists of  $l_B$  AND elements. Several *B*-modules may be combined by using outputs  $E_i'$  or  $F$ .

Using one AND element one can obtain a conjunction of rank  $r$ . To produce a conjunction of rank  $R$  one must combine  $\left\lceil \frac{R}{r} \right\rceil$  AND-elements.\* This is done by connecting the outputs  $E_1'', E_2', \dots, E_{l_B}'$ . For instance, if  $r=3$  and  $R=8$  one must connect  $E_1''$  to  $E_2', E_2''$  to  $E_3'$ .

Thus, using one *B*-module one can realize any conjunction of rank at most  $rl_B$ . Conjunctions of higher rank are formed by connecting several *B*-modules at the point  $E_1'$ .

The disjunction of the resulting conjunctions is obtained (Figure 5) by direct connection of the outputs  $D_1, D_2, \dots, D_{l_B}$ . This is made possible by the diodes connected to the outputs of the AND elements (Figure 1).

When the terms of the disjunction are conjunctions formed by two or more *B*-modules, the latter are directly connected at the points  $F$ .

### c. *C* -module

To eliminate undesirable competition in each feedback circuit and at each output of the automaton, filters must be introduced [1]. This is done by a module of type *C*. Each *C*-module contains  $l_C$  filters (Figure 6).

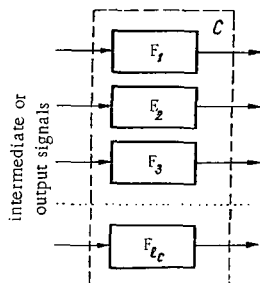


FIGURE 6. Circuit of *C*-module.

## 3. MINIMIZING THE NUMBER OF *B*-MODULES

In automata synthesis it often happens that the same conjunction occurs in more than one of the equations describing the automaton. To simplify our method, we introduce the following restriction. Every conjunction is realized as many times as it occurs in equations (1), (2). Thus we always have  $q_{AND}=1$ .

In view of this restriction, each of the equations describing the automaton must be simplified independently of the other equations in the system.

\* Here and below  $\lceil a \rceil$  denotes the smallest integer greater than  $a$ .

Minimization of equations (1), (2) yields a system of  $k+m$  equations; the  $i$ -th equation contains  $p_i$  prime implicants (conjunctions) of rank

$R_{ij}$  ( $1 \leq j \leq p_i$ ,  $1 \leq i \leq k+m$ ). To realize the  $ij$ -th conjunction,  $G_{ij} = \left\lceil \frac{R_{ij}}{r} \right\rceil$  AND elements are needed. Thus, the lower bound for the number of  $B$ -modules required to realize the  $i$ -th equation is

$$L_{Li} = \left\lceil \frac{G_i}{l_B} \right\rceil = \left\lceil \frac{\sum_{j=1}^{p_i} G_{ij}}{l_B} \right\rceil,$$

and for all  $k+m$  equations:

$$L_{LB} = \sum_{i=1}^{k+m} L_{Li}. \quad (3)$$

#### 4. AUTOMATON-SYNTHESIS ALGORITHM

The foregoing considerations yield the following algorithm for synthesis of an automaton on the basis of modules of type  $A$ ,  $B$ , and  $C$ .

1. Determine the system of equations (minimal disjunctive normal forms) of the given algorithm by the method of [1]. Simplify each equation separately, independently of the others. The equation system will then

contain  $\sum_{i=1}^{k+m} p_i$  prime implicants, some of which may coincide.

2. If the negation of the  $i$ -th (input or intermediate) signal occurs  $v_i$  times in the equation system, its realization requires  $\left\lceil \frac{v_i}{q_{\text{NOT}}} \right\rceil$  NOT elements. If the number of negations occurring in the system is  $s$ , the total number of NOT elements needed is  $N = \sum_{i=1}^s \left\lceil \frac{v_i}{q_{\text{NOT}}} \right\rceil$ . Thus the required number of  $A$ -modules (not counting amplification of input and intermediate signals) is

$$L_A = \left\lceil \frac{N}{l_A} \right\rceil. \quad (4)$$

3. The number of  $C$ -modules is

$$L_C = \left\lceil \frac{k+m}{l_C} \right\rceil. \quad (5)$$

4. Given the rank of the  $ij$ -th prime implicant ( $1 \leq j \leq p_i$ ,  $1 \leq i \leq k+m$ ) the number of AND elements required for its realization is

$$G_{ij} = \left\lceil \frac{R_{ij}}{r} \right\rceil.$$

5. Find the prime implicants for which  $G_{ij} \geq l_B$ ; for each of these, choose an integer  $v_{ij}$  such that the difference  $G'_{ij} = G_{ij} - v_{ij}l_B$  satisfies the inequality  $0 \leq G'_{ij} < l_B$ .

If  $G'_{ij} = 0$ , the corresponding prime implicant requires exactly  $v_{ij}$   $B$ -modules, and does not figure in the following steps (7, 8).

If  $G'_{ij} > 0$ , more than  $v_{ij}$  (but not more than  $v_{ij} + 1$ ) modules are necessary. Therefore, having determined the value of  $v_{ij}$ , in the next steps we shall replace  $G_{ij}$  by  $G'_{ij}$  as the number of AND elements necessary for the corresponding prime implicant.

For each  $i$ , find the number  $L'_i$  of  $B$ -modules for the  $i$ -th equation, by adding all the corresponding values of  $v_{ij}$ .

6. For the remaining prime implicants, satisfying  $G_{ij} < l_B$ , take  $G'_{ij} = G_{ij}$ .

7. Construct a loading table for each equation, with entries for all prime implicants such that  $G'_{ij} > 0$ . If the number of these implicants in the  $i$ -th equation is  $\rho_i$  ( $0 \leq \rho_i \leq \rho_i$ ), the loading table first contains  $2^{\rho_i}$  rows, each containing  $\rho_i$  zeros and units. Each entry in the table corresponds to one of the numbers  $G'_{ij}$ .

We retain in the table only rows for which the sum of the  $G'_{ij}$  for the unit entries is at most  $l_B$ .

Simplify the table by eliminating all rows which are absorbed by other rows (one row is absorbed by another if, apart from units in the same positions as those in the latter, the former contains at least one additional unit).

Denote the remaining rows by  $c_{i1}, c_{i2}, \dots, c_{iu_i}$ .

8. Using the simplified table, construct a function  $\Phi_i$ , which is a conjunction of  $\rho_i$  disjunctions, for the  $i$ -th equation. Each disjunction corresponds to a column in the table, with as many terms as there are units in the corresponding column.

Opening brackets and simplifying the resulting expression, we obtain a disjunction of a certain number of conjunctions in the variables  $c_{i1}, c_{i2}, \dots, c_{iu_i}$ . Choose the conjunction containing the minimum number of variables.

Realization of the prime implicants in the  $i$ -th equation is based on this conjunction. Each of the variables  $c_{i1}, c_{i2}, \dots, c_{iu_i}$  occurring therein is realized by one  $B$ -module. Given the  $G'_{ij}$  that correspond to the unit entries in the row corresponding to this variable, we can determine what prime implicants are realized by the given  $B$ -module. If the prime implicant is such that  $v_{ij} > 0$ , we determine how to link this module to the other  $v_{ij}$  modules to realize the implicant.

The rank of the selected conjunction determines the number  $L''_i$  of  $B$ -modules required to synthesize the prime implicants with  $v_{ij} = 0$ .

9. Determine the total number of  $B$ -modules required to realize the  $i$ -th equation,  $L_i = L'_i + L''_i$ . The entire system of equations then requires

$$L_B = \sum_{i=1}^{k+m} L_i \quad (6)$$

$B$ -modules.

10. Using (4)–(6), determine the total number of modules of types *A*, *B*, and *C* required to realize equations (1), (2):

$$L = L_A + L_B + L_C.$$

The inertial subautomata and input functions are combined in a single automaton.

## 5. EXAMPLES

Example 1. Using modules of types *A*, *B*, and *C* ( $q_{\text{NOT}}=5, q_F=3, r=3, l_A=5, l_B=8, l_C=2$ ), let us synthesize the automaton given by the following numerical expression:

$$\begin{aligned} Z(A_1, A_2, A_3, A_4, A_5, A_6, A_7, A_8, A_9) = & \Sigma (103 Z, 177 Z, 179 Z, \\ & 185 Z, 187 Z, 264, 268, 296, 300, 310, 311, 328, 332, 344, 360, 364, \\ & 433 Z, 435 Z, 438, 439, 441 Z, 443 Z, 456, 472). \end{aligned}$$

1. The automaton is described by a single equation. The minimal disjunctive normal form of the function *Z* is:

$$\begin{aligned} Z = & \bar{A}_9 \bar{A}_8 A_7 A_6 \bar{A}_5 \bar{A}_4 A_3 A_2 A_1 Z + A_9 A_7 \bar{A}_6 A_4 \bar{A}_3 \bar{A}_2 A_1 + \\ & + A_9 \bar{A}_7 A_6 A_5 \bar{A}_4 A_3 A_2 + A_6 \bar{A}_8 \bar{A}_5 A_4 \bar{A}_2 \bar{A}_1 + A_8 \bar{A}_7 A_6 A_5 \bar{A}_3 A_1 Z. \end{aligned}$$

2. The numbers of recurring negations of input signals are  $v_1=v_6=v_9=1$  and  $v_2=v_3=v_4=v_5=v_7=v_8=2$ . Since  $q_{\text{NOT}}=5$  and  $l_A=5$ , the required number of *B*-modules is  $L_A=2$ .

3. The required number of *C*-modules is  $L_C=1$  (by assumption,  $l_C=2, k+m=1$ ).

4. Find the ranks of the five prime implicants:  $R_1=10, R_2=R_3=R_5=7$  and  $R_4=6$ . Then the numbers of AND-elements for the prime implicants  $r=3$  are  $G_1=4, G_2=G_3=G_5=3$  and  $G_4=2$ .

5. There are no prime implicants with  $G_j \geq 8, (L'=0)$ .

6. Take  $G_1'=4, G_2'=G_3'=G_5'=3$  and  $G_4'=2$ .

7. Construct the loading table for *B*-modules (Table 1), retaining only rows in which the sum of  $G_j'$  over columns containing units is at most eight.

The resulting simplified table is Table 2, which contains seven rows.

8. Using Table 2, construct the function

$$\begin{aligned} \Phi = & (c_7 + c_6 + c_5)(c_7 + c_6 + c_4 + c_3)(c_7 + c_4 + c_2) \times \\ & \times (c_6 + c_4 + c_1)(c_5 + c_3 + c_2 + c_1) = c_7 c_1 + c_6 c_2 + c_5 c_4 + \\ & + c_7 c_6 c_5 + c_7 c_6 c_3 + c_7 c_6 c_2 + c_7 c_4 c_3 + c_7 c_4 c_2 + c_6 c_4 c_3 + \\ & + c_6 c_4 c_1 + c_5 c_3 c_2 c_1. \end{aligned}$$

Of these conjunctions we select the three ( $c_7 c_1, c_6 c_2$ , and  $c_5 c_4$ ) that involve two variables. Since they are equivalent, we take the first ( $c_7 c_1$ ) and use it as the basis for realization of the prime implicants, with two *B*-modules ( $L''=2$ ). One of these modules corresponds to the first and second prime implicants, the other to the third, fourth, and fifth.

TABLE 1.

0	0	0	0	1
0	0	0	1	0
0	0	0	1	1
0	0	1	0	0
0	0	1	0	1
0	0	1	1	0
0	1	0	0	0
0	1	0	0	1
0	1	0	1	0
0	1	1	0	0
0	1	1	1	0
1	0	0	0	0
1	0	0	0	1
1	0	0	1	0
1	0	1	0	0
1	1	0	0	0
1	1	0	1	0
1	1	1	0	0

TABLE 2.

$c_1$	0	0	0	1	1
$c_2$	0	0	1	0	1
$c_3$	0	1	0	0	1
$c_4$	0	1	1	1	0
$c_5$	1	0	0	0	1
$c_6$	1	1	0	1	0
$c_7$	1	1	1	0	0

9. The total required number of  $B$ -modules is  $L_B=2$ .

10. The total required number of modules of all types is  $L=2+2+1=5$  (Figure 5).

Example 2. Synthesis of the sequential automaton given by Table 3, using modules of type  $A$ ,  $B$ , and  $C$  ( $q_{\text{NOT}}=4$ ,  $q_F=3$ ,  $r=3$ ,  $l_A=4$ ,  $l_B=3$ ,  $l_C=2$ ).

TABLE 3.

$A_3 A_2 A_1$	$Z$	$X_1$	$X_2$	$X_3$	$X_4$	$X_5$	$X_6$	$X_7$	$X_8$
0 0 0	0	0	0	0	0	1	1	1	1
0 0 1	$X_1(1), X_5(0)$	$X_1$	0	$X_5$	$X_5$	$X_5$	$X_1, X_5$	$X_1$	$X_1$
0 1 0	1	0	1	0	0	1	0	1	1
0 1 1	$X_2(1), X_6(0)$	0	$X_2$	$X_6$	$X_6$	$X_2, X_6$	$X_6$	$X_2$	$X_2$
1 0 0	0	0	0	1	1	1	1	0	0
1 0 1	0	0	0	0	0	1	1	1	1
1 1 0	$X_3(1), X_7(0)$	$X_3$	$X_3, X_7$	$X_3$	$X_3$	$X_7$	0	$X_7$	$X_7$
1 1 1	$X_4(1), X_8(0)$	$X_4$	0	$X_4$	$X_4$	$X_8$	$X_4, X_8$	$X_4$	$X_8$



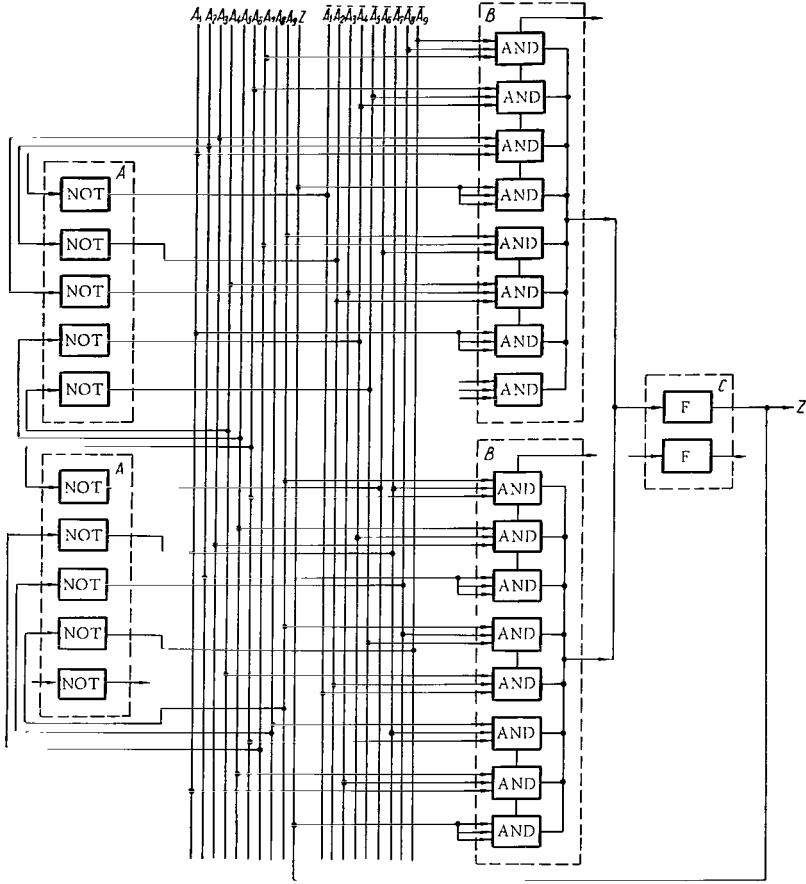


FIGURE 7. Circuit for Example 1.

1. The equation system of the automaton is:

$$\begin{cases} X_1 = \bar{A}_3 \bar{A}_2 A_1 X_1 + A_3 A_2 X_3; \\ X_2 = \bar{A}_3 A_2 X_2 + A_2 \bar{A}_1; \\ X_3 = \bar{A}_3 \bar{A}_2 A_1 \bar{X}_1 + \bar{A}_3 A_2 A_1 \bar{X}_2 + A_3 A_2 X_3 + A_3 \bar{A}_2 \bar{A}_1; \\ Z = \bar{A}_3 \bar{A}_2 A_1 X_1 + \bar{A}_3 A_2 X_2 + A_3 A_2 X_3 + \bar{A}_3 A_2 \bar{A}_1. \end{cases}$$

2. The numbers of repetitions of negations of the signals  $A_1, A_2, A_3, X_1, X_2$  are respectively  $v_1=3, v_2=4, v_3=7, v_4=v_5=1$ . Thus  $L_A=2$ .
3. Since  $k+m=4$  and  $l_C=2$ , it follows that  $L_C=2$ .
4. The ranks of the prime implicants are:

$$\begin{aligned} R_{11} &= 4; R_{12} = 3; \\ R_{21} &= 3; R_{22} = 2; \\ R_{31} &= R_{32} = 4; R_{33} = R_{34} = 3; \\ R_{41} &= 4; R_{42} = R_{43} = R_{44} = 3. \end{aligned}$$

Thus

$$\begin{aligned} G_{11} &= 2; G_{12} = 1; \\ G_{21} &= G_{22} = 1; \\ G_{31} &= G_{32} = 2; G_{33} = G_{34} = 1; \\ G_{41} &= 2; G_{42} = G_{43} = G_{44} = 1. \end{aligned}$$

5. There are no prime implicants with  $G_{ij} \geq 3$ .
6. We take

$$\begin{aligned} G'_{11} &= 2; G'_{12} = 1; \\ G'_{21} &= G'_{22} = 1; \\ G'_{31} &= G'_{32} = 2; G'_{33} = G'_{34} = 1; \\ G'_{41} &= 2; G'_{42} = G'_{43} = G'_{44} = 1. \end{aligned}$$

7. Construct the loading tables for  $B$ -modules. For the inertial subautomata  $X_1$  and  $X_2$ , the tables consist of one row each (each realized by a single  $B$ -module). The simplified tables for the inertial subautomata  $X_3$  and the output function  $Z$  are Tables 4 and 5.

TABLE 4.

$c_{31}$	0	1	0	1
$c_{32}$	0	1	1	0
$c_{33}$	1	0	0	1
$c_{34}$	1	0	1	0
$c_{35}$	1	1	0	0

TABLE 5.

$c_{41}$	0	0	1	1
$c_{42}$	0	1	0	1
$c_{43}$	1	0	0	1
$c_{44}$	1	1	1	0

8. Construct the functions

$$\begin{aligned} \Phi_3 &= (c_{35} + c_{34} + c_{33}) (c_{35} + c_{32} + c_{31}) (c_{34} + c_{32}) (c_{33} + c_{31}) = c_{34} c_{31} + \\ &+ c_{33} c_{32} + c_{35} c_{34} c_{33} + c_{35} c_{32} c_{31} \end{aligned}$$

and

$$\begin{aligned} \Phi_4 &= (c_{44} + c_{43}) (c_{44} + c_{42}) (c_{44} + c_{41}) (c_{43} + c_{42} + \\ &+ c_{41}) = c_{44} c_{43} + c_{44} c_{42} + c_{44} c_{41} + c_{43} c_{42} c_{41} \end{aligned}$$

Select the conjunctions  $c_{34}c_{31}$  and  $c_{44}c_{43}$ ; these are used to realize the functions  $X_3$  and  $Z$  ( $L_3''=2$  and  $L_4''=2$ ).

9. Thus,  $L_1=L_2=1$  and  $L_3=L_4=2$ . Consequently, the required number of  $B$ -modules is  $L_B=6$ .

10. The total number of modules of the three types is  $L=10$  (Figure 8).

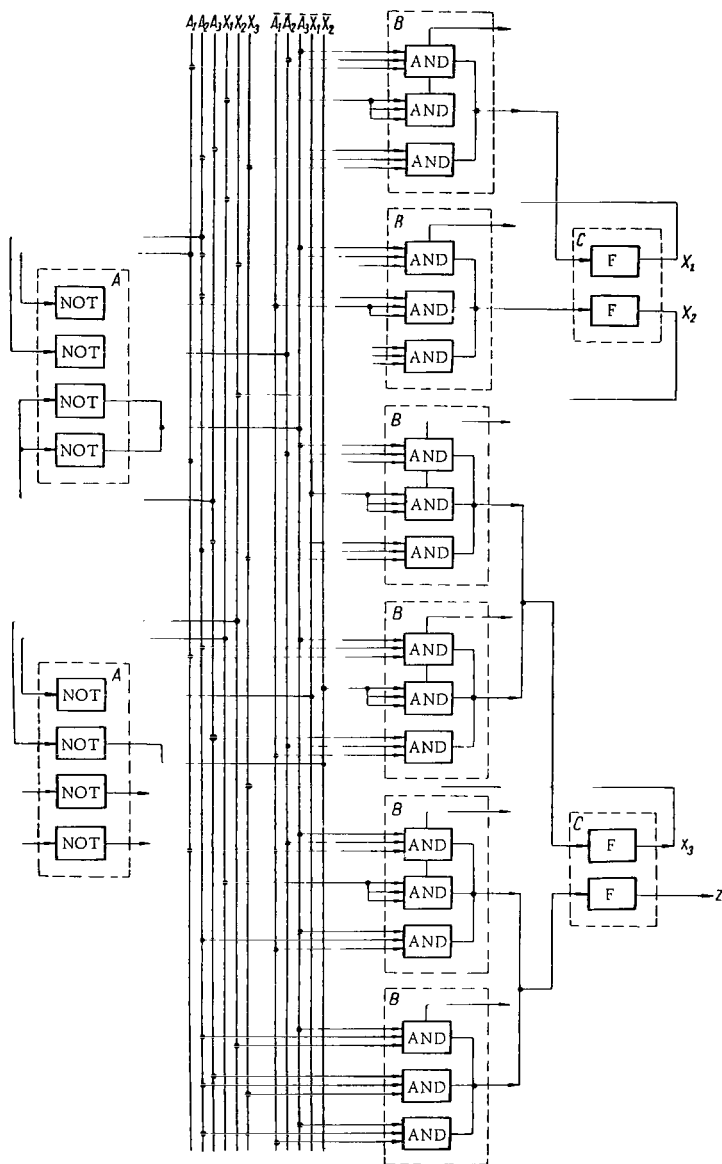


FIGURE 8. Circuit for Example 2.

## Bibliography

1. Yakubaitis, E. A. Asinkhronnyi logicheskii avtomat (An Asynchronous Logical Automaton). — Avtomatika i vychislitel'naya tekhnika, 1. 1967.

*A. A. Kurmit*

*DETERMINING THE INITIAL AND COMPATIBLE  
INTERNAL STATES OF THE INVERSE AUTOMATON  
OF CLASS II BY ANALYZING THE OPERATION OF  
THE ORIGINAL AUTOMATON*

Following /1, 2/ we introduce the concept of the inverse automaton of Class II, in contradistinction to the inverse automaton of Class I defined in /5, 6/. We formulate results for the former similar to those obtained in /5, 6/ for the latter. An example is given.

D. A. Huffman introduced the concept of an information-lossless (ILL) finite automaton in /1, 2/. Two classes of these automata were studied in detail: Class I consists of automata such that the preceding internal state and the output letter uniquely determine the input letter and the present internal state; Class II consists of automata in which the present internal state and output letter uniquely determine the previous internal state and the input letter.

In /2/, ILL automata of finite order (ILLF) were defined as automata in which the initial internal state and a finite output letter sequence determine the original input, therefore also the second internal state. Tests determining whether a given automaton is ILL or ILLF were described in /1-4/. Papers /3, 4/ also describe a method for construction of inverse automata (on the abstract level). Following /1, 2/ we shall call the latter inverse automata of Class I, and the corresponding original automata will be called ILLF automata of Class I.

**Definition 1.** An automaton will be called an ILLF automaton of Class II if the final internal state and any finite output letter sequence determine the immediately preceding internal state and the last input letter.

We shall use the notation and conventions of /5, 6/, unless otherwise stated.

Given the equalities

$$\alpha = a_{i_1} a_{i_2} \dots a_{i_M}, \quad \beta = b_{j_1} b_{j_2} \dots b_{j_P}.$$

Then

$$\alpha^* = a_{i_M} a_{i_{M-1}} \dots a_{i_1}, \quad \beta^* = b_{j_P} b_{j_{P-1}} \dots b_{j_1}.$$

**Definition 2.** Suppose that for any internal state  $s_{1i} \in S_1$  there is an internal state  $s_{2i} \in S_2$  such that for any word  $\alpha'$  of length  $N$  and any word  $\alpha$ , for which there exists  $s_{1i'} \in S_1$  with the property  $\delta_1(s_{1i'}, \alpha'\alpha) = s_{1i}$ , there exists a word  $\alpha''$  of length  $N$  such that

$$\lambda_2(s_{2i}, (\lambda_1(s_{1i'}, \alpha'\alpha))^{-1}) = \alpha''\alpha^*, \quad (1)$$

then the automaton  $A_2$  will be called the automaton of Class II inverse to  $A_1$ , and the number  $N$  will be called the delay.

Henceforth  $A_1$  will denote an ILLF automaton of Class II, and  $A_2$  the automaton of Class II inverse to  $A_1$ , with delay  $N$  (we assume that  $A_2$  exists).

A test verifying whether  $A_1$  is an ILLF automaton of Class II may be derived from the results of [4]. Instead of the diagram of  $A_1$  one must consider the suspended graph obtained from the diagram by changing the directions of all edges.

In analogy with [3, 4], the inverse automaton of Class II may be constructed in the following way. The internal states of  $A_2$  are all pairs  $(s_{1i}, \beta)$  where  $s_{1i} \in S_1$  and  $\beta$  is a word of length  $N$  for which there exist a word  $\alpha$  and an internal state  $s_{1i'} \in S_1$  such that  $\delta_1(s_{1i'}, \alpha) = s_{1i}$ ,  $\lambda_1(s_{1i'}, \alpha) = \beta^*$ . Since an output sequence  $b_1\beta^*$  ( $b_1 \in \Phi$ ) and a final internal state  $s_{1i}$  uniquely determine the preceding internal state  $s_{1i'}$  and the last input letter  $a_{i-1}$ , we can set

$$\begin{aligned} \lambda_2((s_{1i}, \beta), b_1) &= a_{i-1}; \\ \delta_2((s_{1i}, \beta), b_1) &= (s_{1i'}, \beta^*b_1), \end{aligned} \quad (2)$$

where  $\beta$  is the final section of the word  $\beta$  of length  $N-1$ .

In the sequel  $A_2$  will always denote the automaton constructed in this way.

Let  $\mathcal{Z}(s_{1i}, \beta)$  denote the set of all internal states  $s_{1i'} \in S_1$  such that there exists a word  $\alpha$  of length  $N$  with the property  $\delta_1(s_{1i'}, \alpha) = s_{1i}$ ,  $\lambda_1(s_{1i'}, \alpha) = \beta^*$ .

Let  $\mathcal{B}(s_{1i}, \beta)$  denote the set of all words  $\alpha$  of length  $N$  such that there exists an internal state  $s_{1i'} \in S_1$  with the property  $\delta_1(s_{1i'}, \alpha) = s_{1i}$ ,  $\lambda_1(s_{1i'}, \alpha) = \beta^*$ .

In [5] we studied the possibility of determining the internal states of the inverse automaton of Class I constructed in a way similar to that considered here, while in [6] we investigated the selection of an initial internal state for the same automaton.

In this paper we shall consider the same questions for the inverse automaton of Class II. The proofs of the lemmas and theorems, which are essentially identical to the analogous proofs in [6], will be omitted.

**Theorem 1.** The following condition is necessary and sufficient for an internal state  $(s_{1i}, \beta)$  of the automaton  $A_2$  to satisfy (1). Let  $\alpha'$  be a nonempty word and  $\alpha''$  a word of length  $N$  such that there exists an internal state  $s_{1i'} \in S_1$  with the property  $\delta_1(s_{1i'}, \alpha''\alpha') = s_{1i}$ ; then there exist an internal state  $s_{1i'}(x^*\alpha') \in \mathcal{Z}(s_{1i}, \beta)$  and a word  $\alpha'''$  of length  $N$  such that there is an internal state  $s_{1i'} \in S_1$  with the property  $\delta_1(s_{1i'}, \alpha'''\alpha') = s_{1i'}(x^*\alpha')$ ,  $\lambda_1(s_{1i'}, \alpha'''\alpha') = \lambda_1(s_{1i'}, \alpha''\alpha')$ .

**Remark.** As for inverse automata of Class I, it can be shown that for all internal states  $(s_{1i}, \beta_1)$  (fixed  $s_{1i}$ , variable  $\beta_1$ ) the corresponding internal state  $(s_{1i'}(x^*\alpha'), \beta_1)$  is compatible with  $(s_{1i}, \beta_1)$ . Moreover, if  $\beta_2$  is a word such that  $\lambda_2((s_{1i}, \beta_1), \beta_2)$  is defined, then  $\lambda_2((s_{1i'}(x^*\alpha'), \beta_1), \beta_2)$  is also defined.

**Definition 3.** Two internal states  $s_{1i}$  and  $s_{1j}$  are said to be inversely disjoint of order  $M$  if any two internal states  $s_{1i}'$  and  $s_{1j}'$  and any two words  $\alpha'$  and  $\alpha''$  of length  $M$  such that  $\delta_1(s_{1i}', \alpha') = s_{1j}, \delta_1(s_{1j}', \alpha'') = s_{1i}$  satisfy the inequality  $\lambda_1(s_{1i}', \alpha') \neq \lambda_1(s_{1j}', \alpha'')$ .

**Lemma 1.** Suppose the internal states  $(s_{1i}, \beta_i)$  and  $(s_{1j}, \beta_j)$  of the automaton  $A_2$  are compatible,  $s_{1i}'$  and  $s_{1j}'$  are two internal states of the automaton  $A_1$ ; let  $\alpha_i$  and  $\alpha_j$  be two different words of length  $N$  in which the last different letters are in the  $M$ -th position from the end of the word, such that

$$\delta_1(s_{1i}', \alpha_i) = s_{1i}, \delta_1(s_{1j}', \alpha_j) = s_{1j}, \lambda_1(s_{1i}', \alpha_i) = \beta_i^*, \lambda_1(s_{1j}', \alpha_j) = \beta_j^*.$$

Then the internal states  $s_{1i}'$  and  $s_{1j}'$  are inversely disjoint of order  $M$ .

**Definition 4.** Two internal states  $s_{1i}$  and  $s_{1j}$  are said to be inversely noncontradictory with delay  $N$  if any two internal states  $s_{1i}'$  and  $s_{1j}'$  and any two words  $\alpha'$  and  $\alpha''$  of equal length, in which the last different letters are in the  $N+1$ -th position, such that

$$\delta_1(s_{1i}', \alpha') = s_{1i}, \delta_1(s_{1j}', \alpha'') = s_{1j},$$

satisfy the inequality

$$\lambda_1(s_{1i}', \alpha') \neq \lambda_1(s_{1j}', \alpha'').$$

**Lemma 2.** Suppose the internal states  $(s_{1i}, \beta_i)$  and  $(s_{1j}, \beta_j)$  of the automaton  $A_2$  are compatible,  $s_{1i}'$  and  $s_{1j}'$  are two internal states of the automaton  $A_1$ , and  $\alpha_k$  is a word of length  $N$ , such that

$$\delta_1(s_{1i}', \alpha_k) = s_{1i}, \delta_1(s_{1j}', \alpha_k) = s_{1j}, \lambda_1(s_{1i}', \alpha_k) = \beta_i^*, \lambda_1(s_{1j}', \alpha_k) = \beta_j^*.$$

Then the internal states  $s_{1i}'$  and  $s_{1j}'$  are inversely noncontradictory with delay  $N$ .

**Theorem 2.** Suppose the internal states  $(s_{1i}, \beta_i)$  and  $(s_{1j}, \beta_j)$  of the automaton  $A_2$  are compatible.

Then any two internal states  $s_{1i}' \in \mathcal{S}(s_{1i}, \beta_i)$  and  $s_{1j}' \in \mathcal{S}(s_{1j}, \beta_j)$  are

1) inversely disjoint of order  $M$ , if the last different letters of the corresponding words  $\alpha_i \in \mathcal{M}(s_{1i}, \beta_i)$  and  $\alpha_j \in \mathcal{M}(s_{1j}, \beta_j)$  are in the  $M$ -th position from the end of the word;

2) inversely noncontradictory with delay  $N$ , if  $\alpha_i = \alpha_j$ .

**Theorem 3.** Suppose that for any two words  $\alpha_i \in \mathcal{M}(s_{1i}, \beta_i)$  and  $\alpha_j \in \mathcal{M}(s_{1j}, \beta_j)$  all the corresponding internal states  $s_{1i}' \in \mathcal{S}(s_{1i}, \beta_i)$  and  $s_{1j}' \in \mathcal{S}(s_{1j}, \beta_j)$  are

1) inversely disjoint of order  $M$ , if the last different letters in the words  $\alpha_i$  and  $\alpha_j$  are in the  $M$ -th position from the end of the word;

2) inversely noncontradictory with delay  $N$ , if  $\alpha_i = \alpha_j$ ; then the internal states  $(s_{1i}, \beta_i)$  and  $(s_{1j}, \beta_j)$  are compatible.

**Lemma 3.** Suppose that  $A_2$  is a complete automaton, and the internal states  $(s_{1i}, \beta_i)$  and  $(s_{1j}, \beta_j)$  are equivalent. Then  $\mathcal{M}(s_{1i}, \beta_i) = \mathcal{M}(s_{1j}, \beta_j)$ .

**Definition 5.** The automaton  $A_1$  is said to be inversely complete if for any word  $\alpha$  and any internal state  $s_{1i} \in S_1$  there exists an internal state  $s_{1i}' \in S_1$  such that  $\delta_1(s_{1i}', \alpha) = s_{1i}$ .

**Definition 6.** Two internal states  $s_{1i}$  and  $s_{1j}$  of the automaton  $A_1$  are said to be inversely compatible if every word  $\alpha$  and every two internal states  $s_{1i}'$  and  $s_{1j}'$  such that  $\delta_1(s_{1i}', \alpha) = s_{1i}$ ,  $\delta_1(s_{1j}', \alpha) = s_{1j}$  satisfy the equality  $\lambda_1(s_{1i}', \alpha) = \lambda_1(s_{1j}', \alpha)$ .

**Definition 7.** Two inversely compatible internal states of an inversely complete automaton will be called inversely equivalent.

**Lemma 4.** Suppose that  $s_{1i}, s_{1j} \in S_1$  and there exist a word  $\alpha$  of length  $N$  and an internal state  $s_{1i}' \in S_1$  such that

$$\delta_1(s_{1i}, \alpha) = s_{1i}'.$$

If  $A_2$  is a complete automaton, the internal states  $s_{1i}$  and  $s_{1j}$  are inversely noncontradictory with delay  $N$ , and  $s_{1j}$  is inversely disjoint of some order  $M \leq N$  with any internal state  $s_{1i}''$  for which there exists a word  $\alpha''$  of length  $N$  ( $\alpha'' \neq \alpha$ ) such that  $\delta_1(s_{1i}'', \alpha'') = s_{1i}'$ ,  $\lambda_1(s_{1i}'', \alpha'') = \lambda_1(s_{1i}, \alpha)$ , then  $s_{1i}$  and  $s_{1j}$  are inversely compatible.

**Lemma 5.** Let  $A_1$  be an inversely complete automaton. If the internal states  $s_{1i}$  and  $s_{1j}$  are inversely equivalent, they are inversely noncontradictory with delay  $N$ .

**Theorem 4.** Suppose that  $A_2$  is a complete automaton, the internal states  $(s_{1i}, \beta_i)$  and  $(s_{1j}, \beta_j)$  are equivalent, and there exists a word  $\alpha$  of length  $N$  such that at least one of  $\delta_1(s_{1i}, \alpha)$  and  $\delta_1(s_{1j}, \alpha)$  is defined. Then  $\mathfrak{M}(s_{1i}, \beta_i) = \mathfrak{M}(s_{1j}, \beta_j) = \mathfrak{M}$  and every two internal states  $s_{1i}' \in \mathfrak{Z}(s_{1i}, \beta_i)$  and  $s_{1j}' \in \mathfrak{Z}(s_{1j}, \beta_j)$  such that a single word  $\alpha \in \mathfrak{M}$  satisfies both equalities  $\delta_1(s_{1i}', \alpha) = s_{1i}$ ,  $\delta_1(s_{1j}', \alpha) = s_{1j}$  are inversely compatible.

**Theorem 5.** Let  $A_1$  be an inversely complete automaton. Suppose that  $\mathfrak{M}(s_{1i}, \beta_i) = \mathfrak{M}(s_{1j}, \beta_j) = \mathfrak{M}$ , and every two internal states  $s_{1i}' \in \mathfrak{Z}(s_{1i}, \beta_i)$  and  $s_{1j}' \in \mathfrak{Z}(s_{1j}, \beta_j)$  such that a single word  $\alpha \in \mathfrak{M}$  satisfies both equalities  $\delta_1(s_{1i}', \alpha) = s_{1i}$ ,  $\delta_1(s_{1j}', \alpha) = s_{1j}$  are inversely equivalent; then the internal states  $(s_{1i}, \beta_i)$  and  $(s_{1j}, \beta_j)$  are compatible.

**Example.** Let  $\mathfrak{A} = \mathfrak{B} = \{0, 1\}$ , and let the automaton  $A_1$  be given by a table of transitions and outputs (Table 1).

TABLE 1

	0	1		0	1
$a$	$b, 0$	$c, 0$	$e$	$f, 0$	$h, 0$
$b$	$c, 0$	$a, 1$	$f$	$g, 0$	$e, 1$
$c$	—	$f, 0$	$g$	$d, 1$	—
$d$	—	$g, 1$	$h$	$g, 1$	$d, 1$

It can be shown that  $A_1$  is not an ILLF automaton of Class I, but rather an ILLF automaton of Class II with  $N=2$ .

For further analysis, it is convenient to draw up a table of internal states and outputs of  $A_1$  (Table 2).

Using this table, the table of transitions and outputs of the automaton  $A_2$  is easily set up (Table 3).

**Problem 1.** To find all admissible initial internal states of  $A_2$ , given that  $e$  is a final internal state of  $A_1$ .

Clearly, if  $s_{1i}$  is a final internal state of  $A_1$ , the conditions of Theorem 1 are satisfied by all internal states of  $A_2$  of the form  $(\delta_1(s_{1i}, a), (\lambda_1(s_{1i}, \alpha)))$ , where  $\alpha$  is an arbitrary word of length  $N$ . In our case these are  $(g, 00)$  and  $(e, 10)$ . It is clear from the internal-state table of  $A_1$  that the conditions of Theorem 1 are satisfied by the internal states  $g$  and  $h$ . Since  $\mathcal{M}(g, 11) = \{g, h\}$ , it follows that the role of the initial internal state of  $A_2$  may also be played by  $(g, 11)$ .

TABLE 2.

	0	1		0	1
$a$	—	$b, 1$	$e$	—	$f, 1$
$b$	$a, 0$	—	$f$	$e, 0$	$c, 0$
$c$	$b, 0$	$a, 0$	$g$	$f, 0; h, 1$	$d, 1$
$d$	$g, 1$	$h, 1$	$h$	—	$e, 0$

TABLE 3.

	0	1		0	1
$(a, 10)$	—	$(b, 01), 1$	$(f, 00)$	$(c, 00), 1$	$(c, 01), 1$
$(b, 01)$	$(a, 10), 0$	—	$(f, 01)$	$(e, 10), 0$	—
$(c, 00)$	—	$(b, 01), 1$	$(g, 00)$	$(f, 00), 0$	$(f, 01), 1$
$(c, 01)$	$(a, 10), 1$	—	$(g, 10)$	—	$(h, 01), 0$
$(d, 10)$	$(g, 00), 0$	$(h, 01), 1$	$(g, 11)$	$(d, 10), 1$	$(d, 11), 1$
$(d, 11)$	$(g, 10), 0$	$(g, 11), 0$	$(h, 01)$	$(c, 10), 1$	—
$(e, 10)$	$(f, 00), 1$	$(f, 01), 1$			.

**Problem 2.** To find all pairs of compatible internal states of  $A_2$ .

Examination of the set  $S_2$  immediately shows that the following are pairs of inversely disjoint internal states of  $A_1$ , of order 1:  $(a, b)$ ;  $(a, c)$ ;  $(a, f)$ ;  $(a, h)$ ;  $(b, d)$ ;  $(b, e)$ ;  $(c, d)$ ;  $(c, e)$ ;  $(d, f)$ ;  $(d, h)$ ;  $(e, f)$ ;  $(e, h)$ , while the pair  $(b, g)$  is inversely disjoint of order 2.

Apart from the pairs of inversely disjoint internal states of order  $M \leq N$ , the following pairs are inversely noncontradictory with delay  $N=2$ :  $(a, e)$ ;  $(b, f)$ ;  $(c, g)$ ;  $(c, h)$ ;  $(g, h)$ . This can be established by examining the internal-state table of the automaton  $A_1$ . Consideration of the sets  $\mathcal{M}(s_{1i}, \beta_i)$  and  $\mathcal{S}(s_{1i}, \beta_i)$  and the above pairs of inversely disjoint and inversely noncontradictory internal states of  $A_1$  shows that the following internal states of  $A_2$  are compatible

$A_2$ :  $\{(a, 10), (b, 01)\}$ ;  $\{(a, 10), (c, 01)\}$ ;  $\{(a, 10), (e, 10)\}$ ;  $\{(a, 10), (f, 01)\}$ ;  $\{(a, 10), (h, 01)\}$ ;  $\{(b, 01), (c, 00)\}$ ;  $\{(b, 01), (f, 01)\}$ ;  $\{(b, 01), (g, 10)\}$ ;  $\{(c, 00), (c, 01)\}$ ;  $\{(c, 00), (f, 01)\}$ ;  $\{(c, 00), (g, 00)\}$ ;  $\{(c, 00), (h, 01)\}$ ;  $\{(c, 01), (g, 10)\}$ ;  $\{(c, 01), (h, 01)\}$ ;  $\{(f, 01), (g, 10)\}$ ;  $\{(g, 10), (h, 01)\}$ .



## Bibliography

1. Huffman, D. A. Canonical forms for information-lossless finite-state logical machines. — IRE Trans. Circuit Theory, 6, 1959, Spec. Suppl. 41.
2. Huffman, D. A. Notes on information-lossless finite-state automata. — Nuovo cimento, 13, 1959, Suppl. 2, 397.
3. Iven [Even], Sh. Ob avtomatakh konechnogo poryadka bez poteri informatsii (On Information-lossless Automata of Finite Order). Theory of Finite and Probabilistic Automata. — Proceedings of International Symposium on the Theory of Relay Devices and Finite Automata, p. 269. Moscow, "Nauka," 1965.
4. Even, Sh. On Information-lossless automata of finite order. — IEEE Trans. Electronic Comput., 14, 1965, 4, 561.
5. Kurmit, A. A. Obnaruzhenie sovmestimyykh vnutrennikh sostoyanii obratnogo avtomata na osnovanii izucheniya funktsionirovaniya dannogo avtomata (Determining the compatible internal states of the inverse automaton by examining the operation of the original automaton). In sbornik: Teoriya diskretnykh avtomatov. Riga, "Zinatne." 1967.
6. Kurmit, A. A. Nakhozhdenie nachal'nykh vnutrennikh sostoyanii obratnogo avtomata na osnovanii izucheniya funktsionirovaniya dannogo avtomata (Finding the Initial Internal States of the Inverse Automaton by Examining the Operation of the Original Automaton). Present collection.

*A. A. Kurmit*

**FINDING THE INITIAL INTERNAL STATES OF THE  
INVERSE AUTOMATON BY EXAMINING THE  
OPERATION OF THE ORIGINAL AUTOMATON**

It is shown that an internal state of the inverse automaton can play the role of the initial state if and only if, after output of the word characterizing the state under consideration, the corresponding internal state of the original automaton passes into internal states in a definite way related to the initial internal state of the original automaton.

Consider two partial Mealy automata  $A_1$  and  $A_2$ , with the following alphabets of internal states, inputs, and outputs:

$$S_1 = \{s_{11}, \dots, s_{1n_1}\}, \mathfrak{A} = \{a_1, \dots, a_m\}, \mathfrak{B} = \{b_1, \dots, b_l\}, \\ S_2 = \{s_{21}, \dots, s_{2n_2}\}, \mathfrak{B} = \{b_1, \dots, b_l\}, \mathfrak{A} = \{a_1, \dots, a_m\}$$

and the following output and transition functions:

$$\lambda_1(s_{1i}, a_j) = b_{j_i}, \delta_1(s_{1i}, a_j) = s_{1i_j}, \lambda_2(s_{2i}, b_k) = a_{k_i}, \delta_2(s_{2i}, b_k) = s_{2k_i}$$

for

$$s_{1i}, s_{1j_i} \in S_1, s_{2i}, s_{2k_i} \in S_2, a_j, a_{k_i} \in \mathfrak{A}, b_k, b_{j_i} \in \mathfrak{B}.$$

We assume that for any pair  $(s_{1i}, a_j)$  or  $(s_{2i}, b_j)$  the transition function and the output function are either both defined or both undefined.

The letters  $\alpha$  and  $\beta$  (with or without primes and/or subscripts) will denote words on the alphabets  $\mathfrak{A}$  and  $\mathfrak{B}$ , respectively. The functions  $i$  and  $\delta_i$  ( $i=1, 2$ ) are defined in the natural way for words on the alphabets  $\alpha$  and  $\mathfrak{B}$ .

**Definition.** Suppose that for any internal state  $s_{1i} \in S_1$  there exists an internal state  $s_{2j} \in S_2$  such that for any word  $\alpha'$  of length  $N$  and any word  $\alpha$  there is a word  $\alpha''$  of length  $N$  with the property

$$\lambda_2(s_{2j}, \lambda_1(s_{1i}, \alpha\alpha')) = \alpha''\alpha, \quad (1)$$

then the automaton  $A_2$  is said to be inverse to the automaton  $A_1$  and the number  $N$  is called the delay.

**Remark 1.** If  $A_1$  is an initial automaton, it suffices to require that a suitable  $s_{2j}$ , exist for an initial internal state  $s_{1i_0}$ .

**Remark 2.** Use of the notation  $\lambda_1(s_{1i}, \alpha)$  (similarly for  $\lambda_2, \delta_1, \delta_2$ ), always implies that the function is defined for the pair  $(s_{1i}, \alpha)$ .

For a given automaton  $A_1$ , the existence and construction of the inverse automaton and determination of the delay were studied in [1, 2].

In [2], the automaton  $A_2$  was constructed as follows. The internal states of  $A_2$  are all pairs  $(s_{1i}, \beta)$ , where  $s_{1i} \in S_1$  and  $\beta$  is a word of length  $N$  such that there exists a word  $\alpha$  for which  $\lambda_1(s_{1i}, \alpha) = \beta$ .

Suppose that the automaton inverse to  $A_1$ , with delay  $N$ , exists; suppose further that we know an initial state  $s_{1i}$ , and an output sequence  $\beta b_j (b_j \in B)$  of length  $N+1$  emitted by the automaton  $A_1$  when the latter starts from the internal state  $s_{1i}$ . Then the first letter  $a_j$  entering the input of the automaton  $A_1$  is uniquely determined.

The following are therefore well defined:

$$\lambda_2((s_{1i}, \beta), b_j) = a_j, \delta_2((s_{1i}, \beta), b_j) = (\delta_1(s_{1i}, a_j), \beta' b_j), \quad (2)$$

where  $\beta'$  is the final section of length  $N-1$  of the word  $\beta$ .

This automaton  $A_2$  is inverse to  $A_1$  if and only if for every internal state of  $A_1$  there exists an internal state of  $A_2$  satisfying (1) (see also Remark 1).

However, no simple criterion is given in [2] to determine when this is possible and how to choose the corresponding initial internal state of  $A_2$  (of course, the problem may be solved by simply checking all internal states).

This problem is the subject of our paper.

Let  $\mathfrak{M}(s_{1i}, \beta)$  denote the set of all words  $\alpha$  such that  $\lambda_1(s_{1i}, \alpha) = \beta$ .

**Theorem.** An internal state  $(s_{1i}, \beta)$  of the automaton  $A_2$  satisfies (1) if and only if for every word  $\alpha'$  and every word  $\alpha''$  of length  $N$  such that  $\lambda_1(s_{1i}, \alpha' \alpha'')$  is defined there exist a word  $\alpha_{\alpha' \alpha''} \in \mathfrak{M}(s_{1i}, \beta)$  and a word  $\alpha'''$  of length  $N$  with the property

$$\lambda_1(\delta_1(s_{1i}, \alpha_{\alpha' \alpha''}), \alpha' \alpha''') = \lambda_1(s_{1i}, \alpha' \alpha''). \quad (3)$$

**Proof. Sufficiency.** If the condition is satisfied, equality (3) implies

$$\lambda_1(s_{1i}, \alpha_{\alpha' \alpha''} \alpha' \alpha''') = \beta \lambda_1(s_{1i}, \alpha' \alpha''). \quad (4)$$

By construction of the automaton  $A_2$ :

$$\lambda_2((s_{1i}, \lambda_1(s_{1i}, \alpha_{\alpha' \alpha''})), \lambda_1(\delta_1(s_{1i}, \alpha_{\alpha' \alpha''}), \alpha' \alpha''')) = \alpha_{\alpha' \alpha''} \alpha', \quad (5)$$

or, in view of (3):

$$\lambda_2((s_{1i}, \beta), \lambda_1(s_{1i}, \alpha' \alpha'')) = \alpha_{\alpha' \alpha''} \alpha'. \quad (6)$$

This proves that (1) is true.

**Necessity.** Let the internal state  $s_{2j} = (s_{1i}, \beta)$  satisfy (1). Assume the condition of the theorem false, i.e., there exists a nonempty word  $\alpha'$  and a word  $\alpha''$  of length  $N$  such that for any word  $\alpha \in \mathfrak{M}(s_{1i}, \beta)$  and any word  $\alpha'''$  of length  $N$

$$\lambda_1(\delta_1(s_{1i}, \alpha), \alpha' \alpha''') \neq \lambda_1(s_{1i}, \alpha' \alpha''). \quad (7)$$

We consider two cases.

Case 1. There exists a word  $\alpha''$  of length  $N$  and words  $\alpha \in \mathcal{M}(s_{1j}, \beta)$  and  $\alpha_1' (\alpha_1' \neq \alpha')$  such that

$$\lambda_1(\delta_1(s_{1j}, \alpha), \alpha_1' \alpha'') = \lambda_1(s_{1i}, \alpha' \alpha''). \quad (8)$$

Then, by (2) we have

$$\lambda_2((s_{1j}, \beta), \lambda_1(s_{1i}, \alpha' \alpha'')) = \alpha \alpha_1' \neq \alpha \alpha'. \quad (9)$$

Case 2. There are no words  $\alpha''$ ,  $\alpha$ , and  $\alpha_1'$  satisfying (8). Then  $\lambda_2((s_{1j}, \beta), \lambda_1(s_{1i}, \alpha' \alpha''))$  are not defined.

These contradictions prove the theorem.

It follows from the proof that for all internal states of the form  $(s_{1i}, \beta_1)^*$  (fixed  $s_{1i}$ , variables  $\beta_1$ ) the corresponding internal state  $(\delta_1(s_{1j}, \alpha_{\alpha' \alpha''}), \beta_1)$  is compatible with  $(s_{1i}, \beta_1)$ . Moreover, if  $\lambda_2((s_{1i}, \beta_1), \beta_2)$  is defined for some word  $\beta_2$ , then  $\lambda_2((\delta_1(s_{1j}, \alpha_{\alpha' \alpha''}), \beta_1), \beta_2)$  is also defined.

If  $A_2$  is a complete automaton the above internal states  $(s_{1i}, \beta_1)$  and  $(\delta_1(s_{1j}, \alpha_{\alpha' \alpha''}), \beta_1)$  are equivalent.

Example. Let  $S_1 = \{a, b, c, d, e, f, g, h\}$ ,  $\mathcal{A} = \mathcal{B} = \{0, 1\}$ , and define the automaton  $A_1$  by Table 1.

TABLE 1.

	0	1		0	1
$a$	$b, 1$	$c, 0$	$e$	$h, 1$	$c, 0$
$b$	$a, 0$	$f, 0$	$f$	$c, 1$	$b, 0$
$c$	$d, 1$	$e, 1$	$g$	$e, 0$	$d, 0$
$d$	$b, 1$	$g, 0$	$h$	$f, 1$	$a, 1$

The inverse automaton  $A_2$ , constructed by the method of [2], is then given by Table 2.

TABLE 2.

	0	1		0	1
$(a, 01)$	$(c, 10), 1$	$(c, 11), 1$	$(e, 01)$	$(c, 10), 1$	$(c, 11), 1$
$(a, 10)$	$(b, 00), 0$	$(b, 01), 0$	$(e, 11)$	$(h, 10), 0$	$(h, 11), 0$
$(b, 00)$	$(f, 00), 1$	$(a, 01), 0$	$(f, 00)$	$(b, 00), 1$	$(b, 01), 1$
$(b, 01)$	$(a, 10), 0$	$(f, 11), 1$	$(f, 11)$	$(c, 10), 0$	$(c, 11), 0$
$(c, 10)$	$(d, 00), 0$	$(e, 01), 1$	$(g, 00)$	$(d, 00), 1$	$(e, 01), 0$
$(c, 11)$	$(d, 10), 0$	$(e, 11), 1$	$(g, 01)$	$(d, 10), 1$	$(e, 11), 0$
$(d, 00)$	$(g, 00), 1$	$(g, 01), 1$	$(h, 10)$	$(f, 00), 0$	$(a, 01), 1$
$(d, 10)$	$(b, 00), 0$	$(b, 01), 0$	$(h, 11)$	$(a, 10), 1$	$(f, 11), 0$

Problem. To find all internal states of  $A_2$  which can be initial states, if the initial state of the automaton  $A_1$  is  $a$ .

\*  $s_{1i}$  is any internal state of  $A_1$  for which we require an internal state of  $A_2$  satisfying (1).

The condition of the theorem must hold for those internal states of  $A_2$  such that the first element  $s_{1j}$  satisfies  $\delta_1(s_{1j}, \alpha) = a$  with some word  $\alpha$  of length  $N(=2)$ . Examination of the transition table of  $A_1$  easily shows that these states are  $a, d, e$ , and  $f$ .

We can now say that any of the following internal states can be initial states:  $(a, 10)$ ;  $(d, 10)$ ;  $(e, 11)$ ;  $(f, 00)$ .

Since the internal states  $(a, 01)$  and  $(e, 01)$  are equivalent, as are  $(a, 10)$  and  $(d, 10)$ , it follows that the first element  $s_{1j}$  of an initial state of  $A_2$  may also be such that  $\delta_1(s_{1j}, \alpha_1) = d$  and  $\delta_1(s_{1j}, \alpha_2) = e$  for some words  $\alpha_1$  and  $\alpha_2$  of length 2. As before, it turns out that the appropriate internal states of  $A_1$  are  $a, d, e$ , and  $f$ . The corresponding set of internal states of  $A_2$  is:  $(a, 01)$ ;  $(d, 00)$ ;  $(e, 01)$ ;  $(f, 11)$ .

Though our theorem somewhat reduces the necessary amount of checking, the process is nevertheless quite laborious, as is evident from the example.

### Bibliography

1. Levenshtein, V. I. Ob obrashchenii konechnykh avtomatov (On Inversion of Finite Automata). — DAN SSSR, 147 (6): 1300. 1962.
2. Iven, Sh. Ob avtomatakh konechnogo poryadka bez poteri informatsii (On Information-lossless Automata of Finite Order). Theory of Finite and Probabilistic Automata. — Proceedings of International Symposium on the Theory of Relay Devices and Finite Automata, p. 269. Moskva, "Nauka," 1965.

*T.A. Frantsis, G.F. Yanbykh*

# *AUTOMATIC ERROR CORRECTING IN DISCRETE AUTOMATA*

Self-correcting codes are applied to synthesis of asynchronous logical automata by the method of error-correcting inertial subcircuits.

## INTRODUCTION

Reliability of operation is one of the most important properties of any automatic device. However, high-reliability automatic devices cannot be constructed from elements of limited reliability unless redundancy is introduced.

In this paper we consider the introduction of redundancy based on the application of self-correcting codes, suitable for electronic discrete binary finity automata.

There are two approaches to the evaluation of reliability /1/:

1. Reliability is defined as the probability of failproof operation of the entire automaton for given failproof probability of its component elements.
2. Reliability is defined as the maximum admissible number of simultaneously faulty component elements. Conditions governing faults in the component elements may be either specific (listing the component elements in which faults are allowed), or general (specifying the number of elements in which occurrence of faults does not affect operation of the automaton). The only difference between these approaches is methodological, for the failure of some number of component elements is intimately related to the probability of this event, in other words, the latter is an estimate for the former.

The first approach is suitable for the general description of an automaton, since, knowing the failproof probability, one can compare the reliability of various devices.

In automata synthesis, the second approach is more suitable. Given the required reliability of the automaton, the reliability of the component elements available for the synthesis, and the functional circuit of the automaton, one can determine the total number of elements, or the specific elements, in which faults should not affect the operation of the automaton as a whole. M. A. Gavrilov has considered correction of two types of errors:

- 1) The relay remains closed even though the winding is not energized.
- 2) Contacts remain broken even though the winding is energized.

In general, this corresponds to the appearance of a signal "one" instead of "zero" (or vice versa) at the output of the component element. In multistage automata one must distinguish between two types of errors — failures and malfunctions. By failure of a component element we mean a state in which no change of input signal can affect the output signal; if the signal at the output of the faulty element is "one," we say that the element is short-circuited; conversely, if the output is "zero," we say that it is open-circuited. By malfunction we mean a situation in which a component element produces the wrong signal at some stage of the operation of the automaton. In the sequel we shall use the term "error" for both types, unless explicitly stated otherwise.

We make the following assumptions concerning errors in component elements:

1) An error in one component element at some instant is independent of errors in other components at any instant of time.

1) A malfunction in a component element is independent of previous malfunctions in the same element.

In other words, faulty operation of some component element does not affect the normal operating conditions of the other elements, the source of the fault is to be found in the element itself.

In such a situation we shall use the term  $s$ -fold error to mean a simultaneous error in the operation of  $s$  component elements.

Every automaton is characterized by its set of input signals  $X$ , set of output signals  $Z$ , set of internal states  $Q$ , a transition function  $\phi$  and an output function  $f$ . Any automaton may be constructed from functionally complete elementary automata, with two internal states corresponding to two distinct output signals  $z_1, z_2$ , and logic circuits which realize the transition and output functions.

The component elements we shall use are illustrated in Figure 1. In linking these components one must avoid any direct connection between the outputs of two or more elements. Such a connection may be made only through another element.

Every automaton satisfies the relations

$$Q(t+\tau) = \phi[Q(t), X(t)];$$

$$Z(t) = f[Q(t), X(t)],$$

where  $X(t)$  is the input signal at the instant  $t$ ,  $Q(t)$  the internal state at the instant  $t$ ,  $Z(t)$  the output signal at the instant  $t$ , and  $Q(t+\tau)$  the internal state at the following instant  $t+\tau$ .

In this paper we shall restrict ourselves to synchronous automata, in which the input signals, which are pulses, can appear only at fixed intervals of length  $\tau$ .

The transition function of the automaton is determined by the excitation functions (or transition functions) of the elementary automata  $Q_i$ :

$$Q_i(t+\tau) = F[q_i(t)]; \quad (1)$$

$$q_i(t) = \psi_i[Q_1(t), Q_2(t), \dots, Q_k(t), X(t)], \quad (2)$$

where  $i = \overline{1, k}$ ,  $k$  being the number of elementary automata.

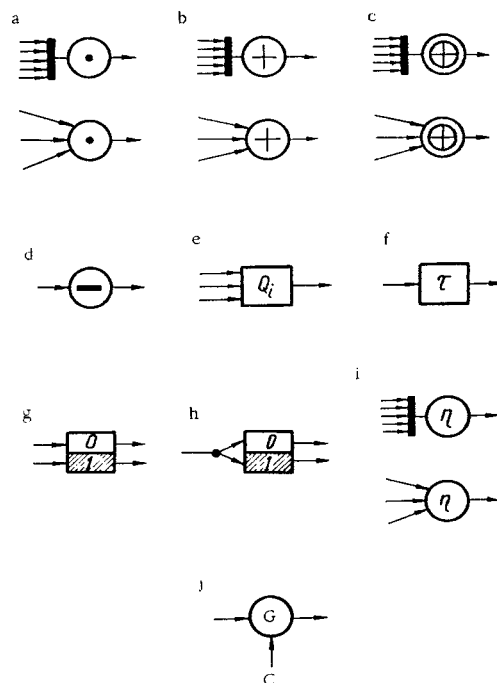


FIGURE 1. Component elements of the automaton:

a — AND-element; b — OR-element; c — addition mod 2; d — NOT-element; e — elementary automaton; f — delay element, with time delay  $\tau$ ; g — two-input trigger (1 — "one" output, 0 — "zero" output); h — complementing trigger; i — threshold element, with threshold  $\eta$ ; j — gate (C — control signal).

The form of the function  $F$  in (1) depends on the internal structure of the elementary automaton; in general, each elementary automaton is specified by a transition table.

The functional circuit of the automaton may be divided into two parts (Figure 2):

- 1) A circuit conveying information about the internal state of the automaton, consisting of elementary automata.
  - 2) A circuit realizing the logic functions, consisting of logic elements.
- The latter in turn may be divided into
- a) a circuit realizing the output function, and
  - b) a circuit realizing the transition function (excitation functions of the elementary automata).

This subdivision facilitates the analysis and synthesis of the circuits, since the probabilities of errors in an elementary automaton and a logic element are often quite different. Moreover, faulty operation of the circuit realizing the transition function entails faulty operation of the elementary automata. Consequently, from this standpoint we shall regard



the elementary automaton and the subcircuit realizing its transition function (assuming that transitions occurring in different elementary automata are independent) as a single internal subcircuit, in which an error in a logic element is equivalent to an error in the elementary automaton.

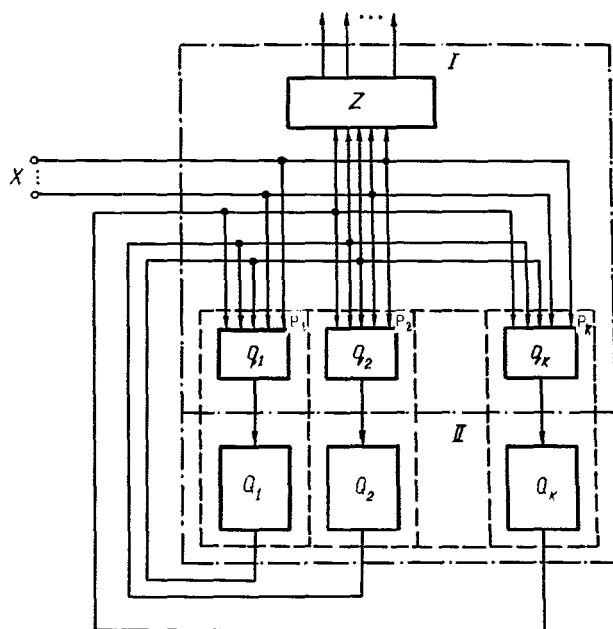


FIGURE 2. Block diagram of a discrete automaton:

$I$  — memory circuit;  $II$  — logic circuit;  $Z$  — output circuit;  
 $q_i$  — transition (excitation) function circuit;  $Q_i$  —  $i$ -th elementary  
 automaton;  $P_i$  —  $i$ -th internal subcircuit.

The reliability of the output function circuit is of particular significance, since it clearly imposes a limit on the reliability of the automaton as a whole. If the output circuit is constructed from logic elements of types AND, OR, NOT, its reliability is determined essentially by the reliability of its output element with respect to errors of the above types. The output circuit must therefore incorporate measures aimed at improving the reliability of the logic elements themselves, as suggested, for instance, by Yu. A. Kosarev [3].

Another method is to employ gate elements, which allow the passage of a signal "one" only in the presence of a control signal [4]. Possibly errors in a gate are:

- 1) short circuit — a signal "one" is emitted in the absence of a control signal;
- 2) open circuit — a signal "one" cannot pass the gate, despite the presence of a control signal.

Since there are no restrictions on connections between the outputs of gates, the outputs of all redundant gates may be connected directly to the load. The situation is thus more analogous to that in devices employing electromagnetic relays than to that in circuits of AND, OR, NOT elements.

## 2. APPLICATION OF SELF-CORRECTING CODES IN CODING THE INTERNAL STATES OF A DISCRETE AUTOMATON

We identify each internal state of the automaton with the corresponding set of internal states of the elementary automata  $Q$ , encoded in binary digits 0, 1, forming a sequence of length  $k$ :

$$\{a_i\}_k = (a_1, a_2, \dots, a_k),$$

where

$$a_i = 0, 1; \quad (i = 1, k).$$

Regarding 0 and 1 as the elements of the field of residues mod 2, we can define addition of sequences of length  $k$

$$\{a_i\}_k + \{b_i\}_k = \{a_i + b_i\}_k$$

and multiplication by a field element  $c$

$$c\{a_i\}_k = \{c a_i\}_k,$$

and thus the internal state of the automaton is characterized by a vector in a vector space over the field of two elements 0 and 1, the dimension of the space being given by the number of elementary automata.

The development of the theory of error-correcting codes (we mention Hamming /5/ as one of the first papers in this connection) has led to applications aimed at improving the reliability of discrete automata. M. A. Gavrilov has proved /1/ that a necessary condition for reliable operation of a multistage relay device is that every two stable states must differ by at least  $d$  single transitions, where  $d$  is defined by the inequality

$$d \geq 2s + 1, \quad (3)$$

$s$  being the number of admissible simultaneous errors.

Regarding the encoded internal state as a vector, it is easily seen that  $d$  is the minimal code distance (in the sense of Hamming) for the correction of  $s$  single errors. R.R. Varshamov /6/ has found an expression relating the number  $r$  of additional parity-check symbols and the number  $k = n - r$  of information symbols to the minimal code distance  $d$ :

$$2^r \geq 1 + \binom{n-1}{1} + \binom{n-1}{2} + \dots + \binom{n-1}{d-2}. \quad (4)$$

Proceeding to the synthesis of a redundant automaton, we must use (4), given  $b$  and  $d$ , to find the number  $n$  of elementary automata that will ensure the given number of internal states, the code distance between which is  $d$ .

Example 1. Consider synthesis of an automaton with one input and one output, given by the following truth table:

TABLE 1

$Z$		0	1
$X$	$Q$	0	1
	0	0	0
	1	1	0

As the elementary automaton we use a delay element, and the logic circuit is constructed from elements of types AND, OR, NOT. The excitation function of the delay element is given by Table 2 [2].

The automaton clearly consists of one delay element and a logic circuit realizing the transition function according to the truth table of the automaton and the excitation function of the delay element (Table 3); this circuit is illustrated in Figure 3a.

TABLE 2

$q(t)$	$Q(t)$	$Q(t+\tau)$
0	0	0
0	1	0
1	0	1
1	1	1

Now suppose that the same component elements are to be used in the synthesis of an automaton realizing the same table with correction of single errors in any one component element of the transition circuit. By (3) the distance between any two internal states of the automaton must be at least  $d=3$ . In this case, the inequality (4) clearly implies that the internal states of the automaton may be designated by the vectors 000 and 111, i. e., we employ a (3, 1) code. The truth table and excitation functions of the resulting automaton are illustrated in Table 4.

Table 4 implies that the excitation functions and the output function are:

$$q_1 = q_2 = q_3 = q = X\bar{Q}_3\bar{Q}_2 + X\bar{Q}_3\bar{Q}_1 + X\bar{Q}_2\bar{Q}_1 \quad (5)$$

and

$$Z = Q_3Q_2 + Q_3Q_1 + Q_1Q_2. \quad (6)$$

By (5) the excitation functions are the same for all elementary automata. This is always the case when the synthesized automaton has only two internal states and the excitation function of the elementary automaton is that given by Table 2.

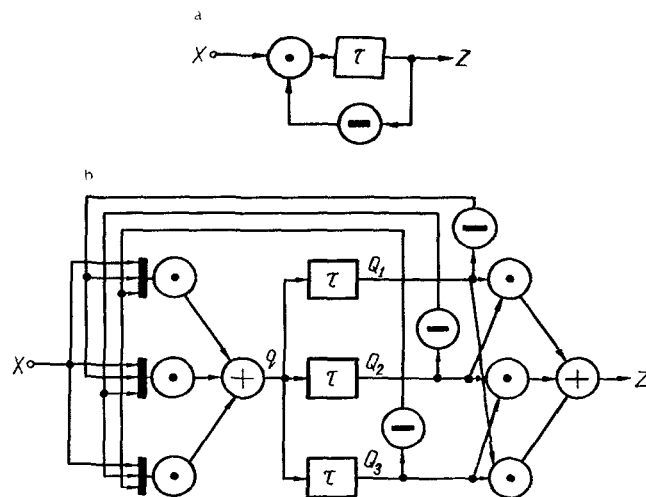


FIGURE 3. Nonredundant (a) and redundant (b) circuit of the synthesized automaton.

TABLE 3.

$x(t)$	$(t)$	$Q(t+\tau)$	$q(t)$	$Z(t)$
0	0	0	0	0
0	1	0	0	1
1	0	1	1	0
1	1	0	0	1

TABLE 4.

$x(t)$	$Q_1(t)$	$Q_2(t)$	$Q_3(t)$	$Q_1(t+\tau)$	$Q_2(t+\tau)$	$Q_3(t+\tau)$	$q_1(t)$	$q_2(t)$	$q_3(t)$	$Z(t)$
0	0 1 0 0	0 0 1 0	0 0 0 1	0	0	0	0 0 0 0	0 0 0 0	0 0 0 0	0
0	1 0 1 1	1 1 0 1	1 1 1 0	0	0	0	0 0 0 0	0 0 0 0	0 0 0 0	1
1	0 1 0 0	0 0 1 0	0 0 0 1	1	1	1	1 1 1 1	1 1 1 1	1 1 1 1	0
1	1 0 1 1	1 1 0 1	1 1 1 0	0	0	0	0 0 0 0	0 0 0 0	0 0 0 0	1

The resulting automaton is illustrated in Figure 3b.

Obviously, all single errors in elementary automata (by elementary automata we mean delay elements and NOT-elements) are corrected in this automaton. The operation of the automaton under various single errors in elements of the logic circuit is illustrated in Table 5. The first column of the table indicates the faulty element (the subscript is the index of the element in Figure 3b) and the type of error (subscript 0—open circuit, 1—short circuit). The second, third, and fourth columns indicate the values of the output function at the instants  $t_0$ ,  $t_0+\tau$  and  $t_0+2\tau$ , respectively. The errors are assumed to occur at the instant  $t_0$ , when the automaton is in state zero and "one" is applied at the input; it is also assumed that a single error in the logic circuit entails no errors in the operation of the elementary automata. Incorrect values of the output function are indicated by bold type.

TABLE 5.

Type of error	$t_0$	$t_0+\tau$	$t_0+2\tau$
	$X$		
	1	0,1	0,1
No error	$Z$		
	0	1	0
$AND_1^0, AND_2^0, AND_3^0$	0	1	0
$AND_1^1, AND_2^1, AND_3^1$	0	1	1
$OR_1^0$	0	<b>0</b>	0,1
$OR_1^1$	0	1	1
$AND_4^0, AND_5^0, AND_6^0$	0	1	0
$OR_2^0$	0	<b>0</b>	0
$OR_2^1$	1	1	1
$AND_4^1, AND_5^1, AND_6^1$	1	1	1

The automaton circuit of Figure 3b is applicable only when the probability of error in an elementary automaton is greater than that of error in a logic element.

To improve the reliability of the transition circuit without having to improve that of its elements, the excitation function of the elementary automata must be organized in as independent a manner as possible.

To improve the reliability of the output circuit, the above-mentioned gate-type elements may be used. Equation (6) may be rewritten in the form

$$Z = Q_1(Q_2 + Q_3) + Q_2Q_3, \quad (6a)$$

according to which the gates form the circuit illustrated in Figure 4. Signals from the corresponding elementary automata are applied to the control inputs of the gates. The gate inputs receive the input current from the load connected to the output of the circuit. Construction of gate circuits from transistors was discussed in [7].

The automaton synthesized in Example 1 is quite trivial; nevertheless, it completely characterizes the method for synthesizing redundant automata and reveals various features of this method.

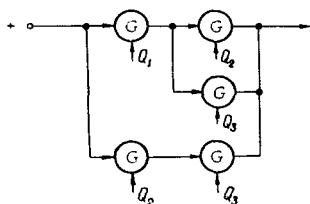


FIGURE 4. Gating in output circuit.

Example 2. Let us construct a decimal counter, counting pulses in increasing order of binary numbers from zero to ten. On the elementary automaton we employ a two-input trigger. The excitation function of this type of trigger is given in Table 6 /2/.

The truth table of the required automaton is given in Table 7. We have used the abbreviation  $q_i(t)=0$  for  $q_{i0}(t)=1$ ,  $q_{i1}(t)=0$ , and  $q_i(t)$  for  $q_{i0}(t)=0$ ,  $q_{i1}(t)=1$ . By Table 7, the excitation functions of the elementary automata are:

$$\left. \begin{aligned} q_{10} &= XQ_1Q_4; \\ q_{11} &= XQ_2Q_3Q_4; \\ q_{20} &= XQ_2Q_3Q_4; \\ q_{21} &= X\bar{Q}_2Q_3Q_4; \\ q_{30} &= XQ_3Q_4; \\ q_{31} &= X\bar{Q}_1\bar{Q}_3Q_4; \\ q_{40} &= XQ_4; \\ q_{41} &= X\bar{Q}_4. \end{aligned} \right\} \quad (7)$$

The synthesized decimal counter is illustrated in Figure 5. Delay elements, with delay  $\theta$  exceeding the duration of the input signals, are needed to prevent undesirable competition.

TABLE 6.

$q_0(t)$	$q_1(t)$	$Q(t)$	$Q(t+\tau)$
0	0	0	0
0	0	1	1
0	1	0	1
0	1	1	1
1	0	0	0
1	0	1	0

The counter is to be synthesized with correction of single errors in the component elements of the transition circuit. By (4), for  $k=4$  and  $d=3$  we have  $n=7$ , i. e., (7, 4) code.

Since the numbering of the separate output functions in the logic circuit is immaterial, we shall regard the first  $k$  symbols of the code vector as information, and the remaining  $r=n-k$  as parity-check symbols. The internal states, encoded in this systematic (7, 4) code, yield vectors which form an orthogonal parity-check matrix  $H/8/$ :

$$H = \begin{bmatrix} 1 & 1 & 0 & \dots & 1 & 1 & 0 & 0 & \dots & 0 \\ 1 & 0 & 1 & \dots & 1 & 0 & 1 & 0 & \dots & 0 \\ 0 & 1 & 1 & \dots & 1 & 0 & 0 & 1 & \dots & 0 \\ \vdots & \vdots & \vdots & \vdots & \vdots & \vdots & \vdots & \vdots & \vdots & \vdots \\ 0 & 0 & 0 & \dots & 1 & 0 & 0 & 0 & \dots & 1 \end{bmatrix}$$

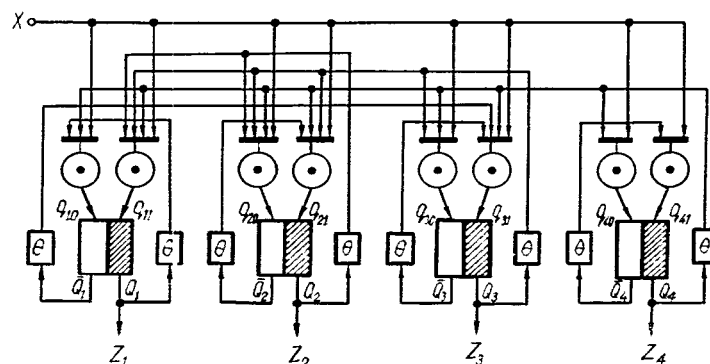


FIGURE 6. Decimal counter constructed from two-input triggers (Example 1).

TABLE 7.

$t$				$t + \tau$				$t$				$t$			
$X$	$Q_1$	$Q_2$	$Q_3$	$Q_1$	$Q_2$	$Q_3$	$Q_4$	$q_1$	$q_2$	$q_3$	$q_4$	$Z_1$	$Z_2$	$Z_3$	$Z_4$
1	0	0	0	0	0	0	1				1	0	0	0	0
1	0	0	0	0	0	0	1				1	0	0	0	1
1	0	0	1	0	0	0	1				1	0	0	0	1
1	0	0	1	1	0	0	1				1	0	0	0	1
1	0	1	0	0	0	0	1				1	0	0	0	1
1	0	1	0	0	0	1	1				1	0	0	0	1
1	0	1	1	0	0	1	1				1	0	0	0	1
1	0	1	1	1	0	1	1				1	0	0	0	1
1	1	0	0	0	0	0	1				1	0	0	0	1
1	1	0	0	0	0	1	1				1	0	0	0	1
1	1	0	1	0	0	0	1				1	0	0	0	1
1	1	0	1	1	0	0	1				1	0	0	0	1
1	1	1	0	0	0	0	1				1	0	0	0	1
1	1	1	0	0	0	1	1				1	0	0	0	1
1	1	1	1	0	0	0	1				1	0	0	0	1

The orthogonality conditions imply the relation

$$QH^T = 0 \quad (8)$$

According to (8), the parity-check inputs of the elementary automata are determined by the relations

$$Q_{k+i} = \sum_{j=1}^k h_{ij} Q_j, \\ (\alpha = \overline{1, r}),$$

where  $h_{ij}$  is the element of the matrix  $H$  in the  $i$ -th row and the  $j$ -th column. In our example

$$H = \begin{bmatrix} 1 & 1 & 0 & 1 & 1 & 0 & 0 \\ 1 & 0 & 1 & 1 & 0 & 1 & 0 \\ 0 & 1 & 1 & 1 & 0 & 0 & 1 \end{bmatrix} \quad (9)$$

After computing the code vectors of the redundant (7, 4) code, we can set up the truth table for a redundant decimal counter (Table 8). To save space, the table has been constructed for error-free performance of the automaton. To represent single errors in the performance of the elementary automata each row of Table 8 must be replaced by 8 rows.

As an example, consider all possible single errors in the states (0000000) and (0001111) (Table 9).

Computation of the transition functions of the separate elementary automata is extremely complicated (Tables 8, 9). It is therefore more convenient to begin by determining the corrected values of the information symbols and to use these alone as the input variables for the transition and output circuits.

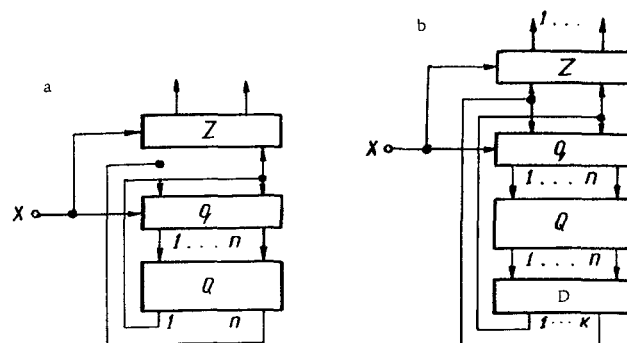


FIGURE 6. Methods for constructing the logic circuits of a redundant automaton:

- a — using the states of all the elementary automata as input variables;
- b — using the corrected values of the states of the information elementary automata as input variables; Z — input circuit; D — decoder circuit;
- Q — memory circuit; q — excitation-function circuit.

Block-diagrams illustrating the two procedures are given in Figures 6a, b. It is clear that when the second method is used the decoder must operate at a high reliability. If necessary, this may be achieved by increasing the reliability of the component elements themselves. Synthesis of a decoder is described in [9], which also gives an example for (7, 4) code. The excitation functions of the elementary automata are, according to Table 8:



TABLE 8.

$t$	$t$							$t+\tau$							$t$							$t$			
	$Q_1^*$	$Q_2^*$	$Q_3^*$	$Q_4^*$	$Q_5^*$	$Q_6^*$	$Q_7^*$	$Q_1$	$Q_2$	$Q_3$	$Q_4$	$Q_5$	$Q_6$	$Q_7$	$q_1$	$q_2$	$q_3$	$q_4$	$q_5$	$q_6$	$q_7$	$Z_1$	$Z_2$	$Z_3$	$Z_4$
1	0	0	0	0	0	0	0	0	0	0	1	1	1	1	0	0	0	1	1	1	1	0	0	0	0
1	0	0	0	1	1	1	1	0	0	1	0	0	1	1	0	0	1	0	0	1	1	0	0	0	1
1	0	0	1	0	0	1	1	0	0	1	1	1	0	0	0	0	1	1	1	0	0	0	0	1	0
1	0	0	1	1	1	0	0	0	1	0	0	1	0	1	0	1	0	1	0	1	0	1	0	1	1
1	0	1	0	0	1	0	1	0	1	0	1	0	1	0	0	1	0	1	0	1	0	0	1	0	0
1	0	1	0	1	0	1	0	0	1	1	0	1	1	0	0	1	1	0	1	1	0	0	1	0	1
1	0	1	1	0	1	1	0	0	1	1	1	1	0	0	1	0	1	1	0	0	1	0	1	1	0
1	0	1	1	1	0	0	1	1	0	0	0	1	1	0	1	0	0	0	1	1	0	0	1	1	1
1	1	0	0	0	1	1	0	1	0	0	1	0	0	1	1	0	0	1	0	0	1	1	0	0	0
1	1	0	0	1	0	0	1	0	0	0	0	0	0	0	0	0	0	0	0	0	0	1	0	0	1

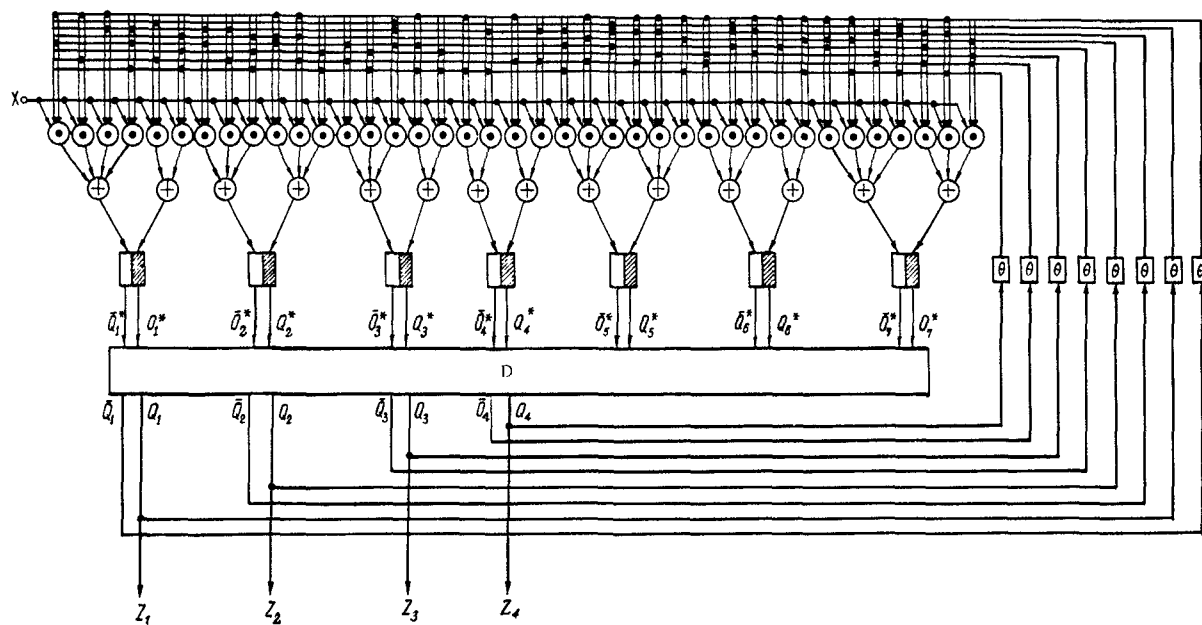


FIGURE 7. Redundant decimal counter using a decoder circuit (D) (Example 2).

$$\begin{aligned}
q_{10} &= X\bar{Q}_1\bar{Q}_3 + X\bar{Q}_1\bar{Q}_4 + X\bar{Q}_1\bar{Q}_2 + X\bar{Q}_2\bar{Q}_3Q_4, \\
q_{11} &= XQ_1\bar{Q}_4 + XQ_2Q_3Q_4; \\
q_{20} &= X\bar{Q}_2\bar{Q}_3 + X\bar{Q}_2\bar{Q}_4 + XQ_2Q_3Q_4; \\
q_{21} &= X\bar{Q}_1Q_2\bar{Q}_3 + X\bar{Q}_1Q_2\bar{Q}_4 + XQ_3Q_4; \\
q_{30} &= X\bar{Q}_3\bar{Q}_4 + XQ_3Q_4 + XQ_1\bar{Q}_2\bar{Q}_3; \\
q_{31} &= X\bar{Q}_1\bar{Q}_3Q_4 + XQ_3Q_4; \\
q_{40} &= X\bar{Q}_1Q_4 + X\bar{Q}_2Q_4; \\
q_{41} &= X\bar{Q}_1\bar{Q}_4 + X\bar{Q}_2\bar{Q}_4; \\
q_{50} &= X\bar{Q}_2\bar{Q}_3Q_4 + X\bar{Q}_1Q_2\bar{Q}_4 + XQ_1\bar{Q}_2\bar{Q}_3; \\
q_{51} &= X\bar{Q}_1\bar{Q}_2\bar{Q}_4 + X\bar{Q}_1\bar{Q}_2Q_3 + X\bar{Q}_1Q_2Q_4; \\
q_{60} &= X\bar{Q}_1Q_3\bar{Q}_4 + XQ_1\bar{Q}_2\bar{Q}_3 + X\bar{Q}_1\bar{Q}_2Q_3; \\
q_{61} &= X\bar{Q}_1\bar{Q}_3 + X\bar{Q}_1Q_2Q_4; \\
q_{70} &= X\bar{Q}_1Q_2\bar{Q}_3 + X\bar{Q}_1Q_2Q_4 + X\bar{Q}_2Q_3\bar{Q}_4 + XQ_1\bar{Q}_2Q_4; \\
q_{71} &= X\bar{Q}_2\bar{Q}_3\bar{Q}_4 + X\bar{Q}_1\bar{Q}_2Q_4 + XQ_2Q_3\bar{Q}_4.
\end{aligned} \tag{10}$$

The synthesized circuit is illustrated in Figure 7.

### 3. REALIZATION OF THE EXCITATION FUNCTIONS USING MAGNETIC DECODERS

When AND-, OR-, NOT-elements are used as component elements, the logic circuit of the automaton becomes extremely complicated. Some simplification is achieved by using magnetic-core decoders. We shall consider a magnetic-core decoder for direct and inverse code, which we call a decoder of the first type and denote by DC1.

The signals of the elementary automata are applied to the inputs of the DC1, and every combination of input signals, i.e., every state of the synthesized automaton, has its own output. Suppose, for instance, that three triggers are used as elementary automata (Figure 8) (the notation for the coils follows 10/), and that it is required to distinguish between the states 010 and 001. Both outputs of each trigger are provided with magnetic cores. The cores of the "zero" output are threaded in accordance with the direct code of the automaton state.

The cores of the "one" outputs are threaded in accordance with the inverse code. Buses corresponding to the direct and inverse codes of each state are connected in series. On the appearance of a clock pulse (CP) an emf is produced only in the windings of the bus corresponding to the given state. An inverter is used to produce the signal at the corresponding output. Figure 8 illustrates the state 010.

In redundant automata the DC1 may be used to determine the internal states, taking all admissible errors of the elementary automata into account.

**Example 3.** Application of the DC1 to the decimal counter of Example 2.

In this case (see Figure 9) there are 8 buses in the DC1 for each row in Table 8, i.e., one bus for each row of Table 9. All 8 buses are connected

TABLE 9.

$t$		$t$						$t+\tau$								$t$							$t$					
$X$		$Q_1$	$Q_2$	$Q_3$	$Q_4$	$Q_5$	$Q_6$	$Q_7$	$Q_1$	$Q_2$	$Q_3$	$Q_4$	$Q_5$	$Q_6$	$Q_7$	$q_1$	$q_2$	$q_3$	$q_4$	$q_5$	$q_6$	$q_7$	$Z_1$	$Z_2$	$Z_3$	$Z_4$		
1		0	0	0	0	0	0	0	}	0	0	0	1	1	1	1	0	0	0	1	1	1	1	0	0	0	0	
		1	0	0	0	0	0	0																				0
		0	1	0	0	0	0	0																				0
		0	0	1	0	0	0	0																				0
		0	0	0	1	0	0	0																				0
		0	0	0	0	1	0	0																				0
		0	0	0	0	0	1	0																				0
		0	0	0	0	0	0	1																				0
1		0	0	0	1	1	1	1	}	0	0	1	0	0	1	1	0	0	1	0	1	1	0	0	0	1		
		1	0	0	1	1	1	1																			1	
		0	1	0	1	1	1	1																			1	
		0	0	1	1	1	1	1																			1	
		0	0	0	1	1	1	1																			1	
		0	0	0	1	0	1	1																			1	
		0	0	0	1	1	0	1																			1	
		0	0	0	1	1	1	0																			1	

via an OR-element, whence a signal is fed to the elementary automata, where it records the code of the next state. If we denote the signal at the output of the DCI for the  $i$ -th state by  $y_i$ , Table 8 yields:

$$\left. \begin{aligned} q_{10} &= y_0 + y_1 + y_2 + y_3 + y_4 + y_5 + y_6; \\ q_{11} &= y_7 + y_8; \\ q_{12} &= y_0 + y_1 + y_2 + y_7 + y_8 + y_9; \\ q_{13} &= y_3 + y_4 + y_5 + y_6; \\ q_{14} &= y_0 + y_3 + y_4 + y_7 + y_8 + y_9; \\ q_{15} &= y_1 + y_2 + y_5 + y_6; \\ q_{16} &= y_1 + y_3 + y_5 + y_7 + y_9; \\ q_{17} &= y_0 + y_2 + y_4 + y_6 + y_8; \\ q_{18} &= y_1 + y_4 + y_6 + y_8 + y_9; \\ q_{19} &= y_0 + y_2 + y_3 + y_5 + y_7; \\ q_{20} &= y_2 + y_5 + y_6 + y_8 + y_9; \\ q_{21} &= y_0 + y_1 + y_4 + y_5 + y_7; \\ q_{22} &= y_2 + y_4 + y_5 + y_7 + y_9; \\ q_{23} &= y_0 + y_1 + y_3 + y_6 + y_8; \\ Z_1 &= y_5 + y_6; \\ Z_2 &= y_4 + y_5 + y_6 + y_7; \\ Z_3 &= y_2 + y_3 + y_6 + y_7; \\ Z_4 &= y_1 + y_3 + y_5 + y_7 + y_9. \end{aligned} \right\} \quad (11)$$

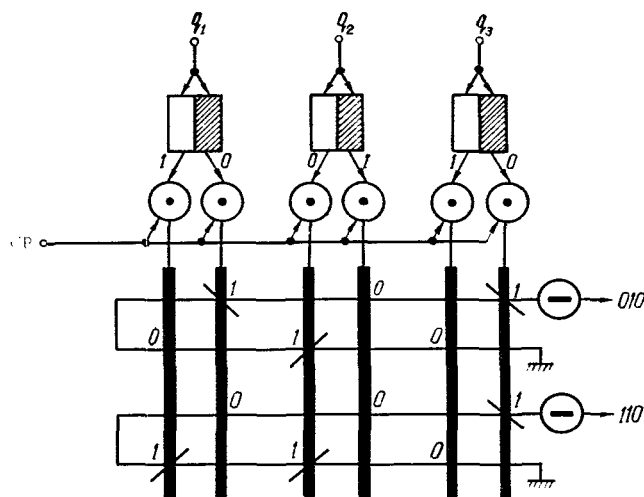


FIGURE 8. Decoder of the first type DCI (CP — clock pulses).

The automaton (see Figure 9) does not correct errors in the NOT- and OR-elements at the outputs of the decoder. Errors in the OR-elements at the trigger inputs, open or short circuits in the magnetizing coils, and failures in individual cores (e.g., mechanical) are equivalent to errors in the elementary automata, and can therefore be corrected.

The number of coils may be reduced by using a decoder with load sharing and voltage addition, proposed by H. Takahasi and E. Goto [11], with a threshold element at each output.

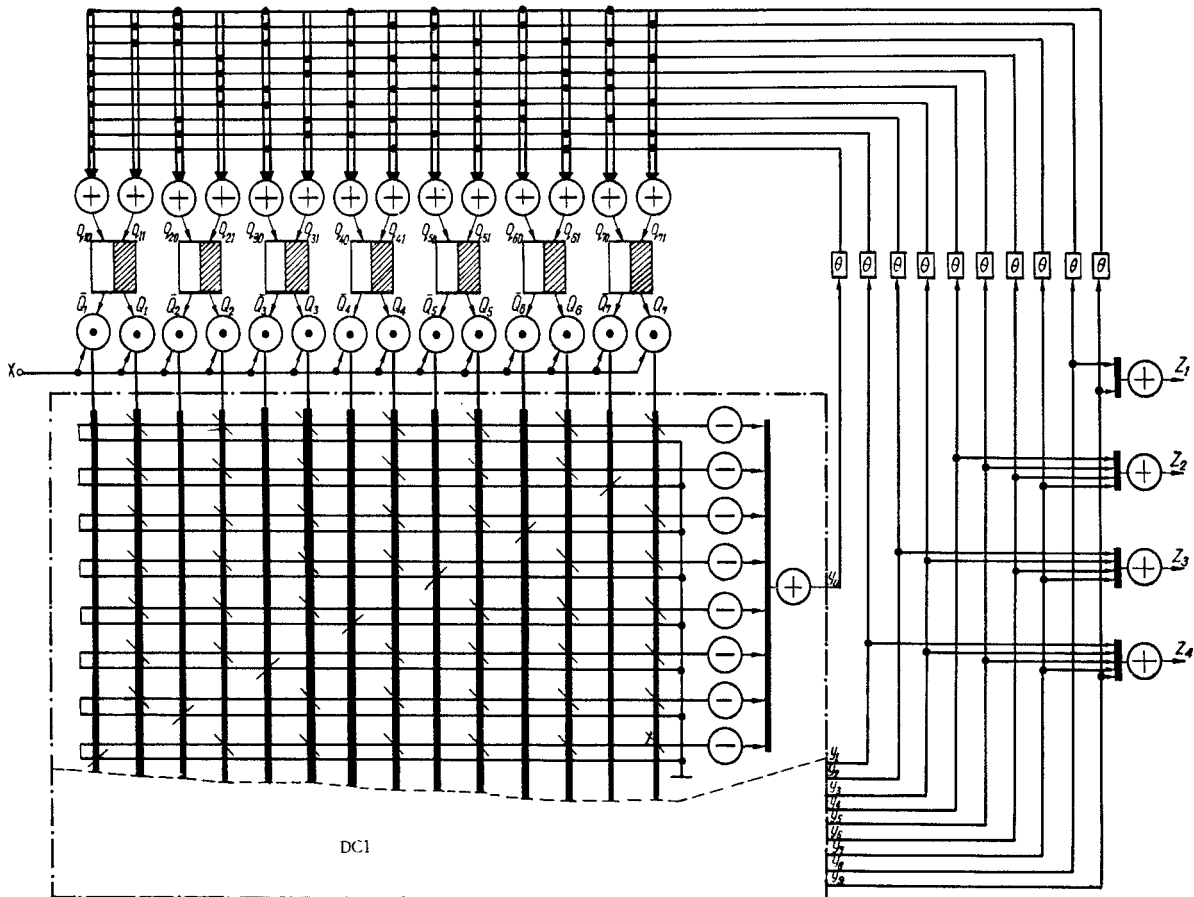


FIGURE 9. Redundant decimal counter using DC1 (Example 3).

We shall call this a decoder of the second type, DC2.

The number of cores in the DC2 is equal to the number of elementary automata (see Example 4). The number of outputs corresponds to the number of internal states of the automaton. The circuit of each output is formed by threading the cores in the direct or inverse direction, according to whether the corresponding component of the state vector is one or zero. When a clock pulse is fed through the core, a direct or inverse current is produced, depending on the state of the corresponding elementary automaton. A positive emf  $+e$  is induced in the output coils if the direction of the current is compatible with the connection of the coil, and a negative emf  $-e$  otherwise. As a result, the maximal signal appears at the output corresponding to the given state of the automaton. If all the elementary automata operate without errors, the resolution  $\rho_0$  of the DC2 is [11]:

$$\rho_0 = \frac{n}{n-2d}, \quad (12a)$$

where  $n$  is the number of elementary automata (code length) and  $d$  the code distance.

If errors occur in  $s$  of the elementary automata, the above factor is obviously reduced to

$$\rho_s = \frac{n-2s}{n-2d+2s}. \quad (12b)$$

The code must be selected with an eye to a value of  $\rho_s$  high enough to ensure practical realization of threshold elements with the given resolution. Thus, for instance, employing codes with code distance  $d = \frac{n}{2}$ , obtained by means of orthogonal matrices (Hadamard matrices) [12], one can take  $\rho_0 = \infty$  and  $\rho_s = \frac{n-2s}{2s}$ .

The selected value of  $\rho_s$  depends on the magnitude of the noise present in the circuit actually used.

**Example 4.** Let us apply a DC2 to the redundant decimal counter of Example 2. By (12b),

$$\rho_1 = \frac{7-2 \cdot 1}{7-2 \cdot 3+2 \cdot 1} = \frac{5}{3}.$$

Suppose this value  $\rho_1 = \frac{5}{3}$  is satisfactory. Consequently, the threshold element at the output must have threshold  $\eta = 3e$ . Since each output of the DC2 corresponds to one internal state of the automaton, the excitation functions of the elementary automata and the output functions are again given by (11), where the  $y_i$  now denote the signals at the outputs of the threshold elements.

The resulting circuit is illustrated in Figure 10.

An automaton incorporating a DC2 corrects all single errors in the elementary automata and all errors equivalent to these (as in Example 3). It does not correct open circuits in the output coils and errors in the threshold elements.

The reliability of the automata synthesized in Examples 3 and 4 may be improved by using magnetic-core threshold elements as elementary automata. There is then no need for input OR-elements, which are replaced by the write winding.

Magnetic decoders seem especially promising with regard to the development and extensive production of ferromagnetic tapes and perforated ferrite wafers. As for the output circuit, this employs the same methods as in Example 1.

Another example will provide a further indication of the possible applications of these decoders.

Example 5. Consider the synthesis of a two-input serial adder using a two-input trigger and AND-, OR-, NOT-elements. Table 10 illustrates the form of the truth table for a nonredundant adder (see, e.g., /2/).

TABLE 10.

$X_1(t)$	$X_2(t)$	$Q(t)$	$Q(t+\tau)$	$Z(t)$	$q(t)$
0	0	0	0	0	0
0	1	0	0	1	0
1	0	0	0	1	0
1	1	0	1	0	1
0	0	1	0	1	0
0	1	1	1	0	1
1	0	1	1	0	1
1	1	1	1	1	1

By Table 10,

$$\left. \begin{aligned} q_1 &= X_1 X_2 + X_1 Q + X_2 Q; \\ q_0 = \bar{q}_1 &= \bar{X}_1 \bar{X}_2 + \bar{X}_1 \bar{Q} + \bar{X}_2 \bar{Q}; \\ Z &= X_1 \bar{X}_2 \bar{Q} + \bar{X}_1 X_2 \bar{Q} + \bar{X}_1 \bar{X}_2 Q + X_1 X_2 Q. \end{aligned} \right\} \quad (13)$$

The resulting circuit for a nonredundant serial adder is illustrated in Figure 11.

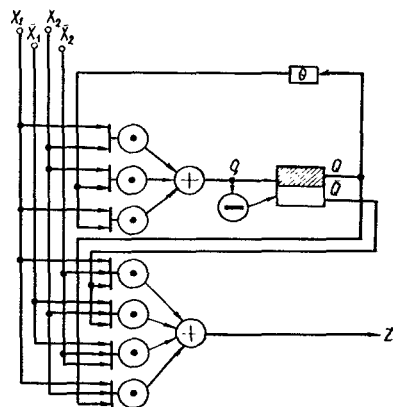


FIGURE 11. Serial adder (Example 5).



To permit correction of single errors in the elementary automata, the internal state of the adder must be encoded, as in Example 1, in (3, 1) code.

The transition function of the redundant automaton is then as described in Table 11.

To determine the actual state of the automaton, i.e., to correct a single error in an elementary automaton, either of the above-mentioned decoders may be used. The excitation functions of the elementary automata are

$$\begin{aligned} q_{10} = q_{20} = q_{30} &= \bar{X}_1 \bar{X}_2 + \bar{X}_1 \bar{Q} + \bar{X}_2 \bar{Q}; \\ q_{11} = q_{21} = q_{31} &= X_1 X_2 + X_1 Q + X_2 Q, \end{aligned}$$

where  $\bar{Q}$  and  $Q$  are the decoder-output signals corresponding to the states "zero" and "one", respectively, of the automaton.

It is clear that the excitation function is the same as that of the nonredundant automaton (13).

Depending on the reliability of the logic elements in comparison with that of the elementary automata, one either employs one transition circuit for all the elementary automata or provides each of them with its own independent circuit, as indicated above.

The redundant adder is illustrated in Figure 12. Its output circuit is the same as that of the nonredundant adder.

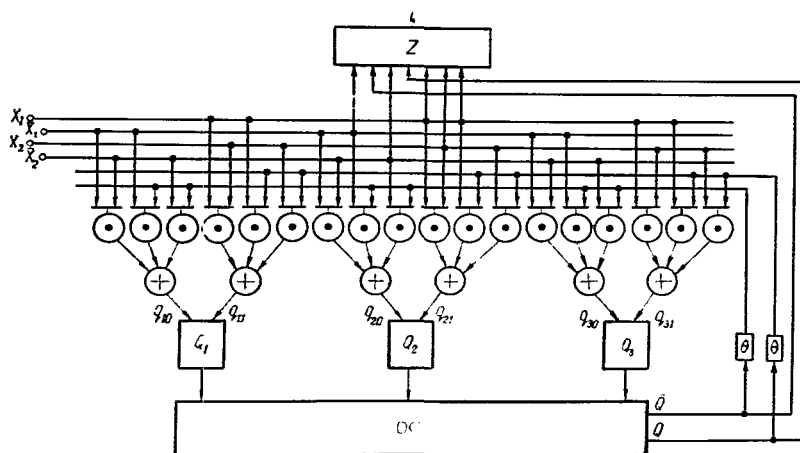


FIGURE 12. Redundant serial adder using a decoder (Example 5).

Z - output circuit; DC - decoder.

Decoders are also conveniently used to determine the information symbols of the input signal in cases where the input signal itself is already redundant.

Example 6. Consider the synthesis of a two-input serial adder, with the input signals encoded in (5, 2) code.

TABLE 11.

$t$		$t$			$t + \tau$			$t$			$t$
$x_1$	$x_2$	$Q_1$	$Q_2$	$Q_3$	$Q_1$	$Q_2$	$Q_3$	$q_1$	$q_2$	$q_3$	$Z$
0	0	0 1 0	0 0 1 0	0 0 0 1	0	0	0	0	0	0	0
0	1	0 1 0 0	0 0 1 0	0 0 0 1	0	0	0	0	0	0	1
1	0	0 1 0 0	0 0 1 0	0 0 0 1	0	0	0	0	0	0	1
1	1	0 1 0 0	0 0 1 0	0 0 0 1	1	1	1	1	1	1	0
0	0	1 0 1 1	1 1 0 1	1 1 1 0	0	0	0	0	0	0	1
0	1	1 0 1 1	1 1 0 1	1 1 1 0	1	1	1	1	1	1	0
1	0	1 0 1 1	1 1 0 1	1 1 1 0	1	1	1	1	1	1	0
1	1	1 0 1 1	1 1 0 1	1 1 1 0	1	1	1	1	1	1	1

After the information symbols of the input signal have been determined by the decoder  $DC_1$  (see Figure 13) and the information symbol of the internal state by decoder  $DC_2$ , the output function and the excitation functions are:

$$q_0 = \mu_0 \bar{Q} + \mu_2 \bar{Q} + \mu_1 \bar{Q} + \mu_0 Q;$$

$$q_1 = \mu_1 \bar{Q} + \mu_2 \bar{Q} + \mu_1 \bar{Q} + \mu_3 Q;$$

$$Z = \mu_2 \bar{Q} + \mu_1 \bar{Q} + \mu_0 \bar{Q} + \mu_3 Q,$$

where  $\mu_i$  is a signal at the output of  $DC_1$  corresponding to an input information symbol ( $i$  is the decimal representation of the input combination);  $\bar{Q}$ ,  $Q$  are the signals at the output of  $DC_2$ .

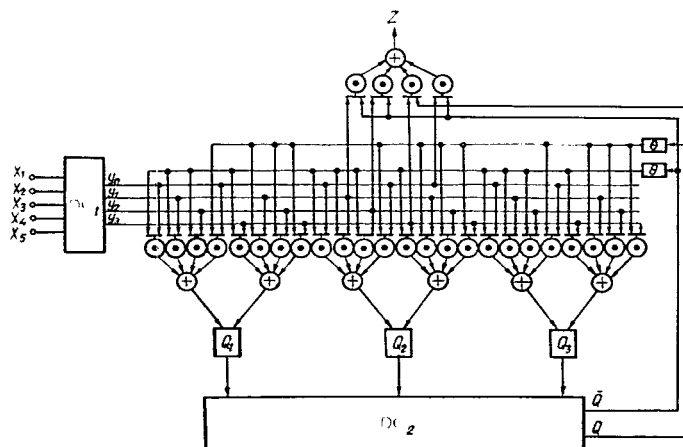


FIGURE 13. Redundant serial adder for the case of an input signal represented in correcting code (Example 6). (DC — decoder).

#### 4. MULTISTAGE ERROR-CORRECTING METHODS

In systems for which speed does not play a decisive role, cyclic codes are suitable for encoding the internal states of an automaton. Errors are then corrected during the time interval between two consecutive performance cycles of the automaton. Using  $n$  subcycles (where  $n$  is the length of the internal-state vector), the code vector is corrected by the correcting circuit, and by the beginning of the next performance cycle the automaton is already in the corrected state, if the error in question is a malfunction. The cyclic character of the code simplifies the correcting circuit. On the other hand, failures cannot be corrected by this method.

Example 7. Let us use a cyclic code to encode the internal states of the decimal counter considered in Example 2 to 4. To store the internal

states of the automaton we use a shift register, formed by connecting elementary automata in series.

The elementary automaton may be either a trigger with separate input OR-elements and a delay element whose function is to prevent simultaneous application of input and shift pulses to the trigger, or one cell of a two-stage magnetic-core shift register. Since there are four information symbols, we use the cyclic Hamming (7, 4) code generated by the polynomial  $x^3+x^2+1$ .

The parity-check matrix is

$$H = \begin{bmatrix} 1 & 0 & 1 & 1 & 1 & 0 & 0 \\ 1 & 1 & 1 & 0 & 0 & 1 & 0 \\ 0 & 1 & 1 & 1 & 0 & 0 & 1 \end{bmatrix} \quad (14)$$

This parity-check matrix may be constructed from adders mod 2 (Figure 14); a signal appears at the output of the matrix whenever a single error occurs in the automaton /13/. This signal proceeds to the shift-pulse generator (SPG) and produces 7 shifts in the shift register. When the combination 001 appears in the output buses of the matrix, the faulty symbol is corrected at the next stage by addition of one mod 2. As in Example 2, the output and transition circuits use only the values of the information symbols as input variables.

Note that this case is slightly different, for the matrix (14) differs from the matrix (9) in the position of the third and fourth columns. As a result, the positions of the variables  $Q_3$  and  $Q_4$  in equations (10) are interchanged. The time interval between two input pulses must be sufficient to allow for 7 shifts in the register, if necessary.

Here the delay elements in the feedback circuit of the automaton (Figure 4) have been replaced by AND-elements whose second input receives a timing pulse (TP) after the error has been corrected.

If one must allow for malfunctions in the register in the course of the parity-check shifts, one or more additional checks must be provided. To this end, one may either reduce the frequency of the input signals, i.e., the performance cycles of the automaton, or increase the frequency of the shift pulses.

To lessen the influence of malfunctions in the course of the parity-check shifts (especially if the shift register contains a large number of elementary automata), the parity-check matrix should be replaced by an error-detecting circuit which divides the state vector by the generating polynomial, together with a decoder at the output (Figure 15). The decoder may be either DC1 or DC2. The division circuit is conveniently constructed from elementary automata in the form of magnetic-core shift-register cells and adders mod 2.

Using a pulse distributor  $P$ , signals are fed into the division circuit successively from all the elementary automata.

If the sequence characterizing the internal state of the automaton is not divisible by the generating polynomial, i.e., an error has occurred, the faulty symbol in the sequence may be determined according to the remainder and then corrected.

To this end, the parity-check shifts are followed by a signal which feeds the contents of the division-circuit cells into the decoder. The output and transition circuits in Figure 15 are the same as in Example 7.

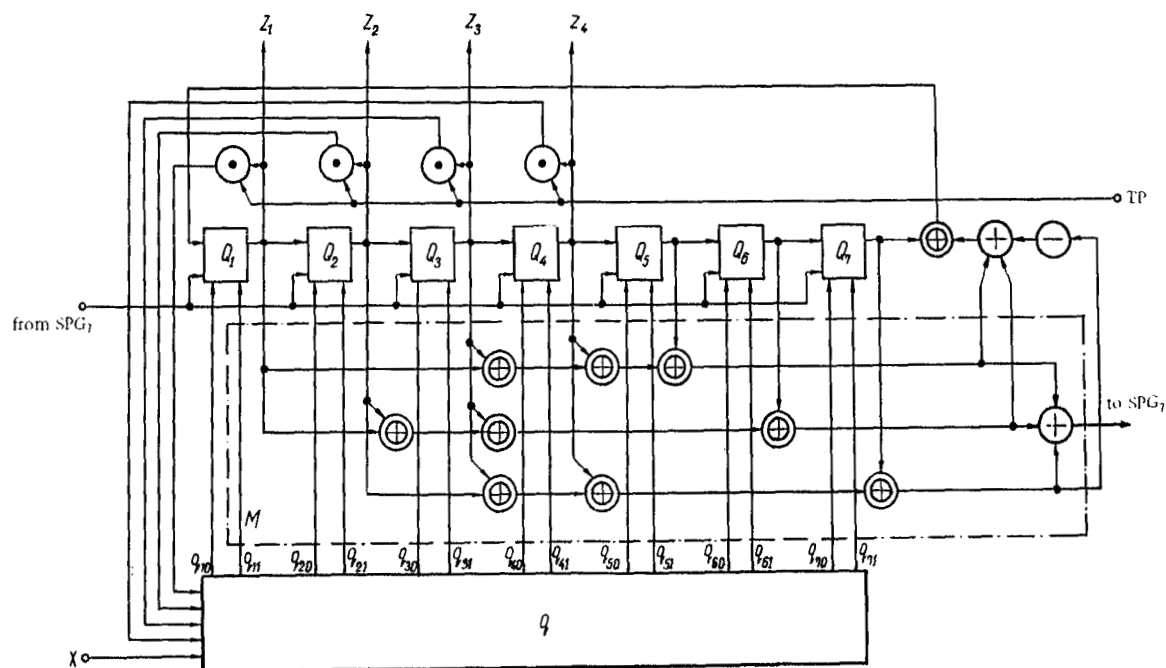


FIGURE 14. Redundant decimal counter with parity-check matrix for multistage single-error correction (Example 7):

$M$  - parity-check matrix;  $q$  - excitation-function circuit.

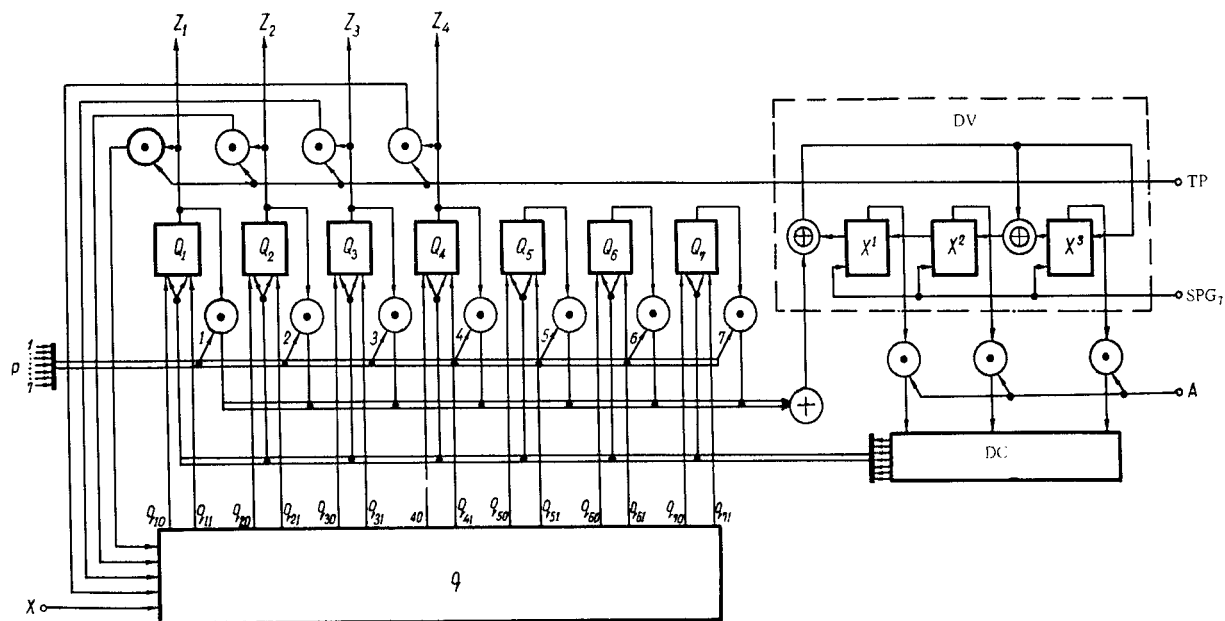


FIGURE 15. Redundant decimal counter with polynomial-division circuit and decoder for multi-stage correction of errors:

$DV$  - division circuit;  $DC$  - decoder;  $X_0$  - excitation-function circuit.

In this automaton, as before, the input signal may be changed only after the error in the current internal state has been corrected. The remainder proceeds from the division circuit to the decoder after appearance of a signal A.

The need for a decoder at the output of the division circuit may be avoided by using a shift register with a unit in one cell as distributor.

The shift register of such a distributor contains as many cells as there are elementary automata. After the internal-state vector has been divided by the generating polynomial and the remainder obtained, shifts occur in the distributor and the division circuit until the signal 001 appears at the output of the latter. The position of the unit in the shift register of the distributor indicates the elementary automaton in which the error has occurred.

## CONCLUSION

It is clear from the examples considered above that in each specific case the method employed for encoding and decoding the internal states of the automaton depends on the relative reliabilities of the memory elements and the logic elements. When the reliability of the output circuit is inadequate, the reliability of its elements must be increased by some method, and the circuit itself constructed from gate elements.

## Bibliography

1. Gavrilov, M. A. Strukturnaya izbytochnost' i nadezhnost' raboty releinykh ustroystv (Structural Redundancy and Reliability of Relay Devices). Trudy 1-go Mezhdunarodnogo kongressa MFAU, Volume 3. Moskva, Izdatel'stvo AN SSSR. 1961.
2. Vavilov, E. N. and G. P. Portnoi. Sintez skhem elektronnykh tsifrovyykh mashin (Synthesis of Electronic Computer Circuits). Moskva, "Sovetskoe Radio." 1963.
3. Kosarev, Yu. A. Rezervirovanie logicheskikh i pereklyuchatel'nykh skhem (Redundancy of Logic and Switching Circuits). In sbornik: Avtomatika, telemekhanika i priborostroenie, p. 256. Moskva-Leningrad, "Nauka." 1965.
4. Glushkov, V. M. Sintez tsifrovyykh avtomatov (Synthesis of Digital Automata). Moskva, Fizmatgiz. 1962.
5. Hamming, R. W. Error-detecting and Error-correcting Codes. —Bell System Technical Journal, 29:147-160. 1950.
6. Varshamov, R. R. Otsenka chisla signalov v kodakh s korrektsiei oshibok (Estimate of the Number of Signals in Error-correcting Codes). —DAN SSSR, 117(5): 739-741. 1957.
7. Hurley, R. B. Transistor Logic Circuits. New York-London. 1961.
8. Peterson, W. W. Error-correcting Codes. Cambridge, Mass., M. I. T. Press. 1961.

9. Frantsis, T. A. O primeneniі korrektruyushchikh kodov dlya povysheniya nadezhnosti kombinatsionnykh logicheskikh skhem (Application of Error-correcting Codes in Increasing the Reliability of Combinational Logic Circuits). In sbornik: Teoriya diskretnykh avtomatov. Riga, "Zinatne." 1967.
10. Kraizmer, L. P. Bystrodeistvuyushchie ferromagnitnye zapominayushchie ustroystva (High-speed Ferromagnetic Storage Devices). Moskva-Leningrad, "Energiya." 1964.
11. Takahasi, H. and E. Goto. Application of Error-correcting Codes to Multiway Switching. UNESCO, International Conference on Information Processing. Paris, 1959.
12. Constantine, C. T. A Load-sharing Matrix Switch. —IBM Journal of Research and Development, 2: 204-211. 1958.
13. Radchenko, A. N. Primery povysheniya nadezhnosti diskretnykh skhem metodom vnutriskhemnogo kodirovaniya sostoyanii (Examples of Increasing the Reliability of Discrete Circuits by the Method of Intra-circuit Coding of States). Leningrad, 1964.



T. A. Frantsis

# ERROR CORRECTING IN ASYNCHRONOUS AUTOMATA

This article discusses the application of self-correcting codes for synthesizing asynchronous logical automata by the method of inertial subcircuits, with correcting errors.

In [1, 2] we considered the application of self-correcting codes to improve the reliability of single-stage and multistage synchronous automata. In the present paper self-correcting codes are used for correction of single errors in asynchronous logical automata synthesized by the method of inertial subcircuits [3, 4] on the basis of truth tables or state diagrams. The memory elements of these automata are inertial subcircuits (IS) (Figure 1, a) which both store and process information. From this standpoint, an IS plays the role of a single transition circuit [2] in a synchronous automaton, consisting of an elementary automaton and its excitation-function circuit.

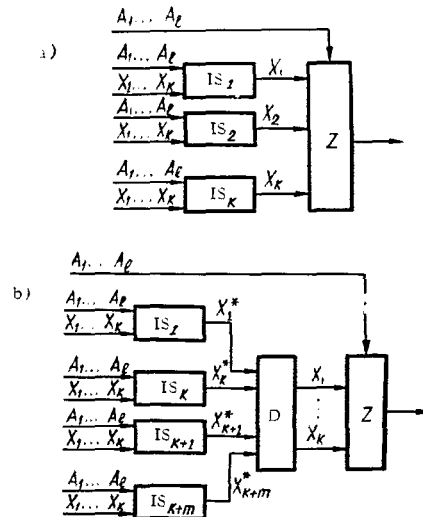


FIGURE 1. Block-diagram of an asynchronous automaton:

a — nonredundant; b — redundant (IS — inertial subcircuit; D — decoder circuit; Z — output circuit;  $X_i$  (in the redundant automaton) — corrected value of the IS output signal  $X_i^*$ ).

Apart from the inertial subcircuits, the automaton contains an output circuit whose inputs receive the input signals of the automaton and the output signals of the IS.

In the sequel we shall consider the correction of errors in any IS. By an error in some logical circuit or individual AND-, OR-, NOT-element we mean the appearance of the wrong signal, zero or one, at the corresponding output.

To prevent an error in a single logic element from affecting more than one IS, the different IS must be mutually independent. By introducing vector addition and multiplication by an element of the field  $GF(2)$ , the set of output signals of an IS may be regarded as a vector over this field.

We shall call the output signals of the nonredundant IS information symbols, and those of the redundant IS — parity-check symbols. The required number of IS is determined by methods of the theory of self-correcting codes in the same way as the number of elementary automata in synchronous automata /2/.

The output vector of the IS of the redundant automaton proceeds to the decoder circuit (D) (Figure 1, b), which is also used in single-cycle automata /1/. The decoder circuit produces the corrected values of the IS-information signals, which in turn proceed to the inputs of the output circuit Z and the corresponding IS.

Just as in single-cycle circuits, it is obvious that the decoder D must have a higher degree of reliability than the rest of the automaton, since otherwise the introduction of redundancy by this method becomes meaningless.

To determine the structure of the parity-check IS, it is convenient to use the coding table of the synthesized automaton /3/; this table is constructed from the truth table and indicates what conjunctions are involved in each IS. The coding table of a nonredundant automaton has as many columns as there are parity-check IS. The values of the parity-check-IS signals are found by summing the corresponding values of the IS-information signals in one row, according to the specific parity-check matrix selected /1, 2, 3/.

As examples, we consider correction of a single error in time-independent and time-dependent automata.

Example 1. Synthesis of the automaton whose state diagram is illustrated in Figure 2, with correction of errors in any single IS. Undesirable competition is prevented by filters.

Table 1 is the truth table based on Figure 2.

TABLE 1.

$A_1$	$A_2$	$Z$	$X_1$	$X_2$
0	0	0	1	1
0	1	$X_2(1), \bar{X}_2(0)$	0	$X_2$
1	0	$X_1(1), \bar{X}_1(0)$	$X_1$	0
1	1	0	0	0

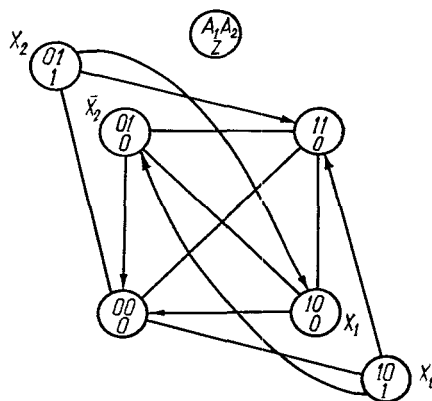


FIGURE 2. State diagram for Example 1.

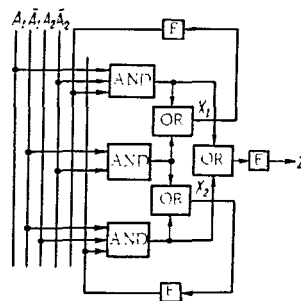


FIGURE 3. Circuit of nonredundant automaton (Example 1).

The truth table yields the following system of equations:

$$\left. \begin{aligned} X_1 &= \bar{A}_1 \bar{A}_2 + A_1 \bar{A}_2 X_1; \\ X_2 &= \bar{A}_1 \bar{A}_2 + \bar{A}_1 A_2 X_2; \\ Z &= A_1 \bar{A}_2 X_1 + \bar{A}_1 A_2 X_2. \end{aligned} \right\} \quad (1)$$

The corresponding automaton is illustrated in Figure 3.

The coding table of the nonredundant automaton is given in Table 2.

Since there are two IS, we see, following [5], that three parity-check IS are needed for single-error correction, i.e., a (5, 2) code is used. Using the parity-check matrix

$$H = \begin{bmatrix} 10100 \\ 11010 \\ 01001 \end{bmatrix},$$

we find the output functions of the parity-check IS:

$$\left. \begin{aligned} X_3 &= X_1; \\ X_4 &= X_1 \oplus X_2; \\ X_5 &= X_2. \end{aligned} \right\} \quad (2)$$

TABLE 2.

	$X_1$	$X_2$
$\bar{A}_1 \bar{A}_2$	1	1
$\bar{A}_1 A_2 X_2$	0	1
$A_1 \bar{A}_2 X_1$	1	0

We add two columns to the coding table (Table 2) in accordance with (2), to obtain the coding table of the redundant automaton (Table 3).

TABLE 3.

	$X_1^*$	$X_2^*$	$X_3^*$	$X_4^*$	$X_5^*$
$\bar{A}_1 \bar{A}_2$	1	1	1	0	1
$\bar{A}_1 A_2 X_2$	0	1	0	1	1
$A_1 \bar{A}_2 X_1$	1	0	1	1	0

According to Table 3, the equations for the IS of the redundant automaton (taking into account that all subcircuits must be independent) are:

$$\left. \begin{aligned} X_1^* &= \bar{A}_1 \bar{A}_2 + \bar{A}_2 X_1; \\ X_2^* &= \bar{A}_1 \bar{A}_2 + \bar{A}_1 X_2; \\ X_3^* &= \bar{A}_1 \bar{A}_2 + \bar{A}_2 X_1; \\ X_4^* &= \bar{A}_1 A_2 X_2 + A_1 \bar{A}_2 X_1; \\ X_5^* &= \bar{A}_1 \bar{A}_2 + \bar{A}_1 X_2; \\ Z &= A_1 \bar{A}_2 X_1 + \bar{A}_1 A_2 X_2. \end{aligned} \right\} \quad (3)$$

To compute the syndrome (see /1/), the decoder circuit must be based on the equations

$$\left. \begin{aligned} s_1 &= X_1^* \oplus X_3^*; \\ s_2 &= X_1^* \oplus X_2^* \oplus X_4^*; \\ s_3 &= X_2^* \oplus X_5^*. \end{aligned} \right\} \quad (4)$$

It is clear from equations (4) that the value of the syndrome corresponding to an error in  $IS_1$  (wrong value of  $X_1$ ) is (110), while for  $IS_2$  it is (011). Consequently, for the error vector we can write

$$\left. \begin{aligned} e_1 &= s_1 s_2; \\ e_2 &= s_2 s_3. \end{aligned} \right\} \quad (5)$$

The circuit of a redundant automaton based on (3-5) is illustrated in Figure 4.

**Example 2.** Synthesis of a time-dependent automaton, with error correction in any one inertial subcircuit. Undesirable competition is eliminated by filters. The automaton operates in the following way. When the input of the automaton receives a signal in the form of a single pulse of duration  $\tau$ , the output of the automaton must emit two pulses of the same duration  $\tau$ ; when the input receives two pulses of equal duration  $\tau$ , the output must emit a single pulse. To simplify matters, we shall assume that the pulse duty factor is  $1/2$ . Thus, the automaton must return to its original state after a time  $4\tau$ .

According to /3, 4/, synthesis of a time-dependent automaton requires either delay elements with delay  $\tau$ , or the introduction of an additional input which receives a signal from a rectangular-pulse generator.

In this example we shall apply the second method, assuming that the appearance of the input signal coincides with the appearance of the supplementary rectangular pulse. The time diagrams of the input and output signals are illustrated in Figure 5.

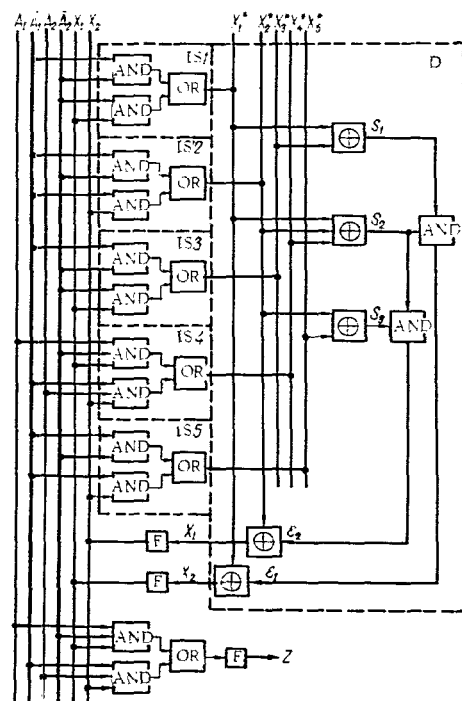


FIGURE 4. Circuit of redundant automaton (Example 1).

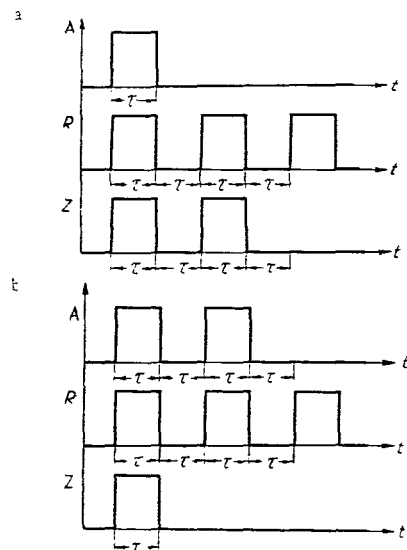


FIGURE 5. Time diagrams for the automaton of Example 2:  
a — one pulse at the input; b — two pulses at the input  
(A — input signal; K — supplementary rectangular pulses; Z — output signal).

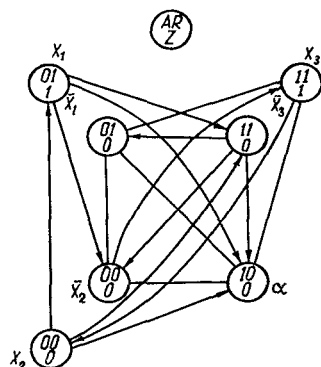


FIGURE 6. State diagram for time-dependent automaton (Example 2).

The state diagram of the synthesized automaton is illustrated in Figure 6. The initial state is  $\bar{X}_2$ . The diagram allows for a possible time lag between the appearance of the initial basic and supplementary input signals — it provides for transitions from the single-valued state  $\alpha$  and the two-valued state  $X_1$  to the state  $X_3$ , which characterizes the appearance of the first output pulse. Moreover, if a noise-signal appears at one of the inputs in the initial state of the automaton, the latter returns to this state after the noise has disappeared — there are transitions from  $\bar{X}_1$  and  $\alpha$  to  $\bar{X}_2$ .

The diagram of Figure 6 corresponds to the following truth table (Table 4).

Table 4 corresponds to the equations

$$\left. \begin{aligned} X_1 &= \bar{A} \bar{R} X_2 + \bar{A} R X_1; \\ X_2 &= \bar{A} \bar{R} X_2 + A R X_3; \\ X_3 &= \bar{A} \bar{R} \bar{X}_2 + \bar{A} R \bar{X}_1 + A R X_3 + A \bar{R}; \\ Z &= A R X_3 + \bar{A} R X_1. \end{aligned} \right\} \quad (6)$$

The nonredundant automaton based on equations (6) is illustrated in Figure 7. It contains three information IS, and therefore, according to /5/, we need three parity-check IS, constructed on the basis of the following parity-check matrix:

$$H = \begin{bmatrix} 1 & 1 & 0 & 1 & 0 & 0 \\ 1 & 0 & 1 & 0 & 1 & 0 \\ 0 & 1 & 1 & 0 & 0 & 1 \end{bmatrix}$$

According to the matrix  $H$ , the parity-check IS must compute the functions

$$\left. \begin{aligned} X_4 &= X_1 \oplus X_2; \\ X_5 &= X_1 \oplus X_3; \\ X_6 &= X_2 \oplus X_3. \end{aligned} \right\} \quad (7)$$

In view of (6) and (7), the coding table of the redundant automaton is that given in Table 5.

It is clear from Table 5 that the parity-check IS of the redundant automaton realize the following functions (after simplification):

$$\left. \begin{aligned} X_4^* &= \bar{A} R X_1 + A R X_3; \\ X_5^* &= \bar{A} + \bar{R} + X_3; \\ X_6^* &= \bar{A} \bar{X}_1 + \bar{R}. \end{aligned} \right\} \quad (8)$$

By /1/, the syndrome circuit must compute the following functions:

$$\left. \begin{aligned} s_1 &= X_1^* \oplus X_2^* \oplus X_4^*; \\ s_2 &= X_1^* \oplus X_3^* \oplus X_5^*; \\ s_3 &= X_2^* \oplus X_3^* \oplus X_6^*. \end{aligned} \right\} \quad (9)$$

TABLE 4.

A	P	Z	X <sub>1</sub>	X <sub>2</sub>	X <sub>3</sub>
0	0	X <sub>2</sub> (0), $\bar{X}_2$ (0)	X <sub>2</sub>	X <sub>2</sub>	$\bar{X}_2$
0	1	X <sub>1</sub> (1), $\bar{X}_1$ (0)	X <sub>1</sub>	0	$\bar{X}_1$
1	0	0	0	0	1
1	1	X <sub>1</sub> (1), $\bar{X}_3$ (0)	0	X <sub>3</sub>	X <sub>3</sub>

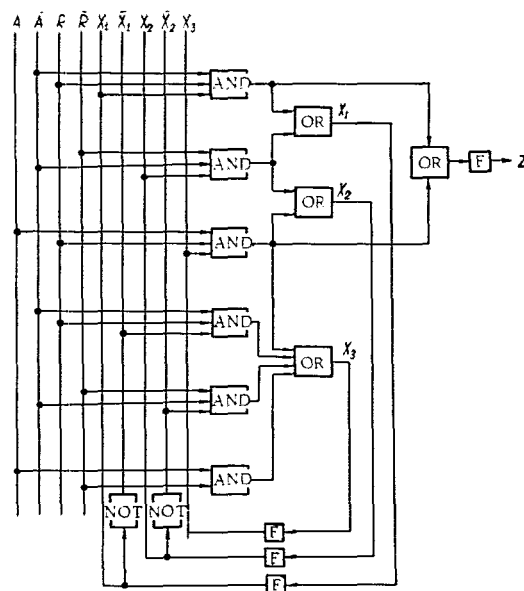


FIGURE 7. Circuit of nonredundant time-dependent automaton (Example 2).

TABLE 5.

	X <sub>1</sub> *	X <sub>2</sub> *	X <sub>3</sub> *	X <sub>4</sub> *	X <sub>5</sub> *	X <sub>6</sub> *
$\bar{A} \bar{R} \bar{X}_2$	0	0	1	0	1	1
$\bar{A} \bar{R} X_2$	1	1	0	0	1	1
$\bar{A} R \bar{X}_1$	0	0	1	0	1	1
$\bar{A} R X_1$	1	0	0	1	1	0
$A \bar{R}$	0	0	1	0	1	1
$A R X_3$	0	1	1	1	1	0

Following [1], the error vector derived from (9) is given by the equations

$$\left. \begin{aligned} e_1 &= s_1 s_2; \\ e_2 &= s_1 s_3; \\ e_3 &= s_2 s_3. \end{aligned} \right\} \quad (10)$$

The circuit of the redundant automaton based on equations (6, 8, 9, 10) is illustrated in Figure 8.

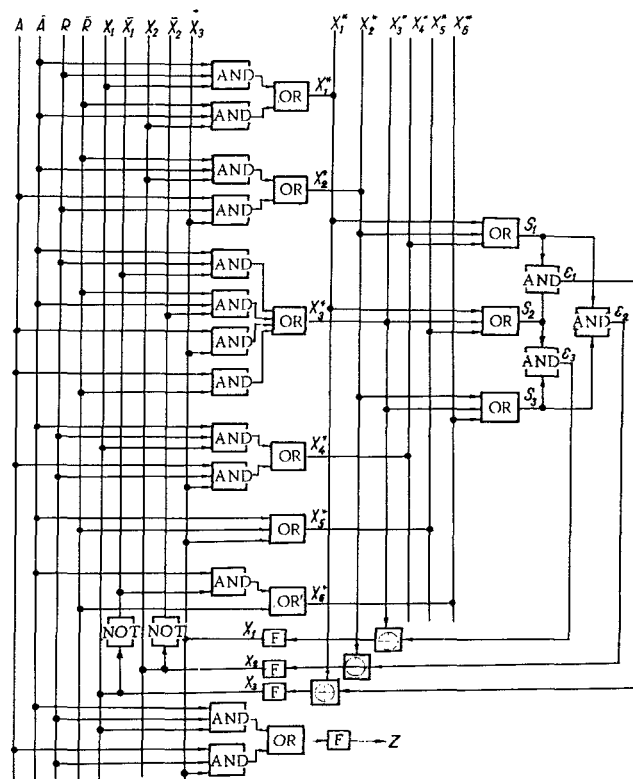


FIGURE 8. Circuit of redundant time-dependent automaton (Example 2).

## CONCLUSION

In synthesizing asynchronous automata, using self-correcting codes to increase reliability, the question arises (just as in the case of single-stage circuits /1/) as to decomposition of the automaton into independent subcircuits larger than inertial subcircuits. The question of optimal decomposition requires further investigation, employing computers. To increase the reliability of the output circuit of an asynchronous automaton one must apply the methods described in /2/ for synchronous automata.

Increase in the reliability of the redundant automaton as a whole, when the latter is synthesized by the above method, depends on the complexity of the nonredundant automaton (i. e., on the number of inertial subcircuits) and the complexity of the individual logic elements. As in the case of single-stage circuits, the more complicated the nonredundant automaton and the more reliable the individual logic element, the greater the increase in the reliability of the redundant automaton in comparison with the nonredundant automaton.



## Bibliography

1. Frantsis, T. A. O primeneniі korrektruyushchikh kodov dlya povysheniya nadezhnosti kombinatsionnykh logicheskikh skhem (Application of Error-correcting Codes in Increasing the Reliability of Combinational Logic Circuits). In sbornik: Teoriya diskretnykh avtomatov. Riga, "Zinatne." 1967.
2. Frantsis, T. A. and G. F. Yanbykh. Avtomaticheskoe ispravlenie oshibok v diskretnykh avtomatakh (Automatic Error Correcting in Discrete Automata). Present collection, p. 36.
3. Yakubaitis, E. A. Asinkhronnye logicheskie avtomaty (Asynchronous Logical Automata). Riga, "Zinatne." 1966.
4. Yakubaitis, E. A. Vremennye asinkhronnye logicheskie avtomaty (Time-dependent Asynchronous Logical Automata). Present collection, p. 1.
5. Peterson, W. W. Error-correcting Codes. Cambridge, Mass., M. I. T. Press. 1961.

*G. F. Fritsnovich*

# *EXTENDING THE FIELD OF APPLICATION OF THE METHOD OF INERTIAL SUBCIRCUITS*

A formal method is given for transforming an arbitrary sequential machine  $P$  with  $n$  inputs and  $m$  outputs into an asynchronous sequential machine  $P^*$  with  $n+1$  inputs and  $m$  outputs whose operation is defined by changes in the input state. The new machine  $P^*$  is information-input equivalent to the original machine  $P$ . This transformation makes the method of inertial subcircuits applicable to the class of all sequential machines.

The basic principles of the method of inertial subcircuits were first described in /1/. Further developments were given in /2-6/.

The basic principle of the method of inertial subcircuits is the construction of the logical structure, satisfying given operating conditions, on the basis of stable states, utilizing the natural internal delays of the logic elements and feedback loops. The role of timing signal may be played by any change of input state, provided the time  $T$  between two consecutive changes is greater than  $\tau_{tp}$ , where  $\tau_{tp}$  is the duration of the transition process initiated by the first state change.

These features of the method naturally impose certain restrictions on its applicability. The method is directly applicable only to the class of sequential asynchronous logic circuits (SALC) /4/, which are asynchronous sequential machines whose timing is determined by changes in the input state /4/ (time-independent logical automata, in the terminology of /2/).

In this paper we shall consider the possibility of extending the method to the class of all sequential machines.\*

The basic notions, introduced in /4/ for SALC, may be extended to the class of all sequential machines. These notions are: input state  $\rho_i$  ( $i=1, 2, \dots, 2^n$ , where  $n$  is the number of input variables), output state  $\lambda_j$  ( $j=1, 2, \dots, 2^m$ , where  $m$  is the number of output variables), internal state  $\kappa_r$  ( $r=1, 2, \dots, 2^k$ , where  $k$  is the number of intermediate variables), and (full) state  $\mu_s$  ( $s=1, 2, \dots, 2^{n+k}$ ). We shall also assume that any sequential machine  $P$  has finite sets of input states  $R=\{\rho_1, \rho_2, \dots, \rho_{2^n}\}$ , output states  $L=\{\lambda_1, \lambda_2, \dots, \lambda_{2^m}\}$ , and (full) states  $M=\{\mu_1, \mu_2, \dots, \mu_{2^{n+k}}\}$ . As in /4/, the set  $M$  is divided into two subsets  $M^s$  and  $M^u$ , where  $M^s$  consists of all stable states and  $M^u$  of all unstable states. It is also convenient to introduce the set  $M^i \subseteq M$  of all utilized states, i. e., all states of the synthesized device for which there exist input states and transitions.

To define the mode of operation of a sequential machine, we shall use the state graph  $G$ .

\* For a definition of sequential machine, see /8/.

By the state graph of a sequential machine we mean a finite directed graph  $G$  whose vertices are interpreted as the states of the machine. A vertex  $g$  of the graph  $G$  is connected to a vertex  $j$  by an edge if and only if there exists a transition from the state  $\mu_i$  (corresponding to the vertex  $g$ ) to the state  $\mu_j$  (corresponding to the vertex  $j$ ).

With each vertex of the graph  $G$  we associate a pair of symbols  $(\rho_i, \lambda_j)$ , where  $\rho_i \in R$  and  $\lambda_j \in L$ . We stipulate that any vertex which corresponds to a stable state of the synthesized machine has a transition from itself to itself (elementary loop), which means that the machine remains in this state until the next change of input state. By the definition of stable states  $/4/$ , a vertex of  $G$  with the designation  $(\rho_i, \lambda_j)$  does not possess a loop if and only if it has a transition to a vertex, the first symbol of whose designation is also  $\rho_i$ . The number of vertices of the graph  $G$  is  $l \leq 2^n$ , coinciding with the cardinality of the set  $M^i$ . In the special case  $M^i \subseteq M$ , the output states and transitions are specified only for the stable states and the state graph  $G$  coincides with the graph of stable states.

In the general case, the requirement that the sequential machine be deterministic and its operation completely defined imposes the following conditions on the graph  $G$ . The  $l$  vertices of the graph (the set of utilized states  $M^i$ ) may be divided into  $2^n$  subsets  $M^i(\rho_1), M^i(\rho_2), \dots, M^i(\rho_i), \dots, M^i(\rho_{2^n})$  each consisting of all vertices whose designation contains the same  $\rho_i$ . Each vertex of the subset  $M^i(\rho_i)$  is the initial point of exactly  $2^n - 1$  edges connecting it to one vertex in each of the remaining  $2^n - 1$  subsets, and one edge which is either a loop or connects the vertex to a vertex of the same subset  $M^i(\rho_i)$ .

If a graph  $G_P$  possesses the above properties, and each of its vertices is assigned a pair of symbols  $(\rho_i, \lambda_j)$ , where  $\rho_i \in R$  and  $\lambda_j \in L$ , we shall say that the graph defines the operation of some sequential machine  $P$ .

Conversely, any graph may be defined by its adjacency matrix  $M_P$ . Suppose that every row (column) of the matrix  $M_P$  is associated with the pair  $(\rho_i, \lambda_j)$  which designates the corresponding vertex of the graph, and that the rows (columns) are arranged in increasing order of the binary representations of the first symbol in the pair  $(\rho_i, \lambda_j)$ .

The matrix  $M_P$  of the state graph  $G$  of a sequential machine possesses the following properties:

- 1) It is of finite dimension  $l \times l$ .
- 2) The matrix may be partitioned by  $2^n - 1$  horizontal lines and  $2^n - 1$  vertical lines in such a way that each of the resulting horizontal (vertical) groups of rows (columns) consists of rows (columns) whose designation involves the same first symbol  $\rho_i$ , and no others; moreover, each row of the submatrices formed by the partition contains exactly one nonzero element.

$$3) \quad \sum_{j=1}^l m_{kj} = 2^n,$$

where  $g=1, 2, \dots, l$  and  $m_{kj}$  is the element of the matrix  $M_P$  at the intersection of the  $g$ -th row and the  $j$ -th column (this follows from property 2).

We shall call these properties the conditions for realizability of a matrix  $M_P$  in the class of sequential machines. By a realization we mean

the construction of a sequential machine whose operation satisfies the conditions implied by the form of the matrix  $M_P$ .

In the special case  $M^i \subseteq M^s$  the state graph  $G$  coincides with the graph of stable states of the sequential machine, and the matrix  $M_P$  has the following properties:

- 1) it is of finite dimension  $l \times l$
- 2)  $m_{gg} = 1$  for  $g = 1, 2, \dots, l$  and  $m_{gg}$  is an element on the principal diagonal of the matrix).
- 3) The submatrices formed by the partition described above have the following properties:
  - a) each row of each submatrix contains exactly one nonzero element;
  - b) the submatrices on the principal diagonal are unit matrices.
- 4)

$$\sum_{j=1}^l m_{kj} = 2^n, \text{ where } g = 1, 2, \dots, l.$$

We shall call these properties the conditions for realizability of the matrix  $M_P$  in the class of sequential asynchronous logical circuits (SALC).

If a given matrix  $M_P$  is not realizable in the class of SALC, but is realizable in the class of all sequential machines, the method of inertial subcircuits is not directly applicable since transitions and output states are specified for unstable as well as stable states. With regard to the state graph, this means that besides edges connecting vertices of subsets  $M^i(\rho_i)$  and  $M^i(\rho_j)$  for  $i \neq j$  (which is the only possibility in SALC), there are edges connecting vertices belonging to the same subset  $M^i(\rho_i)$ . In the latter case we shall speak of a change of state (also output state) of the sequential machine for fixed input state  $\rho_i$ . The presence of such changes means that the timing of the operation of the machine must be "more rapid" than the timing defined by the input-state changes alone. The difficulties involved in defining this "more rapid" timing preclude direct application of the method of inertial subcircuits, which uses the input-state changes as timing signals.

One way of overcoming these difficulties was proposed in [7] — to introduce an auxiliary input signal and utilize the changes in its values as timing signals; thus transitions of the machine from one state to another are possible even when the values of the basic input variables do not change.

We shall indicate a method, convenient for machine synthesis, of introducing an auxiliary input signal when the sequential machine to be synthesized is given by the adjacency matrix of its state graph.

The basic idea is to transform a given sequential machine  $P$  with  $n$  inputs (input variables  $A_1, A_2, \dots, A_n$ ) and  $m$  outputs into a certain sequential machine  $P^*$  with  $n+1$  inputs (input variables  $A_1, A_2, \dots, A_n, A_t$ ) and  $m$  outputs, whose timing is determined by changes of input states. This is done in such a way that the machine  $P^*$  realizes the same information-processing operator (with regard to the basic inputs) as the machine  $P$ .

We shall call the auxiliary input  $A_t$  of the machine  $P^*$  its timing input, and the remaining  $n$  inputs its information inputs.

Starting from a sequential machine  $P$  with  $n$  inputs, set of input states  $R = \{\rho_1, \rho_2, \dots, \rho_{2^n}\}$ , and set of output states  $L = \{\lambda_1, \lambda_2, \dots, \lambda_{2^n}\}$ , we transform it into a sequential machine  $P^*$  with  $n+1$  inputs, set of input states  $F = \{\varphi_1, \varphi_2, \dots, \varphi_{2^{n+1}}\}$ , and set of output states  $L = \{\lambda_1, \lambda_2, \dots, \lambda_{2^n}\}$ , this transformation will be called the introduction of a timing input.

We shall say that the sequential machine  $P^*$  is information-input equivalent to the machine  $P$ , if and only if 1)  $P^*$  is obtained from  $P$  by introduction of a timing input; 2) given any state  $\mu_s$  of  $P$ , there exist two stable states  $\mu_{P^*}$ ,  $\mu_{P^*}$  of  $P^*$  such that, if  $\mu_s$  and either of  $\mu_{P^*}$ ,  $\mu_{P^*}$  are taken as initial states (for  $P$  and  $P^*$ , respectively), and the same sequence of input-state changes applied to an information input\* of  $P^*$  and an input of  $P$ , then both machines  $P$  and  $P^*$  produce the same output sequence, whichever of the states  $\mu_{P^*}$ ,  $\mu_{P^*}$  is chosen as the initial state of  $P^*$ . The solution of our problem is embodied in the following theorem.

**Theorem.** Any sequential machine  $P$  may be transformed by introduction of a timing input into a sequential machine  $P^*$ , information-input equivalent to  $P$ , whose timing is defined by changes of input state.

**Proof.** Let  $P$  be an arbitrary sequential machine with  $n$  inputs, and let  $M_P$  be the adjacency matrix of its state graph  $G_P$ , of dimension  $l \times l$ .

Partition the matrix into submatrices by  $2^n - 1$  horizontal lines and  $2^n - 1$  vertical lines, as described above. Replace every submatrix on the principal diagonal by a unit matrix of the same dimension. The result is a matrix  $M_{P'}$  of the same dimension as  $M_P$ . Form the matrix

$$M_{P^*} = \begin{pmatrix} M_{P'} & M_P \\ M_P & M_{P'} \end{pmatrix}.$$

There is a well-defined correspondence between the rows (columns) of the matrices  $M_P$  and  $M_{P^*}$ , under which each row (column) of  $M_P$  corresponds to exactly two rows (columns) of  $M_{P^*}$ . Thus, the  $g$ -th row (column) of  $M_P$  corresponds to the  $g$ -th and  $l+g$ -th rows (columns) of  $M_{P^*}$  ( $g=1, 2, \dots, l$ ).

Let us assign each row (column) of  $M_{P^*}$  a designation in the form of a pair of symbols  $(\varphi_i, \lambda_j)$  where  $\varphi_i \in F$  and  $\lambda_j \in L$ , in the following way. If the  $g$ -th row (column) of  $M_{P^*}$  has the designation  $(\rho_i, \lambda_j)$ , we designate the  $g$ -th row (column) of  $M_{P^*}$  by the pair  $(\varphi_i, \lambda_j)$  and its  $l+g$ -th row (column) by the pair  $(\varphi_{2^n+i}, \lambda_j)$ , where  $\varphi_i$  and  $\varphi_{2^n+i}$  differ only in the value of the  $(n+1)$ -th input variable. In states  $\varphi_1, \varphi_2, \dots, \varphi_{2^n}$  the  $(n+1)$ -th input variable has value zero, while in  $\varphi_{2^n+1}, \varphi_{2^n+2}, \dots, \varphi_{2^{n+1}}$  its value is one. The values of the other  $n$  input variables in the sets  $\varphi_i$  and  $\varphi_{2^n+i}$  coincide with those of the corresponding input variables in the set  $\rho_i$ .

Once the designations of the rows (columns) of  $M_{P^*}$  have been defined, this matrix defines a certain sequential machine  $P^*$  with  $n+1$  inputs ( $n$  information inputs and one time input) and  $m$  outputs.

Regarding the above transformation of  $P$  into  $P^*$  as the introduction of a time input, the resulting machine  $P^*$  is an asynchronous sequential machine whose timing is defined by changes of input state, since, as follows from its construction, the matrix  $M_{P^*}$  is realizable in the class of SALC.

\* Here we mean a generalized information input, whose state is defined as an ordered set of values of binary variables.

In view of the fact that the sets of all output states of the machines  $P$  and  $P^*$  coincide, the block symmetry of the matrix  $M_P^*$ , and the fact that each of the two rows (columns) of  $M_P^*$  corresponding to a given row (column) of  $M_P$  has a designation with the same second symbol which coincides with the second symbol in the designation of the  $M_P$  row (column), it is not difficult to see that the sequential machine  $P^*$  is information-input equivalent to  $P$ .

The following corollary is of practical importance.

**Corollary.** Any sequential machine may be synthesized by the method of inertial subcircuits.

The procedure is as follows:

- 1) Check the given data for realizability in the class of sequential machines.
- 2) Specify the operating conditions of the required sequential machine in the form of the adjacency matrix of its state graph.
- 3) Check the matrix for realizability in the class of SALC.
- 4) If the machine is realizable in the class of SALC, apply the method of inertial subcircuits.
- 5) If the conditions for realizability in the class of SALC are not satisfied, transform the machine by introduction of a timing input, and synthesize the new machine by the method of inertial subcircuits.

In conclusion, we remark that the above problem may be regarded as a special case of the general problem of timing-conversion of sequential machines /8/. We have studied the conversion of a sequential machine  $P$ , with  $n$  inputs and  $m$  outputs, whose timing is defined by changes of both input state and internal state, into a sequential machine  $P^*$  with  $n+1$  inputs and  $m$  outputs, whose timing is defined by changes of input state, by introduction of a timing input.

This transformation makes it possible to extend any other method of constructing sequential machines, based on stable states, to the class of all sequential machines.

## Bibliography

1. Yakubaitis, E. A. Sintez posledovatel'nostnykh asinkhronnykh logicheskikh skhem (Synthesis of Sequential Asynchronous Logic Circuits). In sbornik: Avtomatika i vychislitel'naya tekhnika, 9. Riga, "Zinatne." 1965.
2. Yakubaitis, E. A. Asinkhronnye logicheskie avtomaty (Asynchronous Logical Automata). Riga, "Zinatne." 1966.
3. Yakubaitis, E. A., A. Yu. Gobzemis, V. G. Gorobets, and G. F. Fritsnovich. Minimizatsiya ob"ema pamyati posledovatel'nostnykh asinkhronnykh logicheskikh skhem (Minimizing the Storage Capacity of Sequential Asynchronous Logic Circuits). In sbornik: Avtomatika i vychislitel'naya tekhnika, 12. Riga, "Zinatne." 1966.
4. Gobzemis, A. Yu. and G. F. Fritsnovich. Analiz funktsionirovaniya posledovatel'nostnykh asinkhronnykh logicheskikh

- skhem (Analysis of the Operation of Sequential Asynchronous Logic Circuits). In sbornik: Avtomatika i vychislitel'naya tekhnika, 15. Riga, "Zinatne." 1966.
5. Fritsnovich, G. F. Spособ zadaniya i raspoznavaniya ekvivalentnykh ustoychivyykh sostoyanii posledovatel'nostnykh asinkhronnykh logicheskikh skhem (A Method for Specification and Detection of Equivalent Stable States in Sequential Asynchronous Logic Circuits). In sbornik: Teoriya diskretnykh avtomatov. Riga, "Zinatne." 1967.
  6. Gobzemis, A. Yu. Minimizatsiya chisla promezhutochnykh peremennykh pri sinteze posledovatel'nostnykh asinkhronnykh logicheskikh skhem (Minimization of the Number of Intermediate Variables in the Synthesis of Sequential Asynchronous Logic Circuits). In sbornik: Teoriya diskretnykh avtomatov. Riga, "Zinatne." 1967.
  7. Yakubaitis, E. A. Vremennye asinkhronnye logicheskie avtomaty (Time-dependent Asynchronous Logical Automata). Present collection, p. 1—15.
  8. Aizerman, M. A., L. A. Gusev, L. I. Rozonoer, I. M. Smirnova, and A. A. Tal'. Logika. Avtomaty. Algoritmy (Logic, Automata, Algorithms). Moskva, Fizmatgiz. 1963.

*A.K. Zuev, L.A. Rastrigin*

**ESTIMATING THE PARAMETERS OF THE  
OBJECT OF OPTIMIZATION**

Estimates are determined for the useful signal and distance to the goal for linear and central objects of optimization in the presence of noise, in a random-search process.

**1. FORMULATION OF THE PROBLEM**

In optimization of systems upon whose quality function random noise is superimposed optimal search strategies cannot be devised unless certain parameters of the object are known. Among these parameters are the level of the useful signal, i.e., the maximum variation of the quality function for a fixed step of the search, and the distance to the goal (extremum point); the latter is used to determine when the system enters a given neighborhood of the extremum, and, consequently, to determine the optimum step size.

Statistical estimates are thus required for these parameters at each step of the search.

We consider an optimizing control system operating by the method of random search with accumulation [1]. The quality functions for a linear and central model of the object are, respectively,

$$Q = (\text{grad } Q \cdot X), \quad (1)$$

$$Q = |\text{grad } Q| |X - X^*|, \quad (2)$$

where the parentheses denote the scalar product.

We assume that the gradient of the quality function depends only on the position, not on the time.  $X = (x_1, \dots, x_n)$  denotes the current state vector and  $X^*$  the position of the goal, where the quality function assumes its maximum value.

The search procedure is carried out by displacing the system from its initial position in a random direction for a distance equal to the trial step size  $g$ , in the space spanned by the parameters  $x_1, \dots, x_n$ . The resulting variation of the quality function of the object is then  $\frac{u}{2} \left( -q \leq \frac{u}{2} \leq q \right)$ , where

$$q = g |\text{grad } Q|. \quad (3)$$



With each measurement, an additive uncorrelated noise function  $\varepsilon \left( \frac{\sigma^2}{2} \right)$  with normal distribution

$$p(\varepsilon) = \frac{1}{\sigma\sqrt{\pi}} \exp\left(-\frac{\varepsilon^2}{\sigma^2}\right). \quad (4)$$

is superimposed on the quality function of the controlled object. The accumulation of the statistic is accomplished as follows. Choose a random direction in the parameter space and sample the quality function on both sides of the initial position, at a distance equal to the trail step size. These two measurements determine the increment of the quality function

$$z = u + \varepsilon(\sigma^2), \quad -\infty < z < \infty. \quad (5)$$

Carrying out similar measurements for different random directions and step sizes we obtain an independent sample

$$z_1, z_2, \dots, z_m, \quad (6)$$

which characterizes the neighborhood of the initial point.

The problem is to determine the unknown parameters  $q$  and  $r = |X - X^*|$  on the basis of the finite sample (6).

To this end we employ standard estimates for the expectation and variance of a random variable  $/2/$ . The estimates will be considered for both linear and central models of the quality of the system.

## 2. LINEAR FIELD

A general expression was derived in  $/3/$  for the probability density of  $u$ :

$$p_n(u) = \frac{\Gamma\left(\frac{n}{2}\right)}{q\sqrt{\pi} \Gamma\left(\frac{n-1}{2}\right)} \left(1 - \frac{u^2}{q^2}\right)^{\frac{n-3}{2}}, \quad (7)$$

where  $\Gamma$  is the gamma-function.

For simplicity we shall consider the case  $n=3$ , and find an estimate for  $q$ . The probability law is

$$p_3(u) = \frac{1}{2q} \quad (8)$$

with expectation zero and variance

$$\sigma_u^2 = \frac{1}{3}q^2. \quad (9)$$

Using (5) we find the variance of the variable  $z$ :

$$\sigma_z^2 = \sigma^2 + \frac{1}{3}q^2. \quad (10)$$

The variance has the standard estimate

$$\hat{\sigma}_z^2 = \frac{1}{m} \sum_{j=1}^m z_j^2. \quad (11)$$

Using (10) and (11) we find the required estimate:

$$\hat{q}^2 = 3 \left( \frac{\sum_{j=1}^m z_j^2}{m} - \sigma^2 \right). \quad (12)$$

Evaluation of the estimate using (12) should involve a fairly large sample. Limit theorems then imply that the estimate  $\hat{q}^2$  is normally distributed. However, it is clear from (12) that when the sample size is finite (as is necessarily the case in practice) some estimates of  $q$  may turn out to be imaginary, while it is evident from physical considerations that  $q$  is essentially real. Samples that lead to imaginary estimates are therefore rejected as unsuitable. The rejection of some of the samples results in a truncated statistical law and a biased estimate.

Strictly speaking, the distribution of the estimate for  $q$  is not normal; nevertheless, in order to obtain approximate estimates we shall assume that it is indeed normal.

An expression for the expectation of a truncated normal distribution is given in [5]. Using this expression one obtains the following unbiased estimate  $\hat{q}_0$  for the parameter  $q$ :

$$\hat{q}_0 = \hat{q} - \frac{2\hat{\sigma}_q^2}{\sqrt{2\pi} \left[ 1 + \Phi \left( \frac{\hat{q}_0}{\hat{\sigma}_q} \right) \right]} \exp \left( -\frac{\hat{q}_0^2}{2\hat{\sigma}_q^2} \right), \quad (13)$$

where  $\hat{\sigma}_q^2$  is an estimate for the variance of the estimate  $\hat{q}$ , and

$$\Phi(x) = \frac{2}{\sqrt{\pi}} \int_0^x e^{-t^2} \cdot dt \quad (\text{see [6]}).$$

The empirical estimates that we cite refer to a small sample and the results are therefore only approximate.

Table 1 gives results of a statistical simulation of the problem using random numbers. 10 experiments were performed, each involving a sample of size  $m=5$ . It was assumed that  $\sigma^2=1$ ,  $q=1$  (imaginary values of  $\hat{q}$  were rejected).

TABLE 1.

No. of sample	1	2	3	4	5	6	7	8	9	10
$\hat{q}_i$	0.794	1.18	1.65	0.96	0.6	0.949	2.3	0.83	1.73	1.78

Table 1 yields

$$\hat{q} = 1.28, \hat{\sigma}_q^2 = 0.28. \quad (14)$$

The unbiased estimate  $\hat{q}_0 \approx 1.06$  is a satisfactory estimate for  $q=1$ . Now consider the question of sample size. It was mentioned above that some samples may yield an imaginary value of  $\hat{q}$ , and then the entire sample is rejected. It is natural to ask whether one can determine a sample size that minimizes the losses resulting from rejected samples. Let us assume that the loss function has the form

$$R'(P_f) = P_f \cdot m \cdot N, \quad (15)$$

where  $P_f$  is the probability of a rejected sample,  $m$  is the sample size, and  $N$  the number of samples. It is more convenient to consider the loss for a single sample:

$$R(P_f) = P_f m. \quad (16)$$

This loss function cannot be given a direct physical interpretation. It is only a rough indication of the average number of unsuitable measurements in one sample.

It is clear from (12) that the sample is rejected if

$$\frac{1}{m} \sum_{j=1}^m z_j^2 < \sigma^2. \quad (17)$$

It is known that the variable  $y = \frac{1}{m} \sum_{j=1}^m z_j^2$  is asymptotically normally distributed:

$$p(y) = \frac{\sqrt{m}}{2\sqrt{\pi} \sigma_z^2} \exp \left[ -\frac{(y - \sigma_z^2)^2}{4 \cdot \frac{\sigma_z^4}{m}} \right] \quad (18)$$

with parameters  $\sigma_z^2$  and  $\sigma_z^4$

$$M \left[ \frac{1}{m} \sum_{j=1}^m z_j^2 \right] = \sigma_z^2 = \sigma^2 + \frac{1}{2} q^2; \quad (19)$$

$$D \left[ \frac{1}{m} \sum_{j=1}^m z_j^2 \right] = \frac{2\sigma_z^4}{m}. \quad (20)$$

The probability that the sample is rejected is

$$P_f = \frac{1}{2} \left\{ 1 + \Phi \left[ \frac{(\sigma^2 - \sigma_z^2) \sqrt{m}}{2 \sigma_z^2} \right] \right\}. \quad (21)$$

When  $\sigma^2 = 1$  and  $q = 1$  this becomes

$$P_f = \frac{1}{2} \left[ 1 - \Phi \left( \frac{\sqrt{m}}{8} \right) \right]. \quad (22)$$

Figure 1 illustrates the specific function for this case,

$$R = \frac{m}{2} \left[ 1 - \Phi \left( \frac{\sqrt{m}}{8} \right) \right], \quad (23)$$

as a function of the probability  $P_f$ .

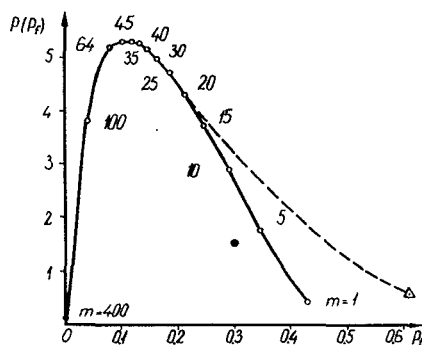


FIGURE 1. Specific losses ( $\sigma^2 = 1$ ,  $q = 1$ ).

distributed random variable has the following density:

$$p(z^2) = \frac{1}{z \sqrt{2\pi} \sigma_z} \exp \left( -\frac{z^2}{2\sigma_z^2} \right). \quad (25)$$

Thus the probability that inequality (24) holds is

$$P_f(z^2 < \sigma^2) = \Phi \left( \frac{\sigma^2}{\sigma_z \sqrt{2}} \right), \quad (26)$$

and the loss for  $m=1$  is

$$R = 0.612.$$

This point is indicated in the figure by a triangle.

It is clear from Figure 1 that the curve has a distinct maximum. For small sample sizes the rejection probability is large, but the sample is small and therefore the losses are small. For large sample sizes  $m=100$  to  $400$ , the rejection probability becomes small and the losses are also insignificant.

Formula (21) is valid for fairly large  $m$ . To evaluate the loss for  $m=1$  other relations must be used. From (12) we see that the sample is rejected if

$$z^2 < \sigma^2. \quad (24)$$

Let us determine the probability that this inequality is valid. It is shown in [7] that the square of a normally

The part of the curve corresponding to  $1 < m < 30$  is based on formula (23), and thus, because of the small sample size, must be regarded as approximate. On the figure we have replaced this branch of the curve by a dotted curve through the point determined above for  $m=1$ . It is clear that the properties of the curve are not affected thereby. We also carried out a numerical simulation of the rejection process for  $m=5$  and  $N=20$ ; the corresponding point is marked by a black dot. Its position obviously does not contradict the above representation. We emphasize that this loss criterion is of tentative value and cannot be used for rigorous determination of sample size. A suitable criterion for optimum sample size would seem to be the average time required to find the extremum, which is beyond the scope of this note. Nevertheless, our criterion does imply one qualitative conclusion: Economical utilization of experiments apparently does not require large sample size.

### 3. CENTRAL FIELD

It follows from [3] that in this case the probability density of the output variable for  $n=3$  is

$$p_3(u) = \frac{1}{2q} \left( 1 - \frac{u}{r} \right) \quad (27)$$

with parameters

$$m_u = - \frac{q^2}{3r} \quad (28)$$

and

$$\sigma_u^2 = \frac{q^2}{3} \left( 1 - \frac{q^2}{3r^2} \right), \quad (29)$$

where  $r$  is the distance to the goal.

This gives the following parameters for the sum (5) of the distributions for  $n=3$ :

$$m_z = m_u = - \frac{q^2}{3r}, \quad (30)$$

$$\sigma_z^2 = \sigma^2 + \frac{q^2}{3} \left( 1 - \frac{q^2}{3r^2} \right). \quad (31)$$

As in the linear case, estimates for  $r$  and  $q$  are obtained by standard techniques — the maximum likelihood estimates for  $m_z$  and  $\sigma_z^2$ :

$$\hat{m}_z = \frac{1}{m} \sum_{j=1}^m z_j, \quad (32)$$

$$\hat{\sigma}_z^2 = \frac{1}{m-1} \sum_{j=1}^m (z_j - \hat{m}_z)^2. \quad (33)$$

Substituting (32) and (33) in the left-hand sides of (30) and (31) and solving the resulting simultaneous equations, we get the following estimates for  $r$  and  $q$ :

$$\hat{r} = - \frac{\hat{\sigma}_z^2 + \hat{m}_z^2 - \sigma^2}{\hat{m}_z}, \quad (34)$$

$$\hat{q} = \sqrt{3[\hat{\sigma}_z^2 + \hat{m}_z^2 - \sigma^2]}. \quad (35)$$

It is clear from these formulas that in practice the estimate for  $r$  may be negative, and that for  $q$  imaginary. Samples having no physical meaning are rejected as unsuitable. As in the linear case, we have thus obtained biased estimates.

Using /5/ we have the following unbiased estimate for  $r$ :

$$\hat{r}_0 = \hat{r} - \frac{2\hat{\sigma}_r}{\sqrt{2\pi} \left[ 1 + \Phi \left( \frac{\hat{r}_0}{\hat{\sigma}_r} \right) \right]} \exp \left( - \frac{\hat{r}_0^2}{2\hat{\sigma}_r^2} \right), \quad (36)$$

where  $\hat{\sigma}_r^2$  is the estimate for the variance of the estimate  $r$ .

An unbiased estimate for  $q$  is given, as in the linear case, by formula (13).

Table 2 cites experimental data for a central field. The initial values of the parameters are  $\sigma^2=1$ ,  $r=1$ ,  $q=1$ , and the sample size  $m=5$ .

TABLE 2.

No. of sample	1	2	3	4	5	6	7	8	9	10
$\hat{r}_i$	0.268	0.85	2.28	0.678	1.45	3.42	0.994	3.76	1.47	1.09
$\hat{q}_i$	0.697	1.33	1.97	1.27	1.68	2.22	1.32	2.12	1.34	1.31

$$\hat{r} = 1.63 \quad \hat{\sigma}_r^2 = 1.11 \quad (37)$$

$$\hat{q} = 1.53 \quad \hat{\sigma}_q^2 = 0.444 \quad (38)$$

Solution of equations (13, 36) by successive approximations using the initial data (37), (38) gives the following unbiased estimates  $\hat{q}_0$  and  $\hat{r}_0$ :

$$\hat{q}_0 \approx 1.3; \quad \hat{r}_0 \approx 1.2.$$

If corrections for bias are taken into account, the experimental results give more satisfactory estimates for the required parameters. To compare formula (34) with the linear version of the estimate, let us apply it to the sample obtained for the linear field. For the expectation  $M[r]$  we obtain

$$M[r] = \lim_{m \rightarrow \infty} \bar{r} = \frac{\frac{1}{2}q^2}{\lim_{m \rightarrow \infty} \frac{1}{m} \sum_{j=1}^m z_j} = \infty. \quad (39)$$

Formula (34) thus agrees with the linear version.

The above approximate estimates for the useful signal and the distance to the goal give satisfactory results in experimental practice. The loss criterion for estimation of the parameters makes it possible to limit the sample size.

On the basis of the estimates of these parameters the trial step size can be corrected, with a view to more precise determination of the extremum of the quality function and reduction of the average time needed for the search.

#### Bibliography

1. Rastrigin, L. A. Sluchainyi poisk v zadachakh optimizatsii mnogoparametricheskikh sistem (Random Search in Optimization Problems for Multi-parameter Systems). Riga, "Zinatne." 1965.
2. Cramer, H. Mathematical Methods of Statistics. Princeton University Press. 1946.
3. Rastrigin, L. A. Vliyanie bluzhdaniya tseli na povedenie sistemy ekstremal'nogo upravleniya (Effect of Randomization of the Goal on the Behavior of Optimizing Control Systems). In sbornik: "Avtomatika i vychislitel'naya tekhnika," 9. Riga, "Zinatne." 1965.
4. Smirnov, N. V. and I. V. Dunin-Barkovskii. Kurs teorii veroyatnostei i matematicheskoi statistiki dlya tekhnicheskikh prilozhenii (Theoretical Course of Probability and Mathematical Statistics in Technical Applications). Moskva. 1965.
5. Shor, Ya. B. Statisticheskie metody analiza i kontrolya kachestva i nadezhnosti (Statistical Methods of Analysis and Control of Quality and Reliability). Moskva, "Sovetskoe radio." 1962.
6. Venttsel', E. S. Teoriya veroyatnostei (Probability Theory). Moskva. "Nauka." 1964.
7. Pugachev, V. S. Teoriya sluchainykh funktsii (Theory of Random Functions). Moskva, Fizmatgiz. 1962.
8. Van der Waerden, B. L. Mathematische Statistik. Berlin, Springer. [Russian translation 1960.]

*L. K. Lapkovskii, L. A. Rastrigin*

# DIAGNOSIS BY COMPLETION

A method is given for diagnosis by completion, applying the method of self-adjusting models. The method may be used to determine the parameters of an inaccessible circuit. As an example we consider the diagnosis of a T-junction shaped bridge.

1. The diagnosis of multipole circuits by simulation, considered in /1/, is based on the assumption that the dynamic properties of the object are accurately represented by the parameters being determined.

Let  $X = (x_1, x_2, \dots, x_n)$  be the vector whose components are the parameters being determined in the diagnosis, and  $A = (a_1, a_2, \dots, a_m)$  the vector of dynamic parameters of the object. For instance, for a linear quadripole circuit the vector  $A$  determined the coefficients of the response function linking the input  $y(t)$  and the output  $z(t)$ :

$$a_1 z^{e-1} + a_2 z^{e-2} + \dots + a_e = a_{e+1} y^{m-e} + \dots + a_m y. \quad (1)$$

It is clear that the dynamic properties of the object establish a correspondence between the  $n$ -dimensional parameter space  $\{X\}$  of the object and the  $m$ -dimensional dynamic-parameter space  $\{A\}$ . This correspondence may be expressed as a relation

$$A = F(X). \quad (2)$$

The physical significance of this relation implies that it is one-valued, i. e., to each value of the vector  $X$  corresponds a unique value of  $A$  (every system has its own specific dynamic behavior). The converse is in general false. This means that for a given type of system there may be a number of vectors  $X$  corresponding to the same vector  $A$ , i. e., in general several systems may exhibit the same dynamic behavior.

The simplest example of such a system is a potential divider, where information concerning the transfer function of the divider conveys no information on the resistances of which it consists. This is illustrated in Figure 1 in schematic form: To one vector  $A$  corresponds a one-parameter manifold of vectors  $X$ .

Diagnosis utilizes the dynamic properties of the system in order to determine its parameters. In the light of the above discussion, it is clear that the diagnosis may not be unambiguous. In /1/ one of the present authors studied the special case in which the relation (2) is one-to-one.



The present paper deals with the more general case in which observation of the dynamic properties does not ensure unambiguous diagnosis. We employ and develop the method of self-adjusting models, using a procedure of multi-parameter optimization [2].

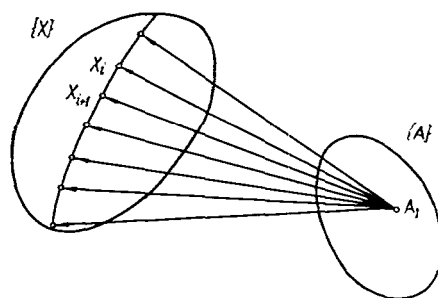


FIGURE 1. Schematic illustration of the relations between the space of the parameters being determined and the space of dynamic parameters.

2. As in [1] it is assumed that the structure (schematic diagram) of the object of diagnosis is given in the form of a multipole circuit certain parts of which are inaccessible to observation. For simplicity we shall confine ourselves to linear passive quadripole circuits (the general case may be treated similarly).

We remark that the method of self-adjusting models is applicable to the synthesis of arbitrary systems, including nonlinear systems [2] — this

is one of its advantages. We confine ourselves to the linear case to simplify the mathematical treatment and to ensure greater visual clarity.

We suppose that the object of diagnosis is "completed," i.e., incorporated in a larger system, in such a way that the required properties can be ascertained. In many cases this can indeed be done. Figure 2 is a block-diagram of completion diagnosis. The system under diagnosis (SD) is provided with blocks 1<sub>i</sub> and 2<sub>i</sub> whose properties may be varied ( $i=1, 2, 3, \dots, l$ ) upon command from the control block (CB). Information on the state of the object and its model (M) in the form of signals  $z(t)$  and  $z'(t)$  is compared, and some function  $Q_i(X')$  measuring the difference between these signals is transmitted to the input of a multichannel optimizer (MO). The latter sets up the quality function

$$Q = \sum_{i=1}^l Q_i(X') \quad (3)$$

and finds its minimum for all realizations of the blocks 1<sub>i</sub> and 2<sub>i</sub>.

The minimum of the function (3) with respect to the model parameters  $X'$  is attained when the model M is identical with the object SD, i.e., it yields the solution of the problem (when the latter exists).

An analogue of this method is in fact widely used in everyday life, when a vacuum tube is tested by inserting it in a radio in place of a tube known to be in working order. If the quality of the reception is unchanged, one concludes that the tube is in working order. The tube is thus "completed" by the radio receiver, the latter revealing the properties of the former.

3. The special features of completion diagnosis will be demonstrated in a simple example. Consider the diagnosis of a T-junction consisting of resistances  $R_1, R_2, R_3$  (enclosed in dashed lines in Figure 3), the junction point being inaccessible. The dynamic properties of the junction are determined by a transfer function, but the latter is not sufficient to

determine the parameters of the former. As indicated above, the junction is adjusted by applying a voltage  $r_1$ , which can assume two values  $r_{11}, r_{12}$ , at the input, and a voltage  $r_2$ , which can also assume two values  $r_{21}, r_{22}$ , at the output. The discrepancy between the bridge and the model is indicated by a galvanometer (see Figure 3).

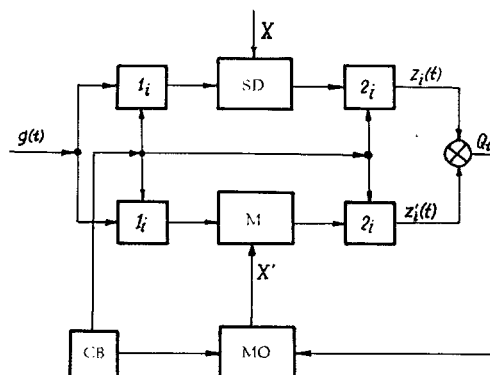


FIGURE 2. Block-diagram of completion diagnosis using a self-adjusting model.

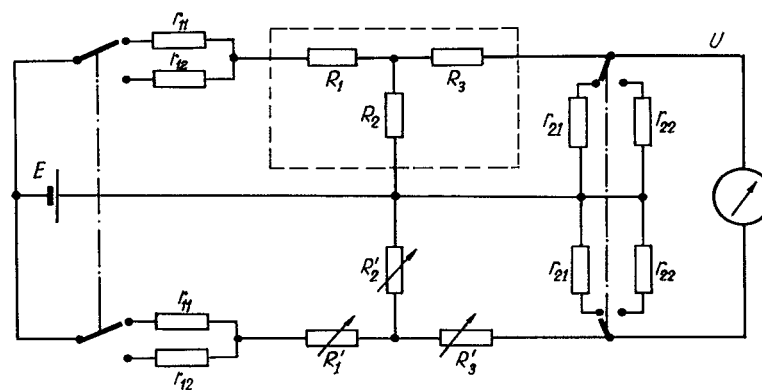


FIGURE 3. Circuit for experimental diagnosis.

The quality function in this example is based on three observations:

$$Q(R') = \sum_{i=1}^3 Q_i(R'), \quad (4)$$

where  $R' = (R'_1, R'_2, R'_3)$  is the vector of optimizing parameters of the model.  $Q_i$  is the absolute value of the galvanometer reading

$$Q_i = |U - U'|, \quad (5)$$

where  $U$  and  $U'$  are the voltages at the outputs of junction and model respectively.

We claim that if  $Q(R') = 0$  then  $R = R'$ . Let us express  $R'_i$  in terms of  $R_i$  by the relation

$$R'_i = R_i(1 + \delta_i), \quad i = 1, 2, 3, \quad (6)$$

where the  $\delta_i$  are assumed fairly small:

$$|\delta_i| \ll 1, \quad (7)$$

which is the case in the neighborhood of the solution. Using (7) and performing a few obvious manipulations we obtain the following expressions from the Kirchhoff equations for the three cases  $i = 1, 2, 3$ :

$$\sum_{j=1}^3 B_{ij} \delta_j = C_i, \quad i = 1, 2, 3; \quad (8)$$

$$\begin{aligned} B_{11} &= -(R_3 + r_{21} + R_2)R_1; & B_{12} &= (R_3 + r_{21})(r_{11} + R_1); \\ B_{13} &= -(r_{11} + R_1 + R_2)R_3; \\ B_{21} &= -(R_3 + r_{22} + R_2)R_1; & B_{22} &= (R_3 + r_{22})(r_{11} + R_1); \\ B_{23} &= -(r_{11} + R_1 + R_2)R_3; \\ B_{31} &= -(R_3 + r_{22} + R_2)R_1; & B_{32} &= (R_3 + r_{22})(r_{12} + R_1); \\ B_{33} &= -(r_{12} + R_1 + R_2)R_3; \end{aligned}$$

$$C_1 = \left(\frac{1}{U_1} - \frac{1}{U'_1}\right)ER_2r_{21}; \quad C_2 = \left(\frac{1}{U_2} - \frac{1}{U'_2}\right)ER_2r_{22};$$

$$C_3 = \left(\frac{1}{U_3} - \frac{1}{U'_3}\right)ER_2r_{22};$$

where  $U_i$  is the voltage at the output of the object in the  $i$ -th observation,  $U'_i$  the corresponding voltage for the model, and  $E$  the source emf.

It is easily seen that when  $Q(R') = 0$  the system (8) is homogenous. Thus if the determinant of the matrix  $\|B_{ij}\|$  is not zero the system has no solution other than the trivial one:

$$\delta_i = 0, \quad i = 1, 2, 3, \quad (9)$$

which means that  $R_i = R'_i$  and proves that the solution of the problem is unique.

Computations show that in general the determinant of the matrix  $\|B_{ij}\|$  is not zero, and the method can therefore be used to determine the parameters of the junction. It is clear that the nonvanishing of the determinant imposes certain restrictions on the choice of the parameters  $r_{ij}$ . However, this condition is not overly restrictive, since one need only find one (readily obtained) solution of an inequality of the form

$$Q(r_{11}, r_{12}, r_{21}, r_{22}) \neq 0. \quad (10)$$

Generalizing the above example, it is easy to formulate a uniqueness condition for a similar multidimensional object with arbitrarily many parameters: the analysis is unique if the rank of the matrix  $\|B_{ij}\|$  based on all the observations, is not smaller than the number of parameters of the object under analysis, when the quality function of the system is a minimum.

The function  $Q(R')$  must be minimized. Indeed, the diagnosis problem could be solved on the basis of the system of linear equations (8) alone. However, in so doing an error is introduced, since these equations were set up subject to the constraint (7), which is in general not satisfied by the initial values of the parameters. One might suggest starting from the exact equations, but the exact equations relating the parameters to be determined and the observations are in general nonlinear, even transcendental, and thus lead to serious computational difficulties. Approximation of these equations by the linear system (8) leads to a solution by iteration and the process determining the exact values of the parameters  $R'$  may be unstable.

4. As an illustration of the discussion, Figure 4 indicates the actual diagnosis process for  $R_1=481$  ohm,  $R_2=1011$  ohm,  $R_3=255$  ohm and supplementary resistances  $r_{11}=1040$  ohm,  $r_{12}=1711$  ohm,  $r_{21}=2090$  ohm,  $r_{22}=7540$  ohm. The optimization was carried out by the method of successive variation of parameters (Gauss-Seidel) with step size 20 ohm. It is clear that the process is convergent, i. e., the model parameters converge to the object parameters.

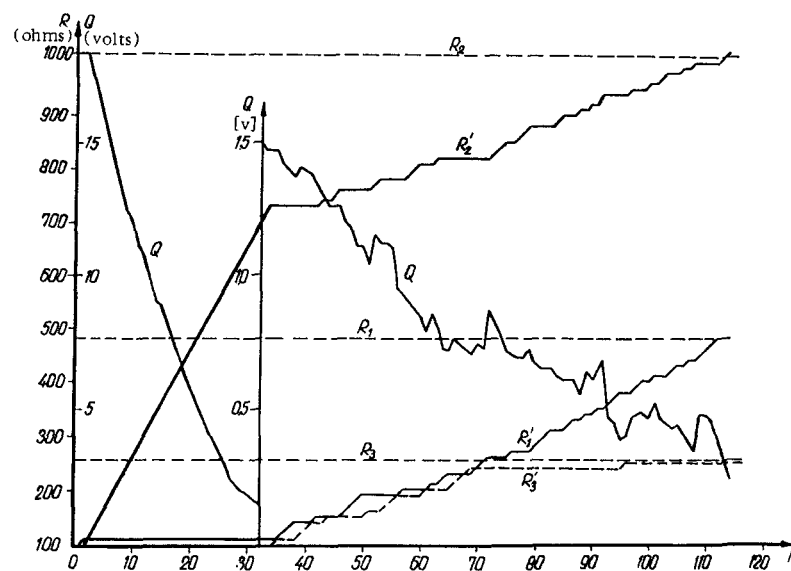


FIGURE 4. Behavior of the quality function  $Q$  and the model parameters  $R_1'$ ,  $R_2'$ ,  $R_3'$  in an actual optimization process to determine the parameters of a T-junction.

Solution of the same problem without minimization yields the values  $\delta_1 = -0.046$ ;  $\delta_2 = -0.034$ ;  $\delta_3 = -0.122$ , while the precise values are  $\delta_1 = -0.80$ ;  $\delta_2 = -0.90$ ;  $\delta_3 = -0.61$ . It is clear that the errors are significant.

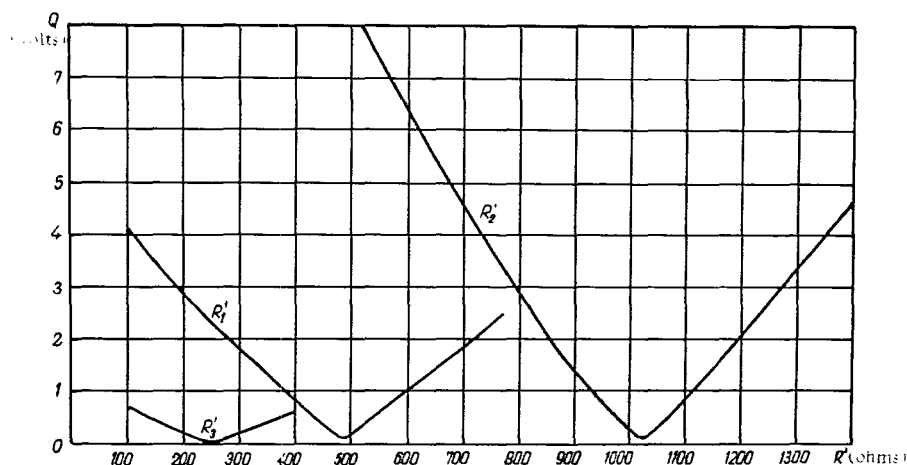


FIGURE 5. Dependence of the quality function  $Q$  on the model parameters.

Figure 5 illustrates the behavior of the quality function when one of the model parameters is varied and the other two coincide with the object parameters. The extremal character of these dependences is obvious, thus emphasizing the need for multiparametric optimization.

We note in conclusion that the diagnostic method proposed here is especially effective in determining the parameters of quadripole circuits with reactive and nonlinear resistances, when the solution of the equations of the object is particularly laborious.

## Bibliography

1. Rastrigin, L. A. Diagnostika sistem putem postroeniya ikh modelei (Diagnostics of Systems by Construction of Models). Izv. AN Latv. SSR, ser. fiziko-tekhnich., 3, 1964.
2. Margolis, M. and S. T. Leonides. O teorii samonastroyayushcheysya sistemy regulirovaniya (metod obuchayushcheysya modeli) (The Theory of a Self-Adjusting Control System (Method of Training Models)). Trudy 1-go mezhdunarodnogo kongressa MFAU, Volume 2. Moskva, Izdatel'stvo AN SSSR, 1961.

*Ya. A. Gel'fandbein, L. V. Kolosov*

**DETERMINATION OF INTERNAL DISTURBANCE IN  
MULTIVARIABLE DYNAMIC SYSTEMS DURING  
PERFORMANCE**

A method is studied for determining the statistical properties of transient disturbances distributed in systems with cross connections, according to realizations of the input and output signals determined during the operation of the system.

The papers /1-4/ are devoted to certain problems concerning the statistical properties of disturbance which is applied at the output and acts during the operation (possibly abnormal) of a system. Of course, in practice it may occur that the disturbance is concentrated at a single point of the system, but such an idealization is highly improbable. In reality the system usually contains several sources of disturbance and it is required to find their statistical characteristics and to eliminate the disturbance itself at the "nodes" of the block-diagram.

We shall consider one method for the solution of this problem, studying as an example the multivariable nonstationary control system whose block diagram is illustrated in Figure 1. The notation is as follows:

- $w_0(t, \xi)$ : pulsed weighting function of the plant;
- $w_1(t, \xi)$ : pulsed weighting function of the controller;
- $w_1(t, \xi), w_2(t, \xi)$ : pulsed weighting functions of the cross connections of the plant;
- $w_a(t, \xi), w_r(t, \xi)$ : pulsed weighting functions of the paths in which the effect of the disturbances may be disregarded;
- $w_b(t, \xi), w_d(t, \xi)$ : pulsed weighting functions of the plant along the paths of disturbances  $f_1(t), f_3(t)$ , respectively;
- $f_2(t), f_4(t)$ : disturbances at the output of the plant.

We shall assume that the statistical characteristics of the signals  $y_1(t)$ ,  $x(t)$ , and  $y_2(t)$  during the performance of the system have already been determined by some method.

It is required to determine the statistical characteristics of the disturbances  $f_1(t), f_2(t), f_3(t), f_4(t)$ .

To solve the problem, we first move the takeoff points 1 and 2 beyond the summing points 3 and 4, respectively, and then move the summing points 1 and 2 beyond the summing points 3 and 4. This results in the block diagram given in Figure 2.

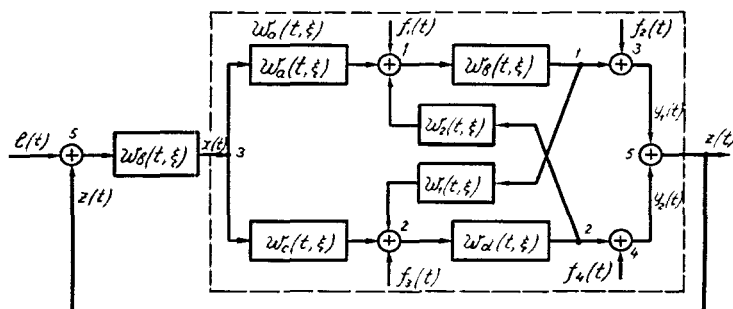


FIGURE 1. Block diagram of a multivariable system with cross connections.

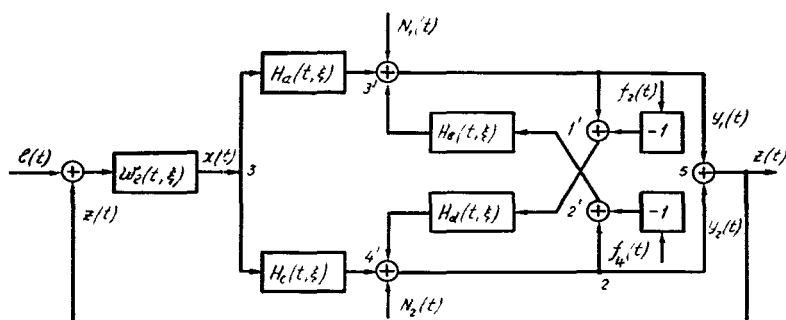


FIGURE 2. Transformed block diagram of the system.

In accordance with the block transformation rules we have the following relations:

$$\left. \begin{aligned} H_a(t, \xi) &= \int_{\xi}^t \omega_a(t, \eta) \omega_b(\xi, \eta) d\eta; & H_b(t, \xi) &= \int_{\xi}^t \omega_2(t, \eta) \omega_b(\xi, \eta) d\eta; \\ H_c(t, \xi) &= \int_{\xi}^t \omega_c(t, \eta) \omega_d(\xi, \eta) d\eta; & H_d(t, \xi) &= \int_{\xi}^t \omega_1(t, \eta) \omega_d(\xi, \eta) d\eta \end{aligned} \right\} \quad (1)$$

and

$$\left. \begin{aligned} N_1(t) &= n_1(t) + f_2(t); & N_2(t) &= n_2(t) + f_4(t); \\ n_1(t) &= \int_0^t \omega_b(t, \xi) f_1(\xi) d\xi; & n_2(t) &= \int_0^t \omega_d(t, \xi) f_3(\xi) d\xi. \end{aligned} \right\} \quad (2)$$

We solve the problem by the method of sequential search. In the first approximation we disregard the cross connections and determine the

statistical characteristics of the applied disturbances  $N_1(t)$  and  $N_2(t)$ . It is clear from Figure 2 that the first approximation is

$$\left. \begin{aligned} N_1'(t) &= y_1(t) - \int_0^t H_a(t, \xi) x(\xi) d\xi; \\ N_2'(t) &= y_2(t) - \int_0^t H_c(t, \xi) x(\xi) d\xi. \end{aligned} \right\} \quad (3)$$

Computing the expectation of both sides of these equalities, we get

$$\left. \begin{aligned} m'_{N_1}(t) &= m_{y_1}(t) - \int_0^t H_a(t, \xi) m_x(\xi) d\xi; \\ m'_{N_2}(t) &= m_{y_2}(t) - \int_0^t H_c(t, \xi) m_x(\xi) d\xi. \end{aligned} \right\} \quad (4)$$

The central values of the disturbances  $N_1'(t)$  and  $N_2'(t)$  are obtained by term-by-term subtraction of (4) from (3):

$$\left. \begin{aligned} \dot{N}_1'(t) &= \dot{y}_1(t) - \int_0^t H_a(t, \xi) \dot{x}(\xi) d\xi; \\ \dot{N}_2'(t) &= \dot{y}_2(t) - \int_0^t H_c(t, \xi) \dot{x}(\xi) d\xi. \end{aligned} \right\} \quad (5)$$

Using the definition of the autocorrelation function as the second-order central moment [5], we get

$$K_{N_1}(t_1, t_2) = M[\dot{N}_1(t_1) \dot{N}_1(t_2)], \quad (6)$$

and by (4), (5)

$$\left. \begin{aligned} K'_{N_1}(t_1, t_2) &= K_{y_1 N_1}(t_1, t_2) - \int_0^{t_1} H_a(t_1, \xi) K_{x' N_1}(\xi, t_2) d\xi; \\ K'_{N_2}(t_1, t_2) &= K_{y_2 N_2}(t_1, t_2) - \int_0^{t_1} H_c(t_1, \xi) K_{x' N_2}(\xi, t_2) d\xi, \end{aligned} \right\} \quad (7)$$

where  $K_{y_1 N_1}(t_1, t_2)$ ,  $K_{x' N_1}(\xi, t_2)$ ,  $K_{y_2 N_2}(t_1, t_2)$  and  $K_{x' N_2}(\xi, t_2)$  are the corresponding cross-correlation functions.

The cross-correlation functions of the disturbances are derived similarly. They have the form

$$K'_{N_1 N_1}(t_1, t_2) = K_{y_1 y_1}(t_1, t_2) - \int_0^{t_1} H_a(t_1, \xi) K'_{x N_1}(\xi, t_2) d\xi. \quad (8)$$



It is clear from these expressions that in order to determine the auto-correlation functions of the reduced disturbances in the first approximation we must know their cross-correlation functions with the input and output signals. In practice, direct determination of these functions under actual operating conditions is often impossible.

Using the definition of the cross-correlation function as the mixed second-order central moment [5], it is easy to derive expressions for the cross-correlation functions appearing in (7):

$$\left. \begin{aligned} K_{y_1 N_1}(t_1, t_2) &= K_{y_1}(t_1, t_2) - \int_0^{t_2} H_a(t_2, \eta) K_{y_1 x_1}(t_1, \eta) d\eta; \\ K_{x N_1}(t_1, t_2) &= K_{x y_1}(t_1, t_2) - \int_0^{t_2} H_a(t_2, \eta) K_{x y_1}(t_1, \eta) d\eta; \\ K_{y_2 N_2}(t_1, t_2) &= K_{y_2}(t_1, t_2) - \int_0^{t_2} H_c(t_2, \eta) K_{y_2 x_2}(t_1, \eta) d\eta; \\ K_{x N_2}(t_1, t_2) &= K_{x y_2}(t_1, t_2) - \int_0^{t_2} H_c(t_2, \eta) K_{x y_2}(t_1, \eta) d\eta; \\ K_{y_1 N_2}(t_1, t_2) &= K_{y_1 y_2}(t_1, t_2) - \int_0^{t_2} H_c(t_2, \eta) K_{y_1 x_2}(t_1, \eta) d\eta. \end{aligned} \right\} \quad (9)$$

It is thus possible to compute first approximations for the statistical characteristics of the disturbances using the statistical characteristics of the input and output signals.

We now determine, again in the first approximation, the statistical characteristics of the disturbances  $f_2(t)$  and  $f_4(t)$ . By Figure 2:

$$\left. \begin{aligned} y_1(t) &= N_1'(t) + \int_0^t H_a(t, \xi) x(\xi) d\xi + \\ &+ \int_0^t H_b(t, \xi) y_2(\xi) d\xi - \int_0^t H_b(t, \xi) f_4(\xi) d\xi, \\ y_2(t) &= N_2'(t) + \int_0^t H_c(t, \xi) x(\xi) d\xi + \\ &+ \int_0^t H_d(t, \xi) y_1(\xi) d\xi - \int_0^t H_d(t, \xi) f_2(\xi) d\xi. \end{aligned} \right\} \quad (10)$$

In the complex domain equations (10) correspond to the following expressions:

$$\left. \begin{aligned} y_1(p) &= N_1'(p) + H_a(p, t) x(p) + H_b(p, t) y_2(p) - H_b(p, t) f_4(p); \\ y_2(p) &= N_2'(p) + H_c(p, t) x(p) + H_d(p, t) y_1(p) - H_d(p, t) f_2(p), \end{aligned} \right\} \quad (11)$$

where  $p = j\omega$ .

This yields

$$\left. \begin{aligned} f_4(p) &= H_b^{-1}(p, t) N_1'(p) + \frac{H_a(p, t)}{H_b(p, t)} x(p) + \\ &\quad + y_2(p) - H_b^{-1}(p, t) y_1(p), \\ f_2(p) &= H_d^{-1}(p, t) N_2'(p) + \frac{H_c(p, t)}{H_d(p, t)} x(p) + \\ &\quad + y_1(p) - H_d^{-1}(p, t) y_2(p). \end{aligned} \right\} \quad (12)$$

Hence it is clear that the first approximations for  $f_4(p)$  and  $f_2(p)$  are

$$\left. \begin{aligned} f_4(t) &= \int_0^t H_b^{-1}(t, \xi) N_1'(\xi) d\xi + \int_0^t G_a(t, \xi) x(\xi) d\xi + \\ &\quad + y_2(t) - \int_0^t H_b^{-1}(t, \xi) y_1(\xi) d\xi, \\ f_2(t) &= \int_0^t H_d^{-1}(t, \xi) N_2'(\xi) d\xi + \int_0^t G_c(t, \xi) x(\xi) d\xi + \\ &\quad + y_1(t) - \int_0^t H_d^{-1}(t, \xi) y_2(\xi) d\xi, \end{aligned} \right\} \quad (13)$$

where  $G_a(t, \xi)$ ,  $G_c(t, \xi)$  are the pulsed weighting functions corresponding to the parametric transfer functions

$$G_a(p, t) = \frac{H_a(p, t)}{H_b(p, t)} \text{ and } G_c(p, t) = \frac{H_c(p, t)}{H_d(p, t)}. \quad (14)$$

From (13) one can derive formulas for the statistical characteristics of the disturbances in the first approximation. Thus, the autocorrelation functions are:

$$\begin{aligned} K_{f_4}(t_1, t_2) &= \int_0^{t_1} H_b^{-1}(t_1, \xi) [K_{N_1'}(\xi, t_2) - K_{y_1'}(\xi, t_2)] d\xi + \\ &\quad + \int_0^{t_1} G_a(t_1, \xi) K_{x'}(\xi, t_2) d\xi + K_{y_2'}(t_1, t_2); \\ K_{f_2}(t_1, t_2) &= \int_0^{t_1} H_d^{-1}(t_1, \xi) [K_{N_2'}(\xi, t_2) - K_{y_2'}(\xi, t_2)] d\xi + \\ &\quad + \int_0^{t_1} G_c(t_1, \xi) K_{x'}(\xi, t_2) d\xi + K_{y_1'}(t_1, t_2). \end{aligned} \quad (15)$$

The cross-correlation functions appearing in (15) are given by

$$\left. \begin{aligned} K_{N_1'}(t_1, t_2) &= \int_0^{t_2} H_b^{-1}(t_2, \eta) K_{N_1}(t_1, \eta) d\eta + \\ &\quad + \int_0^{t_2} G_a(t_2, \eta) K_{N_1 x}(t_1, \eta) d\eta + \\ &\quad + K_{N_1 y_1}(t_1, t_2) - \int_0^{t_2} H_b^{-1}(t_2, \eta) K_{N_1 y_1}(t_1, \eta) d\eta; \end{aligned} \right\} \quad (16)$$

$$\left. \begin{aligned}
K'_{t_1 t_1}(t_1, t_2) &= \int_0^{t_2} H_b^{-1}(t_2, \eta) K'_{y_1 N_1}(t_1, \eta) d\eta + \\
&+ \int_0^{t_2} G_a(t_2, \eta) K_{y_1 x}(t_1, \eta) d\eta + K'_{y_1 y_2}(t_1, t_2) - \\
&- \int_0^{t_2} H_b^{-1}(t_2, \eta) K_{y_1}(t_1, \eta) d\eta; \\
K'_{t_1 t_2}(t_1, t_2) &= \int_0^{t_2} H_b^{-1}(t_2, \eta) K'_{x N_1}(t_1, \eta) d\eta + \\
&+ \int_0^{t_2} G_a(t_2, \eta) K_x(t_1, \eta) d\eta + K_{x y_2}(t_1, t_2) - \\
&- \int_0^{t_2} H_b^{-1}(t_2, \eta) K_{x y_1}(t_1, \eta) d\eta; \\
&\dots \dots \dots \\
K'_{y_1 t_1}(t_1, t_2) &= \int_0^{t_2} H_d^{-1}(t_2, \eta) K'_{y_1 N_1}(t_1, \eta) d\eta + \\
&+ \int_0^{t_2} G_c(t_2, \eta) K_{y_1 x}(t_1, \eta) d\eta + K_{y_1}(t_1, t_2) - \\
&- \int_0^{t_2} H_d^{-1}(t_2, \eta) K_{y_1 y_2}(t_1, \eta) d\eta.
\end{aligned} \right\} \quad (16)$$

It must be remarked that all the cross-correlation functions appearing in (16) may be regarded as known, since they are determined on the basis of the expressions (5), which involve known functions of time:

$$\left. \begin{aligned}
K_{N_1 y_1}(t_1, t_2) &= K_{y_1}(t_1, t_2) - \int_0^{t_1} H_a(t_1, \xi) K_{x y_1}(\xi, t_2) d\xi; \\
K_{N_1 x}(t_1, t_2) &= K_{y_1 x}(t_1, t_2) - \int_0^{t_1} H_a(t_1, \xi) K_x(\xi, t_2) d\xi; \\
&\dots \dots \dots \\
K'_{N_1 y_2}(t_1, t_2) &= K_{y_1 y_2}(t_1, t_2) - \int_0^{t_1} H_a(t_1, \xi) K_{x y_2}(\xi, t_2) d\xi.
\end{aligned} \right\} \quad (17)$$

Thus, in principle one can determine first approximations for the statistical characteristics of all disturbances acting in a multivariable system.

Further note that a first approximation for the cross-correlation function of the disturbances  $f_2(t)$  and  $f_4(t)$  is given by

$$\begin{aligned}
K'_{t_2 t_4}(t_1, t_2) &= \int_0^{t_1} H_d^{-1}(t_1, \xi) K'_{N_2 f_4}(\xi, t_2) d\xi + \\
&+ \int_0^{t_1} G_c(t_1, \xi) K_{x f_4}(\xi, t_2) d\xi + K'_{y_1 f_4}(t_1, t_2) - \\
&- \int_0^{t_1} H_d^{-1}(t_1, \xi) K'_{y_2 f_4}(\xi, t_2) d\xi.
\end{aligned} \quad (18)$$

Using the first approximations (13), we obtain second approximations for the disturbances:

$$\begin{aligned}
 N_1''(t) &= y_1(t) - \int_0^t H_a(t, \xi) x(\xi) d\xi - \int_0^t H_b(t, \xi) y_2(\xi) d\xi + \\
 &\quad + \int_0^t H_b(t, \xi) f_4'(\xi) d\xi; \\
 N_2''(t) &= y_2(t) - \int_0^t H_c(t, \xi) x(\xi) d\xi - \int_0^t H_d(t, \xi) y_1(\xi) d\xi + \\
 &\quad + \int_0^t H_d(t, \xi) f_2'(\xi) d\xi.
 \end{aligned} \tag{19}$$

The corresponding autocorrelation functions are:

$$\begin{aligned}
 K_{N_1}''(t_1, t_2) &= K_{y_1 N_1}''(t_1, t_2) - \int_0^{t_1} H_a(t_1, \xi) K_{x N_1}''(\xi, t_2) d\xi - \\
 &\quad - \int_0^{t_1} H_b(t_1, \xi) K_{y_2 N_1}''(\xi, t_2) d\xi + \\
 &\quad + \int_0^{t_1} H_b(t_1, \xi) K_{f_4' N_1}''(\xi, t_2) d\xi; \\
 K_{N_2}''(t_1, t_2) &= K_{y_2 N_2}''(t_1, t_2) - \int_0^{t_1} H_c(t_1, \xi) K_{x N_2}''(\xi, t_2) d\xi - \\
 &\quad - \int_0^{t_1} H_d(t_1, \xi) K_{y_1 N_2}''(\xi, t_2) d\xi + \int_0^{t_1} H_d(t_1, \xi) K_{f_2' N_2}''(\xi, t_2) d\xi; \\
 K_{N_1 N_2}''(t_1, t_2) &= K_{y_1 N_2}''(t_1, t_2) - \int_0^{t_1} H_a(t_1, \xi) K_{x N_2}''(\xi, t_2) d\xi - \\
 &\quad - \int_0^{t_1} H_b(t_1, \xi) [K_{y_2 N_2}''(\xi, t_2) + K_{f_2' N_2}''(\xi, t_2)] d\xi.
 \end{aligned} \tag{20}$$

The cross-correlation functions appearing in these equations may be computed by formulas similar to (16, 17). It is then not difficult, using formulas similar to (13, 15), to obtain expressions for the disturbances  $f_2''(t)$  and  $f_4''(t)$  and their autocorrelation functions in the second approximation. The known values of  $f_2''(t)$  and  $f_4''(t)$  are then used to obtain a third approximation, and so on.

The computation continues until the difference between consecutive approximations becomes sufficiently small.

Having determined the values of the disturbances  $f_2(t)$  and  $f_4(t)$  after  $n$  iterations, one can use (2) to compute the autocorrelation functions of the reduced disturbances  $n_1(t)$  and  $n_2(t)$ :

$$K_{n_i}(t_1, t_2) = K_{N_i}''(t_1, t_2) - K_{f_i N_i}''(t_1, t_2).$$

The subscript  $n$  indicates that these formulas are based on the  $n$ -th approximation. Similarly

$$K_{n_2}(t_1, t_2) = K_{N_2}^n(t_1, t_2) - K_{f_1 N_2}^n(t_1, t_2).$$

This method, though considerably laborious, may be employed using multivariate correlographs operating concurrently with a high-speed computer.

The extension of our method to steady-state systems presents no difficulties, and we shall therefore omit further reference to this problem.

Note that the pulsed weighting functions of the various blocks of the system needed in the computation may be found by the method of non-correlated actions [1]. To determine the pulsed weighting functions of the separate blocks of the diagram (Figure 1), we need a record of the signals corresponding to the input and output processes of the block under consideration, and also a record of some process in the system which is correlated with the input and output signals of the block but not with the disturbance. The most suitable procedure in applying the above method is nevertheless direct determination of the pulse responses of the blocks by test probing during the debugging process.

Thus, knowing the pulse transition functions of the various parts of a multivariable system, one can approximately determine and localize the noise acting within the system and determine its statistical characteristics on the basis of the input signal of the system and the output signals of its cross channels.

## Bibliography

1. Solodovnikov, V.V. and A. S. Uskov. *Statisticheskii analiz ob'ektov regulirovaniya* (Statistical Analysis of Controlled Objects). Moskva, Mashgiz, 1960.
2. Gel'fandbein, Ya. A. *Statisticheskii metod opredeleniya pomekh v reguliruemyykh sistemakh bez narusheniya normal'nogo rezhima raboty* (A Statistical Method for Determination of Noise in Controlled Systems without Disturbing Normal Operating Conditions). *Izv. AN Latv. SSR, ser. fiziko-tekhich.*, 4, 1964.
3. Gel'fandbein, Ya. A. and L. V. Kolosov. *Opredelenie statisticheskikh kharakteristik pomekhi v funktsioniruyushchei impul'snoi sisteme* (Determination of the Statistical Characteristics of Disturbance in a Sampled-Data System during Operation). Present collection, p. 101.
4. Gel'fandbein, Ya. A. and L. V. Kolosov. *Opredelenie statisticheskikh kharakteristik pomekhi v statsionarnoi impul'snoi sisteme v rezhime ee funktsionirovaniya metodom diskretnykh formiruyushchikh fil'trov* (Determination of the Statistical Characteristics of Noise in a Sampled-Data System under Operating Conditions by the Method of Discrete Shaping Filters). *Referaty dokladov 1-go Vsesoyuznogo simpoziuma po statisticheskim problemam v tekhnicheskoi kibernetike*, 1. Moskva, 1967.

5. Pugachev, V.S. Teoriya sluchainykh funktsii i ee primeneniye k zadacham avtomaticheskogo upravleniya (Theory of Random Functions and its Application to Problems of Automatic Control). Moskva, Fizmatgiz. 1960.

*Ya. A. Gel'fandbein, L. V. Kolosov*

*DETERMINATION OF THE STATISTICAL  
CHARACTERISTICS OF DISTURBANCE IN A  
SAMPLED-DATA SYSTEM DURING OPERATION*

Together with the dynamic characteristics of a system under operating conditions, one often needs estimates for the actual disturbances and internal disturbance acting in the system and affecting the precision of its performance. Internal disturbances in a controlled system are random in nature; as a rule they cannot be accurately determined under operating conditions, but a knowledge of their statistical characteristics may be of considerable assistance to the designer in solving problems of compensation and neutralization of disturbances in debugging. A tentative investigation of this problem for continuous systems may be found in [1, 2]. In this paper we propose a method for determining the autocorrelation functions of internal disturbances in a controller under operating conditions, in particular, for a sampled-data control system, using discrete shaping filters.

Consider a steady-state sampled-data system, whose block diagram is given in fairly general form in Figure 1. The notations are:

- $f[n, 0]$ : random input process;
- $l[n, 0]$ : disturbance whose autocorrelation function is to be determined;
- $v[n, \epsilon]$ : output signal;
- $W_1[n, \epsilon]$ : pulsed weighting function of the reduced continuous block of the controller on which the disturbance has no effect;
- $W_2[n, \epsilon]$ : pulsed weighting function of the block of the controller affected by the disturbance;
- $W_p[n, \epsilon]$ : pulsed weighting function of the controller;
- $W_0[n, \epsilon]$ : pulsed weighting function of the plant.

We assume that during investigation of the system under operating conditions we have already determined (by known methods; see [2, 3]) the autocorrelation functions of the input and output, and the pulsed weighting (or transfer) functions of the controller and the plant, the latter given in discrete form. Moreover, we assume that the internal disturbance and the input are uncorrelated.

Let us apply the discrete Laplace transform to the system, and move the summing point along the path of the signal to the sampler input

(Figure 2). The transfer function of the feedback loop along the path of the disturbance may be expressed as follows:

$$W_3^*(q, \varepsilon) = \frac{W_2^*(q, \varepsilon) W_0^*(q, \varepsilon)}{1 + W_1^*(q, 0) W_2^*(q, 0) W_0^*(q, 0)} \quad (1)$$

and consequently the block diagram of the system may be reduced to that of Figure 3. The pulsed weighting function corresponding to (1) is

$$\begin{aligned} W_3[n, \varepsilon] &= D^{-1} \left\{ \frac{W_2^*(q, \varepsilon) W_0^*(q, \varepsilon)}{1 + W_1^*(q, 0) W_2^*(q, 0) W_0^*(q, 0)} \right\} = \\ &= \frac{1}{2\pi j} \int_{c-j\pi}^{c+j\pi} \frac{W_2^*(q, \varepsilon) W_0^*(q, \varepsilon)}{1 + W_1^*(q, 0) W_2^*(q, 0) W_0^*(q, 0)} e^{qn} dq. \end{aligned} \quad (2)$$

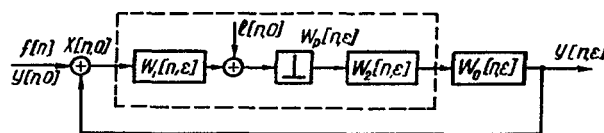


FIGURE 1. Block diagram of a sampled-data control system.

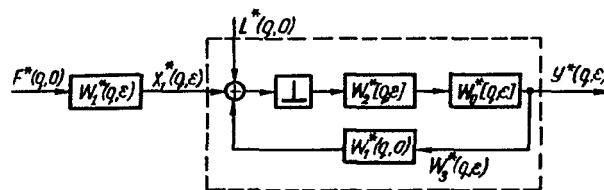


FIGURE 2. Transfer of the input summing point to the input of the sampler pulsed element.

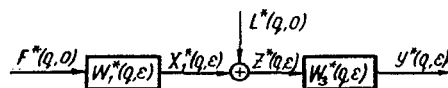


FIGURE 3. Transformed block diagram of the sampled-data system.

We thus obtain the block diagram of a closed-loop sampled-data system equivalent to the system of Figure 1. It is clear from Figure 3 that the output signal  $y[n, \varepsilon]$  is produced upon passage of the signal  $x[n, \varepsilon]$  through a system whose pulsed weighting function  $W_3[n, \varepsilon]$  is (2).



Since

$$z[n, \varepsilon] = \sum_{m=0}^n \beta[m, 0] W_1[n-m, \varepsilon] + \beta[n, 0], \quad (3)$$

it follows that

$$\beta[n, 0] = z[n, \varepsilon] - \sum_{m=0}^n \beta[m, 0] W_1[n-m, \varepsilon]. \quad (4)$$

We shall assume that all signals acting in the system are steady, with expectation zero, i.e.,

$$m_x[n, 0] = m_z[n, \varepsilon] = m_f[n, 0] = m_y[n, \varepsilon] = 0. \quad (5)$$

Since the input and the disturbance are uncorrelated, the autocorrelation function of the disturbance is

$$K_{dd}[n_1, n_2] = K_{zz}[n_1, n_2, \varepsilon] - \sum_{m_1=0}^{n_1} W_1[n_1 - m_1, \varepsilon] \sum_{m_2=0}^{n_2} W_1[n_2 - m_2, \varepsilon] K_{ff}[m_1, m_2]. \quad (6)$$

In view of the fact that the autocorrelation function of a stationary discrete random function depends on the difference between the moments of the discrete argument, expression (6) may be rewritten in the form

$$K_{dd}[r] = K_{zz}[r, \varepsilon] - \sum_{k_1=0}^{\infty} W_1[k_1, \varepsilon] \sum_{k_2=0}^{\infty} W_1[k_2, \varepsilon] K_{ff}[r + k_1 - k_2], \quad (7)$$

where  $n_2 - n_1 = r$ ;  $n_1 - m_1 = k_1$ ;  $n_2 - m_2 = k_2$ .

The autocorrelation function  $K_{zz}[\tau, \varepsilon]$  is determined by the following method.

Assume that the input signal of the block with pulsed weighting function  $W_1[n, \varepsilon]$ , which has the autocorrelation function  $K_{zz}[r, \varepsilon]$ , is produced by a shaping filter with pulsed weighting function  $W_2[n, \varepsilon]$ ; white noise with autocorrelation function of unit intensity, equal to  $\sigma[n-m]/4$ , is applied to the input of the filter. This results in an equivalent sampled-date system with the block diagram of Figure 4.

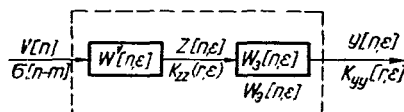


FIGURE 4. Block diagram of the equivalent sampled-data system.

The pulsed weighting function of the equivalent system is

$$W_e[n, \varepsilon] = \sum_{k=0}^n W^v[n-k] W_3[k, \varepsilon], \quad (8)$$

and

$$K_{zz}[r, \varepsilon] = \sum_{k_1=0}^{\infty} W^v[k_1, \varepsilon] \sum_{k_2=0}^{\infty} W^v[k_2, \varepsilon] \sigma[r+k_1-k_2, 0]. \quad (9)$$

In view of the filtering property of the  $\sigma$ -function expression (9) becomes

$$K_{zz}[r, \varepsilon] = \sum_{k_1=0}^{\infty} W^v[k_1, \varepsilon] W^v[r+k_1, \varepsilon]. \quad (10)$$

Thus, to determine the autocorrelation function  $K_{zz}[r, \varepsilon]$  it is sufficient to determine the pulsed weighting function  $W^v[n, \varepsilon]$  of the shaping filter.

Analysis of Figure 4 shows that the equivalent structure of the system under investigation is also a shaping filter, with pulsed weighting function  $W_e[n, \varepsilon]$ , with white noise  $V[n]$  acting at the input and a random process with autocorrelation function  $K_{yy}[r, \varepsilon]$  at the output. Consequently,

$$K_{yy}[r, \varepsilon] = \sum_{k_1=0}^{\infty} W_e[k_1, \varepsilon] \sum_{k_2=0}^{\infty} W_e[k_2, \varepsilon] \sigma[r+k_1-k_2, 0],$$

which leads to an expression similar to (10):

$$K_{yy}[r, \varepsilon] = \sum_{k_1=0}^{\infty} W_e[k_1, \varepsilon] W_e[r+k_1, \varepsilon]. \quad (11)$$

Once the correlation function  $K_{yy}[r, \varepsilon]$  is known and the difference equation for the discrete shaping filter determined, the pulsed weighting function  $W_e[n, \varepsilon]$  of the equivalent system (or its transfer function  $W_e^*(q, \varepsilon)$ ) can be found; using the known functions  $W_e[n, \varepsilon]$  or  $W_3^*(q, \varepsilon)$  it is then easy to determine  $W^v[n, \varepsilon]$  or  $W^{v*}(q, \varepsilon)$ .

The difference equation defining the pulsed weighting function of the equivalent system has the following form /5/:

$$\Phi_m[\Delta, n, \varepsilon] W_e[n-m, \varepsilon] = \Psi_n[\Delta, n, \varepsilon] \sigma[n-m], \quad (12)$$

whence  $W_e^*(q, \varepsilon)$  is determined as the operator quotient

$$W_e^*(q, \varepsilon) = \frac{\Psi_n^*(q, \varepsilon)}{\Phi_m^*(q, \varepsilon)}, \quad (13)$$

and thus

$$W^{v*}(q, \varepsilon) = \frac{W_e^*(q, \varepsilon)}{W_3^*(q, \varepsilon)}. \quad (14)$$

Substituting the expressions (13) for  $W_0^*(q, \varepsilon)$  and (1) for  $W_3^*(q, \varepsilon)$  in this expression, we obtain

$$W^*(q, \varepsilon) = \frac{\Psi_n^*(q, \varepsilon)[1 + W_1^*(q, 0)W_2^*(q, 0)W_0^*(q, 0)]}{\Phi_n^*(q, \varepsilon)W_2^*(q, \varepsilon)W_0^*(q, \varepsilon)}, \quad (15)$$

which gives

$$W^*[n, \varepsilon] = \frac{1}{2\pi j} \int_{\sigma-j\pi}^{\sigma+j\pi} \frac{\Psi_n^*(q, \varepsilon)[1 + W_1^*(q, 0)W_2^*(q, 0)W_0^*(q, 0)]}{\Phi_n^*(q, \varepsilon)W_2^*(q, \varepsilon)W_0^*(q, \varepsilon)} e^{q\varepsilon} dq. \quad (16)$$

Substituting this expression in (10) we can determine the correlation function  $K_{zz}[r, \varepsilon]$ .

One can now use the function  $K_{zz}[r, \varepsilon]$ , the autocorrelation function  $K_z[r]$  of the input, and formula (7) to find the autocorrelation function  $K_u[r]$  of the disturbance at any point of the controller block, assuming the pulsed weighting functions  $W[n, \varepsilon]$  and  $W_2[n, \varepsilon]$  are known beforehand. This makes it possible not only to investigate the path of the internal disturbance in the controller, but also to localize its effective region, corresponding to the maximum correlation in the series of autocorrelation functions defined by (7) for the various blocks of the system described by the pulsed weighting functions  $W_{ii}[n, \varepsilon]$ .

Let us consider an example. Suppose the system (Figure 1) has the following parameters:

$$W_0(p) = \frac{K_0}{T_0 p + 1}; \quad K_0 = 0.8; \quad T_0 = 0.08 \text{ sec};$$

$$W_2(p) = \frac{K_2}{T_1 p + 1}; \quad K_2 = 2.4; \quad T_1 = 0.04 \text{ sec}.$$

The autocorrelation functions of the signals are approximated by

$$K_r[r, 0] = A_r e^{-\alpha_f r} = 0.836 e^{-0.99r};$$

$$K_{zz}[r, \varepsilon] = A_z e^{-\alpha_z |r + \varepsilon|} = 1.56 e^{-0.84|r + \varepsilon|}$$

It is required to find the autocorrelation function of the disturbance, if  $K_1(p) = K_1 = 2$  is the amplifying component and the sampler produces rectangular pulses with pulse duty ratio  $\gamma = 1$  and pulse repetition period  $T = 0.02 \text{ sec}$ .

In terms of dimensionless variables:

$$W_2\left(\frac{q}{T}\right) = \frac{K_2}{\frac{T_1}{T}q + 1} = \frac{1.2}{q + 0.5}$$

and

$$W_0\left(\frac{q}{T}\right) = \frac{K_0}{\frac{T_0}{T}q + 1} = \frac{0.2}{q + 0.25},$$

where

$$q = Tp; \quad p = \frac{q}{T}.$$

After reduction of the circuit as illustrated in Figure 2, we obtain the feedback transfer function along the path of the disturbance:

$$W_{c,1}\left(\frac{q}{T}\right) = \frac{1-e^{-q}}{q} \left[ \frac{1.2}{q+0.5} \cdot \frac{0.2}{q+0.25} \right]. \quad (17)$$

Expressing (17) as a sum of partial fractions, we get

$$W_{c,1}(q) = 0.24(1-e^{-q}) \left[ \frac{C_1}{q-q_1} + \frac{C_2}{q-q_2} + \frac{C_3}{q-q_3} \right].$$

Since

$$\begin{aligned} q_1 &= 0; & q_2 &= -0.5; & q_3 &= -0.25; \\ C_1 &= 8; & C_2 &= 8; & C_3 &= -16, \end{aligned}$$

it follows that

$$\begin{aligned} W_{c,1}^*(q, \varepsilon) &= 1.92(1-e^{-q}) \left[ \frac{e^q}{e^q-1} + \frac{e^q}{e^q-e^{-0.5}} e^{-0.5\varepsilon} + \right. \\ &\quad \left. + 2 \frac{e^q}{e^q-e^{-0.25}} e^{-0.25\varepsilon} \right] \end{aligned}$$

or

$$W_{c,1}^*(q, \varepsilon) = 1.92 \left[ 1 + \frac{e^q-1}{e^q-e^{-0.5}} e^{-0.5\varepsilon} + 2 \frac{e^q-1}{e^q-e^{-0.25}} e^{-0.25\varepsilon} \right].$$

Substituting this expression into (1) and rearranging, we obtain

$$W_s^*(q, \varepsilon) = 0.466 \frac{e^{2q} - 1.59e^q + 0.616}{e^{2q} - 1.58e^q + 0.630}.$$

The transfer function of a filter which produces a random process with autocorrelation function  $K_{yy}[r, \varepsilon]$  is known from [5]:

$$W_e^*(q, \varepsilon) = \frac{e^q}{e^q - e^{-\alpha_y}} \sqrt{A_y(1 - e^{-2\alpha_y})} e^{-\alpha_y \varepsilon},$$

and after substitution of the values of  $A_y$  and  $\alpha_y$  this becomes

$$W_e^*(q, \varepsilon) = 0.44 \frac{e^q}{e^q - 0.43}.$$

The transfer function of a filter which produces a process with autocorrelation function  $K_{zz}[r, \varepsilon]$  at the output is

$$W^{V*}(q, \varepsilon) = \frac{W_e^*(q, \varepsilon)}{W_s^*(q, \varepsilon)} = 0.944 \frac{e^q(e^{2q} - 1.58e^q + 0.63)}{(e^q - 0.43)(e^{2q} - 1.59e^q + 0.616)}.$$

Applying the inverse  $D$ -transformation to this expression, we obtain the pulsed weighting function of the filter:

$$W^1[n, \varepsilon] = D^{-1} \left[ \frac{M e^*(q, \varepsilon)}{N e^*(q, \varepsilon)} \right] = 1.65 e z_3^n + 2.43 e z_2^n - 4.07 e z_1^n.$$

From (10) we get

$$\begin{aligned} K_{zz}[r, \varepsilon] &= 1.65 \sum_{k_1=0}^{\infty} e^{-0.09k_1} e^{-(r-k_1) \cdot 0.09} + \\ &+ 2.43 \sum_{k=0}^{\infty} e^{-0.42k} e^{-(r-k) \cdot 0.42} + 4.07 \sum_{k_2=0}^{\infty} e^{-0.84k_2} e^{-(r-k_2) \cdot 0.84} = \\ &= 5.46 e^{-0.09r} + 2.98 e^{-0.42r} - 4.22 e^{-0.84r}. \end{aligned}$$

The required autocorrelation function of the disturbance can now be defined, using

$$K_{xx}[r, 0] = K_1^2 \cdot K_{ff}[r, 0] = 3.34 \cdot e^{-0.09r},$$

whence

$$\begin{aligned} K_{ff}[r] &= K_{zz}[r] - K_{xx}[r] = \\ &= 2.12 e^{-0.09r} + 2.98 e^{-0.42r} - 4.22 e^{-0.84r}. \end{aligned}$$

## Bibliography

1. Gel'fandbein, Ya. A. Statisticheskii metod opredeleniya pomekh v reguliruemyykh sistemakh bez narusheniya normal'nogo rezhima raboty (A Statistical Method for Determination of Noise in Controlled Systems without Disturbing Normal Operating Conditions). —Izv. AN Latv. SSR, ser. fiziko-tekhnich., 4, 1964.
2. Solodovnikov, V. V. and A. S. Uskov. Statisticheskii analiz ob"ektov regulirovaniya (Statistical Analysis of Controlled Objects). Moskva, Mashgiz, 1964.
3. Gel'fandbein, Ya. A. Opredelenie dinamicheskikh kharakteristik zamknutoi nestatsionarnoi sistemy v normal'nom rezhime ee funktsionirovaniya (Determination of the Dynamic Characteristics of a Nonstationary Closed-Loop System under Normal Operating Conditions). —Izv. AN SSSR, ser. "Tekhnicheskaya kibernetika," 4, 1965.
4. Pugachev, V. S. Osnovy avtomaticheskogo upravleniya (Elements of Automatic Control). Moskva, Fizmatgiz, 1963.
5. Krut'ko, P. D. Statisticheskaya dinamika impul'snykh sistem (Statistical Dynamics of Sampled-Data Systems). Moskva, "Sovetskoe radio." 1963.

*L. A. Gipsh, V. P. Peka*

# *DETERMINATION OF OPTIMAL STOCK LEVEL FOR RANDOM DEMAND*

A method is described for determining the optimal stock level when the demand for the commodity is random (Poissonian). An optimization criterion is chosen and the functional equation of the optimal stock derived for a fixed time interval.

Consider a stockpile of items (spare parts) subject to a demand of random nature, distributed according to a Poisson law:

$$P(i) = e^{-\lambda t} \frac{(\lambda t)^i}{i!}, \quad (1)$$

where  $P(i)$  is the probability that  $i$  demands [each for a single item] are made in the time  $t$ , and  $\lambda$  is the intensity of the demand.

An amount  $v$  of items is stored once in the entire planning period. The unavailability of a single item in the stockpile at the moment of demand entails a loss of  $Q$  rubles.

The cost  $L$  of holding unit stock per unit time (one day) (the stockholding factor) is:

$$L = \frac{q \cdot \eta}{365},$$

where  $q$  is the cost of an item,  $\eta$  the annual percentage income from outlay, and 365 the number of days in a year.

The optimal stock level is determined by considerations of economic expediency. All other considerations may be either reduced to the former or formulated as constraints. A suitable index for the optimal stock is thus the minimum sum of the overhead expenses involved in holding the stock and cost of not being able to meet a demand.

In its most general form, the functional minimizing these losses may be expressed as the sum of the following two products: the stockholding factor  $L$  multiplied by the amount of stock and their holding time, and the penalty factor  $Q$  multiplied by the number of unsatisfied demands:

$$F(v_0) = \min \left[ L \sum_{i=0}^v (v-i) (\mu_{i+1}^t - \mu_i^t) + Q \sum_{i=v+1}^{\infty} (i-v) P(i) \right], \quad (2)$$

where  $v_i$  is the optimal amount of stock,  $i$  is the number of demands, and  $\mu_i^t$  the expectation of the time of the  $i$ -th unsatisfied demand (failure).

The expectation of the time of the  $i$ -th failure is

$$\mu_i^t = \int_0^T f_i(t) \cdot t \cdot dt + T \int_T^\infty f_i(t) dt, \quad (3)$$

where  $T$  is the duration of the planning period and  $f_i(t)$  the probability density of the time of the  $i$ -th failure.

If the failures obey a Poisson law, the probability density of the time of the  $i$ -th failure is governed by an Erlang distribution:

$$f_i(t) = \frac{e^{-\lambda t} \lambda^i t^{i-1}}{(i-1)!} \quad (4)$$

Substituting (4) in (3) and integrating, we obtain

$$\begin{aligned} \mu_i^t = & \frac{i}{\lambda} - e^{-\lambda t} \frac{1}{(i-1)!} [(\lambda^{i-1} t^i + i \lambda^{i-2} t^{i-1} + i(i-1) \lambda^{i-3} t^{i-2} + \dots \\ & \dots + i(i-1) \dots 2 \lambda t + \frac{i!}{\lambda}] + e^{-\lambda t} \frac{1}{(i-1)!} [\lambda^{i-1} t^{i-1} + \\ & + (i-1) \lambda^{i-2} t^{i-2} + (i-1)(i-2) \lambda^{i-3} t^{i-3} + \dots + (i-1)!]. \end{aligned}$$

Multiplying the second expression in square brackets by  $t$ , dividing out by  $e^{-\lambda t} \frac{1}{(i-1)!}$ , and collecting like terms, we obtain

$$\begin{aligned} \mu_i^t = & \frac{i}{\lambda} - e^{-\lambda t} \frac{1}{(i-1)!} \left[ \lambda^{i-2} t^{i-1} + 2(i-1) \lambda^{i-3} t^{i-2} + \right. \\ & + 3(i-1)(i-2) \lambda^{i-4} t^{i-3} + \dots + (i-1)(i-1)! t + \frac{i!}{\lambda} \Big] = \\ = & \frac{1}{\lambda} \left\{ i - e^{-\lambda t} \frac{1}{(i-1)!} [(\lambda t)^{i-1} + 2(i-1)(\lambda t)^{i-2} + \right. \\ & + 3(i-1)(i-2)(\lambda t)^{i-3} + \dots + (i-1)(i-1)! \lambda t + i! \Big] \Big\} = \\ = & \frac{1}{\lambda} \left\{ i - e^{-\lambda t} \left[ \frac{(\lambda t)^{i-1}}{(i-1)!} + 2 \frac{(\lambda t)^{i-2}}{(i-2)!} + 3 \frac{(\lambda t)^{i-3}}{(i-3)!} + \right. \right. \\ & \left. \left. + \dots + (i-1) \lambda t + i! \right] \right\}. \end{aligned}$$

Subtracting  $\mu_i^t$  from  $\mu_{i+1}^t$ :

$$\begin{aligned} \mu_{i+1}^t - \mu_i^t = & \frac{1}{\lambda} \left\{ 1 - e^{-\lambda t} \left[ \frac{(\lambda t)^i}{i!} + \frac{(\lambda t)^{i-1}}{(i-1)!} + \dots + \lambda t + 1 \right] \right\} = \\ = & \frac{1}{\lambda} \left[ 1 - \sum_{j=0}^i e^{-\lambda t} \frac{(\lambda t)^j}{j!} \right]. \end{aligned}$$

The final form of (2) is

$$F(v) = L \sum_{i=0}^v (v-i) \frac{1}{\lambda} \left[ 1 - \sum_{j=0}^i e^{-\lambda t} \frac{(\lambda t)^j}{j!} \right] + \\ + Q \sum_{i=v+1}^{\infty} (i-v) e^{-\lambda t} \frac{(\lambda t)^i}{i!}. \quad (5)$$

Note that if  $v > \lambda t$  the following expression is a good approximation for (5):

$$F(v) = L \frac{2v - \lambda t}{2} + Q \sum_{i=v+1}^{\infty} (i-v) e^{-\lambda t} \frac{(\lambda t)^i}{i!}.$$

### Bibliography

1. Bellman, R. and S. Dreyfus. Applied Dynamic Programming. — Princeton Univ. Press. 1962.
2. Druzhinin, G. V. Nadezhnost' ustroystv avtomatiki (Reliability of Automatic Devices). Moskva, "Energiya." 1964.
3. Feller, W. An Introduction to Probability Theory and its Applications, Volume I. New York, John Wiley and Sons. 1950.



*L.A. Gipsh, V.P. Peka*

**DETERMINATION OF OPTIMAL STOCK  
LEVEL FOR A GROUP OF CUSTOMERS  
UNDER CONDITIONS OF RANDOM DEMAND**

A centralized system supplying a group of customers is considered. A model is set up to determine the optimal central stock level, with an algorithm for its distribution among the customers. The problem is solved on the assumption that the demand at the points of distribution is Poissonian.

Consider a group of customers, each with his own stockpile, and a central stockpile which is used to replenish the customers' stocks (local stockpiles). The central stockpile is provided with an amount  $Y$  of stock once during the entire planning period  $T$  (say a quarter year). The stock in the local stores is replenished in lots of fixed size  $y-x$  when their stock level falls below a given level  $x$ . The time required to deliver the commodity from the central stockpile to a local one is  $\tau$ .

The stock level  $Y$ , the lot size  $y-x$ , and the critical stock level in each local stockpile must be chosen in an optimal manner, i.e., so as to minimize the expected cost of holding stock and the cost of not being able to meet a demand. To determine these costs we use the stockholding factor, i.e., the cost of holding unit stock per unit time, and the dead-time factor  $q$ , i.e., the cost of the customer's dead time as a result of the unavailability of the article during the time  $v$  required for rush delivery from the central stockpile or the manufacturer.

The demand is assumed to obey a Poisson law

$$P(i) = e^{-\lambda t} \frac{(\lambda t)^i}{i!}, \quad (1)$$

where  $P(i)$  is the probability that  $i$  demands are made in time  $t$ ,  $\lambda$  is the intensity of the demand.

We shall determine the stockholding cost in the local stockpile during a single cycle of the supply process, i.e., during the mean time between successive replenishments.

The mean time between successive demands at the local stockpile while the stock level is varying from  $y_k$  to  $x_k+1$  is

$$\mu_k^t = \frac{1}{\lambda_k}. \quad (2)$$

Then the stockholding cost  $L_k$  is given by the expression

$$L_k = l \cdot \frac{1}{\lambda_k} \sum_{i=x_k+1}^{y_k} (y_k - i), \quad (3)$$

or, equivalently,

$$L_k = l \cdot \frac{1}{\lambda_k} \sum_{i=0}^{y_k - x_k - 1} (y_k - i), \quad (4)$$

where  $i$  is the amount of the demand,  $y_k$  is the initial stock level in the  $k$ -th local stockpile,  $x_k$  is the stock level at the  $k$ -th local stockpile at which a replenishment order is made to the central stockpile, and  $\lambda_k$  is the intensity of demand at the  $k$ -th stockpile.

However, during the time  $\tau$  required to fill the order from the central stockpile more demands may be made at the  $k$ -th local stockpile, and the stock level may fall below  $x_k$ . Consequently, after delivery of an amount  $y_k - x_k$  from the central stockpile, the stock level in the  $k$ -th local stockpile when the new supply cycle starts is less than  $y_k$ . The probability that the new cycle will start at level  $y_k$ , or, what is the same, that no demands are made at the  $k$ -th stockpile during the period  $\tau_k$ , is

$$P(0, \tau_k) = e^{-\lambda_k \tau_k},$$

where  $\tau_k$  is the time required to fill an order issuing from the  $k$ -th local stockpile.

The probability that the new cycle will start at a level  $y_k - 1$  may be expressed as follows:

$$P(1, \tau_k) = e^{-\lambda_k \tau_k} \frac{\lambda_k \tau_k}{1!}, \text{ etc.}$$

Expression (4) now becomes

$$L_k = l \cdot \frac{1}{\lambda_k} \sum_{i=0}^{y_k - x_k - 1} (y_k - i) \sum_{j=0}^i e^{-\lambda_k \tau_k} \frac{(\lambda_k \tau_k)^j}{j!}. \quad (5)$$

The stockholding cost during the period  $\tau_k$  is

$$L_k^\tau = l \sum_{i=0}^{x_k} (x_k - i) (\mu_{i+1}^\tau - \mu_i^\tau), \quad (6)$$

where  $\mu_i^\tau$  is the expectation of the time of the  $i$ -th demand.

$$\mu_i^\tau = \int_0^\tau f_i(t) t dt + \tau \int_\tau^\infty f_i(t) dt, \quad (7)$$

where  $f_i(t)$  is the probability density of the time of the  $i$ -th demand.

In our case (assuming a Poisson distribution of demands) this density is Erlangian [2]:

$$f_i(t) = \frac{e^{-\lambda_k t} \lambda_k^i t^{i-1}}{(i-1)!}. \quad (8)$$

Substituting (8) in (7) and integrating, we obtain

$$\mu_i^* = \frac{1}{\lambda_k} \left[ i - \sum_{j=0}^i \sum_{u=0}^j e^{-\lambda_k \tau_k} \frac{(\lambda_k \tau_k)^u}{u!} \right]. \quad (9)$$

A detailed derivation of (9) may be found in [4].

The final expression for the stockholding cost during the time  $\tau_k$  is

$$L_k^* = l \frac{1}{\lambda_k} \sum_{i=0}^{x_k} \left( (x_k - i) \left( 1 - \sum_{j=0}^i e^{-\lambda_k \tau_k} \frac{(\lambda_k \tau_k)^j}{j!} \right) \right) \quad (10)$$

The average number of cycles in a quarter year is

$$n_{cp} = \frac{\lambda_k T}{y_k - x_k}. \quad (11)$$

The total stockholding cost during one supply cycle at the  $k$ -th local stockpile is now obtained by adding (5) and (10):

$$L_k = \left[ l \frac{1}{\lambda_k} \sum_{i=0}^{y_k - x_k - 1} (y_k - i) \sum_{j=0}^i e^{-\lambda_k \tau_k} \frac{(\lambda_k \tau_k)^j}{j!} + \right. \\ \left. + l \frac{1}{\lambda_k} \sum_{i=0}^{x_k} (x_k - i) \left( 1 - \sum_{j=0}^i e^{-\lambda_k \tau_k} \frac{(\lambda_k \tau_k)^j}{j!} \right) \right] \frac{\lambda_k T}{y_k - x_k}. \quad (12)$$

The cost of not being able to meet a demand at the local stockpile is the product of the factor  $q$  and the expectation of the number of unsatisfied demands during the time  $\tau$ . For a single supply cycle, this is

$$Q_k = q \sum_{i=x_k+1}^{\infty} e^{-\lambda_k \tau_k} \frac{(\lambda_k \tau_k)^i}{i!} \cdot (i - x_k), \quad (13)$$

and for the entire planning period

$$Q_k = q \sum_{i=x_k+1}^{\infty} e^{-\lambda_k \tau_k} \frac{(\lambda_k \tau_k)^i}{i!} (i - x_k) \cdot \frac{\lambda_k T}{y_k - x_k}. \quad (14)$$

We now determine the stockholding cost in the central stockpile. With a sufficient degree of accuracy we can assume that the flow of supplies from the central stockpile is Poissonian with parameter

$$\Lambda = \sum_{k=1}^z \lambda_k, \quad (15)$$

where  $z$  is the number of local stockpiles.

The cost of holding an amount of stock  $Y$  in the central stockpile for time  $T$  is determined in the same way as the cost of holding an amount  $x_k$  at the local stockpile, using expressions (6) – (10).

The formula for the central stockpile is

$$L_3 = l \frac{1}{\Lambda} \sum_{i=0}^Y (Y-i) \left( 1 - \sum_{j=0}^i e^{-\Lambda T} \frac{(\Lambda T)^j}{j!} \right). \quad (16)$$

It must be kept in mind that the stock  $Y$  in the central stockpile is limited, and thus it may happen that orders cannot be filled owing to exhaustion of the stock. Let us determine the expectation of the time during which orders from the local stockpiles can be filled, or, equivalently, the expectation of the time of the  $Y$ -th demand at the central stockpile:

$$\mu_Y T = \int_0^T f_Y(t) \cdot t \cdot dt + T \int_T^\infty f_Y(t) dt, \quad (17)$$

where

$$f_Y(t) = \frac{e^{-\Lambda t} \Lambda^Y t^{Y-1}}{(Y-1)!}. \quad (18)$$

Substituting (18) in (17) and integrating, we obtain

$$\mu_Y T = \frac{1}{\Lambda} \left( Y - \sum_{i=0}^{Y-1} \sum_{j=0}^i e^{-\Lambda T} \frac{(\Lambda T)^j}{j!} \right). \quad (19)$$

Dividing (19) by the planning period  $T$ , we obtain the availability factor  $Y$ , i. e., the relative fraction of the planning period during which all demands from the local stockpile can be fulfilled:

$$k_T = \frac{\mu_Y T}{T}. \quad (20)$$

Multiplying (5), (10) by  $k_T$ , we get the stockholding cost for that part of the period  $T$  corresponding to uninterrupted replenishment of stock at the local stockpiles. The cost of unsatisfied demands at a local stockpile during this period is the product of (14) and  $k_T$ . We now determine the stockholding cost for the remaining part  $T - \mu_Y T$  of the planning period. In this case the stock level at the central stockpile is  $Y=0$ , and the stock level

$S_k$  at the  $k$ -th local stockpile may have any value from  $y_k$  down to  $x_k + 1$  with equal probability, in view of our assumption that the arrival of demands at the local stockpile is uniform. Thus

$$y_k \geq S_k \geq x_k + 1,$$

and

$$\varphi(S_k) = \frac{1}{y_k - x_k}. \quad (21)$$

The stockholding cost at the  $k$ -th local stockpile is (see (7) - (10))

$$L_k' = l \sum_{i=0}^{S_k} (S_k - i) \frac{1}{\lambda_k} \left( 1 - \sum_{j=0}^i e^{-\lambda_k(T - \mu_Y T)} \frac{[\lambda_k(T - \mu_Y T)]^j}{j!} \right), \quad (22)$$

and by (21)

$$L_k' = l \sum_{S_k=x_k+1}^{y_k} \varphi(S_k) \cdot \sum_{i=0}^{S_k} (S_k - i) \frac{1}{\lambda_k} \left( 1 - \sum_{j=0}^i e^{-\lambda_k(T - \mu_Y T)} \frac{[\lambda_k(T - \mu_Y T)]^j}{j!} \right). \quad (23)$$

The cost of not being able to meet demands at the local stockpile, due to interruption of deliveries from the central stockpile, is the product of the probability that all the local stockpiles receive demands exceeding the stock level  $Y$  at the center and the conditional expectation of the number of unsatisfied demands in each subdivision due to exhaustion of stock at the local stockpiles, when the total number of unsatisfied demands is  $i$ .

The probability that the number of demands exceeds the total available stock by  $i$  is

$$P(Y+i) = e^{-\Lambda T} \frac{(\Lambda T)^{Y+i}}{(Y+i)!}. \quad (24)$$

The probability that a given demand reaches the  $k$ -th local stockpile is the ratio of the corresponding intensity of demand to the total intensity for all  $z$  stockpiles:

$$P_k = \frac{\lambda_k}{\Lambda}. \quad (25)$$

The probability that exactly  $j$  demands reach the  $k$ -th stockpile when there is a total of  $i$  demands at all  $z$  local stockpiles is determined by considering a suitable system of Bernoulli trials:

$$P_k(j) = C_i' P_k^j q_k^{i-j}, \quad (26)$$

where  $C_i'$  is the number of combinations of  $i$  items  $j$  at a time, and  $q_k = 1 - P_k$ .

At the moment the stock  $Y$  in the central stockpile is exhausted, the  $k$ -th local stockpile still contains  $S_k$ . The expectation of a unsatisfied demand at the  $k$ -th stockpile under these conditions is

$$\mu(S_k) = \sum_{j=S_k+1}^i C_i^j P_k^j q_k^{i-j} \cdot (j - S_k). \quad (27)$$

The probability that the stock level at the  $k$ -th local stockpile is  $S_k$  is given by (21).

The expectation of an unsatisfied demand at the  $k$ -th stockpile due to the central stockpile being exhausted is

$$\mu_k = \sum_{S_k=x_k+1}^{y_k} \varphi_k(S_k) \sum_{j=S_k}^i C_i^j P_k^j q_k^{i-j} \cdot (j - S_k). \quad (28)$$

The cost incurred by unavailability of articles at the central stockpile is

$$Q_0 = q \sum_{i=0}^{\infty} l^{-\Delta T} \frac{(\Lambda T)^{(Y+i)}}{(Y+i)!} \sum_{k=1}^z \sum_{S_k=x_k+1}^{y_k} \varphi_k(S_k) \sum_{j=S_k+1}^i C_i^j P_k^j q_k^{i-j} \cdot (j - S_k). \quad (29)$$

All told, the cost of holding stock and being unable to meet demands for all  $z$  local stockpiles and the central stockpile supplying them is

$$F(Y, x_k, y_k) = L_0 + \sum_{k=1}^z (L_k + L_k') + Q_0 + \sum_{k=1}^z Q_k. \quad (30)$$

Substituting the actual values of  $L$  and  $Q$  in (30), we obtain the following expression:

$$\begin{aligned} F(Y, x_k, y_k) = & l \sum_{i=0}^y (Y-i) \frac{1}{\Lambda} \left( 1 - \sum_{j=0}^i e^{-\Delta T} \frac{(\Lambda T)^j}{j!} \right) + \\ & + \sum_{k=1}^z \left\{ l \frac{1}{\lambda_k} \sum_{i=0}^{y_k-x_k-1} (y_k-i) \sum_{j=0}^i e^{-\lambda_k \tau_k} \frac{(\lambda_k \tau_k)^j}{j!} + \right. \\ & + l \sum_{i=0}^{x_k} (x_k-i) \frac{1}{\lambda_k} \left( 1 - \sum_{j=0}^i e^{-\lambda_k \tau_k} \frac{(\lambda_k \tau_k)^j}{j!} \right) \left. \right\} \frac{\lambda_k T}{y_k - x_k} \frac{1}{\Lambda T} \times \\ & \times \left( Y - \sum_{i=0}^{Y-1} \sum_{j=0}^i e^{-\Delta T} \right) \frac{(\Lambda T)^j}{j!} + l \sum_{S_k=x_k+1}^{y_k} \varphi(S_k) \sum_{i=0}^{S_k} (S_k-i) \frac{1}{\lambda_k} \left( 1 - \right. \\ & \left. - \sum_{j=0}^i e^{-\lambda_k (T-\mu_y \tau)} \right) \frac{[\lambda_k (T-\mu_y \tau)]^j}{j!} \left. \right\} + q \sum_{i=0}^{\infty} e^{-\Delta T} \frac{(\Lambda T)^{(Y+i)}}{(Y+i)!} \times \end{aligned}$$

$$\begin{aligned}
& \times \sum_{k=1}^z \sum_{S_k=x_k+1}^{y_k} q_k(S_k) \sum_{j=S_k+1}^i C_i^j P_k^j q_k^{i-j} (j-S_k) + \\
& + \sum_{k=1}^z q_k \sum_{i=x_k+1}^{\infty} e^{-\lambda_k \tau_k} \frac{(\lambda_k \tau_k)^i}{i!} \times \\
& \times (i-x_k) \cdot \frac{\lambda_k T}{y_k - x_k} \cdot \frac{1}{\Lambda T} \left( Y - \sum_{i=0}^{Y-1} \sum_{j=0}^i e^{-\Lambda T} \frac{(\Lambda T)^j}{j!} \right). \quad (31)
\end{aligned}$$

The value of  $\mu_Y T$  is given by (19).

The optimum values of  $Y$ ,  $x_k$ , and  $y_k$  may be determined by minimizing the function (31).

### Bibliography

1. Bellman, R. and S. Dreyfus. Applied Dynamic Programming. — Princeton Univ. Press. 1962.
2. Druzhinin, G. V. Nadezhnost' ustroystv avtomatiki (Reliability of Automatic Devices). Moskva, "Energiya." 1964.
3. Feller, W. An Introduction to Probability Theory and its Applications, Volume 1. New York, John Wiley and Sons. 1950.
4. Gipsh, L. A. and V. P. Peka. Opredelenie optimal'nogo razmera zapasa pri sluchainom sprosye (Determination of Optimal Stock Level for Random Demand). Present collection, p. 108.

S. G. Zvonov

*APPLICATION OF THE TWO-DIMENSIONAL  
Z-TRANSFORM IN DETERMINING THE  
AUTOCORRELATION FUNCTION OF THE INPUT  
SIGNAL IN A LINEAR SAMPLED-DATA SYSTEM*

The two-dimensional z-transform is defined, a table given, and a method described for seeking the statistical characteristics of the input signal of a linear sampled-data system with constant parameters. All these problems are considered in relation to unbiased discrete functions of two arguments  $f(n, m)$ .

The value of operator methods in investigations of automatic control systems has long been recognized. Operator methods are applied to the statistical dynamics of automatic systems in the monograph /1/, whose main subject is continuous systems.

Together with continuous systems, sampled-data systems have been extensively developed, and operator methods play an important role in their analysis /2, 5/. Much credit is due to Ya. Z. Tsypkin for the development and extension of these methods. The statistical dynamics of sampled-data systems is studied in /4, 5, 6/, in which the analysis and synthesis are based on the theory of finite-difference equations, the basic dynamic characteristic of sampled-data systems in the time domain being the pulsed weighting function.

We wish to investigate the use of operator methods analogous to those considered in /1/, in particular, the two-dimensional z-transform, in the dynamic analysis of sampled-data systems.

# 1. BASIC NOTIONS AND DEFINITIONS

Let  $f(n, m)$  be a discrete function of two variables  $n$  and  $m$  ( $n, m = 0, 1, 2, \dots$ ), representing a two-dimensional train of  $\delta$ -pulses of a definite amplitude, with period  $T=1$  in each of the variables; the function is assumed to increase at most exponentially, so that

$$\lim_{n \rightarrow \infty} \frac{|f(n, m)|}{Me^{cn+dm}} = \lim_{m \rightarrow \infty} \frac{|f(n, m)|}{Me^{cn+dm}} = 0, \quad (1)$$



where  $M, c, d$  are certain constants;  $c$  and  $d$  are the growth indicators of  $f(n, m)$  in the variables  $n$  and  $m$ , respectively.

The expression

$$F(z, z_1) = \sum_{n=0}^{\infty} \sum_{m=0}^{\infty} f(n, m) z^{-n} z_1^{-m} = Z_2[f(n, m)], \quad (2)$$

where  $z = e^p$ ,  $z_1 = e^{p_1}$ ,  $p$  and  $p_1$  being the complex arguments of the corresponding Laplace transform, is called the two-dimensional  $z$ -transform of the function  $f(n, m)$ , and the latter is called the pre-image of its transform.

Formula (2) may be written

$$F(z, z_1) = \sum_{n=0}^{\infty} z^{-n} \sum_{m=0}^{\infty} f(n, m) z_1^{-m}, \quad (3)$$

where the inner sum is the one-dimensional  $z$ -transform of the function  $f(n, m)$  in the variable  $m$  with parameter  $n$ . Denoting the one-dimensional  $z$ -transform in the variable  $m$  by  $Z_m$ , we write

$$Z_m[f(n, m)] = \sum_{m=0}^{\infty} f(n, m) z_1^{-m} = F_m(n, z_1). \quad (4)$$

Expression (2) then becomes

$$F(z, z_1) = \sum_{n=0}^{\infty} F_m(n, z_1) z^{-n} = Z_n[F_m(n, z_1)], \quad (5)$$

where  $Z_n$  denotes the one-dimensional  $z$ -transform in the variable  $n$ , with parameter  $z_1$ .

In view of (4),

$$F(z, z_1) = Z_n\{Z_m[f(n, m)]\} \quad (6)$$

and so

$$Z_2 = Z_n Z_m. \quad (7)$$

Thus the two-dimensional  $z$ -transform is equivalent to successive application of two one-dimensional one-sided transforms in the respective variables; moreover, the order of application is immaterial:

$$Z_n Z_m = Z_m Z_n. \quad (8)$$

If  $F(z, z_1) = Z_2[f(n, m)]$ , the analogues of (6) and (7) for the inverse two-dimensional  $z$ -transform  $Z_2^{-1}$  are

$$Z_2^{-1} = Z_n^{-1} Z_m^{-1} \quad (9)$$

and

$$f(n, m) = Z_2^{-1}[F(z, z_1)]. \quad (10)$$

Applying the inversion formula for the one-dimensional  $z$ -transform to  $Z_n$  and  $Z_m$  [2, 5], we derive the following inversion formula for the two-dimensional  $z$ -transform:

$$f(n, m) = -\frac{1}{4\pi^2} \oint_{|z|=e^c} \oint_{|z_1|=e^d} F(z, z_1) z^{n-1} z_1^{m-1} dz dz_1, \quad (11)$$

where  $|z|=e^c$  and  $|z_1|=e^d$  are circles whose interiors contain all the poles of  $F(z, z_1)$  as a function of  $z$  and  $z_1$ , respectively.

The basic properties of the two-dimensional  $z$ -transform are analogous to those of the two-dimensional Laplace transform [1]; they may be proved on the basis of (7) and the corresponding properties of the one-dimensional  $z$ -transform [2, 5].

## 2. RELATION OF THE TWO-DIMENSIONAL $z$ -TRANSFORM TO THE LIMIT ONE-DIMENSIONAL TRANSFORM

In investigations of the statistical properties of discrete systems it is often necessary to use functions of two arguments  $n$  and  $m$ , corresponding to two instants of time in the operation of the system. In the steady-state case it is convenient to introduce the new variable

$$l = n - m. \quad (12)$$

To distinguish between transient and steady regimes in the performance of the system we introduce the notion of the preset period of the system's operation

$$N = \min(n, m). \quad (13)$$

The condition for transition to a steady regime is  $N \rightarrow \infty$ . When this condition is satisfied the quantity  $l = n - m$  has a definite sense, though both variables  $n$  and  $m$  approach infinity.

Thus, we must determine properties of the two-dimensional  $z$ -transform which determine the behavior of the pre-image not only when  $n = \infty$  and  $m = \infty$  but also when  $N \rightarrow \infty$ .

Suppose some property of a discrete system is described by a function  $f(n, m)$  whose two-dimensional  $z$ -transform is

$$\Phi(z, z_1) = \sum_{n=0}^{\infty} \sum_{m=0}^{\infty} f(n, m) z^{-n} z_1^{-m}. \quad (14)$$

The domain of summation consists of the entire first quadrant of the  $n, m$ -plane (Figure 1). Let us divide this domain into two domains  $G_1$  and  $G_2$  as illustrated; summing separately in each of these domains and along the bisector, we have

$$\Phi(z, z_1) = \sum_{n=0}^{\infty} \sum_{m=n}^{\infty} f(n, m) z^{-n} z_1^{-m} + \sum_{m=0}^{\infty} \sum_{n=m}^{\infty} f(n, m) z^{-n} z_1^{-m} - \sum_{n=0}^{\infty} f(n, n) z^{-n} z_1^{-n}. \quad (15)$$

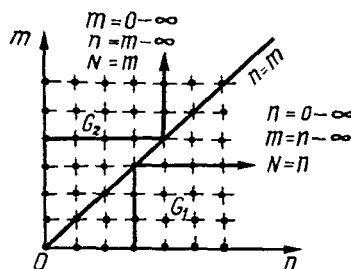


FIGURE 1. Domains, order, and limits of summation in (14).

We now replace the variables  $n$  and  $m$  by  $l=n-m$  and  $N=\min(n, m)$ . In the domain  $G_2$ ,  $m \geq n$ , therefore

$$l < 0, \quad n = N, \quad m = N - l. \quad (16)$$

In  $G_1$  we have  $n \geq m$ , and

$$l > 0, \quad m = N, \quad n = N + l. \quad (17)$$

After appropriate changes in the limits of summation, we obtain

$$\Phi(z, z_1) = \sum_{N=0}^{\infty} (z, z_1)^{-N} \left[ \sum_{l=0}^{\infty} f(N+l, N) z^{-l} + \sum_{l=-\infty}^{\infty} f(N, N-l) z_1^l - f(N, N) \right]. \quad (18)$$

It is clear that

$$\sum_{l=0}^{\infty} f(N+l, N) z^{-l} = F_1(z, N) \quad (19)$$

and

$$\sum_{l=-\infty}^0 f(N, N-l) z_1^l = F_2(z_1, N) \quad (20)$$

are the one-dimensional one-sided  $z$ -transforms of the functions  $f(N+l, N)$  and  $f(N, N-l)$  in the variable  $l$ , with parameter  $N$ . Thus (18) may be written

$$\Phi(z, z_1) = \sum_{N=0}^{\infty} (zz_1)^{-N} [F_1(z, N) + F_2(z_1, N) - f(N, N)]. \quad (21)$$

Formula (21) is the one-dimensional  $z$ -transform of the function  $F_1(z, N) + F_2(z_1, N) - f(N, N)$  in the variable  $N$ .

By the theorem on the finiteness of the one-dimensional  $z$ -transform

$$\lim_{N \rightarrow \infty} [F_1(z, N) + F_2(z_1, N) - f(N, N)] = \lim_{z z_1 \rightarrow 1} \frac{z z_1 - 1}{z z_1} \Phi(z, z_1). \quad (22)$$

Let us consider some particular cases.

Let  $f(n, m) = f(n - m)$ . Then  $f(N, N) = f(0)$ ,  $f(N + l, N) = f_1(l)$ , and  $f(N, N - l) = f_2(-l)$ . The corresponding one-dimensional transforms are

$$F_1(z) = \sum_{l=0}^{\infty} f_1(l) z^{-l}, \quad (23)$$

$$F_2(z_1) = \sum_{l=0}^{\infty} f_2(-l) z_1^{-l}, \quad (24)$$

and (21) becomes

$$\Phi(z, z_1) = \frac{z z_1}{z z_1 - 1} [F_1(z) + F_2(z_1) - f(0)]. \quad (25)$$

If  $f(l)$  is an even function, i. e.,

$$f(n, m) = f(|n - m|),$$

then

$$\Phi(z, z_1) = \frac{z z_1}{z z_1 - 1} [F(z) + F(z_1) - f(0)]. \quad (26)$$

However, if  $f(n, m)$  depends not only on the difference between the arguments but also on  $N$ , then in the general case the input process is a transient which approaches a steady process as  $N \rightarrow \infty$ . The steady-state condition may be derived from (21) and (22) by setting

$$\left. \begin{aligned} \lim_{N \rightarrow \infty} F_1(z, N) &= F_1(z), \\ \lim_{N \rightarrow \infty} F_2(z_1, N) &= F_2(z_1), \\ \lim_{N \rightarrow \infty} f(N, N) &= f(0). \end{aligned} \right\} \quad (27)$$

Accordingly, we have

$$\lim_{z z_1 \rightarrow 1} \frac{z z_1 - 1}{z z_1} \Phi(z, z_1) = F_1(z) + F_2(z^{-1}) - f(0). \quad (28)$$

If  $f(n, m) = f(|n - m|)$ , then  $F_1(z) = F_2(z) = F(z)$ , and

$$\lim_{z z_1 \rightarrow 1} \frac{z z_1 - 1}{z z_1} \Phi(z, z_1) = F(z) + F(z^{-1}) - f(0). \quad (29)$$

Note that for a steady regime (29) coincides with the formula for the two-sided  $z$ -transform [2, 5].

### 3. RELATION BETWEEN THE TWO-DIMENSIONAL $z$ -TRANSFORMS OF THE AUTOCORRELATION FUNCTIONS OF THE INPUT AND OUTPUT SIGNALS OF A LINEAR SAMPLED-DATA SYSTEM

As shown in [4], the autocorrelation function  $K_y(n, m)$  of the output signal is related to the autocorrelation function  $K_x(n, m)$  of the input signal of a nonstationary sampled-data system, whose pulsed weighting function is  $\omega(n, m)$ , by the formula

$$K_y(n, m) = \sum_{l=0}^n \sum_{k=0}^m \omega(n, l) \omega(m, k) K_x(l, k). \quad (30)$$

Multiplying both sides of (30) by  $z^{-n}z_1^{-m}$  and summing over  $n$  and  $m$  from 0 to  $\infty$ , we obtain

$$\begin{aligned} & \sum_{n=0}^{\infty} \sum_{m=0}^{\infty} K_y(n, m) z^{-n} z_1^{-m} = \\ & = \sum_{n=0}^{\infty} \sum_{m=0}^{\infty} z^{-n} z_1^{-m} \left[ \sum_{l=0}^n \sum_{k=0}^m \omega(n, l) \omega(m, k) K_x(l, k) \right]. \end{aligned} \quad (31)$$

Denote the two-dimensional  $z$ -transform of the output-signal autocorrelation function by  $\Phi_{K_y}(z, z_1)$ , and change the order of a summation on the right-hand side; then

$$\Phi_{K_y}(z, z_1) = \sum_{l=0}^{\infty} \sum_{k=0}^{\infty} K_x(l, k) \left[ \sum_{n=l}^{\infty} \omega(n, l) z^{-n} \sum_{m=k}^{\infty} \omega(m, k) z_1^{-m} \right]. \quad (32)$$

By analogy with the incomplete one-sided Laplace transform, we call the expressions in square brackets

$$\left. \begin{aligned} \sum_{n=l}^{\infty} \omega(n, l) z^{-n} &= W_1(z, l), \\ \sum_{m=k}^{\infty} \omega(m, k) z_1^{-m} &= W_1(z_1, k) \end{aligned} \right\} \quad (33)$$

the incomplete one-sided  $z$ -transforms of the weighting function.

Therefore, (32) may be written

$$\Phi_{K_y}(z, z_1) = \sum_{l=0}^{\infty} \sum_{k=0}^{\infty} W_1(z, l) W_1(z_1, k) K_x(l, k). \quad (34)$$

Thus the two-dimensional transform of the output-signal autocorrelation function is determined by the input-signal autocorrelation function and the incomplete  $z$ -transforms of the weighting function.

For stationary systems we have

$$\left. \begin{aligned} W_1(z, l) &= z^{-l} W(z); \\ W_1(z_1, k) &= z_1^{-k} W(z_1), \end{aligned} \right\} \quad (35)$$

where  $W(z)$  is the transfer function of the system.

Substituting (35) in (34) and denoting the transform of the input-signal autocorrelation function by  $\Phi_{K_x}(z, z_1)$ , we obtain the equality

$$\Phi_{K_y}(z, z_1) = W(z) W(z_1) \Phi_{K_x}(z, z_1), \quad (36)$$

which determines the transform of the output-signal autocorrelation function for a system with constant parameters and weighting function  $w(n-m)$ .

#### 4. AUTOCORRELATION FUNCTION OF THE OUTPUT SIGNAL

Let us consider the case of a sampled-data dynamic system whose input is a steady random signal  $x(n)$  with autocorrelation function  $K_x(l)$  ( $l=n-m$ ).

The two-dimensional  $z$ -transform of the output-signal autocorrelation function is then given by (36).

$K_x(l)$  is an even function with one-dimensional transform

$$F_x(z) = \sum_{l=0}^{\infty} K_x(l) z^{-l}, \quad (37)$$

so that by (26) and (36)

$$\Phi_{K_x}(z, z_1) = \frac{zz_1}{zz_1 - 1} [F_x(z) + F_x(z_1) - K_x(0)]; \quad (38)$$

$$\Phi_{K_y}(z, z_1) = \frac{zz_1}{zz_1 - 1} W(z) W(z_1) [F_x(z) + F_x(z_1) - K_x(0)]. \quad (39)$$

The one-dimensional  $z$ -transforms of most autocorrelation functions may be expressed in the form of a proper fraction

$$F_x(z) = \frac{L(z)}{N(z)}. \quad (40)$$

The same holds for transfer functions of sampled-data systems:

$$W(z) = \frac{Q(z)}{R(z)}. \quad (41)$$

Let us write (39) in the form

$$\Phi_{K_y}(z, z_1) = \frac{zz_1}{zz_1 - 1} [\mathcal{W}(z) \mathcal{W}(z_1) F_x(z) + \\ + \mathcal{W}(z) \mathcal{W}(z_1) F_x(z_1) - \mathcal{W}(z) \mathcal{W}(z_1) K_x(0)] \quad (42)$$

and express  $\mathcal{W}(z)$  and  $\mathcal{W}(z) F_x(z)$  as sums of partial fractions:

$$\mathcal{W}(z) = \sum_{i=1}^r \frac{A_i z}{z - a_i}; \quad (43)$$

$$\mathcal{W}(z) F_x(z) = \sum_{k=1}^{r+v} \frac{B_k z}{z - a_k}, \quad (44)$$

where  $a_i = e^{-\lambda_i}$ ,  $a_k = e^{-\lambda_k}$ , and  $r$  are the numbers of poles of  $\mathcal{W}(z)$  and  $F_x(z)$ , respectively.

The coefficients of the expansions are determined by the usual rules:

$$A_i = \frac{Q(a_i)}{R'(a_i)}, \quad (46)$$

$$B_k = \frac{Q(a_k) L(a_k)}{[R(a_k) N(a_k)]}. \quad (47)$$

Similarly,

$$\mathcal{W}(z_1) = \sum_{i=1}^r \frac{A_i z_1}{z_1 - a_i}, \quad (48)$$

$$\mathcal{W}(z_1) F_x(z_1) = \sum_{k=1}^{r+v} \frac{B_k z_1}{z_1 - a_k}. \quad (49)$$

Assuming that all the poles of  $\mathcal{W}(z)$  and  $F_x(z)$  are simple and that these functions have no common poles, we use (43), (44), (48), (49) to transform (42) to the form

$$\Phi_{K_y}(z, z_1) = \sum_{i=1}^r \sum_{k=1}^{r+v} A_i B_k F(a_i, a_k) - \frac{1}{2} K_x(0) \sum_{i=1}^r \sum_{k=1}^r A_i A_k F(a_i, a_k), \quad (50)$$

where

$$F(a_i, a_k) = \frac{zz_1}{zz_1 - 1} \left[ \frac{zz_1}{(z_1 - a_i)(z - a_k)} + \frac{zz_1}{(z - a_i)(z_1 - a_k)} \right]. \quad (51)$$

To determine the autocorrelation function we must return to the pre-image space. Using the linearity of the direct and inverse two-dimensional z-transform, we find that (50) corresponds to the following pre-image:

$$K_y(n, m) = \sum_{i=1}^r \sum_{k=1}^{r+v} A_i B_k K_x(a_i, a_k) - \frac{1}{2} K_x(0) \sum_{i=1}^r \sum_{k=1}^r A_i A_k K_x(a_i, a_k), \quad (52)$$

where  $K_x(a_i, a_k)$  is the pre-image of  $F(a_i, a_k)$ .

Let us determine the pre-image of the transform

$$F(z, z_1) = \frac{zz_1}{zz_1 - 1} \left[ \frac{zz_1}{(z - a_i)(z_1 - a_k)} + \frac{zz_1}{(z_1 - a_i)(z - a_k)} \right]. \quad (53)$$

Writing the inversion formula for the expression

$$F_1(z, z_1) = \frac{zz_1}{zz_1 - 1} \frac{zz_1}{(z - a_i)(z_1 - a_k)}$$

for  $n \geq m$  in the form

$$f_1(n, m) = \frac{1}{2\pi j} \oint_{|z|=c} \frac{z}{z - a_i} z^{n-1} \left[ \frac{1}{2\pi j} \oint_{|z_1|=c} \frac{zz_1^2}{(zz_1 - 1)(z_1 - a_k)} z^{m-1} dz_1 \right] dz \quad (54)$$

and using the Residue Theorem, we obtain

$$f_1(n, m) = \frac{a_i^{n-m}}{1 - a_i a_k} [1 - (a_i a_k)^{m+1}], \quad n \geq m. \quad (55)$$

To find the pre-image of  $F_1(z, z_1)$  for  $m \geq n$ , we must rewrite (54) in the form

$$f_1(n, m) = \frac{1}{2\pi j} \oint_{|z_1|=c} \frac{z_1}{z_1 - a_k} z_1^{m-1} \left[ \frac{1}{2\pi j} \oint_{|z|=c} \frac{z^2 z_1}{(zz_1 - 1)(z - a_i)} z^{n-1} dz \right] dz_1. \quad (56)$$

Application of the Residue Theorem yields

$$f_1(n, m) = \frac{a_k^{m-n}}{1 - a_i a_k} [1 - (a_i a_k)^{n+1}], \quad m \geq n. \quad (57)$$

We introduce new variables for the domains  $G_1$  and  $G_2$  (Figure 1):

$$l = |n - m| \text{ and } N = \min(n, m),$$

since in the domain  $G_1$  ( $n \geq m$ )

$$n - m = l, \quad n = N,$$

and in  $G_2$  ( $m \geq n$ )

$$n - m = -l, \quad m = N.$$



In terms of the new variables, formulas (55) and (57) become

$$\left. \begin{aligned} f_1(n, m) &= \frac{a_i^{l_i}}{1 - a_i a_k} [1 - (a_i a_k)^{N+1}], \quad n \geq m, \\ f_1(n, m) &= \frac{a_k^{l_k}}{1 - a_i a_k} [1 - (a_i a_k)^{N+1}], \quad m \geq n. \end{aligned} \right\} \quad (58)$$

The pre-images of the transform

$$F_2(z, z_1) = \frac{zz_1}{zz_1 - 1} \cdot \frac{2zz_1}{(z_1 - a_i)(z - a_k)}$$

for  $n \geq m$  and  $m \geq n$  differ from (58) only in that  $a_i$  and  $a_k$  are interchanged. Thus

$$\left. \begin{aligned} f_2(n, m) &= \frac{a_k^{l_k}}{1 - a_i a_k} [1 - (a_i a_k)^{N+1}], \quad n \geq m, \\ f_2(n, m) &= \frac{a_i^{l_i}}{1 - a_i a_k} [1 - (a_i a_k)^{N+1}], \quad m \geq n. \end{aligned} \right\} \quad (59)$$

Adding (58) and (59), we see that for all  $n \geq 0$  and  $m \geq 0$  the two-dimensional  $z$ -transform (53) has the pre-image

$$f(n, m) = \frac{1}{1 - a_i a_k} (a_i^{l_i} + a_k^{l_k}) [1 - (a_i a_k)^{N+1}] \quad (60)$$

Let us consider some special cases.

1. One of the terms of the transform  $\Phi_{K_0}(z, z_1)$  has the form

$$F(a_i, a_i) = \frac{zz_1}{zz_1 - 1} \cdot \frac{2zz_1}{(z - a_i)(z_1 - a_i)}. \quad (61)$$

Setting  $a_k = a_i$  in (60), we obtain

$$f(a_i, a_i) = \frac{2a_i^{l_i}}{1 - a_i^2} [1 - a_i^{2(N+1)}]. \quad (62)$$

2. When  $a_i \rightarrow 1$ , the right-hand side of (62) becomes an indeterminate expression of the type  $\frac{0}{0}$ . Using l'Hospital's rule, we find that the transform

$$F(1, 1) = \frac{zz_1}{zz_1 - 1} \cdot \frac{2zz_1}{(z - 1)(z_1 - 1)} \quad (63)$$

has the pre-image

$$f(1, 1) = 2(N+1). \quad (64)$$

3. If  $a_k = a_i^{-1}$ , the right-hand side of (60) is again indeterminate; reasoning as before, we see that the two-dimensional transform

$$F(a_i, a_i^{-1}) = \frac{zz_1}{zz_1 - 1} \left[ \frac{zz_1}{(z - a_i)(z_1 - a_i^{-1})} + \frac{zz_1}{(z_1 - a_i)(z - a_i^{-1})} \right] \quad (65)$$

has the pre-image

$$f(a_i, a_i^{-1}) = (N+1)(a_i^{|k|} + a_i^{-|k|}). \quad (66)$$

4. When  $a_i \rightarrow 0$ , the two-dimensional transform

$$F(0, 0) = \frac{zz_1}{zz_1 - 1} \quad (67)$$

has the pre-image

$$f(0, 0) = \begin{cases} 1 & \text{if } l=0, \\ 0 & \text{if } l \neq 0. \end{cases} \quad (68)$$

The function (68) coincides with the lattice  $\sigma$ -function [4], which is the discrete analogue of the Dirac  $\delta$ -function for  $l = n - m$ :

$$\sigma(n-m) = \begin{cases} 1 & \text{if } n=m; \\ 0 & \text{if } n \neq m. \end{cases} \quad (69)$$

We collect all our results in a table of transforms and pre-images, which contains all the data required for determining the statistical characteristics of the output variable in a sampled-data dynamic system.

TABLE 1.

Transform $F(z, z_1)$	Pre-image $f(n, m)$
$\frac{zz_1}{zz_1 - 1}$	$\sigma(n-m) = \begin{cases} 1 & \text{if } n=m, \\ 0 & \text{if } n \neq m. \end{cases}$
$\frac{zz_1}{zz_1 - 1} \frac{2zz_1}{(z-1)(z_1-1)}$	$2(N+1), \quad N = \min(n, m).$
$\frac{zz_1}{zz_1 - 1} \frac{2zz_1}{(z-a)(z_1-a)}$	$\frac{2a^{ k }}{1-a^2} [1-a^2(N+1)], \quad \begin{matrix} l = n-m, \\ a = e^{-\lambda}. \end{matrix}$
$\frac{zz_1}{zz_1 - 1} \left[ \frac{zz_1}{(z-a)(z_1-a^{-1})} + \frac{zz_1}{(z-a^{-1})(z_1-a)} \right]$	$(N+1)(a^{ k } + a^{- k })$
$\frac{zz_1}{zz_1 - 1} \left[ \frac{zz_1}{(z-a_i)(z_1-a_k)} + \frac{zz_1}{(z-a_k)(z_1-a_i)} \right]$	$\frac{1}{1-a_i a_k} (a_i^{ k } + a_k^{ k }) [1 - (a_i a_k)^{N+1}];$ $a_i = e^{-\lambda_i}, \quad a_k = e^{-\lambda_k}.$

Using Table 1 and formulas (50), (52) one can solve various problems in the statistical analysis of sampled-data systems. In so doing the presence of the factor  $[1 - (a_i a_k)^{N+1}]$  in the component (60) of the

autocorrelation function makes it possible to use the table and the formulas to study transients in sample-data systems.

## 5. EXAMPLES

1. Let us find the autocorrelation function at the output of a sampled-data system with transfer function

$$W(z) = \frac{1.4z^2 - 1.068z}{z^2 - 1.556z - 0.607} \quad (70)$$

when the input is discrete white noise of unit intensity, whose autocorrelation function is  $K_x(n, m) = \sigma(n-m)/4$ .

The two-dimensional transform of the input-signal autocorrelation function is, according to Table 1,

$$\Phi_{Kx}(z, z_1) = \frac{zz_1}{zz_1 - 1}.$$

In applying (43) - (49), note that

$$W(z) = \frac{z}{z - e^{-0.2}} + \frac{0.4z}{z - e^{-0.3}} \quad (71)$$

and

$$\begin{aligned} a_1 &= e^{-0.2}, & A_1 &= B_1 = 1, \\ a_2 &= e^{-0.3}, & A_2 &= B_2 = 0.4. \end{aligned}$$

By (50) and (51),

$$\begin{aligned} \Phi_{Ky}(z, z_1) &= \frac{zz_1}{zz_1 - 1} \left[ \frac{zz_1}{(z - a_1)(z_1 - a_1)} + \frac{0.4zz_1}{(z - a_1)(z_1 - a_2)} + \right. \\ &\quad \left. + \frac{0.4zz_1}{(z - a_2)(z_1 - a_1)} + \frac{0.16zz_1}{(z - a_2)(z_1 - a_2)} \right]. \end{aligned} \quad (72)$$

Using Table 1 and formula (52), we find the output-signal autocorrelation function:

$$\begin{aligned} K_y(n, m) &= 3.035e^{-0.2|n-m|} \{ [1 - e^{-0.4(N+1)}] + 0.335(1 + e^{-0.1|n-m|}) \times \\ &\quad \times [1 - e^{-0.5(N+1)}] + 0.117e^{-0.1|n-m|} [1 - e^{-0.6(N+1)}] \}. \end{aligned} \quad (73)$$

Letting  $N \rightarrow \infty$  in (73), we can determine  $K_y(n, m)$  for the steady regime.

2. Let us determine the transfer function  $W(z)$  of a discrete filter which transforms discrete white noise of unit intensity into a random process  $y(n)$  with autocorrelation function

$$K_y(n, m) = D e^{-\alpha|n-m|}. \quad (74)$$

By Table 1:

$$\Phi_{Ky}(z, z_1) = \frac{zz_1}{zz_1 - 1} \frac{zz_1 D(1 - e^{-2\alpha})}{(z - e^{-\alpha})(z_1 - e^{-\alpha})[1 - e^{-2\alpha(N+1)}]}, \quad (75)$$

$$\Phi_{Kx}(z, z_1) = \frac{zz_1}{zz_1 - 1}. \quad (76)$$

Using (36), (75), and (76), we have

$$W(z)W(z_1) = \frac{zz_1 D(1 - e^{-2\alpha})}{(z - e^{-\alpha})(z_1 - e^{-\alpha})[1 - e^{-2\alpha(N+1)}]}, \quad (77)$$

whence

$$W(z) = \frac{z}{z - e^{-\alpha}} \sqrt{\frac{D(1 - e^{-2\alpha})}{1 - e^{-2\alpha(N+1)}}}. \quad (78)$$

For the steady regime, we let  $N \rightarrow \infty$  in (78) and obtain

$$W(z) = \frac{z\sqrt{D(1 - e^{-2\alpha})}}{z - e^{-\alpha}}. \quad (79)$$

Formula (79) was obtained in [4] in the form of a difference equation.

The author is indebted to A. N. Sklyarevich for valuable advice and assistance.

#### Bibliography

1. A. N. Sklyarevich. *Operatornye metody v statisticheskoi dinamike avtomaticheskikh sistem* (Operator Methods in the Statistical Dynamics of Automatic Systems). Moskva, "Nauka," 1965.
2. Ya. Z. Tsypkin. *Teoriya lineinykh impul'snykh sistem* (Theory of Linear Sampled-Data Systems). Moskva, Fizmatgiz, 1963.
3. A. A. Krasovskii and G. S. Pospelov. *Osnovy avtomatiki i tekhnicheskoi kibernetiki* (Fundamentals of Automatics and Technical Cybernetics). Moskva-Leningrad, Gosenergoizdat, 1962.
4. Krut'ko, P. D. *Statisticheskaya dinamika impul'snykh sistem* (Statistical Dynamics of Sampled-Data Systems). Moskva, "Sovetskoe Radio," 1963.
5. Kuzin, L. T. *Raschet i proektirovanie diskretnykh sistem upravleniya* (Design and Planning of Discrete Control Systems). Moskva, Mashgiz, 1962.
6. Perov, V. P. *Statisticheskii sintez impul'snykh sistem* (Statistical Synthesis of Sampled-Data Systems). Moskva, "Sovetskoe Radio," 1959.

*Ya. Ya. Osis*

# MINIMIZATION OF THE NUMBER OF CHECK POINTS

The author considers the minimization of the number of check points for the state of a complex object, the latter being represented by a so-called graph-model.

The essence of the method is to find minimal externally stable subsets of a directed graph. Algorithms are given for solution of this problem on a computer.

The proposed graph-model may also be used for localization and detection of errors if the sets of parameters are disjoint.

In this paper we consider the problem of minimizing the number of check points or diagnostic-information outputs. To this end we propose the representation of complex mechanical, biological, physiological and other systems by graph-models; the method may also be used to develop procedures for detection and localization of errors.

From the mathematical viewpoint the graph-model of a system is given by the following data:

- 1) a finite set of parameters (symptoms)

$$X = \{a, b, c, \dots, x, y, z\}, \quad (1)$$

the vertices of the graph;

- 2) a finite set of edges  $U$ , where

$$X \cap U = \emptyset; \quad (2)$$

- 3) a ternary predicate, the incidence predicate:

$$P(x, u, y), \quad x, y \in X, \quad u \in U; \quad (3)$$

- 4) statement formulas

$$\forall x, y [P(x, u, y) \rightarrow ] P(y, u, x)]; \quad (4)$$

- 5)  $\exists x P(x, u, x).$  (5)

By (3) and (4) a graph-model is a directed graph. Formula (5) states that the graph may contain loops at single vertices. Since the graph may be disconnected, the parameters of the system under consideration need not be correlated.

The more reliable the initial information, the more reliable the graph as a mathematical model of the system. Once the graph has been set up, one can use the formal mathematical apparatus of Graph Theory [1].

We first formulate the basic idea underlying the algorithm for minimization of the number of controlled parameters by means of a graph-model of the object. The number of vertices (parameters) in the graph-model is reduced by mapping the vertices rejected in the minimization process onto the remaining vertices by considering the shortest path from the former to the latter:

$$l \leq 1, \quad (6)$$

where  $l$  is the number of edges in the shortest path.

Thus any member of the initial set of vertices is either a member of the minimizing subset or is the initial vertex of an edge whose other vertex is in the minimizing subset.

Mathematically, the problem is solved by finding the minimal externally stable subsets of the graph. An externally stable subset of the graph is a subset

$$T \subseteq X, \quad (7)$$

which satisfies the formula

$$\forall x [x \in X, x \notin T \rightarrow (\Gamma_x \cap T \neq \emptyset)], \quad (8)$$

where  $\Gamma_x$  is the image of  $X$  under the (many-valued) mapping described above.

We are not interested in the whole family of externally stable subsets  $\Gamma$ , where

$$X \in \Gamma, T \in \Gamma, \quad (9)$$

but only in the minimal subsets:

$$\Gamma_{\min} \subseteq \Gamma, T_{\min} \in \Gamma_{\min}. \quad (10)$$

where  $\Gamma_{\min}$  is the family of minimal externally stable subsets.

There is a well-known algorithm, due to C. Berge [1], for finding  $T_{\min}$ ; it is based on repeated constructions of graphs.

In this paper we try to establish algorithms which are more formal in nature and more suitable for computer applications.

A theoretical approach to the definition of  $\Gamma_{\min}$  may be based on the equality

$$\Gamma_{\min} = (\Gamma_a \cup \Gamma_a) \cap (\Gamma_b \cup \Gamma_b) \cap \dots \cap (\Gamma_n \cup \Gamma_n) \cap \dots \cap (\Gamma_z \cup \Gamma_z), \quad (11)$$

where

$$\forall x (\Gamma_x \subseteq \Gamma, T_x \in \Gamma_x, x \in T_x) \quad (12)$$

and

$$\forall x (\Gamma_x = \Gamma_m \cup \Gamma_{m+1} \cup \dots \cup \Gamma_r), \quad (13)$$

Theorem. If  $T \in \Gamma$ , then the minor

$$D = [d_{s,t}], \quad (26)$$

of the matrix  $C$ , consisting of the rows, such that

$$\forall s (s \in I \wedge s \notin L) \quad (27)$$

and the columns, such that

$$\forall t (t \in L) \quad (28)$$

satisfies the condition

$$\forall s \exists t (d_{s,t} = 0). \quad (29)$$

Since the algebraic algorithm is a matrix representation of externally stable subsets, the proof follows from (8). The minimal externally stable subsets are those satisfying (29) for  $t = t_{\min}$ .

In practice,  $T_{\min}$  may be constructed by considering the vertices for which the sum of elements of the corresponding rows of  $C$  is minimal:

$$\sum_{j=1}^n C_{ij} = r_{i \min} \quad (30)$$

and the vertices with maximal sum of elements of the corresponding columns of the matrix  $D$ :

$$\sum_{s=1}^n d_{s,t} = k_{t \max}. \quad (31)$$

Corollary. All the externally stable subsets contain vertices corresponding to zero rows of the matrix  $C$ , i. e.,

$$\forall i (r_i = 0 \rightarrow i \in T). \quad (32)$$

Let us consider an example. The adjacency matrix of the graph of Figure 1 is

$$A = \begin{matrix} & \begin{matrix} a & b & e & g & f \end{matrix} \\ \begin{matrix} a \\ b \\ e \\ g \\ f \end{matrix} & \begin{bmatrix} 0 & 0 & 0 & 0 & 0 \\ 1 & 0 & 0 & 0 & 0 \\ 0 & 1 & 0 & 0 & 0 \\ 0 & 0 & 1 & 0 & 0 \\ 0 & 1 & 0 & 1 & 0 \end{bmatrix} \end{matrix} \quad (33)$$

For  $t=1$  and  $t=2$  there is no matrix  $D$  satisfying condition (29). For  $t=3$  we get four matrices:

$$\begin{aligned}
 D_1 &= \begin{array}{c} \begin{array}{ccc} & a & b & e \end{array} \\ \begin{array}{c} g \\ f \end{array} \begin{array}{|ccc|} \hline 0 & 0 & 1 \\ 0 & 1 & 0 \\ \hline \end{array} \end{array} \\
 D_2 &= \begin{array}{c} \begin{array}{ccc} & a & b & g \end{array} \\ \begin{array}{c} e \\ f \end{array} \begin{array}{|ccc|} \hline 0 & 1 & 0 \\ 0 & 1 & 1 \\ \hline \end{array} \end{array} \\
 D_3 &= \begin{array}{c} \begin{array}{ccc} & a & e & g \end{array} \\ \begin{array}{c} b \\ f \end{array} \begin{array}{|ccc|} \hline 1 & 0 & 0 \\ 0 & 0 & 1 \\ \hline \end{array} \end{array} \\
 D_4 &= \begin{array}{c} \begin{array}{ccc} & a & e & f \end{array} \\ \begin{array}{c} b \\ g \end{array} \begin{array}{|ccc|} \hline 1 & 0 & 0 \\ 0 & 1 & 0 \\ \hline \end{array} \end{array}
 \end{aligned} \tag{34}$$

Thus  $t_{\min}=3$ , i. e., the minimal externally stable subsets consist of three elements. The sets  $T_{t_{\min}}$  themselves are given in (21). Note that all  $T_{t_{\min}}$  contain the vertex  $a$  (corresponding to the zero row of  $A$ ), so that condition (32) is satisfied.

The algebraic algorithm is sufficiently simple for computer realization.

In conclusion, we remark that the graph-model is a detailed structural representation which takes into account all interconnections between the parameters, and may also serve as a mathematical model for the investigation of other logical and information processes which require no knowledge of the quantitative relations between the parameters and their dependence on time. This formulation of the problem is characteristic not only of numerous problems of control and diagnostics; it is also applicable to empirical mathematical descriptions of complex biological and physiological systems. In the opinion of the authors of /3/, it is difficult to represent the latter by analytic mathematical models such as systems of algebraic or differential equations; other types of models are needed, among them also qualitative causal models. In addition, our approach makes it possible to carry out analysis of the object with regard to localization of errors, if the superposition of the functions (parameters) is discontinuous.

In the future we propose to improve the graph-model technique by the introduction of weighting and probabilistic categories, and by allowance for the demands of specific problems of control and diagnosis.

### Bibliography

1. Berge, C. The Theory of Graphs and its Applications. New York, John Wiley and Sons. 1962.



2. Shikhanovich, Yu. A. Vvedenie v sovremennuyu matematiku (Introduction to Modern Mathematics). Moskva, "Nauka." 1965.
3. Amosov, N. M. and V. A. Lishchuk. Primenenie metodov kibernetiki v fiziologii (Application of Cybernetical Methods in Physiology). In sbornik: "Modelirovanie v biologii i meditsine" (Simulation in Biology and Medicine). Kiev. 1965.

L. N. Volkov

# AN ENGINEERING METHOD FOR ANALYTIC LEAST-SQUARES OPTIMIZATION OF REALIZABLE SYSTEMS

In solving certain problems involved in the least-squares optimization of systems whose input consists of random signals with nonzero expectation  $g(t)$ , the functions  $g(t)$  are expanded in Taylor series over some time interval. Solution of these problems yields pulsed weighting functions which are quite difficult to realize [1, 4]. However, by choosing a suitable representation of the function  $g(t)$  over the time interval, one can obtain the optimal pulsed weighting function in the form

$$k(\tau) = \sum_{i=1}^n D_i t^{-a_i \tau} + D_{n+1} \delta(\tau), \quad \tau \geq 0, \quad \operatorname{Re} a_i > 0. \quad (1)$$

Moreover, as we shall demonstrate below, the number of terms in this expansion is easily determined before the actual solution of the problem. It is known [3] that the pulsed weighting function in the above form is easily realized by means of elements with constant lumped parameters. The following problem is therefore of interest.

The input of a linear dynamic system with constant lumped parameters consists of a useful signal  $y(t)$  and noise  $n(t)$ ; both signals are given in statistical terms. The expectation of the useful signal is  $g(t)$ , nonzero at  $t=0$ , either decreasing as  $t \rightarrow \infty$  or periodic.

The central useful signal  $m(t) = y(t) - g(t)$  and the noise  $n(t)$  are stationary random uncorrelated functions with autocorrelation functions  $R_m(\tau)$ ,  $R_n(\tau)$ , respectively. The desired signal at the output of the linear system is  $h(t)$ . The pulsed weighting function of the ideal system, which converts  $y(t)$  into  $h(t)$ , is  $\kappa(\tau)$ . Let the output signal of the actual system be  $x(t)$ ; then the total error of the system  $\varepsilon(t) = x(t) - h(t)$  may be expressed in the form

$$\varepsilon(t) = \varepsilon_{\text{ran}}(t) + \varepsilon_{\text{dyn}}(t),$$

where

$$\varepsilon_{\text{ran}}(t) = \int_0^\infty \varphi(t-\tau) k(\tau) d\tau - \int_{-\infty}^\infty m(t-\tau) \kappa(\tau) d\tau \quad (2)$$

is the random component, and

$$\varepsilon_{\text{dyn}}(t) = \int_0^t g(t-\tau)k(\tau)d\tau - \int_{-\infty}^t g(t-\tau)x(\tau)d\tau \quad (3)$$

is the nonrandom (dynamic) component, where

$$\varphi(t) = m(t) + n(t).$$

It is required to find a system with pulsed weighting function (1) with minimal sum of squared errors,

$$\varepsilon_0^2 = \varepsilon_{\text{stat}}^2 + v \varepsilon_{\text{dyn}}^2, \quad (4)$$

where

$$\begin{aligned} \varepsilon_{\text{stat}}^2 = & \int_0^\infty \int_0^\infty R_\varphi(\tau-\theta)k(\tau)k(\theta)d\tau d\theta - \\ & - 2 \int_0^\infty \int_{-\infty}^\infty R_\pi(\tau-\theta)k(\tau)x(\theta)d\tau d\theta + \\ & + \int_{-\infty}^\infty \int_{-\infty}^\infty R_m(\tau-\theta)x(\tau)x(\theta)d\tau d\theta \end{aligned} \quad (4a)$$

(see, e.g., [4]);

$$\varepsilon_{\text{dyn}}^2 = \int_0^\infty \left\{ \int_0^t g(t-\tau)k(\tau)d\tau - \int_{-\infty}^t g(t-\tau)x(\tau)d\tau \right\}^2 dt, \quad (4b)$$

and  $v$  is a weighting factor.

In the general case, as is known [1], the autocorrelation functions  $R_m$ ,  $R_n$ , and  $R_\varphi$  of the steady signals may be expressed in the form

$$\left. \begin{aligned} R_m(\tau) &= \sum_{j=1}^m A_j e^{-b_j|\tau|}; \quad R_n(\tau) = \sum_{j=m+1}^l A_j e^{-b_j|\tau|}; \\ R_\varphi(\tau) &= R_m(\tau) + R_n(\tau) = \sum_{j=1}^l A_j e^{-b_j|\tau|}. \end{aligned} \right\} \quad (5)$$

Let us express the function  $g(t)$  in the form

$$g(t) = \sum_{k=1}^r d_k e^{-a_k t}. \quad (5a)$$

This is possible both for a decreasing or periodic function of time, and for a polynomial in  $t$  over a finite time interval. In many cases the signal (5a) is an exact description of the different physical processes.

Solutions of the above problem are known for various particular cases (see /1, 4, 5, 6/, and others); however, these usually involve auxiliary functions /4/ or two-dimensional Laplace transforms /6/, which complicate application of the results in engineering practice.

Below we present a general solution of the problem which is both simpler and more suitable for practical applications.

Using the usual variational method (as in /4/), we derive the condition for  $s_0[k(\tau)]$  to be a minimum with respect to  $k(\tau)$ :

$$\begin{aligned} & \int_0^{\infty} R_{\varphi}(\tau-\theta)k(\theta)d\theta - \int_{-\infty}^{\infty} R_m(\tau-\theta)\kappa(\theta)d\theta + \\ & + \nu \int_{\tau}^{\infty} g(t-\tau) \left[ \int_0^t g(t-\theta)k(\theta)d\theta - \int_{-\infty}^t g(t-\theta)\kappa(\theta)d\theta \right] dt = 0. \end{aligned} \quad (6)$$

Substituting (3), (5), (5a) in (6) and transforming the resulting expression, we obtain

$$\begin{aligned} & \sum_{j=1}^l A_j e^{-b_j \tau} \left[ \sum_{i=1}^n \frac{D_i}{a_i - b_j} + D_{n+1} \right] - \sum_{j=1}^m A_j \int_{-\infty}^{\infty} e^{-b_j |\tau-\theta|} \kappa(\theta) d\theta - \\ & - \sum_{i=1}^n D_i e^{-a_i \tau} \left[ \sum_{j=1}^l \frac{2A_j b_j}{a_i^2 - b_j^2} + \nu \sum_{p=1}^r \sum_{k=1}^r \frac{d_p d_k}{(a_i - g_p)(a_i + g_p)} \right] + \\ & + \nu \sum_{p=1}^r \sum_{k=1}^r d_p d_k \left[ \frac{e^{-g_p \tau}}{g_p + g_k} \left( \sum_{i=1}^n \frac{D_i}{a_i - g_p} + D_{n+1} \right) - \right. \\ & \left. - e^{-g_k \tau} \int_{\tau}^{\infty} \int_{-\infty}^t e^{-g_k t} e^{-g_p(t-\theta)} \kappa(\theta) d\theta dt \right] = 0. \end{aligned} \quad (7)$$

Condition (7) will hold identically for all  $\tau \geq 0$  if and only if the following conditions are satisfied:

$$\sum_{j=1}^l \frac{2A_j b_j}{a_i - b_j} + \nu \sum_{p=1}^r \sum_{k=1}^r \frac{d_p d_k}{(a_i - g_p)(a_i + g_k)} = 0, \quad i = 1, 2, \dots, n; \quad (8a)$$

$$\left\{ \begin{aligned} & \sum_{j=1}^l A_j e^{-b_j \tau} \left[ \sum_{i=1}^n \frac{D_i}{a_i - b_j} + D_{n+1} \right] - \sum_{j=1}^m A_j \int_{-\infty}^{\infty} e^{-b_j |\tau-\theta|} \kappa(\theta) d\theta + \\ & + \nu \sum_{p=1}^r \sum_{k=1}^r d_p d_k \left[ \frac{e^{-g_p \tau}}{g_p + g_k} \left( \sum_{i=1}^n \frac{D_i}{a_i - g_p} + D_{n+1} \right) - \right. \\ & \left. - e^{-g_k \tau} \int_{\tau}^{\infty} \int_{-\infty}^t e^{-g_k t} e^{-g_p(t-\theta)} \kappa(\theta) d\theta dt \right] = 0. \end{aligned} \right. \quad (8b)$$

The first  $n$  equations of system (8) are identical in form and define the  $n$  exponents  $a_i$  of the optimal pulsed weighting function, the  $i$ -th equation being an algebraic equation of degree  $l+r-1$  for  $a_i$ . Solution of any of these equations yields the same roots, so that to determine all possible values of

$a_i$  it is sufficient to consider one equation. Among the  $z(l+r-1)$  roots of this equation there are  $l+r-1$  with positive real part, and by the condition  $\operatorname{Re} a_i > 0$  and equation (8a) these are the exponents of the optimal pulsed weighting function. Hence it is clear that the number of terms of the optimal  $k(\tau)$  is the sum of the numbers of terms in the autocorrelation function  $R_x(\tau)$  and the expectation  $g(t)$ .

Thus the optimal system will be completely determined if we determine the  $n+1$  coefficients  $D_i$  from (8b).

To determine the coefficients  $D_i$  we must know the form of the ideal pulsed weighting function  $\kappa(\tau)$ .

We shall consider three types of  $\kappa(\tau)$ , which are the most important in practice: filter ( $\kappa(\tau) = \delta(\tau)$ ), differentiation with filter ( $\kappa(\tau) = \delta'(\tau)$ ), delay with filter ( $\kappa(\tau) = \delta(\tau + t_0)$ ).

In these cases substitution of the corresponding form of  $\kappa(\tau)$  in (8b) gives the following equations:

$$\left. \begin{aligned} & \sum_{j=1}^l A_j e^{-b_j \tau} \left[ \sum_{i=1}^n \frac{D_i}{a_i - b_j} + D_{n+1} \right] - \sum_{j=1}^m A_j e^{-b_j \tau} + \\ & + v \sum_{p=1}^r \sum_{k=1}^r \frac{d_p d_k}{g_p + g_k} e^{-g_p \tau} \left[ \sum_{i=1}^n \frac{D_i}{a_i - g_p} + D_{n+1} - 1 \right] = 0; \end{aligned} \right\} \quad (9)$$

$$\left. \begin{aligned} & \sum_{j=1}^l A_j e^{-b_j \tau} \left[ \sum_{i=1}^n \frac{D_i}{a_i - b_j} + D_{n+1} \right] - \sum_{j=1}^m A_j b_j e^{-b_j \tau} + \\ & + v \sum_{p=1}^r \sum_{k=1}^r \frac{d_p d_k}{g_p + g_k} e^{-g_p \tau} \left[ \sum_{i=1}^n \frac{D_i}{a_i - g_p} + D_{n+1} - 1 \right] = 0; \end{aligned} \right\} \quad (10)$$

$$\left. \begin{aligned} & \sum_{j=1}^l A_j e^{-b_j \tau} \left[ \sum_{i=1}^n \frac{D_i}{a_i - b_j} + D_{n+1} \right] - \sum_{j=1}^m A_j e^{-b_j t_0} e^{-b_j \tau} + \\ & + v \sum_{p=1}^r \sum_{k=1}^r \frac{d_p d_k}{g_p + g_k} e^{-g_p \tau} \left[ \sum_{i=1}^n \frac{D_i}{a_i + g_p} + D_{n+1} - e^{-g_p t_0} \right] = 0. \end{aligned} \right\} \quad (11)$$

It is clear from (9)–(10) that the total error is a minimum if and only if  $k(\tau) = \sum_{i=1}^n D_i e^{-a_i \tau} + D_{n+1} \delta(\tau)$  involves all  $l+r-1$  exponents  $a_i$  (with positive real parts) which satisfy (8a). In fact, equations (9)–(10) contain  $l+r$  different functions of the variable  $\tau$ , the coefficients of each of these functions vanish simultaneously only if there are  $l+r$  different optimized parameters. The role of these parameters is played by the  $n+1$  coefficients  $D_i$ , so that a necessary condition for the optimum is  $n+1 = l+r$ .

A necessary and sufficient condition for equations (9)–(11) to hold is thus the validity of the following respective systems of algebraic equations:

$$\left. \begin{aligned} & \sum_{i=1}^n \frac{D_i}{a_i - b_j} + D_{n+1} - 1 = 0; \quad j = 1, 2, \dots, m; \\ & \sum_{i=1}^n \frac{D_i}{a_i - b_j} + D_{n+1} = 0; \quad j = m+1, m+2, \dots, l; \\ & \sum_{i=1}^n \frac{D_i}{a_i - g_p} + D_{n+1} - 1 = 0; \quad p = 1, 2, \dots, r; \end{aligned} \right\} \quad (12)$$

$$\left. \begin{aligned}
& \sum_{i=1}^n \frac{D_i}{a_i - b_j} + D_{n+1} - b_j = 0; \quad j=1, 2, \dots, m; \\
& \sum_{i=1}^n \frac{D_i}{a_i - b_j} + D_{n+1} = 0; \quad j=m+1, m+2, \dots, l; \\
& \sum_{i=1}^n \frac{D_i}{a_i - g_p} + D_{n+1} - g_p = 0; \quad p=1, 2, \dots, r; \\
& \sum_{i=1}^n \frac{D_i}{a_i - b_j} + D_{n+1} - e^{-b_j y} = 0; \quad j=1, 2, \dots, m; \\
& \sum_{i=1}^n \frac{D_i}{a_i - b_j} + D_{n+1} = 0; \quad j=m+1, m+2, \dots, l; \\
& \sum_{i=1}^n \frac{D_i}{a_i - g_p} + D_{n+1} - e^{-g_p y} = 0; \quad p=1, 2, \dots, r.
\end{aligned} \right\} \quad (13)$$

$$\left. \begin{aligned}
& \sum_{i=1}^n \frac{D_i}{a_i - b_j} + D_{n+1} - e^{-b_j y} = 0; \quad j=1, 2, \dots, m; \\
& \sum_{i=1}^n \frac{D_i}{a_i - b_j} + D_{n+1} = 0; \quad j=m+1, m+2, \dots, l; \\
& \sum_{i=1}^n \frac{D_i}{a_i - g_p} + D_{n+1} - e^{-g_p y} = 0; \quad p=1, 2, \dots, r.
\end{aligned} \right\} \quad (14)$$

Each of the systems (12)–(14) consists of  $l+r=n+1$  linear equations for the  $n+1$  coefficients  $D_i$ . Solution of the corresponding system for the  $D_i$  leads to the final determination of the pulsed weighting function of the optimal system. Similar methods may be used to determine the optimal  $k(\tau)$  for other functions  $x(\tau)$ .

After determining the optimal  $k(\tau)$  we wish to find the minimal value of the total squared error. To determine  $\varepsilon_{0\min}^2$  we substitute the minimum condition (6) and (4a), (4b) in (4):

$$\begin{aligned}
\varepsilon_{0\min}^2 = & \int_{-\infty}^{\infty} x\Theta d\Theta \left[ \int_0^{\infty} R_m(\tau - \Theta) k(\tau) d\tau - \int_{-\infty}^{\infty} R_m(\tau - \Theta) x(\tau) d\tau \right] + \\
& + v \int_0^t \int_{-\infty}^t g(t - \Theta) x(\Theta) d\Theta \left[ \int_0^t g(t - \tau) k(\tau) d\tau - \right. \\
& \left. - \int_{-\infty}^t g(t - \tau) x(\tau) d\tau \right].
\end{aligned} \quad (15)$$

In the three cases mentioned above expression (15) has the form

$$\begin{aligned}
\varepsilon_{0\min}^2 = & \int_0^{\infty} R_m(\tau) k(\tau) d\tau - R_m(0) + \\
& + v \int_0^{\infty} g(t) dt \left[ \int_0^t g(t - \tau) k(\tau) dt - g(t) \right];
\end{aligned} \quad (16)$$

$$\begin{aligned}
\varepsilon_{0\min}^2 = & R_m''(0) - \int_0^{\infty} R_m'(\tau) k(\tau) d\tau - \\
& - v \int_0^{\infty} \left\{ \int_0^t g(t - \tau) g'(t) k(\tau) d\tau - [g'(t)]^2 \right\} dt;
\end{aligned} \quad (17)$$

$$\epsilon_0^2 \min = \int_0^\infty R_m(\tau - t_y) k(\tau) d\tau - R_m(0) + \\ + v \int_0^\infty g(t - t_y) dt \left\{ \int_0^t g(t - \tau) k(\tau) d\tau - g(t - t_y) \right\}. \quad (18)$$

The above results are clearly applicable to engineering computations of optimal systems (for complex input signals —  $l+r \geq 5$  — the expressions easily lend themselves to computer solution).

The method may also be used to obtain a feasible solution for functions  $g(t)$  involving a constant component. In fact, express the constant term  $d_k$  in the form  $d_k e^{-g_k t}$ , where  $g_k < 1$ ; then use the resulting formulas to find the optimal pulsed weighting function, in which none of the  $a_i$  tend to zero as  $g_k \rightarrow 0$ . One can also use formulas (12) — (14), setting the corresponding  $g_k$  equal to zero in the equations.

Analogous results are obtained when  $g(t)$  is a polynomial. In this case  $g(t)$  has the representation

$$g(t) = \sum_{k=1}^r d_k t^{k-1} e^{-g_k t}, \quad (19)$$

where  $g_k \rightarrow 0$ ,  $k=1, 2, \dots, r$ .

By the same method one can determine the best system in the sense of the minimal  $\epsilon_{\text{ran}}^2$  for given  $\epsilon_{\text{dyn}}^2$ , or vice versa (minimal  $\epsilon_{\text{dyn}}^2$  for given  $\epsilon_{\text{ran}}^2$ ). When this is done the optimum condition is again equation (6), in which  $v$  should be regarded as a Lagrange multiplier.

Our method makes it possible to solve a more general problem in which

$$g(t) = \sum_{k=1}^r d_k(t) e^{-g_k t},$$

where

$$d_k(t) = \sum_{v=0}^{r_k} d_{kv} t^v. \quad (20)$$

To determine the coefficients  $d_{kv}$  in the representation (20) of an arbitrary time function  $f(t)$ , the following formula can be used:

$$d_{kv} = \frac{1}{(r_k - v)! v!} \frac{d^{r_k - v}}{d\rho^{r_k - v}} [(\rho + g_k)^{r_k + 1} F(\rho)] \rho = -g_k;$$

this formula is derived in [6].

Let us consider an example. Let

$$g(t) = 1 - e^{-t}; \quad m(t) \equiv 0; \quad R_n(\tau) = e^{-5|\tau|}; \\ \kappa(\tau) = \delta(\tau); \quad v = 0.25 \text{ sec}^{-1}.$$

In this case  $d_1 = d_2 = 1$ ;  $A_1 = 1$ ;  $b_1 = 5$ ;  $g_1 = 0$ ;  $g_2 = 1$ ;  $l = 1$ ;  $m = 0$  and (8b) is

$$\frac{2A_1b_1}{a^2-b_1^2} + v \left[ \frac{d_1^2}{(a^2-g_1^2)} + \frac{d_2^2}{(a^2-g_2^2)} + \frac{2d_1d_2(a^2-g_1g_2)}{(a^2-g_1^2)(a^2-g_2^2)} \right] = 0;$$

$$\frac{D_1}{a_1-b_1} + \frac{D_2}{a_2-b_1} + D_3 = 0;$$

$$\frac{D_1}{a_1-g_1} + \frac{D_2}{a_2-g_1} + D_3^{-1} = 0;$$

$$\frac{D_1}{a_1-g_2} + \frac{D_2}{a_2-g_2} + D_3^{-1} = 0.$$

Substituting the given coefficients in the first equation, we get

$$11a^4 - 35.25a^2 + 6.25 = 0,$$

whence  $a_1 = 1.74$ ,  $a_2 = 0.43$ ; these values are substituted in the remaining equations:

$$\begin{cases} -0.307D_1 - 0.219D_2 + D_3 = 0; \\ 0.58D_1 + 2.38D_2 + D_3 - 1 = 0; \\ 1.35D_1 - 1.75D_2 + D_3 - 1 = 0. \end{cases}$$

Solution of this system of linear equations yields the  $D_i$ :

$$D_1 = -0.188; D_2 = 0.45; D_3 = 0.097.$$

The optimal pulsed weighting function is thus

$$k(\tau) = -0.188 e^{-1.74\tau} + 0.45 e^{-0.43\tau} + 0.097 \delta(\tau).$$

The optimal transfer function is

$$W(\rho) = \frac{0.124\rho + 0.6\rho + 1}{(0.57\rho + 1)(2.32\rho + 1)}.$$

This transfer function may be realized in the form of an RC-circuit /3/.

### Bibliography

1. Laning, J. H. and R. H. Battin. Random Processes in Control Theory. New York, McGraw-Hill. 1956.
2. Osnovy avtomaticheskogo regulirovaniya (Elements of Automatic Control), Volume I. Moskva, Mashgiz. 1954.
3. Osnovy avtomaticheskogo regulirovaniya (Elements of Automatic Control), Volume II. Moskva, Mashgiz. 1959.
4. Solodovnikov, V. V. Statisticheskaya dinamika lineinykh sistem avtomaticheskogo upravleniya (Statistical Dynamics of Linear Automatic Control Systems). Moskva, Fizmatgiz. 1960.
5. Osnovy avtomaticheskogo upravleniya (Fundamentals of Automatic Control). Moskva, Fizmatgiz. 1963.
6. Sklyarevich, A. N. Operatornye metody v statisticheskoi dinamike avtomaticheskikh sistem (Operator Methods in the Statistical Dynamics of Automatic Systems). Moskva, Fizmatgiz. 1965.



*A. N. Sklyarevich*

**INITIAL DATA FOR THE ORGANIZATION OF  
PREVENTIVE MAINTENANCE IN A SYSTEM  
WITH A POSSIBLE STRUCTURAL FAULT**

Initial data are found for the organization of preventive maintenance in a system with one possible structural fault: the probability of a fault, the average required number of standby components. Methods are indicated for specification of the working time of the system and the preventive maintenance period. [Throughout the paper we use the abbreviation p. m. for "preventive maintenance."]

Consider a non-renewable system during whose performance a structural fault may occur. It was shown in [1] that relatively simple graphical methods may be used to compute the optimal duration  $t_w$  of the working cycle of the system and to estimate the efficiency of the system under deviations from this optimum, provided the following factors are known: the calendar service life  $T$  of the system, the mean duration  $t_{pm}$  of p. m., the intensity  $\lambda$  of faults, and intensity  $\mu$  of system failure when a fault has occurred.

The main inadequacy of this method is that the quantity  $t_{pm}$  is assumed known. In actual fact only certain components of this period may be regarded as known — the time  $t_1$  needed to locate a fault and the time  $t_r$  needed to repair it. Now, when the system is standing idle during p. m., it is not necessarily true that a fault has occurred; therefore the equality

$$t_{pm} = t_1 + t_r \quad (1)$$

is in general false, and must be replaced by an equality

$$t_{pm} = t_1 + q t_r, \quad (2)$$

where  $q$  is the probability that the system, when idle during p. m., has suffered a fault. In the general case  $q$  is a function of the working cycle of the system, and so a more accurate equality is

$$t_{pm} = t_1 + q(t_w) t_r, \quad (3)$$

which shows that the optimal working cycle  $t_w$  and the average p. m. time  $t_{pm}$  must be determined simultaneously. These data, and also the function  $q(t_w)$ , are basic for organization of the system and implementation of p. m. The value of  $q(t_w)$  governs not only the duration of p. m. but also the required number of standby elements, if faults are repaired by replacing defective components.

To determine the value of  $q(t_w)$ , let us analyze the formula /1/

$$F(t) = e^{-\lambda t} + \frac{\lambda}{\mu - \lambda} (e^{-\lambda t} - e^{-\mu t}), \quad (4)$$

which determines the probability of satisfactory performance of a system with a single structural fault at an instant  $t$ , on the assumption that all other components of the system are reliable. The right-hand side of this expression involves two terms: the first determines the probability that no structural fault occurs during time  $t$ , and the second the [conditional] probability of satisfactory performance during the same time interval, on the assumption that a structural fault has occurred. Applying Bayes' formula /2/, we see that the probability of the presence of a fault during satisfactory performance of the system is given by the relation

$$q(t) = \frac{1 - e^{-\nu t}}{\frac{\mu}{\lambda} - e^{-\nu t}}, \quad (5)$$

where

$$\nu = \mu - \lambda. \quad (6)$$

Substituting  $t = t_w$  in (5), we get the probability of the presence of a structural fault in the system when p. m. is initiated.

The behavior of the function  $q(t)$ , or that of its complementary function

$$p(t) = \frac{\frac{\mu}{\lambda} - 1}{\frac{\mu}{\lambda} - e^{-\nu t}} = \frac{\nu}{\mu - \lambda e^{-\nu t}}, \quad (7)$$

which is the conditional probability that there is no fault in the system, given its satisfactory performance during time  $t$ , depends on the ratio of the characteristics  $\mu$  and  $\lambda$ , or, what is the same, on the sign of  $\nu$ .

Let us analyze the behavior of these functions, and of the simpler characteristic

$$r(t) = \frac{q(t)}{p(t)} = \frac{\lambda}{\nu} (1 - e^{-\nu t}), \quad (8)$$

which is the ratio of the probability that there is a fault to the probability that there is no fault, both on the assumption that the system is operating satisfactorily during time  $t$ ; we shall carry out the analysis for the three possible cases:  $\mu > \lambda$  ( $\nu > 0$ ),  $\mu < \lambda$  ( $\nu < 0$ ) and  $\mu = \lambda$  ( $\nu = 0$ ).

Note first that in all cases

$$\left. \begin{aligned} q(0) &= 0, & p(0) &= 1, & r(0) &= 0, \\ q'(0) &= \lambda, & p'(0) &= -\lambda, & r'(0) &= \lambda, \end{aligned} \right\} \quad (9)$$

i. e., the initial part of any of the experimentally determined curves  $p(t)$ ,  $q(t)$ ,  $r(t)$  determines  $\lambda$ , which in turn determines the average time to the first fault.

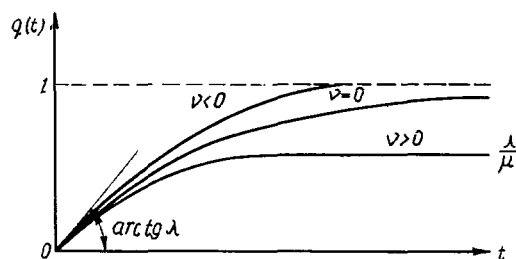


FIGURE 1. Graph of the function  $q(t)$ .

If  $\mu > \lambda$  (the average time to the first fault is greater than the average time to failure of the system with a fault), then as  $t \rightarrow \infty$  the functions  $p(t)$ ,  $q(t)$ ,  $r(t)$  asymptotically approach well-defined limits (Figures 1 to 3):

$$q(\infty) = \frac{\lambda}{\mu}; \quad p(\infty) = \frac{\nu}{\mu}; \quad r(\infty) = \frac{\lambda}{\nu}, \quad (10)$$

and, consequently, after a certain time during the operation of the system the probabilities of the presence or absence of a structural fault are in practice completely defined and in principle independent of the actual performance of the system. When the value of  $\lambda$  is known, any one of these probabilities may be used to evaluate  $\mu$ .

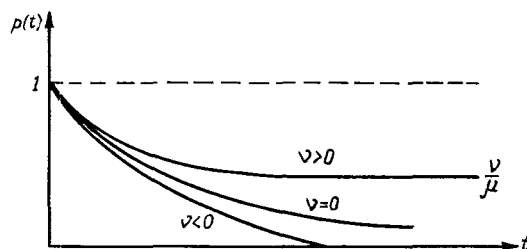


FIGURE 2. Graph of the function  $p(t)$ .

If  $\lambda > \mu$  (the average time to the first fault is less than the average time to failure of the system with a fault), then  $\nu < 0$ , and so as  $t \rightarrow \infty$  (Figures 1 to 3)

$$q(t) \rightarrow 1; \quad p(t) \rightarrow 0; \quad r(t) \rightarrow \infty,$$

i.e., after a certain time practically all satisfactorily performing systems suffer a structural fault. It is obvious that in this case

$$t_{pm} = t_1 + t_r$$

and the value of  $\mu$  cannot be determined by finding the proportion of all satisfactorily performing systems in which structural faults occur.

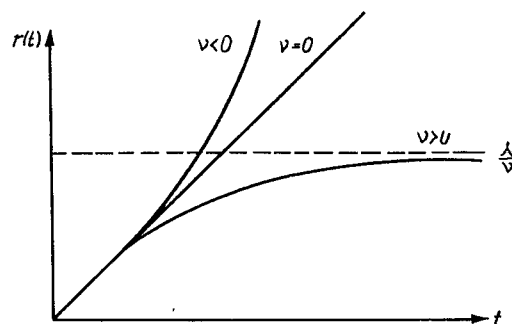


FIGURE 3. Graph of the function  $r(t)$ .

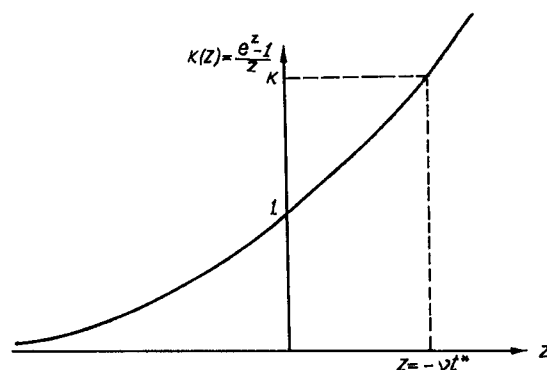


FIGURE 4. Graph of the function  $k(z)$ .

To determine the value of  $\mu$  in the case  $\lambda > \mu$  we suggest the following method (Figure 4). After a certain time  $t^*$  from the start of the system, determine the function  $r(t^*)$  and evaluate

$$k = \frac{r(t^*)}{\lambda t^*}. \quad (11)$$

Substituting  $t = t^*$  in (8) and denoting

$$z = -v t^*,$$

we find that the quantities  $k$  and  $z$  satisfy the transcendental equation

$$kz = e^z - 1, \quad (12)$$

which we solve for given  $k$  (e.g., by a graphical method, as in Figure 4), finding the value of  $z$  and hence the required failure rate  $\mu$ :

$$\mu = \lambda - \frac{z}{t^*}. \quad (13)$$

Finally, we analyze the third case,  $\lambda = \mu$  (the average time to the first fault is equal to the average time from the fault to failure of the system).

If  $\lambda = \mu$ , then  $v = 0$  and therefore equalities (5), (7), (8) become indeterminate expressions of type  $\frac{0}{0}$ . Using de l'Hospital's rule, we get

$$p(t) = \frac{1}{1 + \lambda t}; \quad q(t) = \frac{\lambda t}{1 + \lambda t}; \quad r(t) = \lambda t, \quad (14)$$

and therefore, as  $t \rightarrow \infty$ ,

$$p(t) \rightarrow 0, \quad q(t) \rightarrow 1, \quad r(t) \rightarrow \infty. \quad (15)$$

Moreover, for all values of

$$k = \frac{r(t)}{\lambda t} = 1. \quad (16)$$

This equality may be used as a test for the condition  $\lambda = \mu$ . It is clear from (15) that, as in the previous case, if the system performs satisfactorily for a certain time after it starts, a structural fault will almost always occur.

Now that we know how to determine the function  $q(t)$ —the probability of a fault in the system for given  $\lambda$  and  $\mu$ —we can find the time required to implement p.m., and hence the optimal p.m. period. To solve the latter problem on the basis of the dependence of the p.m. time on the p.m. period, we suggest the method of successive approximations. We first assume that the p.m. time is defined by (1), find the periodicity of the p.m., determine  $q(t_w)$  according to the working cycle  $t_w$ , and then improve the p.m. period. After several iterations a stable result is obtained, i.e., the result remains practically unchanged upon further iterations. These results may be used as initial data for the organization of p.m.

We shall now find the average number of standby components required in the course of the calendar service life to replace unserviceable components during p.m. Since the first p.m. cycle is implemented with probability  $F(t_w)$  and the conditional probability of a fault being found during p.m. is  $q(t_w)$ , it follows that with probability  $F(t_w) q(t_w)$  the first p.m. cycle will involve the replacement of an unserviceable component. This means that to maintain the first cycle for a single system an average of  $F(t_w) q(t_w)$  standby components are needed.

The second cycle begins with probability  $F(t_w)$  and end with probability  $F^2(t_w)$ . Since the structure of the system is completely renewed during p.m.,

the conditional probability of the occurrence of a fault during the second cycle is found by the same arguments as during the first; therefore the average number of standby components required for a single system in the course of the second cycle is  $F^2(t_w)q(t_w)$ . Similarly, for the third p. m. period we have  $F^3(t_w)q(t_w)$ , and for the  $N$ -th —  $F^N(t_w)q(t_w)$ .

If the calendar service life of the system involves  $N$  p. m. cycles, then the average total number of standby components required for a single system is

$$m = \sum_{i=1}^N q(t_w) F^i(t_w)$$

or

$$m = q(t_w) F(t_w) \frac{1 - F^N(t_w)}{1 - F(t_w)}. \quad (17)$$

Let us compare this formula with that defining the average working time of the system during its calendar service life  $/1/$ :

$$T_{av} = \frac{1 - F^N(t_w)}{1 - F(t_w)} \int_0^{t_w} F(t) dt. \quad (18)$$

The result is

$$m = \frac{T_{av}}{\int_0^{t_w} F(t) dt} q(t_w) F(t_w). \quad (19)$$

Since  $q(t_w)F(t_w)$  is the unconditional probability of a fault in the system occurring during p. m., and

$$\frac{T_{av}}{\int_0^{t_w} F(t) dt} \approx \frac{T_{av}}{t_w} \approx N', \quad (20)$$

where  $N'$  is the average number of working cycles of the system during its calendar service life, we see that (19) indicates that the average number of standby components required to guarantee p. m. is just the product of the unconditional probability of a fault being found during p. m. and the average number of working cycles of the system during its calendar service life. This structure of the formula for  $m$  is obvious, though its derivation involves rigorous arguments.

## CONCLUSIONS

1. We have found the law governing the probability of the presence or absence of a fault during performance of a system with one possible structural fault.
2. We have improved the technique of determining the optimal p. m. time and the optimal duration of p. m. for a system of this type.
3. We have determined the average number of components required for replacing faulty components during the service life of the system (assuming that the replacements are carried out during preventive maintenance).

## Bibliography

1. Sklyarevich, A. N. and E. N. Tsvetkova. Optimal'nye sroki polnoi profilaktiki sistemy s vozmozhnyimi narusheniyami struktury (Optimal Duration of Preventive Maintenance for a System with Possible Structural Faults). — In press.
2. Venttsel', E. S. Teoriya veroyatnostei (Probability Theory). Moskva, Fizmatgiz, 1962.

*L. P. Leont'ev*

**EVALUATING THE RELIABILITY OF A SYSTEM WITH  
AFTEREFFECTS UNDER INCOMPLETE PREVENTIVE  
MAINTENANCE—A SPECIAL CASE**

An equation is derived for the reliability of complex systems with preventive maintenance (p. m.), assuming that the periods of satisfactory performance of the components and the time from failure of one component to failure of the system are exponentially distributed. We obtain recursion relations for systems with two types of faults, which provide an estimate of reliability after any working cycle when only one fault is eliminated or when both are eliminated successively.

In /1/ we derived general formulas for the reliability of systems with accumulation in which incomplete preventive maintenance (p. m.) is implemented at some time  $\tau$ , i. e., certain faults are eliminated, in accordance with a preassigned schedule. It is of considerable interest to estimate the reliability of such systems when the probability density of the occurrence of the  $i$ -th fault is  $\lambda_i e^{-\lambda_i t}$ , while the aftereffect density, i. e., the probability density of the time from the occurrence of the  $k$ -th combination faults to failure of the system, is  $\mu_k e^{-\mu_k t}$ , where  $\mu_k$  is the intensity of the failures of the system following a combination of  $k$  faults. These distributions are based on experimental data, but they may also be derived from the physical nature of the occurrence of failures over sufficiently varied ranges of working times.

It is known /1/ that the probability of failproof performance of the system on the assumption that incomplete p. m. is initiated at the instant  $\tau$ , is given by the formula

$$P_m(t) = \sum_{k=0}^m \sum_{i=0}^r S(\tau, (A_m^k x) A_r^i y) \cdot \sum_{i=0}^m \sum_{j=0}^r S(\eta, (A_m^i x), (A_r^j y) / \tau, (A_m^k x), (A_r^i y)). \quad (1)$$

As in /1/ we shall assume that faults of type  $x$  with intensities  $\lambda_1, \lambda_2, \lambda_3, \dots, \lambda_m$  are eliminated during the process, while faults of type  $y$ , with intensities  $\lambda_1', \lambda_2', \lambda_3', \dots, \lambda_r'$ , are not disregarded.

Consider the unconditional probability  $P_m(\tau)$ :

$$P_m(\tau) = \sum_{k=0}^m \sum_{i=0}^r S(\tau, (A_m^k x), (A_r^i y)). \quad (2)$$



$P_m(\tau)$  is the probability of satisfactory performance of the system in the time interval  $0, \tau$ . For exponential distributions

$$P_m(\tau) = \sum_{k=0}^m \sum_{l=0}^r \sum_{x_1=1}^m \sum_{x_2=1}^m \dots \sum_{x_k=1}^m \sum_{y_1=1}^r \sum_{y_2=1}^r \dots \sum_{y_l=1}^r \frac{\lambda_1 \lambda_2 \dots \lambda_k \lambda_1' \lambda_2' \dots \lambda_l'}{Q'(\beta_i, x_1, \dots, x_k, y_1, \dots, y_l)} e^{-\beta_i \tau} \quad (3)$$

The formula for the conditional probability may be derived from the equation

$$P(\eta/\tau) = \sum_{v=0}^m \sum_{u=0}^{m-v} \sum_{i=0}^k \sum_{j=0}^{m-k} \sum_{\pi=0}^r S(\eta, (A_v^i \bar{x}), (A_u^j x), (A_r^\pi y) / \tau, (A_m^k \bar{x}), (A_l^j y)) \quad (4)$$

where

$$\begin{aligned} S(\eta, (A_v^i \bar{x}), (A_u^j x), (A_r^\pi y) / \tau, (A_m^k \bar{x}), (A_l^j y)) = \\ = \sum_{\bar{x}_1=1}^k \sum_{\bar{x}_2=1}^k \dots \sum_{\bar{x}_i=1}^k \sum_{x_1=1}^{m-k} \sum_{x_2=1}^{m-k} \dots \sum_{x_j=1}^{m-k} \sum_{y_1=1}^r \sum_{y_2=1}^r \dots \sum_{y_\pi=1}^r \prod_{j=1}^k P_{\bar{x}_j}(\eta) \frac{\prod_{i=\pi+1}^{m-k} P_{x_i}(\tau)}{\prod_{i=1}^{m-k} P_{x_i}(\tau)} \times \\ \times \frac{\prod_{i=\pi+1}^r P_{y_i}(\tau)}{\prod_{i=1}^r P_{y_i}(\tau)} \int_{t_1}^{\eta} \int_{t_2}^{\eta} \dots \int_{t_i}^{\eta} \int_{t_2'}^{\eta} \int_{t_3'}^{\eta} \dots \int_{t_{i+1}}^{\eta} \int_{t_{i+2}}^{\eta} \dots \int_{t_{\pi-1}}^{\eta} \prod_{j=1}^i f_{\bar{x}_j}(t_j') \times \\ \times \prod_{i=1}^j f_{x_i}(\tau + t_i') \prod_{k=i+1}^{\pi} f_{y_k}(\tau + \tau_k) \Phi_{\bar{x}_1, \dots, \bar{x}_i, x_1, \dots, x_j, y_1, \dots, y_{l+1}, \dots, y_\pi} \\ (\eta, t_1, t_2, \dots, t_i, t_1', t_2', \dots, t_j', \tau_{i+1}, \tau_{i+2}, \dots, \tau_\pi / \tau, y_1, y_2, \dots, y_l) \times \\ \times dt_1 \dots dt_i dt_1' \dots dt_j' d\tau_{i+1} \dots d\tau_\pi. \end{aligned} \quad (5)$$

Denote the intensities of component failures of type  $x$  by  $\lambda_1', \lambda_2', \dots, \lambda_i'$  and the intensities of the corresponding aftereffect times by  $\mu_1', \mu_2', \dots, \mu_i', \mu_1', \mu_2', \dots, \mu_i$ , in the case that the components fail in the interval  $0, \tau$ . Otherwise we use the notation  $\lambda_1, \lambda_2, \dots, \lambda_i, \mu_1, \mu_2, \dots, \mu_i, \mu_1, \mu_2, \dots, \mu_i$ . The intensities of failures and aftereffects of type  $y$  are denoted by  $\bar{\lambda}_1, \bar{\lambda}_2, \dots, \bar{\lambda}_i, \bar{\mu}_1, \bar{\mu}_2, \dots, \bar{\mu}_i, \bar{\mu}_1, \bar{\mu}_2, \dots, \bar{\mu}_i$ . Then equation (5) becomes

$$S(\eta, A_v^i \bar{x}, (A_u^j x), (A_r^\pi y) / \tau, (A_m^k \bar{x}), (A_l^j y)) = \sum_{\bar{x}_1=1}^k \sum_{\bar{x}_2=1}^k \dots \sum_{\bar{x}_i=1}^k \sum_{x_1=1}^{m-k} \sum_{x_2=1}^{m-k} \dots \sum_{x_j=1}^{m-k} \sum_{y_1=1}^r \sum_{y_2=1}^r \dots \sum_{y_\pi=1}^r \times \quad (6)$$



Let us determine the conditional probability corresponding to the unconditional probabilities (9) and (10). In this case the system starts in the interval  $\eta$  with a fault of type 2 which occurred in the previous working period. The next working period of the system (the interval  $\eta = t - \tau$ ) ends either with one fault of type 2 or with a fault of both types. The conditional probability of the former event is

$$P(\eta/\tau, y) = e^{-(\lambda_1 + \nu_2)\eta}, \quad (13)$$

while that of the latter is

$$F(\eta/\tau, xy) = \int_0^\eta e^{-\mu_2 t_1} \lambda_1 e^{-\lambda_1 t_1} e^{-\mu_{12}(\eta - t_1)} dt_1. \quad (14)$$

The required conditional probability is

$$P(\eta/\tau, y) + F(\eta/\tau, xy) = e^{-\lambda_1 \eta} \left\{ \frac{\mu_{12} - \mu_2}{\nu_{12} - \nu_2} e^{-\nu_2 \eta} - \frac{\lambda_1}{\nu_{12} - \nu_2} e^{-\nu_{12} \eta} \right\}. \quad (15)$$

Since

$$P(t) = \{P_0(\tau) + P_x(\tau)\}P(\eta) + \{P_y(\tau) + P_{xy}(\tau)\}\{P(\eta/\tau, y) + P(\eta/\tau, xy)\}, \quad (16)$$

it follows that the reliability of a system with two possible faults one of which is eliminated during p. m. is given by the following explicit expression:

$$\begin{aligned} P(t) = & e^{-\lambda t} \left\{ 1 + \frac{\lambda_1}{\nu_1} (1 - e^{-\nu_1 \tau}) \right\} \left\{ 1 + \frac{\lambda_1}{\nu_1} (1 - e^{-\nu_1 \eta}) + \right. \\ & + \frac{\lambda_2}{\nu_2} (1 - e^{-\nu_2 \eta}) + \lambda_1 \lambda_2 \left[ \frac{1}{\nu_1 \nu_{12}} + \frac{1}{\nu_2 \nu_{12}} \frac{1}{\nu_1 (\nu_1 - \nu_{12})} e^{-\nu_1 \eta} + \right. \\ & + \left. \frac{1}{\nu_2 (\nu_2 - \nu_{12})} e^{-\nu_2 \eta} + \frac{1}{\nu_{12} (\nu_{12} - \nu_1)} e^{-\nu_{12} \eta} + \frac{1}{\nu_{12} (\nu_{12} - \nu_2)} e^{-\nu_{12} \eta} \right] \Big\} + \\ & + e^{-\lambda t} \left\{ \frac{\lambda_2}{\nu_2} (1 - e^{-\nu_2 \tau}) + \lambda_1 \lambda_2 \left[ \frac{1}{\nu_1 \nu_{12}} + \frac{1}{\nu_2 \nu_{12}} + \frac{1}{\nu_1 (\nu_1 - \nu_{12})} e^{-\nu_1 \tau} + \right. \right. \\ & + \left. \frac{1}{\nu_2 (\nu_2 - \nu_{12})} e^{-\nu_2 \tau} + \frac{1}{\nu_{12} (\nu_{12} - \nu_1)} e^{-\nu_{12} \tau} + \frac{1}{\nu_{12} (\nu_{12} - \nu_2)} e^{-\nu_{12} \tau} \right] \Big\} \times \\ & \times \left\{ \frac{\mu_{12} - \mu_2}{\nu_{12} - \nu_2} e^{-\nu_2 \eta} - \frac{\lambda_1}{\nu_{12} - \nu_2} e^{-\nu_{12} \eta} \right\}. \end{aligned} \quad (17)$$

We introduce the notation

$$\begin{aligned} \psi_1(\tau) &= \frac{\lambda_1}{\nu_1} (1 - e^{-\nu_1 \tau}); \\ \psi_2(\tau) &= \frac{\lambda_2}{\nu_2} (1 - e^{-\nu_2 \tau}); \\ \psi_{12}(\tau) &= \lambda_1 \lambda_2 \left\{ \frac{\nu_1 + \nu_2}{\nu_1 \nu_2 \nu_{12}} + \frac{1}{\nu_1 (\nu_1 - \nu_{12})} e^{-\nu_1 \tau} + \frac{1}{\nu_2 (\nu_2 - \nu_{12})} e^{-\nu_2 \tau} + \right. \\ &+ \left. \left[ \frac{1}{\nu_{12} (\nu_{12} - \nu_1)} + \frac{1}{\nu_{12} (\nu_{12} - \nu_2)} \right] e^{-\nu_{12} \tau} \right\}; \\ \varphi(\tau) &= \frac{\mu_{12} - \mu_2}{\nu_{12} - \nu_2} e^{-\nu_2 \tau} - \frac{\lambda_1}{\nu_{12} - \nu_2} e^{-\nu_{12} \tau}. \end{aligned}$$

With this notation (17) becomes

$$P(t) = e^{-\Lambda t} \{1 + \psi_1(\tau)\} \{1 + \psi_1(\eta) + \psi_2(\eta) + \psi_{12}(\eta)\} + e^{-\Lambda t} \{\psi_2(\tau) + \psi_{12}(\tau)\} \varphi(\eta) \quad (18)$$

or

$$P(t) = e^{-\Lambda t} \{1 + \psi_1(\tau)\} \{1 + \psi_1(\eta)\} + e^{-\Lambda t} \{[1 + \psi_1(\tau)][\psi_2(\eta) + \psi_{12}(\eta)] + \varphi(\eta)[\psi_2(\tau) + \psi_{12}(\tau)]\}. \quad (19)$$

The first term on the right-hand side of (19) defines the probability that the system has either no faults or a fault of type 1 at the end of the interval  $\eta$ . The second term is the probability that by the end of the interval  $\eta$  the system involves either a fault of type 2 or faults of types 1 and 2. When the duration of the cycles between the p. m. times is the same, i. e.,  $\eta = \tau$ , formula (19) becomes

$$P(2\tau) = e^{-2\Lambda\tau} \{1 + \psi_1(\tau)\}^2 + e^{-2\Lambda\tau} \{[1 + \psi_1(\tau)][1 + \varphi(\tau)][\psi_2(\tau) + \psi_{12}(\tau)]\}. \quad (20)$$

Let us find recursion relations for the reliability of the system at the end of  $n$  working periods (i. e.  $n-1$  p. m. periods).

Denote the probability that there are no faults after  $n-1$  p. m. periods by  $P_0((n-1)\tau)$  and the probability that there is a fault of type 2 by  $P_y((n-1)\tau)$ .

Then

$$P(n\tau) = P_0((n-1)\tau) \{1 + \psi_1(\tau) + \psi_2(\tau) + \psi_{12}(\tau)\} e^{-\Lambda\tau} + P_y((n-1)\tau) \varphi(\tau) e^{-\Lambda\tau}, \quad (21)$$

or

$$P(n\tau) = e^{-\Lambda\tau} \{P_0((n-1)\tau)[1 + \psi_1(\tau)] + P_0((n-1)\tau)[\psi_2(\tau) + \psi_{12}(\tau)] + P_y((n-1)\tau)\varphi(\tau)\}, \quad (22)$$

where

$$e^{-\Lambda\tau} \{P_0((n-1)\tau)[\psi_2(\tau) + \psi_{12}(\tau)] + P_y((n-1)\tau)\varphi(\tau)\} = P_y(n\tau); \quad (23)$$

$$e^{-(n-1)\Lambda\tau} [1 + \psi_1(\tau)]^{n-1} = P_0((n-1)\tau); \quad (24)$$

$$[\psi_2(\tau) + \psi_{12}(\tau)] e^{-\Lambda\tau} = P_y(\tau). \quad (25)$$

We now consider a more general case; in even-numbered p. m. periods faults of type 2 are eliminated, and in odd-numbered ones — faults of type 1.

Let us write (16) in a somewhat different form:

$$P(2\tau) = \{P_0(\tau) + P_x(\tau)\} \{P_0(\eta) + P_y(\eta)\} + \{P_0(\tau) + P_x(\tau)\} \{P_x(\eta) + P_{xy}(\eta)\} + e^{-\Lambda\tau} \{\psi_2(\tau) + \psi_{12}(\tau)\} P(\eta/\tau, \eta) + P(\eta/\tau, xy) \{\psi_2(\tau) + \psi_{12}(\tau)\}, \quad (26)$$

where

$$P(\eta/\tau, y) = e^{-(\Lambda + v_2)\eta}; \quad (27)$$

$$P(\eta/\tau, xy) = e^{-\Lambda\eta} \varphi_{21}(\eta);$$

$$P_0(\tau) = e^{-\Lambda\tau}; \quad P_x(\tau) = e^{-\Lambda\tau} \psi_1(\tau); \quad P_y(\tau) = e^{-\Lambda\tau} \psi_2(\tau); \quad (28)$$

$$P_{xy}(\tau) = e^{-\lambda \tau} \psi_{12}(\tau); \quad \varphi_{21}(\tau) = \frac{\lambda_1}{\nu_{12} - \nu_2} (e^{-\nu_2 \tau} - e^{-\nu_{12} \tau}).$$

Since a fault of type 2 is eliminated during the second p. m. period, it follows that when the latter ends the probability that there are no faults is

$$P_0(2\tau) = e^{-2\lambda \tau} \{1 + \psi_1(\tau)\} \{1 + \psi_2(\tau)\} + e^{-2\lambda \tau} \{\varphi_2(\tau) + \psi_{12}(\tau)\} e^{-\nu_2 \tau}, \quad (29)$$

while the probability that there is a fault of type 1 is

$$P_x(2\tau) = e^{-2\lambda \tau} \{1 + \psi_1(\tau)\} \{\psi_1(\tau) + \psi_{12}(\tau)\} + e^{-2\lambda \tau} \{\psi_2(\tau) + \psi_{12}(\tau)\} \varphi_{21}(\tau). \quad (30)$$

For the third working period we have the relation

$$P(3\tau) = P_0(2\tau) e^{-\lambda \tau} \{1 + \psi_1(\tau) + \psi_2(\tau) + \psi_{12}(\tau)\} + P_x(2\tau) \{e^{-\nu_1 \tau} + \varphi_{12}(\tau)\} e^{-\lambda \tau} \quad (31)$$

or

$$P_0(3\tau) = P_0(2\tau) \{1 + \psi_1(\tau)\} e^{-\lambda \tau} + P_x(2\tau) e^{-(\lambda + \nu_1) \tau} + P_0(2\tau) \{\psi_2(\tau) + \psi_{12}(\tau)\} e^{-\lambda \tau} + P_x(2\tau) \varphi_{12}(\tau) e^{-\lambda \tau}, \quad (32)$$

where

$$\varphi_{12}(\tau) = \frac{\lambda_2}{\nu_{12} - \nu_1} (e^{-\nu_1 \tau} - e^{-\nu_{12} \tau}). \quad (33)$$

Thus the reliability of the system at the end of the  $n$ -th working period ( $t = n\tau$ ) is

a) for odd  $n$ :

$$P(n\tau) = P_0((n-1)\tau) \{1 + \psi_1(\tau)\} e^{-\lambda \tau} + e^{-\lambda \tau} P_x((n-1)\tau) e^{-\nu_1 \tau} + P_0((n-1)\tau) e^{-\lambda \tau} \{\psi_2(\tau) + \psi_{12}(\tau)\} + P_x((n-1)\tau) e^{-\lambda \tau} \varphi_{12}(\tau); \quad (34)$$

b) for even  $n$ :

$$P(n\tau) = P_0((n-1)\tau) e^{-\lambda \tau} \{1 + \psi_2(\tau) + e^{-\lambda \tau} P_y((n-1)\tau) e^{-\nu_2 \tau} + P_0((n-1)\tau) e^{-\lambda \tau} \{\psi_1(\tau) + \psi_{12}(\tau)\} + P_y((n-1)\tau) e^{-\lambda \tau} \varphi_{21}(\tau). \quad (35)$$

Computations using formulas (22), (34), and (35) present no essential difficulties, since once the initial functions  $\psi_1$ ,  $\psi_2$ ,  $\psi_{12}$ ,  $\varphi_{12}$  and  $\varphi_{21}$  have been computed the solution involves only algebraic operations—addition and multiplication.

### Bibliography

1. Leont'ev, L. P. Otsenka nadezhnosti apparatury pri uchete profilaktiki s nepolnym ustraneniem nakoplenykh narushenii (Evaluation of the Reliability of Equipment Allowing for Preventive Maintenance with Incomplete Elimination of Cumulative Faults). — In press.
2. Sklyarevich, A. N. Nadezhnost' sistem so strukturnymi narusheniyami (Reliability of Systems with Structural Faults). — Avtomatika i Telemekhanika, 3. 1967.

*V. I. Levin*

**A METHOD FOR ANALYSIS OF RANDOM  
PROCESSES WITH INDEPENDENT  
INCREMENTS AND DISCRETE STATES**

A method is considered for the analysis of discrete-time random processes with independent stationary increments, discrete states. Underlying the method is the fact that for fixed parameters of the process (i.e., the number of positive, negative, and zero changes of state) its probability characteristics may be computed by geometric methods. The constant parameters are then replaced by random parameters corresponding to the conditions of the problem, using the total probability formula.

The method is applicable to the analysis of "accumulation-elimination" processes, such as failure-renewal processes in radio-electronic devices.

**INTRODUCTION**

An important problem in the investigation of random processes is to compute the probability of some well-defined property of the process in the time-state coordinate system. The best-known problems of this type are related to the probability characteristics of the overshoot of the process beyond a given level and are of great importance in reliability theory. Overshoot problems have been solved only for certain types of processes [1, 2]. At the same time, there are a great many analogous complex problems whose solution by probabilistic and analytical methods involves serious difficulties. An example is the determination of probability characteristics of the maxima, minima, and monotonicity intervals of a random process.

The application of geometric methods seems promising for the solution of these problems. Their applicability depends on the fact that each realization of a random process conforms to certain geometric laws. An example of the method for a certain random process with independent increments was given in [3].

In the present paper we consider a more general type of discrete-time processes with independent increments and discrete states; at each stage the process either remains in its present state  $M$  or passes to one of two neighboring states ( $N$  or  $L$ ). The transition probabilities for  $M \rightarrow M$ ,  $M \rightarrow N$ ,  $M \rightarrow L$  are not necessarily equal and are independent of the time and  $M$ . We present a geometric method for studying these processes in time-state coordinates.

1. Formulation of the problem. A process of the type described above may be represented graphically by a set of realizations or paths (Figure 1). Each path is a polygonal line whose straight-line segments are either parallel to the time-axis (present state preserved)

or inclined to it (transition to one of two neighboring states). It will be clear from the sequel that our method is also applicable to processes involving transitions to any finite set of states.

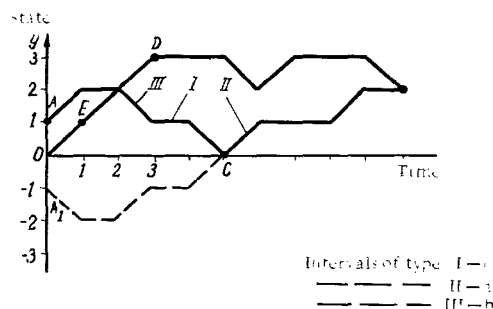


FIGURE 1.

Since this is a process with independent increments, the state changes in any time interval  $\Delta t_i = t_{i+1} - t_i$  occur independently of the behavior of the process in the intervals  $\Delta t_0, \dots, \Delta t_{i-1}, \Delta t_{i+1}, \dots$ . The following probabilities are given for each interval, independently of  $i$ :

$N$  — the probability that the state at the instant  $t_i$  is unchanged at the instant  $t_{i+1}$ ;

$P$  — the probability of transition to a "higher" state during  $\Delta t_i$ ;

$Q$  — the probability of transition to a "lower" state during  $\Delta t_i$ .

By definition there are no other transitions, so that

$$P + Q + N = 1. \quad (1)$$

Every path (Figure 1) is characterized by its initial point and the following parameters:

$a$  — the number of time intervals in which the transition is to the next-highest state;

$b$  — the number of time intervals in which the transition is to the next-lowest state;

$c$  — the number of time intervals in which the state does not change.

For the random process under consideration these parameters are random variables governed by the following probability distribution:

$$F(a, b, c) = \frac{t!}{a! b! c!} P^a Q^b N^c, \quad a + b + c = t. \quad (2)$$

We present a simple method for computing the probabilities of the positions of the realizations of the process in time-state coordinates. The basic idea is as follows:

At the first stage the parameters  $a, b, c$  of the paths (realizations of the process) are fixed. It follows from (2) that different paths of the resulting set are equiprobable. Thus the probability  $R(z/a, b, c)$  of a path with parameters  $a, b, c$  occupying position  $z$  is the ratio of the number of such

paths to the total number of paths with parameters  $a, b, c$ . The former number may usually be computed by geometric methods. The latter is

$$A(a, b, c) = \frac{t!}{a! b! c!}, \quad a+b+c=t. \quad (3)$$

At the second stage the parameters  $a, b, c$  are randomized, in accordance with the conditions of the problem. The probability of a realization occupying position  $z$  in time  $t$  is determined by the total probability formula:

$$P(z, t) = \sum_{a+b+c=t} R(z/a, b, c) \cdot F(a, b, c). \quad (4)$$

2. First stage of the computation. We now substantiate and illustrate the application of geometric methods for computation of the probability  $R(z/a, b, c)$ . In so doing we shall consider points  $z$  that are of practical interest. The methods considered here are analogous to those applied in [3] to the investigation of simpler processes.

1. Proposition 1. (Reflection Principle) (Figure 1). The number of paths  $AB$  ( $y_A \geq 0, y_B \geq 0$ ) with parameters  $a, b, c$  having at least one point on the time-axis is equal to the number of all paths  $A_1B$  with parameters  $a_1 = a + y_A, b_1 = b - y_A, c_1 = c$ , where  $A_1$  is the reflection of the point  $A$  in the time-axis.

Proof. Let  $ACB$  be any path with parameters  $a, b, c$  which has a point on the time-axis. Let  $C$  be the first such point (in direction of increasing time). With every path  $ACB$  we associate, in one-to-one fashion, the path  $A_1CB$ , in such a way that the segments  $CB$  of both paths coincide while the sections  $AC$  and  $A_1C$  are symmetric with respect to the time-axis. Thus the only differences between the parameters of the paths  $ACB$  and  $A_1CB$  derive from the different parameters of  $AC$  and  $A_1C$ . The latter satisfy the equations

$$\left. \begin{aligned} a_{A_1B} + b_{A_1B} &= a_{AB} + b_{AB}; \\ b_{A_1B} - a_{A_1B} &= y_A; \\ a_{A_1B} &= b_{AB}; \\ b_{A_1B} &= a_{AB}, \end{aligned} \right\} \quad (5)$$

whence it follows that

$$a_{A_1B} = a_{AB} + y_A, \quad b_{A_1B} = b_{AB} - y_A. \quad (6)$$

It is also obvious that  $c_{A_1B} = c_{AB}$ .

This completes the proof. It is analogous to the proof of the particular case  $c=0$  in [3]. The difference is due to the fact that when  $c=0$  the parameters of the paths are completely determined by their initial and terminal points, so that there is no need to discuss the relations between the parameters of  $ACB$  and  $A_1CB$ .

2. Let us compute the probability that a path  $OB, B(t, y_B \geq 0)$ , with parameters  $a \geq 1, b, c$ , neither touches nor cuts the time-axis for  $0 < x \leq t$  (Figure 1).

It is clear that any path  $OB$  with no points on the time-axis must pass through the point  $E(1, 1)$  and the total number of these paths is the total number of paths  $EB$  minus the number of paths  $EB$  having at least one point



161

Substituting  $A$  from (3), we obtain, after a few manipulations,

$$A(y > -d/a, b, c) = \begin{cases} A(a, b, c) \left[ 1 - \frac{(b-d+1) \dots b}{(a+1) \dots (a+d)} \right], & b \geq d, a-b > -d, \\ A(a, b, c), & b < d, a-b > -d, \\ 0, & a-b \leq -d. \end{cases} \quad (11)$$

Hence the required probability is

$$P(y > -d/a, b, c) = \begin{cases} 1 - \frac{(b-d+1) \dots b}{(a+1) \dots (a+d)}, & b \geq d, a-b > -d, \\ 1, & b < d, a-b > -d, \\ 0, & a-b \leq -d. \end{cases} \quad (12)$$

4. The probability that a path  $OB$ ,  $B(t, y_B)$ , with parameters  $a, b, c$  will have nonnegative ordinates for  $0 \leq x \leq t$  may be derived from (12):

$$P(y \geq 0/a, b, c) = P(y > -1/a, b, c) = \begin{cases} 1 - \frac{b}{a+1}, & a-b \geq 0, \\ 0, & a-b < 0. \end{cases} \quad (13)$$

A particular case of (13), for  $a=b, c=0$  is derived in [3].

5. Let us compute the probability that a path  $OB$ ,  $B(t, y_B \leq d)$  with parameters  $a, b, c$  neither touches nor cuts the line  $y=d$ .

The number  $A(y < d/a, b, c)$  of paths that have no point on the line  $y=d$  is equal to the number of all paths  $OB$  with parameters  $a, b, c$  minus the number of paths  $OB$  that have at least one point on the line  $y=d$ .

By Proposition 1 the latter is the total number of paths from the point  $N(0, 2d)$ , symmetric to  $O$  with respect to the line  $y=d$ , to the point  $B$ . The parameters of these paths are  $a_1=a-d, b_1=b+d, c_1=c$ . Thus

$$A(y < d/a, b, c) = A(a, b, c) - A(a-d, b+d, c), \quad (14)$$

or, substituting  $A$  from (3),

$$A(y < d/a, b, c) = \begin{cases} A(a, b, c) \left[ 1 - \frac{(a-d+1) \dots a}{(b+1) \dots (b+d)} \right], & a \geq d, \\ A(a, b, c), & a < d. \end{cases} \quad (15)$$

Thus the required probability is

$$P(y < d/a, b, c) = \begin{cases} 1 - \frac{(a-d+1) \dots a}{(b+1) \dots (b+d)}, & a \geq d, \\ 1, & a < d. \end{cases} \quad (16)$$

6. The probability that a path  $OB$ ,  $B(t, y_B \leq 0)$  with parameters  $a, b, c$  has nonpositive ordinates for  $0 \leq x \leq t$  may be derived from (16); it is

$$P(y \leq 0/a, b, c) = P(y < 1/a, b, c) = 1 - \frac{a}{b+1}. \quad (17)$$

7. Let us compute the probability that a path with parameters  $a, b, c$  first reaches the level  $y=d$  at its final point  $R(r=a+b+c, d)$ .

To this end we shall use the method of "inverted" paths [3]. By "inversion" we mean the one-to-one correspondence whereby every path  $OR$  whose ordinates (in order) are  $y_0=0, y_1, \dots, y_r=d$  corresponds to the path  $(OR)'$  with ordinates

$$y_i' = y_r - y_{r-i}. \quad (18)$$

It is obvious that the initial and terminal points and the parameters of both paths are the same.

To see that this correspondence is indeed one-to-one, note that the twice inverted path  $(OR)''$  coincides with  $OR$ , as follows from the equalities

$$y_i'' = y_r' - y_{r-i}' = y_r - (y_r - y_i) = y_i. \quad (19)$$

Thus the number of paths  $OR$  is equal to the number of paths  $(OR)'$ . Since  $R$  is the first point at which the path  $OR$  reaches the level  $y=d$ , it follows from (18) that the path  $(OR)'$  has positive ordinates for  $0 < x \leq r$ . Thus the probability  $P(d=y_r > y_i, i < r)$ , that the path first reaches  $y=d$  at the point  $R$  is equal to the probability that the path  $(OR)'$  has positive ordinates for  $0 < x \leq r$ , provided  $a-b=d$ . This probability is given by (9), so that, together with the obvious case  $a-b \neq d$

$$P(d=y_r > y_i, i < r) = \begin{cases} \frac{d}{r}, & a-b=d, \\ 0, & a-b \neq d. \end{cases} \quad (20)$$

8. Let us compute the probability that the first point on the time axis at which a path  $OS$  with parameters  $a, b, c$  changes direction is its terminal point  $S(s=a+b+c, 0)$  (Figure 2).

If  $a \neq b$  this probability is zero. Consider the case  $a=b$ . It is then immaterial whether the path is in the positive or the negative domain when the change of direction occurs; to fix ideas we consider the first case.

The number  $A(S/a, b, c)$  of paths  $OS$  with nonnegative ordinates which first change direction on the time axis at the point  $S$  is the number of paths  $OT, T(s-1, 1)$ , with parameters  $a_1=a, b_1=a-1, c_1=c$  which neither touch nor cut the time axis for  $0 < x \leq s-1$ . The latter number is given by (9). Thus

$$A(S/a, a, c) = \frac{1}{s-1} A(a, a-1, c). \quad (21)$$

The required probability is

$$P(S/a, a, c) = \frac{A(S/a, a, c)}{A(a, a, c)}. \quad (22)$$

Substituting the values of  $A$  obtained from (3) and (21) and adding the case  $a=b$ , we get

$$P(S/a, b, c) = \begin{cases} \frac{a}{s(s-1)}, & a=b, \\ 0, & a \neq b. \end{cases} \quad (23)$$

The following conclusion may be drawn from the above examples. Geometric methods employing the principles of reflection, inversion, and truncation are fairly effective for the computation of the probabilities of various positions (in time-state coordinates) of the realizations of a discrete-time random process with independent increments and discrete states. Combination of these methods with other methods (especially inductive methods) yields many useful results. Some details may be found in [3], where geometric methods are applied to the investigation of processes whose realizations have two parameters  $a$  and  $b$ ,  $c=0$ .

3. Second stage of the computation. According to the formulation of the problem, formula (4) is the basis for the general method of computing the probability that the realizations of the process occupy given positions during the time  $t$ . Let us solve a specific problem.

Consider a radio-electronic system under the following conditions: at random instants certain components fail, or standby components replace faulty one. The probabilities of failure (replacement) of a single component in unit time are given. The probability that two or more components fail (are replaced) in unit time is neglected. The failures (replacements) of components in different time intervals are assumed independent, and failures and replacements of components are mutually independent. For normal operation of the system (on the assumption that replacement of a faulty component is instantaneous) the accumulated difference between the number of replaced components and the number of faulty components must be nonnegative, otherwise a critical situation is deemed to have occurred. We wish to compute the probability that there will be no critical situations during time  $t$ .

The state of the system may be characterized by a single parameter  $y(t)$ --the accumulated difference between the number of replaced and faulty components during the time  $t$ . It is clear that  $y(t)$  is a discrete-time random process with independent increments and discrete states. The increment of  $y(t)$  in unit time can only have the values 0, 1, -1. Thus the problem reduces to computing the probability that no realization of the process enters the negative domain during the time  $t$ .

The same or a similar formulation is applicable to many problems arising in various fields of technology and economy and involving the accumulation and expenditure of resources. For example:

- 1) reliability computations for discrete automata with memory, possessing control and error-correction systems;
- 2) hopper-type devices in assembly-lines;
- 3) water-reservoir computations;
- 4) trade-network computations.

In the last two cases it is assumed that the time and the states (water level in the reservoir, quantity of sold goods) are discrete.

With a view to including various possible applications in our discussion, we shall consider the problem of this section as follows: Given a discrete-time random process with independent increments and discrete states, to find the probability that the realizations of the process do not enter the negative ordinate domain during the time  $t$ . It is assumed that the state transitions in the realizations and the corresponding probabilities satisfy the conditions of the formulation of the problem, and that the initial state of the process is the origin.

By (4) the required probability is

$$P(y \geq 0, t) = \sum_{a+b+c=t} P(y \geq 0/a, b, c) F(a, b, c). \quad (24)$$

Substituting the corresponding probabilities from (2), (13) into (24), we get

$$P(y \geq 0, t) = \sum_{\substack{a+b+c=t \\ a-b \geq 0}} \frac{t!}{a! b! c!} P^a Q^b N^c - \sum_{\substack{a+b+c=t \\ a-b \geq 0}} \frac{t!}{a! b! c!} P^a Q^b N^c \left( \frac{b}{a+1} \right). \quad (25)$$

Expressing  $c$  in terms of  $a, b, t$  and setting  $a+b=k$ , the two sums in (25) may be written as follows:

$$\begin{aligned} & \sum_{k=0}^t C_t^k N^{t-k} \sum_{b=0}^{[0.5 k]} C_k^b P^{k-b} Q^b, \\ & \sum_{k=0}^t C_t^k N^{t-k} \sum_{b=0}^{[0.5 k]} C_k^{b-1} P^{k-b} Q^b. \end{aligned} \quad (26)$$

Thus the probability of a nonnegative state of the process during time  $t$  is

$$P(y \geq 0, t) = \sum_{k=0}^t C_t^k N^{t-k} \sum_{b=0}^{[0.5 k]} (C_k^b - C_k^{b-1}) P^{k-b} Q^b. \quad (27)$$

For at all significant values of  $t$  this formula involves a formidable number of computations. Fortunately, in practice the most interesting cases are usually those in which at least one of the probabilities  $P, Q, N$  is negligibly small. Let us consider these cases.

a)  $Q \ll P$ .

In this case the inner sum in (27) may be replaced by its first term ( $b=0$ ). The result is

$$P(y \geq 0, t) \approx \sum_{k=0}^t C_t^k N^{t-k} P^k = (N+P)^t = (1-Q)^t. \quad (28)$$

This formula has a simple physical interpretation. For instance, in the case of a radio-electronic system (see above) it means that if failures are relatively rarer than replacements by standby components, then the absence of critical situations and the absence of failures are equivalent events.

b)  $Q=P$ .

In this case the inner sum in (27) is equal to  $P^k C_k^{[0.5k]}$ , and thus

$$P(y \geq 0, t) = \sum_{k=0}^t C_k^{[0.5 k]} C_t^k N^{t-k} P^k. \quad (29)$$

It is considerably easier to compute the sum in (29) than the double sum in the general formula (27). In practice the most interesting case is  $Q=P \approx 0$  ("slowly changing" process). Computation can then be limited to the first  $n$  terms of (29). The absolute error involved in this approximation for large  $t$  is at most

$$\Delta_{\max} = \frac{2^{t+1} P^{n+1}}{\pi t}. \quad (30)$$

The actual value of the absolute error is usually much smaller. For example, let  $P=10^{-5}$ ,  $t=100$ , and suppose the sum is limited to 11 terms. By (30) the error is at most 0.01. However, even if we compute the first term alone we get

$$P(y \geq 0, 100) > N^{100} = (1 - 2 \cdot 10^{-5})^{100} > 1 - 2 \cdot 10^{-3},$$

so that the absolute error  $\Delta$  is at most 0.002.

Note that when  $tP \ll 1$  computations of formula (29) can always be limited to the first term. The physical meaning of this assertion is simple: if the input and output of even one unit of the resources is an almost impossible event, then the nonnegativity of the resources during time  $t$  is equivalent to the latter maintaining their initial (zero) level.

c)  $Q \gg P$ .

In this case it is sufficient to compute the  $[0.5k]$ -th term of the inner sum in (29). The result is

$$P(y \geq 0, t) = \sum_{k=0}^t C_t^k (C_k^{[0.5k]} - C_k^{[0.5k]-1}) N^{t-k} P^{k-[0.5k]} Q^{[0.5k]}. \quad (31)$$

The case  $Q \approx 0$  is of practical interest. Moreover, if  $tQ \ll 1$  the computation can be limited to the first term of (31). In general, if the first  $n$  terms of (31) are taken into account, the absolute error cannot exceed

$$\Delta_{\max} = \frac{(2N)^t}{\pi \sqrt{tQ}} \left( \frac{2\sqrt{PQ}}{N} \right)^{n+1}. \quad (32)$$

Thus, if  $t = 100$ ,  $P = 10^{-5}$ ,  $Q = 10^{-2}$  and the 9 first terms of (31) are computed, then the absolute error cannot exceed  $1.4 \cdot 10^{-4}$ . This degree of accuracy is quite reasonable. In fact, the right-hand side of (31) is greater than

$$N^{100} = (1 - 10^{-2} - 10^{-5})^{100} \approx 0.04,$$

so that the relative computation error is at most

$$\delta = \frac{1.4 \cdot 10^{-4}}{0.04} = 3.5 \cdot 10^{-3};$$

d)  $N=0$  ("rapidly changing" process).

In this case only the  $t$ -th term of the outer sum in (27) is not zero. Thus

$$P(y \geq 0, t) = \sum_{b=0}^{[0.5k]} (C_t^b - C_t^{b-1}) Q^b (1-Q)^{t-b} \quad (33)$$

or, after simple manipulations, for  $Q < 1$

$$P(y \geq 0, t) = \frac{(1-2Q)^{t+1}}{(1-Q)^{t+1}} \sum_{b=0}^{[0.5k]} C_t^b Q^b (1-Q)^{t-b} + C_t^{[0.5k]} Q^{[0.5k]+1} (1-Q)^{t-[0.5k]}, \quad (34)$$

Computation of (34) is a simple, since tables are available for the sum in the right-hand side [4]. A particular case of this formula, for  $P=Q=0.5$ , may be found in [3].

## CONCLUSIONS

1. We have proposed a method for the analysis of discrete-time random processes with independent increments and discrete states, based on simple geometric principles [3].

2. The method is also applicable to continuous processes. In this case formula (2) must be replaced by the probability density of the number of positive and negative increments of the realizations of the process as functions of a continuous time-variable.

3. The only processes actually studied in the paper were such that each step involved an increment of at most one unit. It is easy to generalize the results to the case when the state changes are numbers from the interval  $[-K, +L]$ , where  $K$  and  $L$  are positive integers.

4. The method is applicable to the analysis of systems whose operation involves the input and output of resources, such as radio-electronic systems with failure and renewal.

## Bibliography

1. Levin, B. R. *Teoriya sluchainykh funktsii i ee primeneniye v radio-tekhnike* (The Theory of Random Functions and its Application to Radio-Technology). Moskva, "Sovetskoe Radio." 1960.
2. Skorokhod, A. V. *Sluchainye protsessy s nezavisimymi prirashcheniyami* (Random Processes with Independent Increments). Moskva, "Nauka." 1964.
3. Feller, W. *An Introduction to Probability Theory and its Applications*, Volume I. New York, Wiley. 1950.
4. Roming, H. C. *50-100 Binomial Tables*. New York, Wiley. 1953.

A. M. Margulis

**STANDBY REDUNDANCY SYSTEM AS A PARTICULAR  
CASE OF SYSTEMS WITH POSSIBLE STRUCTURAL  
FAULTS**

Formulas for the reliability of standby redundancy systems are derived from the corresponding formulas for systems with possible structural faults, assuming the conditional failure intensities of the system in the presence of working components to be zero. When all the components have failed the conditional failure intensity of the system is assumed infinite.

In [1] A. N. Sklyarevich determined the probability of failproof performance for time  $t$  of a nonrenewable system with  $n$  possible structural faults. Failures of components are considered independent.

If the probability of failproof performance of a component for time  $t$  and  $k$  the conditional probability of failproof performance of the system with  $k$  structural faults ( $k \leq n$ ) are described by exponential laws, then the probability of failproof performance of the system is given by the following formula:

$$G(t) = F(t) \left\{ 1 + \sum_{k=1}^n \sum_{i_1=1}^N \sum_{i_2=1}^{N_1} \dots \sum_{i_k=1}^{N_1} \sum_{l=0}^k \frac{\lambda_{i_1} \lambda_{i_2} \dots \lambda_{i_k}}{Q^l(\beta_{i_1, i_2, \dots, i_k})} e^{-\beta_{i_1, i_2, \dots, i_k} t} \right\}, \quad (1)$$

where  $N$  is the number of components in the system,

$$Q(z, i_1, i_2, \dots, i_k) = (-1)^k z(z - v_{i_1})(z - v_{i_2, i_1}) \dots (z - v_{i_1, i_2, \dots, i_k}), \quad (2)$$

$$v_{i_1, i_2, \dots, i_k} = \mu_{i_1, i_2, \dots, i_k} - \lambda_{i_1} - \lambda_{i_2} - \dots - \lambda_{i_k}, \quad (3)$$

and  $\lambda_{i_1}, \lambda_{i_2}, \dots, \lambda_{i_k}$  are the failure intensities of the components of the system,  $\mu_{i_1, i_2, \dots, i_k}$  is the conditional failure intensity of the system in the presence of a combination of failures  $i_1, i_2, \dots, i_k$ , and finally

$$F(t) = e^{-\sum_{i=1}^N \lambda_i t}.$$

We shall show that standby redundancy systems are special cases of systems with possible structural faults.

A common feature of both types of system is that they can perform satisfactorily despite several faulty components. The specific features of standby redundancy systems are:

a) the failure intensities of the components are equal:

$$\lambda_{i_1} = \lambda_{i_2} = \dots = \lambda_{i_N} = \lambda; \quad (4)$$



b) the conditional failure intensity of the system when less than  $N$  components fail is zero:

$$\mu_{i_1, i_2, \dots, i_k} = 0, \quad (5)$$

while it is infinite when all components fail:

$$\mu_{i_1, i_2, \dots, i_N} = \infty.$$

Thus

$$v_{i_1, i_2, \dots, i_k} = -k\lambda$$

and

$$v_{i_1, i_2, \dots, i_N} = \infty. \quad (6)$$

In view of (4)–(6) formula (1) assumes a simpler form:

$$\begin{aligned} G(t) &= e^{-N\lambda t} \left\{ 1 + \sum_{k=1}^{N-1} C_N^k k! \sum_{i=0}^k \frac{\lambda^k}{Q'(\beta, i_1, \dots, i_k)} e^{-\beta t} \right\} = \\ &= e^{-N\lambda t} \left\{ 1 + \sum_{k=1}^{N-1} (-1)^k C_N^k (1 - e^{-\lambda t})^k \right\}. \end{aligned} \quad (7)$$

Opening the braces and changing signs within the parentheses, we get

$$G(t) = e^{-N\lambda t} + \sum_{k=1}^{N-1} C_N^k e^{-(N-k)\lambda t} (1 - e^{-\lambda t})^k. \quad (8)$$

Formula (8) is identical with the formula for the probability of failproof performance of a standby redundancy system, derived by different arguments in [2, 4] and other sources.

The methods considered in [1] for evaluating the reliability of systems with possible structural faults are also applicable when each component is subject to two types of failure – "short circuits" and "open circuits."

Consider a system of  $N$  components, each of which is liable to failures of either open-circuit or short-circuit type, these failures being independent. The system can be represented by a system containing  $2N$  components, consisting of two  $N$ -component subsystems. The components of the first subsystem are liable only to short circuit failures, those of the second to open circuit failures. The system is considered to be performing satisfactorily if both subsystems are performing satisfactorily. Then the probability of failproof operation of the system is

$$G(t) = G_0(t) G_1(t), \quad (9)$$

where  $G_1(t)$  is the corresponding probability for the first subsystem (short circuits) and  $G_0(t)$  for the second (open circuits).

In evaluating the reliability of a system with regard to specific types of failures the schematic diagram describing the connections between the components plays an essential role. Let us consider this problem for the

case of series-parallel systems. The reasoning for other types (such as bridge circuits) is analogous. The only modification is in the combinations of failures causing failure of the system as a whole.

Let us determine these combinations for a series-parallel system. A failure of the first subsystem occurs if all the components of a single line are short-circuited.

Assuming that the conditional failure intensity of the system for all combinations of faults that cause failure of the entire system is infinite, we obtain

$$\mu_{i_{s1}, i_{s2}, \dots, i_{sr}, \dots, i_{sn}} = \infty \quad (s=1, 2, \dots, m), \quad (10)$$

where  $i_{sr}$  indicates the failure of the  $r$ -th component from the left in the  $s$ -th line, and  $n$  is the number of components connected in series in a single line.

It also follows from (10) that the first subsystem breaks down if the number of faults occurring in it exceeds  $N-n$ .

The probability of failproof performance of the first subsystem during time  $t$  is

$$G_s(t) = F_s(t) \left\{ 1 + \sum_{k=1}^{N-n} \sum_{i_1=i_{11}=1}^N \sum_{i_2=i_{12}=1}^N \dots \sum_{i_k=i_{1k}=1}^N \frac{\lambda_{i_1}, \dots, \lambda_{i_k}}{Q'(\beta_t, i_1, \dots, i_k)} e^{-\beta_t t} \right\}, \quad (11)$$

where  $k=n(s-1)+r$ ,  $\lambda_i$  is the failure intensity of the  $i$ -th component (short circuit), and

$$F_s(t) = e^{-\sum_{i=1}^N \lambda_i t}.$$

A failure occurs in the second subsystem if all the lines are open-circuited. Therefore

$$\mu_{i_{1k}, i_{2l}, \dots, i_{mr}} = \infty \quad (k, l, \dots, r=1, 2, \dots, n). \quad (12)$$

The second subsystem breaks down if the number of faulty components exceeds  $N-m$ , where  $m$  is the number of lines connected in parallel.

The probability of failproof performance of the second subsystem during time  $t$  is

$$G_o(t) = F_o(t) \left\{ 1 + \sum_{k=1}^{N-m} \sum_{i_1=i_{11}=1}^N \sum_{i_2=i_{12}=1}^N \dots \sum_{i_k=i_{1k}=1}^N \frac{\lambda_{i_1}, \dots, \lambda_{i_k}}{Q'(\beta_t, i_1, \dots, i_k)} e^{-\beta_t t} \right\}, \quad (13)$$

where  $k=n(s-1)+r$ ,

$$F_o(t) = e^{-\sum_{i=1}^N \lambda_i t};$$

$\lambda_i$  is the open-circuit failure intensity of the  $i$ -th component, and  $e^{-\lambda_i t}$  is the probability that the  $i$ -th component is not open-circuited during time  $t$ .

Substituting (11) and (13) in (9), we obtain a formula for the probability of failproof performance of the entire system during time  $t$ :

$$G(t) = F_0(t) F_s(t) \left\{ 1 + \sum_{k=1}^{N-n} \sum_{i_1=1}^N \sum_{i_2=1}^{N'} \dots \dots \dots \sum_{i_k=1}^{N'} \sum_{l=0}^k \frac{\lambda_{i_1}, \dots, \lambda_{i_k}}{Q'(\beta_l, i_1, \dots, i_k)} e^{-\beta_l t} \right\} \times \left\{ 1 + \sum_{k=1}^{N-m} \sum_{i_1=1}^N \sum_{i_2=1}^{N'} \dots \dots \dots \sum_{i_k=1}^{N'} \sum_{l=0}^k \frac{\lambda_{i_1}, \dots, \lambda_{i_k}}{Q'(\beta_l, i_1, \dots, i_k)} e^{-\beta_l t} \right\}. \quad (14)$$

Formula (14) may be written as follows:

$$G(t) = F(t) \left\{ 1 + \sum_{k=1}^{N-(m+n)} \sum_{i_1=1}^{2N} \sum_{i_2=1}^{2N'} \dots \dots \dots \sum_{i_k=1}^{2N'} \sum_{l=0}^k \frac{\lambda_{i_1}, \dots, \lambda_{i_k}}{Q'(\beta_l, i_1, \dots, i_k)} e^{-\beta_l t} \right\}, \quad (15)$$

where  $F(t) = F_0(t) F_s(t)$  and the conditional failure intensities of the system for all combinations of faults that imply the combinations involved in (10) and (12) are infinite.

In [3, 4, 5] and in other sources a formula is derived for the probability of failproof performance of a series-parallel standby redundancy system during time  $t$ , in the presence of two types of component failure (open and closed circuits). Separate expressions are given there for the two types of failure. It may then be shown by manipulations of the expressions (11) and (13), rather than (15) itself, that when condition (4) holds the formula (15) and the formula for the probability of failproof performance of a standby redundancy system are identical.

Assuming the failure intensities of the components equal, let us find the probability that the first subsystem fails when failures occur in less than  $N-n$  components (i. e., in the presence of the combinations involved in condition (10):

$$\begin{aligned} & C_m^1 e^{-(N-n)\lambda_i t} (1 - e^{-\lambda_i t}) + C_m^1 C_{N-n}^1 e^{-(N-n-1)\lambda_i t} \times (1 - e^{-\lambda_i t})^{n+1} + \dots \\ & \dots + (C_m^1 C_{N-n}^n - C_m^2) e^{-(N-2n)\lambda_i t} \times (1 - e^{-\lambda_i t})^{2n} + \dots + \\ & + [C_m^1 C_{N-n}^{(m-2)n} - C_m^2 C_{N-2n}^{(m-2)n} + \dots + \\ & + (-1) C_m^{m-1} C_{N-(m-1)n}^1] e^{-n\lambda_i t} (1 - e^{-\lambda_i t})^{N-n} = \\ & = \sum_{k=n}^{N-n} \sum_{i=1}^s (-1)^{i-1} C_m^i C_{(m-i)n}^{k-in} e^{-in\lambda_i t} (1 - e^{-\lambda_i t})^{N-in}. \end{aligned}$$

where  $k = sn + r$ ;  $s = 0, 1, \dots, (m-1)$ ;  $(r < n)$ .

In view of (15) and (4), formula (11) may be written as follows:

$$G_s(t) = e^{-N\lambda_d t} + \sum_{k=1}^{n-1} C_N^k e^{-(N-k)\lambda_d t} (1 - e^{-\lambda_d t})^k + \\ + \sum_{k=n}^{N-n} \sum_{i=1}^s (C_N^k + (-1)^k C_{m,i}^k C_{(m-i)n}^{k-in}) e^{-in\lambda_d t} (1 - e^{-\lambda_d t})^{N-in}, \quad (16)$$

Simple manipulations yield

$$G_s(t) = [1 - (1 - e^{-\lambda_d t})^n]^m. \quad (17)$$

Similarly, using (4) and (12) we can derive from (13) an expression for the probability that the system is not open-circuited during the time  $t$ :

$$G_o(t) = 1 - (1 - e^{-n\lambda_d t})^m. \quad (18)$$

Formulas (16) and (17) coincide with the corresponding formulas in the above-mentioned sources.

Example. Let us derive a formula for the probability of failproof performance of a system consisting of two lines connected in parallel, each line consisting of two components connected in series.

1) The probability that no failure occurs owing to short-circuiting during time  $t$  is:

$$G_s(t) = e^{-4\lambda_d t} [1 - C_4^1 (1 - e^{\lambda_d t})] + (C_4^2 - C_4^1) (1 - e^{\lambda_d t}) = \\ = e^{-4\lambda_d t} [1 - 2(1 - e^{\lambda_d t})] = [1 - (1 - e^{-\lambda_d t})^2]^2.$$

2) The probability that no failure occurs owing to open-circuiting during time  $t$  is

$$G_o(t) = e^{-4\lambda_d t} [1 - C_4^1 (1 - e^{\lambda_d t}) + (C_4^2 - C_2^1 C_2^1) (1 - e^{\lambda_d t})^2] = \\ = 2e^{-2\lambda_d t} - e^{-4\lambda_d t} = 1 - (1 - e^{-2\lambda_d t})^2.$$

3) The probability of failproof performance of the system during time  $t$  is

$$G(t) = [1 - (1 - e^{-\lambda_d t})^2]^2 [1 - (1 - e^{-2\lambda_d t})^2].$$

## Bibliography

1. Sklyarevich, A. N. Nadezhnost' sistem so strukturnymi narusheniyami (Reliability of Systems with Structural Faults). — In press.
2. Epifanov, A. D. Nadezhnost' avtomaticheskikh sistem (Reliability of Automatic Systems). Moskva, Mashinostroenie. 1964.
3. Leont'ev, L. P. Sintez nadezhnykh sistem iz nadezhnykh elementov (Synthesis of Reliable Systems from Reliable Components). — Izv. AN Latv. SSR, ser. fiziko-tekhnich., 2. 1962.
4. Polovko, A. M. Osnovy teorii nadezhnosti (Fundamentals of Reliability Theory). Moskva, "Nauka." 1964. [English Translation: Academic Press, New York. 1968.]
5. Sinitsa, M. A. Rezervirovanie radioelektronnoi apparatury (Redundancy in Radio-electronic Equipment). — Radioelektronnaya promyshlennost', 5. 1958.

*V. P. Chapenko*

**APPLICATIONS OF STRUCTURAL REDUNDANCY  
TO INCREASE THE RELIABILITY OF ANALOGUE-  
DIGITAL FUNCTIONAL CONVERTERS**

A method is proposed for the construction of analogue-digital time-pulse function converters of high reliability, based on the application of structural methods for the introduction of redundancy.

**1. INTRODUCTION**

To improve the reliability of digital computers (DC) with components of limited reliability one must introduce redundancy. In this connection much attention is being focused on structural methods for the introduction of redundancy in DC, are based on the application of correcting codes and various types of redundancy [2, 3, 4, 6, 7]. At present these methods are inadequately employed in increasing the reliability of the input units of DC being used as analogue-digital converters (ADC).

The majority of current designs for ADC consist of both analogue devices (linearly-varying voltage generators, comparison circuits, etc.) and digital devices (registers, counters, switches, commutators).

The operation of ADC involves errors of three types:

1) Errors governed by gradual deviation of the working parameters of the device beyond the limits laid down by the designer (drift failures). In ADC this type of error is characteristic primarily for the analogue devices, whose input parameter is a continuous quantity. The admissible deviations of this quantity are quite limited, since they determine the accuracy of analogue-digital conversion. For the digital devices, the range of admissible variations in the working parameters is wider, and they are therefore less susceptible to errors of this type.

2) Catastrophic failures, usually due to faults in the components (open or short circuits).

3) Short-duration (or self-eliminating) failures, due to disturbances by external and internal interference.

The two last types of errors may occur in both analogue and digital units of the ADC. In the sequel, reference to an error of an ADC unit will mean any of these three types.

Modern methods for increasing the interference-stability of digital devices use error-correcting codes (arithmetic AN-codes for errors in the adders of a DC; nonarithmetic codes (such as Hamming codes for errors in information-transmission and information-processing networks). Since these codes employ digital representation of information, they are not applicable to detection and correction of errors in analogue devices.

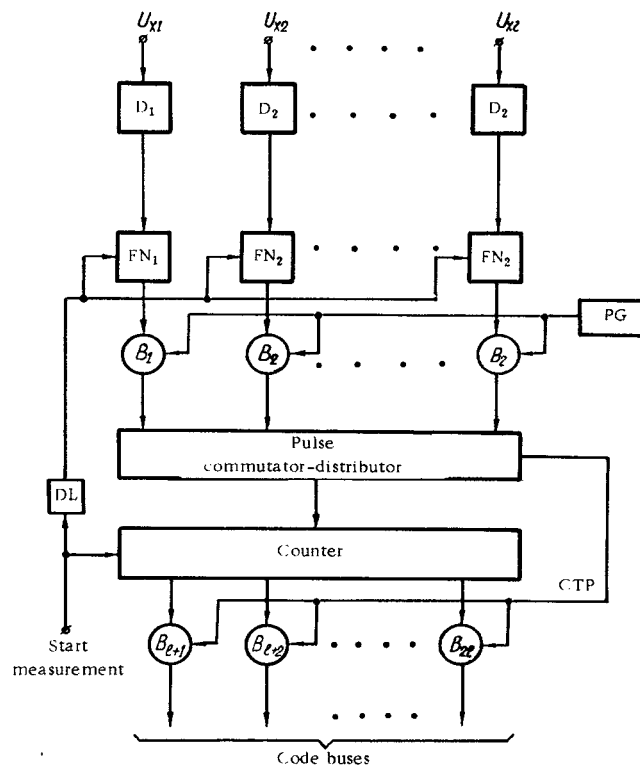


FIGURE 1. Block-diagram of a multichannel ADC.

Various forms of redundancy have gained widespread acceptance as a means for increasing the reliability of computing equipment. The smaller the degree of redundancy, the greater the reliability of the DC. With regard to ADC this means that it is more advantageous to introduce redundancy at the component level than to reproduce the entire converter.

To illustrate the possibilities of constructing analogue-digital converters which correct errors arising during operation, we consider a multichannel sequential-count ADC with intermediate conversion into a time interval  $1/f$  (Figure 1).

The operation of the converter proceeds as follows. Voltages  $U_{x1}-U_{xn}$  from the sensors of measured quantities  $D_1-D_n$  are applied to fantastrons  $FN_1-FN_n$ . A pulse "start measurement" sets the triggers of the counter to zero and, through a delay line (DL), starts the fantastrons. The duration of the output pulse of each fantastron  $FN_i$  is proportional to the corresponding  $U_{xi}$ . At the same time the gates  $B_1-B_n$  are opened and they receive pulses from a generator (PG). The commutator-distributor opens the outputs of the gates in sequence, for periods equal to the maximum duration of conversion in a single measurement channel, and the counter receives the PG pulses from

the  $i$ -th channel. The reading of the counter is proportional to the input voltage  $U_{xi}$ . On completion of a conversion cycle in the  $i$ -th channel, the commutator-distributor produces a code-transmission pulse CTP which opens the gates  $B_{i+1} \dots B_n$ . Through these gates the state of the counter is transmitted to a channel linking it to the DC.

## 2. INCREASING THE RELIABILITY OF THE ANALOGUE UNITS OF THE ADC BY ERROR CORRECTING METHODS

Redundancy can be introduced in analogue devices by triplication and the use of a selective circuit (majority element). When an error occurs in [only] one of the three redundant devices, an error-free signal is produced at the output of the majority element. If we regard the output analogue-variables as the elements of a code, then three-fold redundancy with a majority element is equivalent to a (3, 1) code for correction of single errors. In terms of Boolean algebra, the output function  $M(x, y, z)$  of the majority element has the form

$$M(x, y, z) = (x \wedge y) \vee (x \wedge z) \vee (y \wedge z), \quad (1)$$

where  $x, y, z$  are binary input signals.

Expression (1) is valid for bistable digital devices. The operation of a majority element with analogue inputs may be described in terms of continuous logic [5]. The logical OR function  $\vee$  is the selection of the great greater of two continuous variables  $x$  and  $y$ :

$$x \vee y = \max(x, y).$$

The logical AND function  $\wedge$  is the selection of the smaller of  $x$  and  $y$ :

$$x \wedge y = \min(x, y).$$

Expression (1) now becomes

$$M(x, y, z) = \max[\min(x, y), \min(x, z), \min(y, z)]. \quad (2)$$

If  $x = y \neq z$ , then

$$M(x, y, z) = \max[x, \min(x, z), \min(y = x, z)] = x = y. \quad (3)$$

Expression (3) corresponds to the selection of two identical quantities out of three.

Simulation of the operations min and max by electrical circuits is described in [5]. The block-diagram of a majority element with three analogue function units is illustrated in Figure 2a. The signal at the output of the circuit is that described (2) (Figure 2b).

In the converter circuit under consideration, the fantastron plays the role of a generator of rectangular pulses of variable duration. The basic parameter of this component is the relative time-error factor /1/; deviation of this parameter beyond the admissible limits gives rise to an error. By three-fold redundancy of the fantastron with a majority element single-error correction can be achieved. The input variables of the selective circuit are the durations of the fantastron pulses. A single error occurs when the durations of two pulses coincide and the time error in the third exceeds the admissible limits. The output function of the majority element is

$$\tau_{out} = \max[\min(\tau_1, \tau_2), \min(\tau_1, \tau_3), \min(\tau_2, \tau_3)], \quad (4)$$

where  $\tau_1, \tau_2, \tau_3$  are the durations of the output pulses of the fantastron and  $\tau_{out}$  is the duration of the output pulse of the majority element.

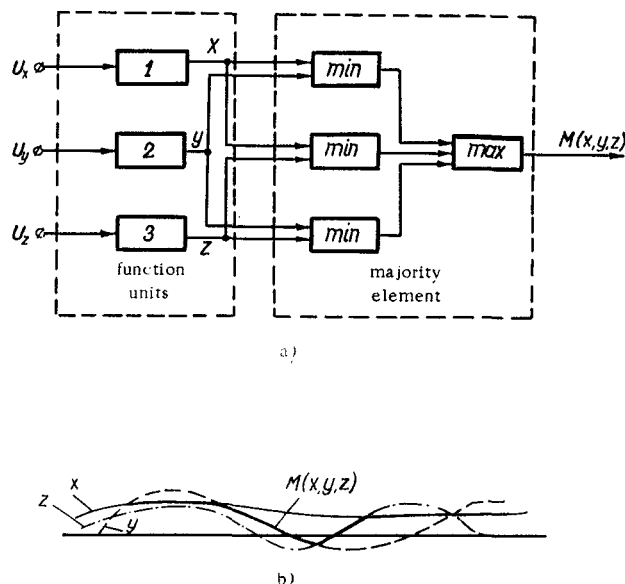


FIGURE 2. Block-diagram (a) and majority selection of a continuous signal from three input signals (b).

To construct a majority element which selects the maximal and minimal pulse durations, one can use binary-logic AND and OR circuits. The pulse duration at the output of the AND circuit is determined by the time during which the input signals coincide. The duration of the output pulse of the OR circuit corresponds to the greatest input-pulse duration. The use of binary AND and OR circuits may increase the error of the fantastron converter, owing to variations in the duration of the rectangular pulse at the output of the majority element. Below we describe a method for correction of instrumental errors in the ADC.



A redundant circuit of fantastrons with a majority element and a time diagram describing its operation are illustrated in Figures 3, a, b.

The increase in the reliability of the fantastron when this method is used is limited by the reliability of the selective element itself. Some increase in the reliability of the majority element in comparison with that of the fantastrons may be achieved by series-parallel redundancy of the digital circuits. In the selective circuit one can use gate circuits, as suggested in [7]. A signal is applied to the gate inputs only in the presence of a control voltage (as in electromagnetic relays). The methods for improving the reliability of gates are analogous to those used for switching devices [4].

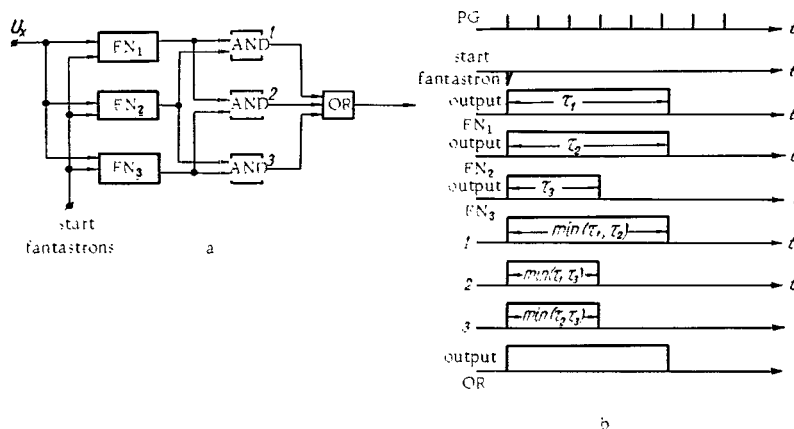


FIGURE 3. Schematic diagram of a three-fold-redundant fantastron circuit with majority element (a), time diagram (b).

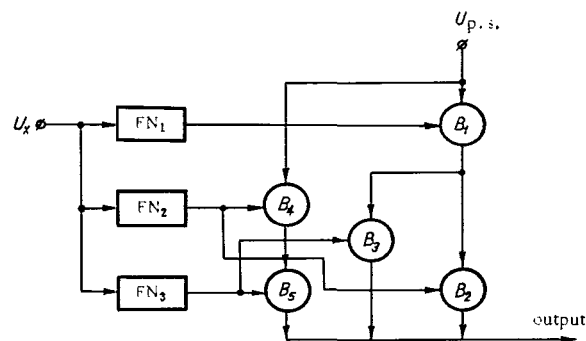


FIGURE 4. Schematic diagram of majority element constructed from gates.

The gates in the majority element are connected as indicated in Figure 4. The output pulse of the gate circuit is determined by the duration of the pulse at the control and gate inputs. The fantastron pulses are applied to the control inputs of the gates  $B_1 - B_5$ . The power supply feeds into the gate inputs  $B_1$  and  $B_4$ . The durations of the pulses at the inputs of  $B_1$  and  $B_4$  are  $\tau_{11}$  and  $\tau_{12}$ , respectively. From the output of  $B_1$  the pulse proceeds to the gate inputs  $B_2$  and  $B_3$ , while that from  $B_4$  proceeds to the gate input  $B_5$ . The outputs of  $B_2$ ,  $B_3$ ,  $B_5$  produce pulses of durations  $\min(\tau_{f1}, \tau_{f2})$ ,  $\min(\tau_{f1}, \tau_{f3})$ ,  $\min(\tau_{12}, \tau_{13})$ , respectively.

### 3. INCREASING THE RELIABILITY OF THE PULSE COUNTERS AND DISTRIBUTORS OF THE ADC

The function of the pulse counter in the ADC is to convert the measured analogue quantity into a digital sample and to act as output register for transmission of the digital code to the DC. The errors in the ADC depend to a significant degree on the fact that the binary counter is a source of random errors. A single error may give rise to errors in several digits of the digital code of the measured quantity. It is thus necessary to correct errors in the binary counter. However, the existing methods for constructing error-correcting counters, based on the use of error-correcting codes, considerably complicate the structure of the counter and increase its cost /6, 7/.

The code states of a counter are usually represented by binary or decimal residue-class arithmetic /8/. The counter consists of several ring shift-registers (ring counters) which successively move a "one" (or a "zero") from bit to bit. The bits of a ring counter are memory cells which are energized by a "one" signal during a single bit-time. The bit-times of all the ring counters are synchronized by a clock. The number of states of a ring counter is determined by the number  $n_i$  of bits it contains.

Calculating circuits employing ring counters have a number of advantages:

1. Ring counters are easily constructed from ferrite elements, which are more reliable than transistor elements.
2. The reliability of ring shift-registers may be considerably improved by employing redundancy with cross-connections of ferrite-diode cells, as suggested, e.g., by L. G. Ivanova /10/. A register of this type performs reliably when there are "open-circuit" -type failures in any combination of up to half the ferrites, barring errors in two ferrites of a single bit. Connection of the diodes in series can lessen the danger of "short-circuit"-type failures. The gain in reliability is achieved by relatively simple means, while the increase in the size and weight of the circuit is fairly small.

3. The load on a ring shift-register is constant, since the memory cells of the counter always contain the code "one."

It is thus advantageous to use ring shift-registers of ferrite-diode cells in ADC as highly reliable pulse counters and pulse distributors.

The structure of a system of ring counters is based on the following conditions /8/:

1) The numbers of bits in the ring counters must be pairwise prime:

$$(n_i, n_j) = 1, \quad i \neq j; \quad (5)$$

2) the total number  $N$  of states of the system is defined by

$$N = \prod_{i=1}^m n_i, \quad (6)$$

where  $m$  is the number of ring counters;

3) given the capacity  $N$  of the system, one must find the minimal sum of pairwise prime numbers  $S_{\min}$  whose product is at least  $N$ :

$$\prod_{i=1}^m n_i \geq N; \quad \sum_{i=1}^m n_i = S_{\min}; \quad (7)$$

$$(n_i, n_j) = 1; \quad 1 \leq i \leq m; \quad 1 \leq j \leq m; \quad i \neq j.$$

$S_{\min}$  is the minimal number of bits of the ring counters yielding the given capacity.

As an example, suppose the greatest number of pulses entering the counter of the ADC is  $63 = 2^6 - 1$ , corresponding to maximum converted continuous voltage. Using tables of prime decompositions of the numbers from 63 to 127 into pairwise prime factors one finds that  $S_{\min} = 14$  for two numbers  $N_1$  and  $N_2$  ( $N_1 = 70 = 2 \times 5 \times 7$ ,  $N_2 = 84 = 3 \times 4 \times 7$ ). Choose a system of ring counters with  $n_1 = 3$ ,  $n_2 = 4$ ,  $n_3 = 7$ . The sequence of states of this system is given in Table 1, and Figure 5 is a block-diagram of the corresponding circuit.

TABLE 1.

bit-time	counter states		
	$n_1$	$n_2$	$n_3$
1	100	0111	1000000
2	010	1011	0100000
3	001	1101	0010000
4	100	1110	0001000
5	010	0111	0000100
6	001	1011	0000010
...	...	...	...
63	001	1101	0000001
...	...	...	...
84	001	1110	0000001

Any bit-time number smaller than 84 corresponds to a definite state of the ring counters.

To express the readings of the ring counters in a binary representation system their states may be decoded by a read-only memory unit (ROM). When this is done the ring registers fulfill the function of a pulse distributor controlling the sequential read-out of the numbers recorded in the ROM in binary representation, which correspond to the states of the ring-counter system. Existing ROMs are simple in design and construction, small in size, and highly reliable [9]. Today ROMs are made from various ferromagnetic elements, diode and capacity matrices, and perforated ferrite plates.

Another important advantage of ROMs for ADC circuits is the possibility of representing the binary numbers recorded in the memory unit in noise-stable code.

The numbers recorded in a binary representation system have  $k$  information digits and  $m$  parity-check digits, corresponding to the representation of the measured analogue quantity in error-correcting code, say Hamming code. This renders transmission of discrete information from the ADC to the DC more reliable.

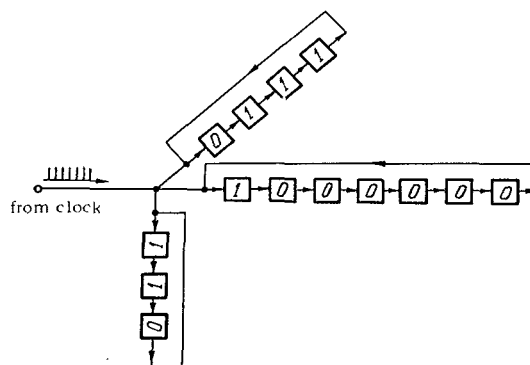


FIGURE 5. Block-diagram of a system of three ring counters.

For instance, with the system of ring counters of Figure 5 one can obtain 6-digit binary code at the output of the ADC. Thus representation of the numbers recorded in the ROM requires  $k=6$  information digits and  $m=4$  parity-check digits. The total capacity of the ROM is

$$m+k=4+6=10.$$

Yet another advantage of ROMs is their low energy consumption, since the information is read out at the instant the conversion cycle ends.

Figure 6 is the block-diagram of a single-channel ADC with two ring counters of capacities  $n_1$  and  $n_2$  and an ROM storing  $(m+k)$ -digit codes. A "package" of clock pulses, whose number is determined by the duration of the pulses of the fantastron FN, reaches the ring counters, which fulfill the function of a pulse distributor controlling the sequential read-out of information from the ROM. At the end of the measurement a "transfer code" pulse (TCP) is fed to the ROM. The number selected by the ring counters proceeds to the output register. Let us consider the operation of a pulse distributor consisting of ring counters with  $n_1=3$  and  $n_2=4$  bits (Figure 7). Suppose the state of the three-bit counter is 100, while that of the four-bit counter is 0111. The clock pulses, entering through the gate B, move the information through the ring counters. The energized bits of the counters (state "one") send a pulse to the inputs of the corresponding gates  $B_1 - B_7$ . The other input of each gate receives a set pulse. When the pulses

at each input of the gate coincide, the output produces a current pulse. The outputs of  $B_1 - B_7$  form a coordinate-transformer matrix of dimension  $3 \times 4$ . Each coordinate-transformer acts as a switch operating on the principle of anticoinciding currents; it is a pulse transformer with four windings on a toroidal core with rectangular hysteresis loop. The matrix cores are at first negatively magnetized (state "zero"). This is ensured by a bias current  $I_{bi}$  passing through the bias windings of the coordinate transformer. At the end of the measurement cycle the pulse TCP starts the set-pulse shapers PS-1 and PS-2. A negative current pulse  $-I_c$  proceeds from the output of PS-1 to the gates  $B_1 - B_4$ , and passes through all gates corresponding to state "one" in the bits of the counter  $n_2$ .

The gates  $B_1, B_2, B_3$  receive a positive current pulse  $+I_c$  from the output of PS-2. As a result, the core of the magnetic switch at the intersection of a nonenergized row and an energized column is magnetized, enters state "one," and sends a pulse to the output winding of a magnetic switch loaded with a number bus consisting of 10 cores with rectangular hysteresis loop. The current pulses which reach the output windings of the bit cores of the number line proceed through amplifiers  $A_1 - A_{10}$  to the output register.

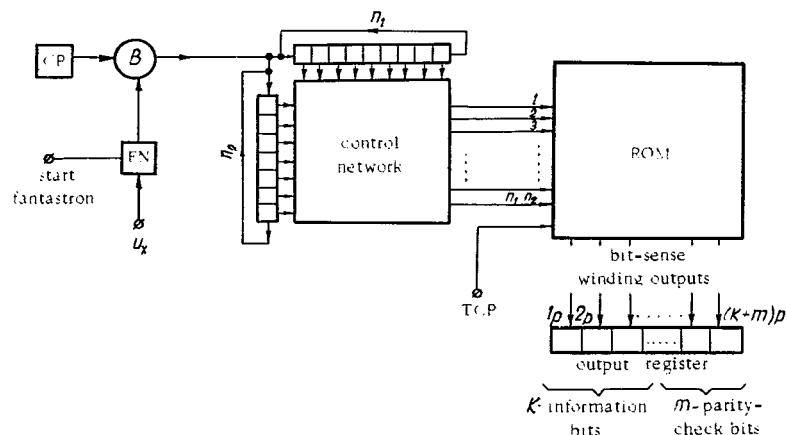


FIGURE 6. Block-diagram of ADC with ROM.

Today several versions of small-size and compact ROMs are available in which the number of memory cores in the number buses is considerably smaller than the total capacity of the ROM in binary units /9/. This is achieved by threading several numerical set-windings on each core. The information in these ROMs is determined by mechanical considerations — the threading of the cores.

In the ROM circuit of Figure 7 there is a single number line on which are threaded 12 set windings from the corresponding coordinate transformers of the pulse distributor.

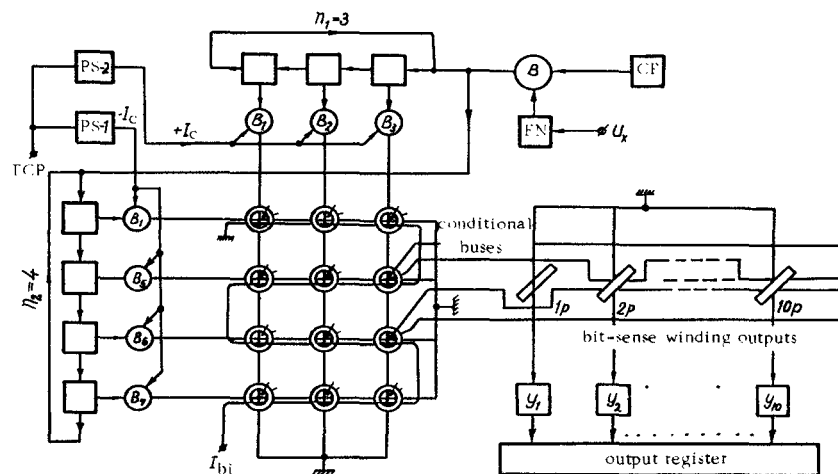


FIGURE 7. Schematic diagram of ROM of capacity  $3 \times 4$ .

The above mode of operation of a pulse distributor with two ring counters can be extended to systems of several ring counters, using well-known methods [9] for the construction of multicoordinate networks of ferrite cores. Design of multicoordinate ROMs is also not difficult.

By employing redundancy with cross-connections of ring counters, one can ensure normal performance of the pulse distributor despite catastrophic failures. Random errors are not corrected. In this connection we mention the design of error-correcting pulse distributors from linear transformer decoders, based on the principle of addition of voltages [3]. The performance index of a transformer decoder is its resolution factor  $C$ , defined as the ratio of the voltage in a selected bus of the decoder to the maximal voltage in the other buses:

$$C = \frac{n}{n-2d}, \quad (8)$$

where  $n$  is the number of binary-code digits in the register at the decoder input, and  $d$  is the code distance between the input binary numbers of the decoder.

The operation of a linear transformer decoder is controlled by a shift-register in which the information is represented by noise-resistant code. The circuit corrects errors arising both in the register itself and in the decoder. At present the disadvantage of such circuits is the need for threshold elements at the decoder input in order to select the output signals in the selected and nonselected buses.

Utilization of codes with code distance  $d = \frac{n}{2}$ , developed with the aid of orthogonal matrices [2], provides complete suppression of noise in the non-selected buses. However, application of this method in an ADC increases the size of the equipment.

#### 4. FUNCTION CONVERSION IN THE ADC

For function conversion of an analogue quantity into digital code, ROMs can be used. The numerical cells contain information in error-correcting code, in accordance with the given function-conversion operator. In recording in the ROM, various instrumental faults of the ADC may be taken into account: the nonlinearity of the response of the sensors for the measured quantities, the nonlinear dependence of the duration of the fantastron pulse on the control voltage, the variations of pulse duration in the majority element. This is especially important when a multichannel ADC has a set of identical sensors, such as temperature sensors in an industrial remote-control system.

Suppose that the temperature sensors are thermoelectric pyrometers [11]. The dependence of the emf induced in the thermocouples on the

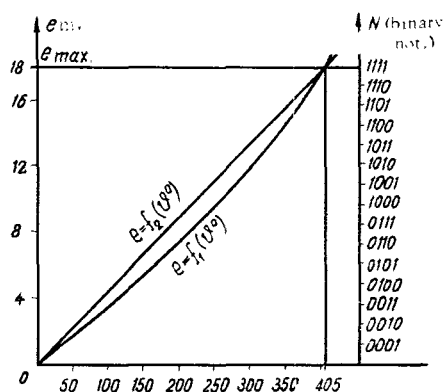


FIGURE 8. Static response of a thermoelectric pyrometer.

temperature  $\theta^{\circ}$  is described by a nonlinear function (the curve  $e=j_1(\theta^{\circ})$  in Figure 8). The reading of the thermoelectric pyrometer is to be converted into digital code with an accuracy of 1, 15. The nonlinear function  $e=j_1(\theta^{\circ})$  is approximated by a straight line  $e=j_2(\theta^{\circ})$ , with a certain error. Table 2 gives numerical standards for the temperature when the response of the thermocouples is approximated by a linear function and for the true response. The numerical qualities are represented in Hamming (7, 4) code.

In a similar way the nonlinearity of the fantastrons in an ADC can be corrected.

If the converter output is to produce both the current value of the measured quantity and a given function thereof, the capacity of the ROM must

be enlarged. The memory cell can therefore store the binary code of both the function itself and its increment in each working cycle of the ADC. The numerical values of the increments proceed from the ROM to a counter-type adder, where they are added or subtracted, according to the sign of the increment. The number of bits in the adder may be greater than that of the ADC itself. For example, when the measured quantity is squared, increments enter the adder in accordance with the expression

$$1+3+5+7+\dots+2^n-1,$$

where  $n$  is the capacity of the ADC.

Here we are using the fact that the sum of the first  $m$  odd numbers is  $m^2$ . The counter-type adder contains  $2n$  bits.

To increase the reliability of the counter-type adder one can use error-correcting codes, such as  $AN$ -codes.

TABLE 2.

$\theta^\circ$	Digital standards		
	$e = f_2(\theta^\circ)$	$e = f_1(\theta^\circ)$	
		information symbols	parity-check symbols
27	0001	0001	111
54	0010	0010	011
81	0011	0011	100
108	0100	0011	100
135	0101	0100	101
162	0110	0101	010
189	0111	0110	110
216	1000	0111	001
243	1001	1000	110
270	1010	1001	001
297	1011	1010	101
324	1100	1011	010
351	1101	1100	011
378	1110	1101	100
405	1111	1111	111

## CONCLUSION

The above methods for increasing the reliability of multichannel ADC of time-pulse type may also be used for other types of analogue-digital converters, introducing redundancy in the individual units of the ADC.

## Bibliography

1. Shevelev, P. N. Fantastronnyi preobrazovatel' tipa "napryazhenie-chislo" (Fantastron Converter of the "Voltage-Number" Type). Trudy Rzhskogo instituta inzhenerov GVF, Number 6. Riga. 1961.
2. Peterson, W. W. Error-correcting Codes. Cambridge, Mass. M. I. T. Press. 1961.
3. Radchenko, A. N. Primery povysheniya nadezhnosti diskretnykh skhem metodom vnutriskhemnogo kodirovaniya sostoyanii (Examples of Improving the Reliability of Digital Circuits by Intracircuit Coding of States). Leningrad. 1964.
4. Kosarev, Yu. A. Rezervirovanie logicheskikh i pereklyuchatel'nykh skhem (Redundancy in Logic and Switching Circuits). In sbornik: "Avtomatika, telemekhanika, priborostroenie. "Moskva-Leningrad. 1965.
5. Ginsburg, S. A. Logicheskii metod sinteza funktsional'nykh preobrazovatelei (A Logical Method for the Synthesis of Function Converters). Trudy Mezhdunarodnogo kongressa MFAU, volume 4. Moskva, AN SSSR. 1961.
6. Russo, R. L. IEEE Trans. Electronic Computers, 14: 3, 359. 1965.
7. Frantsis, T. A. and G. F. Yanbykh. Avtomaticheskoe ispravlenie oshibok v diskretnykh avtomatakh (Automatic Error Correcting in Discrete Automata). Present collection.



8. Pivovarov, A. N. O predstavlenii natural'nykh chisel sistemoi kol'tsevykh schetchikov s poparno-vzaimno-prostymi chislami razryadov (On Representation of Natural Numbers by Ring Counters with Pairwise Prime Numbers of Bits). —Izv. AN SSSR (tekhnicheskaya kibernetika), 4. 1965.
9. Kraizmer, A. P. Bystrodeistvuyushchie ferromagnitnye zapominayushchie ustroystva (High-speed Ferromagnetic Memory Units). Moskva-Leningrad, "Energiya." 1964.
10. Ivanova, L. G. Povyshenie nadezhnosti sdvigayushchikh registrov (Increasing the Reliability of Shift-Registers). Sbornik rabot po voprosam elektromekhaniki, Number 7. Moskva-Leningrad. 1962.
11. Maizel', M. M. Osnovy avtomatizatsii tekhnologicheskikh protsessov (Fundamentals of the Automation of Technological Processes). Moskva. 1960.

*L. P. Leont'ev, B. M. Kopelevich*

**THEORETICAL GAIN IN RELIABILITY BY  
MEANS OF SERIES-PARALLEL AND PARALLEL-  
SERIES STANDBY REDUNDANCY**

Equations are considered for determining the reliability of series-parallel and parallel-series redundant systems with constantly connected standby components. Failure of each component may be due to either of two independent reasons. It is shown that these schemes may be used to obtain reliability arbitrarily close to unity.

In /1, 2, 3/ methods were considered for determining the reliability of series, parallel, and combined standby redundancy systems. Criteria were developed for selecting the method whereby the main and standby components are connected, and various properties of the reliability function of standby redundancy systems were studied.

In this paper we study the question whether one can achieve a given reliability, arbitrarily close to unity, by means of series-parallel and parallel-series standby redundancy.

In /3/ it was shown if open and short circuits are mutually incompatible events, then the reliability of systems in which the standby components are connected in series-parallel and parallel-series is given by the equations

$$P_{n, m} = (1 - q_s^n)^m - (1 - p_o^n)^m; \quad (1)$$

$$P_{m, n} = (1 - q_o^m)^n - 1(-p_s^m)^n, \quad (2)$$

where  $p_o$  is the reliability of each component as regards open circuits,

$$q_o = 1 - p_o,$$

and  $p_s$  its reliability as regards short circuits.

$$q_s = 1 - p_s;$$

$m$  is the number of elements in a line or the number of elements connected in parallel in a single branch (Figure 1, 2), and  $n$  the number of parallel lines or the number of branches connected in series (Figure 1, 2).

Since the inequalities

$$q_o < p_s \text{ and } q_s < p_o \quad (3)$$

are always true, it follows that equations (1) and (2) may be combined in a single equivalent equation:

$$P_{k, r} = (1 - \alpha^k)^r - (1 - \beta^k)^r, \quad (4)$$

where

$$0 < \alpha < 1; \quad 0 < \beta < 1; \quad \alpha < \beta. \quad (5)$$

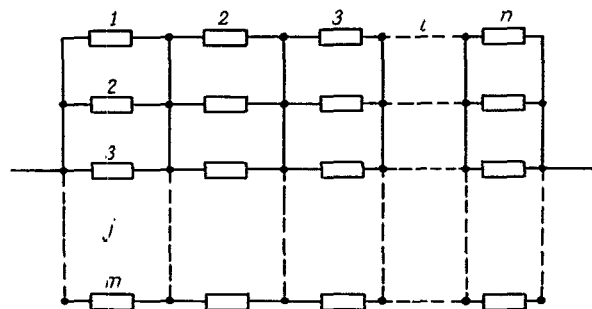


FIGURE 1. Parallel-series connection of elements

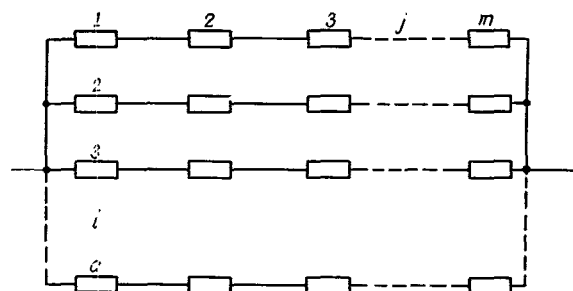


FIGURE 2. Series-parallel connection of elements.

We wish to prove that for any  $\alpha$  and  $\beta$  satisfying conditions (5) and any  $k_1 > k$  ( $1 \leq k \neq \infty$ ), there exists  $r_1 > r$  ( $1 \leq r \neq \infty$ ) such that

$$P_{k_1, r_1} > P_{k, r}. \quad (6)$$

in explicit form, inequality (6) is

$$(1 - \alpha^{k+y})^{r+x} - (1 - \beta^{k+y})^{r+x} > (1 - \alpha^k)^r - (1 - \beta^k)^r. \quad (7)$$

Since no restrictions are imposed on  $k$  other than  $1 \leq k \neq \infty$ , we must prove the following assertion:

I. For any  $1 \leq k \neq \infty$ ,  $1 \leq r \neq \infty$ , and  $k_1 = k + y$  ( $y > 0$ ), there exists  $0 < x$  such that inequality (7) holds.

In equality (7) may be written in the form

$$(1 - \alpha^{k+y})^{r+x} - (1 - \alpha^k)^r > (1 - \beta^{k+y})^{r+x} - (1 - \beta^k)^r. \quad (8)$$

Both sides of (8) may be regarded as values of a function of a single argument  $z$ , with  $z = \alpha$  in the left-hand side and  $z = \beta$  in the right-hand side.

The conditions  $0 < z < 1$ ,  $z_1 = \alpha < z_2 = \beta$  must be satisfied. Inequality (8) becomes

$$\varphi(z_1) > \varphi(z_2), \quad (9)$$

where

$$\varphi(z) = (1 - z^{k+y})^{r+x} - (1 - z^k)^r. \quad (10)$$

Thus Proposition I reduces to the following assertion:

II. For any  $z_1 < z_2$  ( $0 < z_1 < 1$ ), ( $0 < z_2 < 1$ ) and any  $k_1 = k + y$  ( $0 < k \neq \infty$ ,  $0 < y \neq \infty$ ), there exists  $x$  ( $0 < x \neq \infty$ ) such that inequality (8) holds.

To prove II, we must show that the conditions imposed on the values of  $x$ ,  $y$ ,  $k$ ,  $r$  ensure that

$$\frac{d\varphi}{dz} < 0, \quad (11)$$

$$\frac{d\varphi}{dz} = -(p+x)(k+y)z^{k+y-1}(1-z^{k+y})^{r+x-1} + krz^{k-1}(1-z^k)^{r-1}. \quad (12)$$

Substituting  $\frac{d\varphi}{dz}$  from (12) into (11), we get the inequality

$$(r+x)(k+y)z^{k+y-1}(1-z^{k+y})^{r+x-1} > krz^{k-1}(1-z^k)^{r-1}. \quad (13)$$

Inequality (13) may be replaced by the stronger inequality

$$(r+x)(k+y)z^y(1-z^{k+y})^x > kr. \quad (14)$$

For if (14) holds, then since

$$(1 - z^{k+y}) > (1 - z^k) \quad (15)$$

in the domain  $y > 0$  under consideration, it follows that (13) is true.

Consider the left-hand side of (14). The product of the first two factors is always greater than  $kr$ :

$$(r+x)(k+y) > kr, \quad (16)$$

while the product of the remaining two factors  $z^y(1-z^{k+y})^x$  is always smaller than unity for  $x, y > 0$ .

Inequality (14) will be satisfied if we can find conditions under which

$$z^y(1-z^{k+y})^x \quad (17)$$

is a nondecreasing function of  $x$  and  $y$ .

Consider the partial derivative  $\frac{\partial \psi(x, y)}{\partial y}$ , where  $\psi(x, y) = z^y(1-z^{k+y})^x$ ;

$$\frac{\partial \psi(x, y)}{\partial y} = z^y(1-z^{k+y})^x \ln z - z^y x(1-z^{k+y})^{x-1} z^{k+y} \ln z. \quad (18)$$

Inequality (14) will be satisfied if we can find conditions guaranteeing that the partial derivative

$$\frac{\partial \Psi(x, y)}{\partial y} \quad (19)$$

is positive. The condition  $\frac{\partial \Psi(x, y)}{\partial y} > 0$  is equivalent to

$$(1 - z^{k+y})^x > x (1 - z^{k+y})^{x-1} z^{k+y}. \quad (20)$$

Hence

$$x < \frac{1}{z^{k+y}} - 1. \quad (21)$$

It is clear from (21) that for any  $x > 0$  there exist infinitely many values of  $y$  satisfying (21), hence also (14).

We have thus proved that there are conditions under which the functions defined by equations (1) and (2) are monotonically increasing functions of  $m$  and  $n$ . This means that once the arguments  $m$  and  $n$  have been suitably chosen it is always possible to increase the reliability. We claim that the reliability may be made arbitrarily close to unity.

Consider the limit of the expression

$$(1 - \alpha^k)^r = \left[ (1 - \alpha^k)^{\frac{1}{\alpha^k}} \right]^{r \alpha^k}. \quad (22)$$

The expression in square brackets tends to  $e^{-1}$  as  $k \rightarrow \infty$ . Therefore \*

$$\lim_{\substack{k \rightarrow \infty \\ r \rightarrow \infty}} (1 - \alpha^k)^r = e^{-\lim_{\substack{k \rightarrow \infty \\ r \rightarrow \infty}} r \alpha^k}. \quad (23)$$

The following conditions are necessary for the expression (4) to tend to unity as  $r \rightarrow \infty$  and  $k \rightarrow \infty$ :

$$\left. \begin{aligned} \lim_{\substack{r \rightarrow \infty \\ k \rightarrow \infty}} (1 - \alpha^k)^r &= 1; \\ \lim_{\substack{r \rightarrow \infty \\ k \rightarrow \infty}} (1 - \beta^k)^r &= 0. \end{aligned} \right\} \quad (24)$$

But the limit (23) is unity if

$$\lim_{\substack{r \rightarrow \infty \\ k \rightarrow \infty}} r \alpha^k = 0. \quad (25)$$

\* [Translator's note: This argument is far from rigorous, but the final conclusion is nonetheless correct.]

The relation (25) will be satisfied if  $r \rightarrow \infty$  to the same order as  $\frac{1}{(\alpha + \varepsilon_1)^k}$ , where  $\varepsilon_1$  is an arbitrarily small positive number. On the other hand,

$$\lim_{\substack{r \rightarrow \infty \\ k \rightarrow \infty}} (1 - \beta^k)^r = 0,$$

if  $r\beta^k$  also tends to  $\infty$  as  $r \rightarrow \infty$  and  $k \rightarrow \infty$ . This is the case if  $r \rightarrow \infty$  to the same order as  $\frac{1}{(\beta - \varepsilon_2)^k}$ , where  $\varepsilon_2$  is another arbitrarily small quantity.

Consequently, the following condition is sufficient for (24) to hold:

$$\frac{1}{\beta^k} \leq r \leq \frac{1}{\alpha^k}. \quad (26)$$

Since  $\beta > \alpha$ , this condition may always be ensured.

We have thus proved that for given  $\alpha$  and  $\beta$  satisfying conditions (5) one can always find sequences  $k_n \rightarrow \infty$  and  $r_n \rightarrow \infty$  such that  $\lim_{\substack{r_n \rightarrow \infty \\ k_n \rightarrow \infty}} [(1 - \alpha^{k_n})^{r_n} - (1 - \beta^{k_n})^{r_n}] = 1$ .

## Bibliography

1. Leont'ev, L. P. Sintez nadezhnykh skhem iz nadezhnykh elementov (Synthesis of Reliable Systems from Reliable Components). Izv. AN Latv. SSR, ser. fiziko-tekh., 2. 1962.
2. Leont'ev, L. P. Ob opredelenii optimal'nogo sposoba soedineniya osnovnogo i rezervnykh elementov (Determination of the Optimal Manner for Connecting the Main Component and the Standby Components). In sbornik: Avtomatika i vychislitel'naya tekhnika, 6. Izdatel'stvo AN Latv. SSR. Riga. 1963.
3. Leont'ev, L. P. and A. M. Margulis. Vozmozhnostipovysheniya nadezhnosti putem primeneniya posledovatel'nostno-parallel'nykh i parallel'no-posledovatel'nykh skhem postoyannogo rezervirovaniya (Possibilities of Increasing Reliability by Means of Series-Parallel and Parallel-Series Standby Redundancy). In sbornik: Avtomatika i vychislitel'naya tekhnika, 12. Riga, "Zinatne." 1966.

V. F. Yadina

# FAILURE INTENSITY OF A SYSTEM ALLOWING FOR STRUCTURAL FAULTS

The author considers the time-dependence of the  $\Lambda$ -characteristic of systems with structural faults. Formulas are derived for the settling time of the  $\Lambda$ -characteristic of the system.

One of the basic quantitative characteristics of reliability is the failure intensity  $\Lambda(t)$  of the system, that is, the conditional probability density of a failure at the instant  $t$ , given the satisfactory performance of the system up to this instant [2]:

$$\Lambda(t) = -\frac{G'(t)}{G(t)}, \quad (1)$$

where  $G(t)$  is the probability of the satisfactory performance of the system.

In studying reliability one usually considers models in which any failure or fault in the system leads to immediate breakdown. In this case the  $\Lambda$ -characteristic is usually assumed constant (without regard for the role played by running-in and aging of the components), and then

$$G(t) = e^{-\lambda t}$$

(the lower curve in Figure 1), where  $\lambda$  is the intensity of the occurrence of a fault in a component.

We shall consider the case in which the system may continue to perform satisfactorily, or with certain aftereffects, despite occurrence of a failure. The above considerations are then no longer true, and it is the aim of this paper to determine the behavior of the  $\Lambda$ -characteristic for such systems, allowing for the cumulative effect of one or more faults. The unconditional probability of failproof performance of the system in time  $n$  when  $t$  cumulative faults may occur is determined by the following expression [1]:

$$G(t) = F(t) \left\{ 1 + \sum_{k=1}^n \sum_{i_1=1}^n \dots \sum_{i_k=1}^n \sum_{l=0}^k \frac{\lambda_{i_1} \dots \lambda_{i_n}}{Q'(\beta_{e_1, i_1}, \dots, i_k)} e^{-\beta_{e_1} t} \right\}, \quad (2)$$

where

$$Q(\beta_{e_1, i_1}, \dots, i_k) = (-1)^k z(z - v_{i_1}) (z - v_{i_1, i_2}) \dots (z - v_{i_1, \dots, i_k});$$

$$v_{i_1, \dots, i_k} = \mu_{i_1, \dots, i_k} - \lambda_{i_1} - \dots - \lambda_{i_k};$$

$\lambda_i$  is the intensity of the occurrence of the  $i$ -th fault, and  $\mu_{i_1} \dots \mu_{i_k}$  the conditional intensity of the failure of the system when a combination of faults  $i_1, \dots, i_k$  has occurred. The roots of the above polynomial are  $0, \nu_{i_1}, \dots, \nu_{i_k}$ . The function  $F(t)$  is the probability of failproof performance in the absence of faults.

Consider the case when

$$G_1(t) = e^{-k\lambda t} \left\{ 1 + \frac{k\lambda}{\nu} (1 - e^{-\nu t}) \right\}, \quad (3)$$

where  $k$  is the number of components in the system.

Formula (3) describes the reliability of the system when a fault may occur in any one component (and the system itself does not break down). The intensity of the occurrence of a fault for all the components is constant, as is the conditional intensity of the failure of the system due to these faults.

Similarly, if

$$G_2(t) = G_1(t) + e^{-k\lambda t} \cdot 2C_k^2 \lambda^2 \left[ \frac{1}{\nu \cdot \nu_{1,2}} + \frac{e^{-\nu t}}{\nu(\nu - \nu_{1,2})} + \frac{e^{-\nu_{1,2}t}}{\nu_{1,2}(\nu_{1,2} - \nu)} \right], \quad (4)$$

then a fault may occur both in any one component and in any pair of components. Figure 1 illustrates the reliability of the systems represented by (3) (middle curve) and (4) (upper curve). The graphs correspond to the cases  $\mu_i = \text{const}$  and  $\mu_{i_1, i_2} = \text{const}$ .

In systems without aftereffects the behavior of the  $\Lambda$ -characteristic is affected only by the intensities of faults (failures) of the individual components. When there are aftereffects the failure intensity of the system also depends on the intensities of the failures caused by these faults. For systems with a single fault, formulas (1) and (3) give

$$\Lambda_1(t) = k\lambda - \frac{e^{-k\lambda t} e^{-\nu t} k\lambda}{G_1(t)}. \quad (5)$$

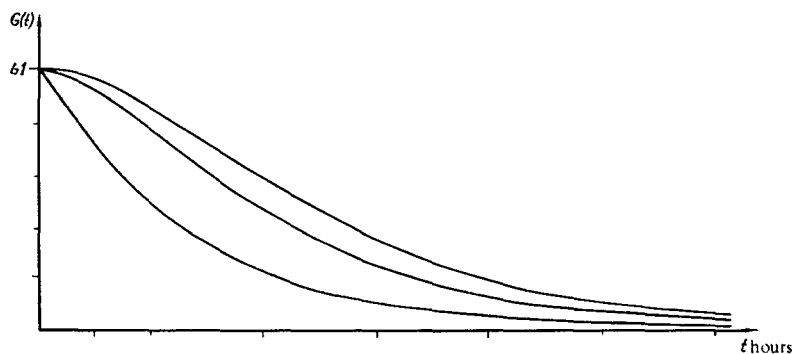


FIGURE 1. Reliability of systems with one and two structural faults.



With accumulation of two faults:

$$\Lambda_2(t) = k\lambda - \frac{e^{-k\lambda t} [k\lambda e^{-\nu t} - 2C_k^2\lambda(e^{-\nu t} - e^{-\nu_1 t})]}{G_2(t)}. \quad (6)$$

We shall consider the behavior of the  $\Lambda$ -characteristic of systems with one possible fault in three cases:

- 1)  $\mu > \lambda$ , i. e.,  $\nu > 0$ ;
- 2)  $\mu < \lambda$ , i. e.,  $\nu < 0$ ;
- 3)  $\mu = \lambda$ , i. e.,  $\nu = 0$ .

1. If  $\mu > \lambda$  and  $\nu > 0$ , it is easy to see from (5) that  $\Lambda \rightarrow k\lambda$  as  $t \rightarrow \infty$ , i. e., as  $t$  increases the failure intensity of the system approaches a constant value, approximately  $k\lambda$ . The behavior of the  $\Lambda$ -characteristic in this case is illustrated in Figure 2a—the straight line parallel to the time axis is situated at the level  $k\lambda$ .

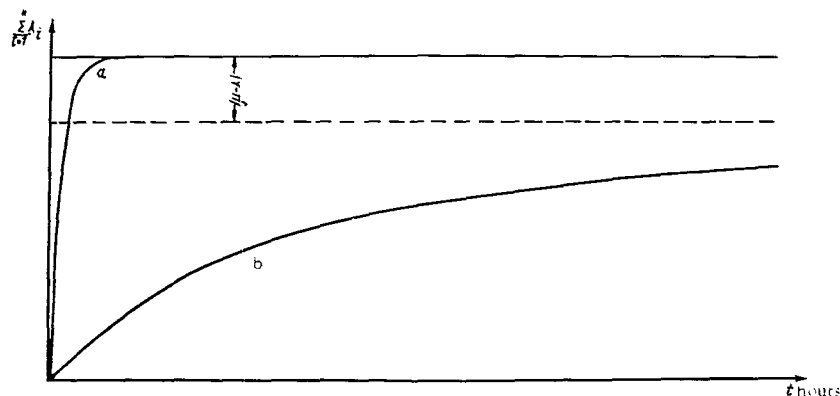


FIGURE 2. Behavior of the  $\Lambda$ -characteristic for  $\nu \geq 0$  and  $\nu < 0$ .

2. If  $\mu < \lambda$  and  $\nu < 0$ , it is convenient to transform (5) into the form

$$\Lambda_1(t) = k\lambda \left[ 1 - \frac{1}{\frac{1}{e^{-\nu t}} + \frac{k\lambda}{\nu} \left( -1 + \frac{1}{e^{-\nu t}} \right)} \right]. \quad (7)$$

Letting  $t \rightarrow \infty$ , we see that  $\Lambda_1(t) \rightarrow k\lambda + \nu$  (Figure 2b).

3. If  $\mu = \lambda$ ,  $\nu = 0$ , the expression  $\frac{k\lambda \left( \frac{1}{e^{-\nu t}} - 1 \right)}{\nu}$  is an indeterminate expression of type  $\frac{0}{0}$ . Using de l'Hospital's rule, we obtain

$$\frac{k\lambda \left( \frac{1}{e^{-\nu t}} - 1 \right)}{\nu} = k\lambda t, \quad \nu = 0.$$

Then

$$\Lambda_1(t) \rightarrow k\lambda \text{ as } t \rightarrow \infty.$$

Thus the final result for our model is:

- 1) when  $v \geq 0$ ,  $\Lambda_1(t) \rightarrow k\lambda$  as  $t \rightarrow \infty$ ;
- 2) when  $v < 0$ ,  $\Lambda_1(t) \rightarrow k\lambda + v$  as  $t \rightarrow \infty$ .

In practice one usually considers the value of  $\Lambda(t)$  steady when it has  $v \geq 0$  reached 95% of its limit value. For  $v < 0 - 0.95(k\lambda + v)$ . The obvious problem is now to determine the settling time of  $\Lambda(t)$  in each case. To determine the dependence of the settling time on the parameters  $\lambda$  and  $\mu$ , the left-hand side of (5) must first be equated to  $0.95k\lambda$ , then to  $0.95(k\lambda + v)$  one can then find the required values of  $t$  for various  $\lambda$  and  $\mu$ , for the cases  $v \geq 0$  and  $v < 0$ .

Sample computation:

1.  $v \geq 0$ . Then

$$k\lambda - \frac{k\lambda e^{-k\lambda t} e^{-vt}}{G_1(t)} = 0.95 k\lambda$$

or

$$\frac{e^{-k\lambda t} e^{-vt}}{G_1(t)} = 0.05.$$

Substituting the expression for  $G_1(t)$ , we get

$$e^{-vt} = \frac{1 + \frac{k\lambda}{v}}{20 + \frac{k\lambda}{v}}. \quad (8)$$

We shall not look for the dependence of the settling time on the failure intensity of the system to the level  $k\lambda$  in explicit form; instead we shall determine the dependence of  $\lambda^*$  on  $\frac{\lambda}{\mu}$  (where  $\lambda^* = \lambda t$ ), so that all three parameters will be described by a single graph.

Introduce the notation

$$\frac{\lambda t}{\mu t} = \frac{\lambda^*}{\mu^*} = m,$$

then

$$\lambda t - \mu t = \frac{(m-1)\lambda^*}{m}.$$

In this notation equation (2) becomes

$$e^{\frac{(m-1)\lambda^*}{m}} = \frac{1 + k \frac{m}{1-m}}{20 + k \frac{m}{1-m}}. \quad (9)$$

The graph of this function is illustrated in Figure 3a. The computation was performed for the case  $k=1$ .

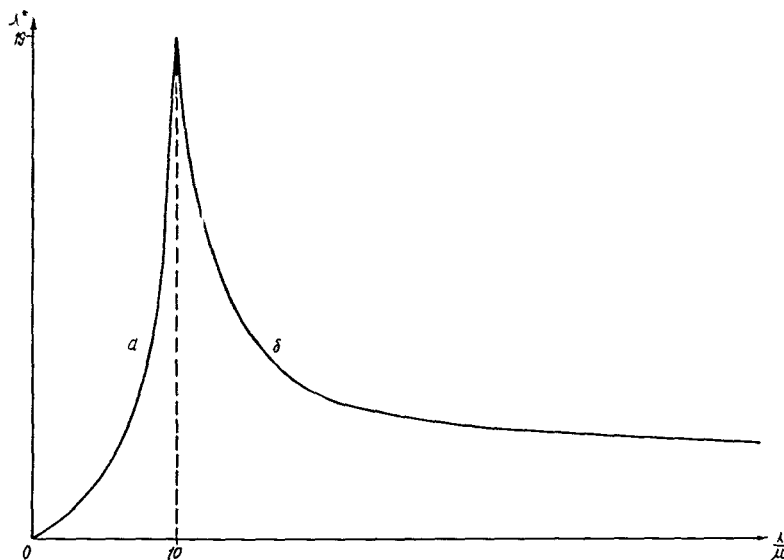


FIGURE 3 Dependence of  $\lambda^*$  on  $\frac{\lambda}{\mu}$  for  $v \geq 0$  and  $v < 0$

2.  $v < 0$ . Reasoning as before, we obtain

$$k\lambda - \frac{k\lambda e^{-k\lambda t} e^{-v t}}{G_1(t)} = 0,95 (k\lambda + v)$$

or

$$e^{\frac{(m-1)\lambda^*}{m}} = \frac{k^2 m^2 - 19(1-m)^2 - 18mk(1-m)}{k^2 m^2 - mk(1-m)}.$$

Carrying out the same operations as before, we again determine the dependence of the settling time of the  $\lambda$ -characteristic on the parameters  $\lambda$  and  $\mu$ . The corresponding graph is that of Figure 3b.

### Bibliography

1. Sklyarevich, A. N. Nadezhnost' sistem so strukturnyminarusheniyami (Reliability of Systems with Structural Faults). Avtomatika i telemekhanika, 3. 1967.
2. Gnedenko, B. V., Yu. K. Belyaev, and A. D. Solov'ev. Matematicheskie metody v teorii nadezhnosti (Mathematical Methods in the Theory of Reliability). Moskva, "Nauka." 1965.

G. A. Volounik

**EXPERIMENTAL DETERMINATION OF THE  
PARAMETERS OF THE RELIABILITY FUNCTION  
FOR A SYSTEM WITH POSSIBLE FAULTS**

In computing the operational characteristics of complex systems, the need arises to represent a system with an arbitrary number of faults (which do not cause immediate failure of the system) by a fictitious system with a limited number of faults in such a way that the reliability functions of the two systems are reasonably close to each other. The general form of the reliability function of a system with possible faults was obtained in [1]. Figure 1 illustrates a typical reliability curve.

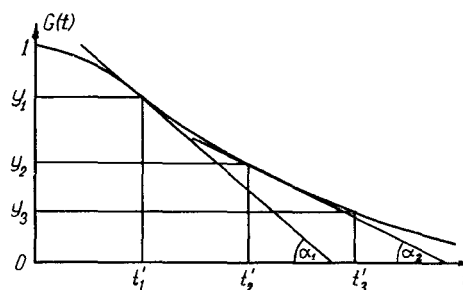


FIGURE 1. Reliability function of a system with possible faults.

In this paper we describe methods for determining the parameters of the reliability function for a system with "generalized" faults, on the basis of the empirical reliability function. Among these parameters are the intensity  $\lambda$  of the occurrence of "generalized" faults, and the intensity  $\mu$  of the failure of the system in the presence of a fault.

Underlying these methods are the results of an analytic investigation of reliability for a system with a single fault:

$$G(t) = e^{-\lambda t} + \frac{\lambda}{\mu - \lambda} (e^{-\lambda t} - e^{-\mu t}). \quad (1)$$

Let  $t'_k$  be the instants of time defined by

$$t'_k = k t'_1 \quad (k = 1, 2, \dots), \quad (2)$$

where  $t'_1$  is the abscissa of the point of inflection.

It can be shown that these instants satisfy the relations

$$\lambda^k e^{-\lambda t'_k} = \mu^k e^{-\mu t'_k} \quad (k=1, 2, \dots), \quad (3)$$

which express the interchangeability of the intensities  $\lambda$  and  $\mu$  with respect to the reliability function, i. e., permutation of the coefficients does not alter the reliability law defined by (1).

Let  $y_k$  be the ordinates of the reliability function corresponding to the points  $t'_k$  and  $\alpha_k$  the angles between the tangents to the function at these points and the time axis; these quantities are determined by the following expressions:

$$y_k = \frac{\mu^{k+1} - \lambda^{k+1}}{\mu^k(\mu - \lambda)} e^{-\lambda t'_k} = \sum_{l=0}^k e^{-(k-l)\lambda + l\mu} t'_l \quad (k=1, 2, \dots); \quad (4)$$

$$\operatorname{tg} \alpha_k = \frac{\lambda \mu (\mu^k - \lambda^k)}{\mu^k(\mu - \lambda)} e^{-\lambda t'_k} \quad (k=1, 2, \dots). \quad (5)$$

The values of  $y_k$  and  $\operatorname{tg} \alpha_k$  may be measured with a certain degree of accuracy on the graph of the empirical reliability function. The auxiliary constructions required to this end are illustrated in Figure 1. To determine the parameters  $\lambda$  and  $\mu$  in the general case, one need only solve the system of two equations (4) and (5).

We describe in detail two methods which are the most suitable from the standpoint of the results and the required amount of computation. In so doing we shall confine ourselves to equations (4) and (5) for  $k=1$  and  $k=2$ , and therefore we only need the empirical reliability function over a finite time interval.

Method I. The basis of the method is equation (5) for  $k=1$ :

$$\operatorname{tg} \alpha_1 = \lambda e^{-\lambda t'_1}, \quad (I)$$

which directly determines the intensity  $\lambda$ . In the general case equation (5) will have two roots. By (3), the second root gives the intensity  $\mu$ . If there is a double root, this means that  $\lambda = \mu$ .

The following procedure is recommended for solution of the transcendental equation (1). Multiplying both sides by  $t'_1$ , we get a system of two equations:

$$\begin{cases} y = \frac{\operatorname{tg} \alpha_1}{u}; \\ y = e^{-u}, \end{cases} \quad (Ia)$$

which are easily solved for  $u = \lambda t'_1$  by graphical methods.

Method II. The basic equations

$$\begin{cases} y_1 = e^{-\lambda t'_1} + e^{-\mu t'_1}; \\ y_2 = e^{-2\lambda t'_1} + e^{-(\lambda+\mu)t'_1} + e^{-2\mu t'_1} \end{cases} \quad (II)$$

lead to a quadratic equation in  $e^{-\lambda t'_1}$ :

$$e^{-2\lambda t'_1} - p e^{-\lambda t'_1} + q = 0, \quad (IIa)$$

where

$$p=y_1; \quad q=(y_1)^2-y_2. \quad (11b)$$

After solving equation (11a), the intensity  $\lambda$  may be computed,  $t_1'$  being known, for example, by using tables. The second root of the equation yields the intensity  $\mu$ .

Method II does not involve the tangent to the empirical reliability function at the inflection point, and is therefore more accurate than Method I. Moreover, Method II yields an approximation of the reliability function over a longer time interval.

If the empirical reliability function exhibits no clear-cut inflection point, this means that one of the parameters ( $\lambda$  or  $\mu$ ) is considerably greater than the other. In this case the dominant intensity may be determined by standard methods for the exponential reliability law.

### Bibliography

1. Sklyarevich, A.N. Nadezhnost' sistem so strukturnymi narusheniyami (Reliability of Systems with Structural Faults). Avtomatika i telemekhanika, 3. 1967.

*I. Ya. Bilinskii, E. K. Gulevskii*

### TUNNEL DIODE SWITCHING DELAY

This article examines tunnel diode switching delay under the action of a linearly increasing voltage. By means of an approximate analytical solution for a nonlinear differential equation describing the initial stage of the switching process, the delay dependence on the parameters of the signal, tunnel diode and circuit is obtained. The derived formula is useful for calculating the regime and deviation of the discriminators which operate when the input voltage exceeds a certain level, the appropriate upper limit of increment for input pulse signals, and the delay variation limits for a given variation in the tunnel diode parameters.

The concept of the transfer function is not usual for tunnel-diode (TD) pulse units. One can, however, attempt to derive a function expressing the correlation between the output for a specific type of input signal, taking into account the TD and the circuit parameters. Obviously, such a function will constitute the mathematical expression of the TD switching process.

If our aim is to obtain a relationship appropriate both for qualitative and quantitative analysis, the TD characteristic has to be approximated by a complex expression and the desired relationship which results is even more involved and inconvenient for analysis. The switching process can, however, be split into separate stages which can be separately examined. Each switching stage will then correspond to a certain segment of the TD characteristic, for which a good approximation will be far easier to find than for the entire characteristic. The results thus obtained should indicate the influence of the signal, circuit and TD parameters upon each switching stage and, in addition will help in calculating the operating conditions and circuit properties (resolution, transconductance of the front, output signal amplitude, etc.).

Below we shall study the switching delay of a quiescent TD (Figure 1, a) under the effect of an increasing voltage applied to the circuit input.

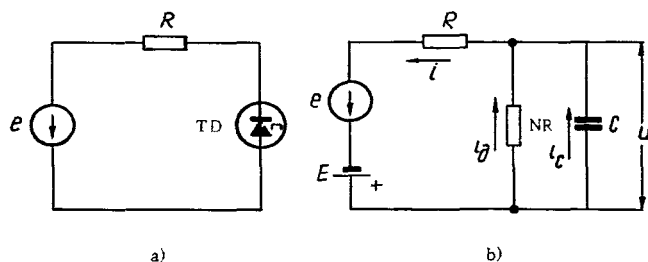


FIGURE 1. Cut-off TD circuit:

a — circuit diagram; b — equivalent circuit.

Let  $t_d$  be the time delay from the onset of the signal until the instant when the voltage  $u$  across the TD attains a value of  $U_2$ , which corresponds to the intersection of the  $R$ -load line and the current-voltage characteristic of the TD (Figure 2) for an input signal  $e$  equal to the static operation threshold  $U_m$ . The delay of a real circuit can be expressed as a sum

$$t_d = t_m + \Delta t.$$

The first term represents the time elapsed from the onset of the signal until the signal attains the value  $U_m$ .

The magnitude of  $t_m$  depends on the starting position of the working point and the statics of the circuit. The magnitude  $\Delta t$  characterizes the circuit inertia, i.e., its dynamic properties. The signal parameters mainly affect  $\Delta t$ ; the transconductance of the front of the output voltage for different signals remains almost unchanged [1].

A linearly increasing voltage was chosen as the input signal, as this most often adequately approximates the actual TD switching conditions. In fact,  $\Delta t$  is influenced only by that part of the input voltage, which corresponds to the passage of the working point through the maximum-current domain. This usually enables us to consider the input signal as a linearly increasing voltage, since for a reliable operation of pulse circuits the amplitude of the input pulses is chosen in such a way as to exceed the dynamic operation threshold  $E_m$  even under the most unfavorable conditions in the operating range. Therefore, switching on is effected by the leading edge, a portion of which may usually be replaced in calculations by a linearly increasing voltage.

Inasmuch as the switching delay corresponds to the passage of the working point along the tunnel admittance branch, only that part of the TD characteristic will be approximated when writing the initial equations. We stress the fact that as long as the working point moves along the tunnel-admittance branch, the TD constitutes a small resistance and the time constant of the circuit is very small. Hence, the initial position of the working point influences neither  $\Delta t$  nor the difference  $\Delta e = E_m - U_m$  (see Figure 2), when this position does not exceed  $0.8 I_1$ , even for comparatively large time constants [2].

For analysis, the circuit in Figure 1(a) is replaced by the equivalent circuit in Figure 1(b), i.e., the TD is replaced by a nonlinear resistance (NR), having the current-voltage characteristic of a linear capacitance  $C$ :

$$i_\partial = \alpha u^2 + \beta u + z \quad (1)$$

(Equation (1) fairly accurately approximates the tunnel-admittance branch of the current-voltage characteristic of the TD (see Figure 2, curve 2).

The equivalent circuit is represented by the system of equations

$$\left. \begin{aligned} E + e &= i R + u; \\ i &= i_\partial + i_c; \\ i_\partial &= \alpha u^2 + \beta u + z; \\ i_c &= C \frac{du}{dt}; \\ e &= k t, \end{aligned} \right\} \quad (2)$$





Since

$$\frac{d i_{\partial'}}{d u'} = 2 \alpha u' + \beta,$$

then, at the point of the maximum,

$$0 = 2 \alpha \frac{U_{09}}{2} + \beta$$

or

$$\beta = -\alpha U_{09}. \quad (5)$$

By substituting the value  $\beta$  into equation (4), we obtain

$$0.1 I_1 = \alpha \frac{U_{09}^2}{4} - \alpha \frac{U_{09}^2}{2},$$

whence

$$\alpha = -\frac{0.4 I_1}{U_{09}^2}. \quad (6)$$

By determining  $\alpha$  at the level  $n I_1$ , where  $n = \frac{I_n}{I_1}$ , we similarly obtain

$$\alpha = -\frac{4(1-n)I_1}{U_n^2},$$

whence

$$\frac{0.1}{U_{09}^2} = \frac{1-n}{U_n^2}$$

and

$$U_n = \sqrt{\frac{1-n}{0.1}} U_{09}.$$

Then

$$\beta = -\alpha U_n = \frac{0.4 I_1}{U_{09}} \sqrt{\frac{1-n}{0.1}}. \quad (7)$$

By substituting the value of  $\alpha$  and  $\beta$  into equation (3), we obtain

$$\frac{d u'}{d t} = \frac{0.4 I_1}{U_{09}^2 C} u'^2 - \left( \frac{0.4 \sqrt{\frac{1-n}{0.1}} R I_1 + U_{09}}{U_{09} R C} \right) u' + \frac{k t}{R C} \quad (8)$$

or, designating the coefficients of  $u'^2$ ,  $u'$  and  $t$  by the letters  $a$ ,  $b$  and  $h$ , respectively, we have

$$\frac{d u'}{d t} = a u'^2 + b u' + h t. \quad (9)$$

This is a Riccati equation for which an exact solution cannot be found. Let us therefore search for an approximate solution by the perturbation method [3].

We multiply the nonlinear term of the equation by the dimensionless parameter  $\mu$ , equal to unity:

$$\dot{u}' = b u' + h t + \mu a u'^2. \quad (10)$$

Let us assume a series solution

$$u' = u_0 + \mu u_1 + \mu^2 u_2 + \mu^3 u_3 + \dots \quad (11)$$

Substituting into equation (10), we obtain

$$\begin{aligned} \dot{u}_0 + \mu \dot{u}_1 + \mu^2 \dot{u}_2 + \mu^3 \dot{u}_3 = & b(u_0 + \mu u_1 + \mu^2 u_2 + \mu^3 u_3) + h t + \\ & + \mu a (u_0 + \mu u_1 + \mu^2 u_2 + \mu^3 u_3)^2. \end{aligned} \quad (12)$$

The dots indicate derivatives with respect to  $t$ . We obtain the terms of the series (11) by equating the terms of equation (12), containing corresponding powers of  $\mu$ . To determine the generating solution, we write

$$\dot{u}_0 = b u_0 + h t \text{ for } t=0; u_0=0.$$

Then

$$u_0 = \frac{h}{b^2} (e^{bt} - bt - 1). \quad (13)$$

To determine the first-order correction term we equate the terms of equation (12) containing equal powers of  $\mu$ .

$$\dot{u}_1 = b u_1 + a u_0^2.$$

By substituting the value derived for  $u_0$ , we obtain:

$$\dot{u}_1 = b u_1 + \frac{a h^2}{b^3} (e^{bt} - bt - 1)^2.$$

The solution of this differential equation at zero initial conditions gives

$$u_1 = \frac{a h^2}{b^3} [e^{2bt} + e^{bt} (4 - 2 b t - b^2 t^2) - b^2 t^2 - 4 b t - 5]. \quad (14)$$

To determine the second-order correction term, we write

$$\dot{u}_2 = b u_2 + 2 a u_0 u_1.$$

The second-order correction has the following form:

$$u_2 = \frac{2a^2h^3}{b^8} \left[ \frac{1}{2} e^{3bt} + e^{2bt} (-b^2t^2 - b^2t + 4) + e^{bt} \left( \frac{1}{4} b^4t^4 + \frac{3}{8} b^3t^3 - 3b^2t^2 - 9bt + \frac{51}{2} \right) - b^3t^3 - 8b^2t^2 - 25bt - 30 \right]. \quad (15)$$

We find the third-order correction from the equation

$$u^3 = b u_3 + a u_1^2 + 2 a u_0 u_2. \quad (16)$$

If in this equation we substitute the expressions defining  $u_0$ ,  $u_1$  and  $u_2$ , equation (16) becomes very cumbersome. Since we are interested in solving equation (8) within a certain range of parameters, let us see if the terms containing the factor  $e^{bt}$  can be dropped for our case. This can obviously be done if, in the worst case,

$$e^{bt} \frac{b^4 t^4}{4} < bt. \quad (17)$$

The expression for  $b$  is

$$b = -0.4 \sqrt{\frac{1-n}{0.1}} \frac{R I_1}{U_{09}} + 1 \frac{1}{RC}.$$

Here, the worst case corresponds to a 2 ma TD with high capacitance. Since the 2 ma TD tunnel-admittance branch is approximated by a high resistance, then, after solving equation (8) for high  $C$ -values, the origin  $O'$  must not be chosen higher than  $0.8 I_1$ , i.e.,  $n = 0.8$ . Assuming  $R \geq 2 \frac{U_1}{I_1}$  and  $U_1 \approx U_{09}$ ,

$$b = -(0.4 \cdot 2\sqrt{2} + 1) \frac{1}{RC}.$$

If  $C = 10$  pF and  $R = 150$  ohm,  $b \approx -1.4 \cdot 10^9 \text{ sec}^{-1}$ . Then, at  $t = 2 \cdot 10^{-9} \text{ sec}$ ,  $bt \approx 3e^{bt} \frac{b^4 t^4}{4}$ . In other words, if we are interested not in the shape of the curve  $u'(t)$  but in the values of  $\Delta t$  and  $\Delta e$ , which characterize the dynamic properties of the circuit, we can drop those terms in equations (13–15) which contain the factor  $e^{bt}$ . By doing this, we obtain the third-order correction:

$$u_3 = -\frac{a^3 h^4}{b^7} (5b^4t^4 + 64b^3t^3 + 350b^2t^2 + 960bt + 1105). \quad (18)$$

By substituting the expressions for  $u_0$ ,  $u_1$ ,  $u_2$  and  $u_3$  into equation (11) and taking  $\mu = 1$ , we obtain

$$u' = A_4t^4 + A_3t^3 + A_2t^2 + A_1t + A_0. \quad (19)$$

where

$$\begin{aligned}
 A_4 &= -\frac{5a^3 h^4}{b^7}; \\
 A_3 &= -\frac{2a^2 h^3}{b^8} (b^3 + 32ah); \\
 A_2 &= -\frac{a h^2}{b^9} (b^5 + 16ahb^3 + 350a^2 h^2); \\
 A_1 &= -\frac{h}{b^{10}} (b^9 + 4ahb^6 + 50a^2 h^2 b^3 + 960a^3 h^3); \\
 A_0 &= -\frac{h}{b^{11}} (b^9 + 5ahb^6 + 60a^2 h^2 b^3 + 1105a^3 h^3).
 \end{aligned} \tag{19a}$$

By substituting the expressions defining  $a$ ,  $b$  and  $h$  in (19a), we obtain an equation describing the variation with time of the voltage across the TD as a function of the parameters of the signal, TD and resistance  $R$ :

$$\begin{aligned}
 A_4 &= \frac{0.32}{s^7} I_1^3 R^3 k^4 U_{09}; \\
 A_3 &= \frac{0.32}{s^8} I_1^2 R^2 k^3 U_{09} (s_3 - 12.8\lambda q_0); \\
 A_2 &= \frac{0.4}{s^9} I_1 R k^2 U_{09} (s^6 - 6.4\lambda q_0 s^3 + 56\lambda^2 q_0^2); \\
 A_1 &= \frac{k U_{09}}{s^{10}} (s^9 - 1.6\lambda q_0 s^6 + 8\lambda^2 q_0^2 s^3 - 61.44\lambda^3 q_0^3); \\
 A_0 &= \frac{R k U_{09} q_0}{s^{11}} (-s^9 + 2\lambda q_0 s^6 - 9.6\lambda^2 q_0^2 s^3 + 70.72\lambda^3 q_0^3),
 \end{aligned} \tag{19b}$$

where

$$\begin{aligned}
 s &= 0.4R I_1 \sqrt{\frac{1-n}{0.1}} + U_{09}; \\
 \lambda &= I_1 R^2 k; \\
 q_0 &= C U_{09}.
 \end{aligned}$$

If  $t=t_3$   $u'=U_2'$ . Therefore, by equating equation (19) with  $U_2'$  and solving for  $t$ , we can, in principle, obtain the sought delay time. But an analytical solution of an algebraic equation of the fourth degree is practically impossible. To determine  $\Delta t$  we therefore use Taylor's formula

$$u'(t_m' + \Delta t) \approx u'(t_m') + \Delta t \left. \frac{d u'}{d t} \right|_{t=t_m'}$$

whence

$$\Delta t \approx \frac{U_2' - u'(t_m')}{\left. \frac{d u'}{d t} \right|_{t=t_m'}}. \tag{20}$$

The error involved in using formula (20) becomes smaller for smaller  $\Delta t$  values. We therefore assume that

$$\Delta t = \Delta_1 t + \Delta_2 t, \tag{21}$$

and rearrange formula (20) to calculate  $\Delta_2 t$ ; then

$$\Delta_2 t \approx \frac{U_2' - u'(t_m' + \Delta_1 t)}{\left. \frac{d u'}{d t} \right|_{t=t_m' + \Delta_1 t}}. \quad (22)$$

We choose  $\Delta_1 t$  arbitrarily, in order to have  $\Delta_1 t + t_m' < t_d$ . If  $\Delta_1 t$  is chosen correctly, then  $\Delta_2 t \ll \Delta t_1$ .

To determine  $U_2'$  and  $t_m'$ , we solve the system of equations (2) for  $C=0$ . We obtain the equation

$$\alpha u'^2 + \beta u' = \frac{e(t) - u'}{R},$$

whence

$$u' = \frac{-(R\beta + 1) + \sqrt{(R\beta + 1)^2 + 4R\alpha e(t)}}{2R\alpha}, \quad (23)$$

$$U_2' = -\frac{R\beta + 1}{2R\alpha} = \frac{0.4 \sqrt{\frac{1-n}{0.1}} R I_1 U_{09} + U_{09}^2}{0.8 R I_1} \quad (24)$$

and

$$t_m' = -\frac{(R\beta + 1)^2}{4R\alpha k} = \frac{1.6(1-n)R^2 I_1^2 + 0.8 \sqrt{\frac{1-n}{0.1}} R I_1 U_{09} + U_{09}^2}{1.6 R I_1 k}. \quad (25)$$

Allowing for (19), (21) and (22), we finally obtain:

$$\Delta t = \Delta_1 t + \frac{U_2' - (A_4 t_0^4 + A_3 t_0^3 + A_2 t_0^2 + A_1 t_0 + A_0)}{4 A_4 t_0^3 + 3 A_3 t_0^2 + 2 A_2 t_0 + A_1}, \quad (26)$$

where  $t_0 = t_m' + \Delta_1 t$ .

From the system of equations (2) and expression (26) we find  $\Delta e$ :

$$\Delta e = k \Delta t. \quad (27)$$

Adding the  $\Delta t$  and  $\Delta e$  values found by means of formulas (26) and (27) to the corresponding static values, we can calculate the delay time  $t_d$  and the dynamic operation threshold  $E_m$ . In this case, the choice of the initial position of the working point, i.e., the magnitude of the shift, will only affect  $t_m$  and  $U_m$ , but not  $\Delta t$  and  $\Delta e$ . When calculating the static values  $U_m$  and  $t_m$ , formulas (24) and (25) should not be used, since they are derived for a coordinate system with origin at  $O'$  in order to obtain expressions determining  $\Delta t$  and  $\Delta e$ .

Let us designate by the letter  $p$  any of the parameters  $I_1$ ,  $U_{09}$ ,  $C$ ,  $R$  and  $k$ . The variation limit of the parameter will be designated by  $\Delta p$ , and the corresponding variations in the magnitudes  $t_d$ ,  $t_m$ ,  $\Delta t$ ,  $U_m$ ,  $\Delta e$  and  $E_m$  by the symbols  $\delta t_d$ ,  $\delta t_m$ ,  $\delta t$ ,  $\delta U_m$ ,  $\delta e$  and  $\delta E_m$ , respectively.

Obviously,

$$\left. \begin{aligned} \delta t_d &= \delta t_{in} + \delta t; \\ \delta U_{in} &= k \delta t_{in}; \\ \delta E_{in} &= \delta U_{in} + \delta e. \end{aligned} \right\} \quad (28)$$

If  $\Delta p$  is comparatively small,

$$\delta t \approx \frac{\partial(\Delta t)}{\partial p} \Delta p = \frac{\left( \frac{\partial U_2'}{\partial p} - \frac{\partial u'}{\partial p} \right) \frac{du'}{dt} - (U_2' - u') \frac{\partial}{\partial p} \frac{du'}{dt}}{\left( \frac{du'}{dt} \right)^2} \Delta p; \quad (29)$$

$$\delta t_{in} \approx \frac{\partial t_{in}}{\partial p} \Delta p; \quad (30)$$

then  $u'$  and  $\frac{du'}{dt}$  in expression (29) can be evaluated at  $t=t_0$ .

To calculate  $\delta t_d$  and  $\delta E_{in}$  for the given limits  $\Delta k$  and  $\Delta C$ , formulas (28) and (29) are simplified; thus, if

$$\delta t_{in} = 0, \quad \delta U_{in} = 0 \quad \text{and} \quad \frac{\partial U_2'}{\partial p} = 0$$

and noting that

$$\frac{U_2' - u'}{\frac{du'}{dt}} = \Delta_2 t,$$

we obtain

$$\delta t = \delta t_d \approx \frac{-\frac{\partial u'}{\partial p} - \Delta_2 t \frac{\partial}{\partial p} \frac{du'}{dt}}{\frac{du'}{dt}} \Delta p. \quad (31)$$

These formulas help in analyzing the comparative influence of the various parameters upon the switching-on delay and the dynamic operation threshold; moreover, they help in calculating, for instance, the following magnitudes:

- 1)  $i_c$  for  $u' = U_2'$ , i.e., the initial conditions for calculating the subsequent switching stages — the intermittent increase of  $u'$ ;
- 2) the additional shift, equal to  $\Delta e$ , for discriminators that must operate when the input voltage reaches a given level /1, 2/;
- 3) the discrimination errors for variation of the input voltage slope within the given limits;
- 4) the upper incremental limit, equal to  $\Delta e$ , for impulse signals. Increments exceeding  $\Delta e$  no longer reduce the switching-on delay /2/;
- 5) the variation limits of the delay and dynamic operation threshold for given limits of variation in the TD parameters.

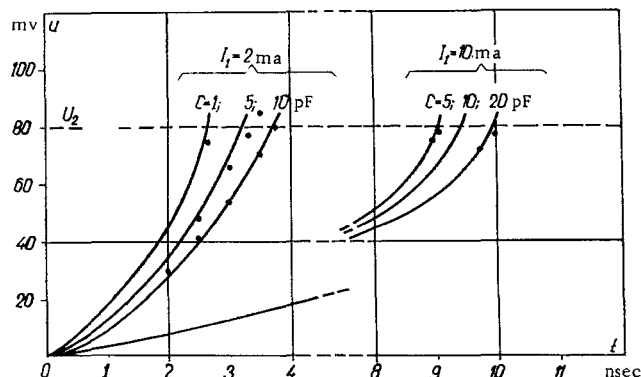


FIGURE 3. Variation of voltage  $u'$  with time.

In order to assess to what extent the derived analytical expression  $u'(t)$  approaches the exact solution of the differential equation (8), the latter was solved on an electronic digital computer. The curves thus obtained are shown in Figure 3. The dots indicate the calculation results obtained by employing formulas (19) and (19b). The check was carried out for an AsGa tunnel diode having the parameters given in Figure 3 for  $k = 0.5 \cdot 8.357 \cdot 10^7$  v/sec and various  $R$ -values. The error in determination of  $\Delta t$  from the above-mentioned formulas was found to be within 3 to 10%. The error was smallest when the calculations were carried out for a very large  $n$ , i.e., when the origin of coordinates  $n$  was located as high as possible. The magnitude may be increased as long as we can still assume that  $i_c = 0$  at  $t = 0$  [2]. For example, for the calculations, the results of which are marked as dots in the graphs (see Figure 3),  $n$  has been taken in the range 0.75–0.925. For  $I_1 = 2$  ma and  $C = 5$ –10 pF,  $n = 0.75$ . As can be seen from the figure, the accuracy obtained for  $C = 5$  pF is lower owing to the small  $n$ . For  $I_1 = 2$  ma and  $C = 1$  pF,  $n = 0.9$  (the same  $n$  was taken for  $I_1 = 10$  ma and  $C = 20$  pF). For  $I_1 = 10$  ma and  $C = 5$  pF,  $n = 0.925$ .

## CONCLUSION

1. The dynamic properties of a switched-on tunnel diode cannot be described merely by the parameters  $I_1$ ,  $U_1$  and  $C$ . It is necessary to indicate the width of the characteristic near to the maximum, for example, at the 0.9  $I_1$  level; in other words, the dynamic properties of a TD are characterized by the parameters  $I_1$ ,  $U_{0.9}$  and  $C$ .

2. A check of the solution obtained for the nonlinear differential equation describing the first stage in the switching process indicated that the formulas derived suffice for quantitative calculations when the parameters of the TD and the signal vary widely within the above-mentioned limits.



3. The derived formulas also apply when the TD operates as an active resistance. It suffices to determine the parameters of the total current-voltage characteristic of the TD and the load resistance.

### Bibliography

1. Beiners, E.G. and I.Ya. Bilinskii. Investigation of the Threshold Properties of Tunnel Diodes on an Analog Computer. — In the collection: Avtomatika i vychislitel'naya tekhnika (Automation and Computer Technology). 12. 'Zinatne', Riga. 1966.
2. Beiners, E.G., I.Ya. Bilinskii and P.P. Treis. Some Threshold Properties of Tunnel Diodes. — In Sbornik: Avtomatika i vychislitel'naya tekhnika (Automation and Computer Technology). 12. 'Zinatne', Riga. 1966.
3. Cunningham, V. Introduction to the Theory of Nonlinear Systems (Russian translation), GEI, Moscow. 1962.

*M. F. Grinkhof*

**DESIGN OF A TWO-CYCLE SHIFT FERRITE-DIODE REGISTER WITH ALLOWANCE FOR COMPONENT TOLERANCES**

The design of a two-cycle shift register using transformer-type ferrite-diode elements is described, taking into account the tolerances in core and diode parameters and in cycle current. The results obtained by this procedure are compared with the results which are derived assuming exact values of the parameters. The derivation of the design equation is described. The method can be used to draw up design equations for other particular types of ferrite diode shift registers.

The design procedure for ferrite-diode elements using the exact values of the magnetic and electric parameters has been developed to a considerable extent. This procedure makes allowance for parameter deviations due to changes in temperature from their nominal values. The results of this design procedure, however, are not fully consistent with the experiment, and tedious and time-consuming adjustment is therefore inevitable for all ferrite-diode elements. The main reason for this discrepancy is that the design calculations are based on the statistical averages, and thus ignores the intrinsic scatter of the core and diode parameters.

In the present paper we have tried to devise a design procedure for a two-cycle shift register using transformer-type ferrite-diode elements with one coupling diode, taking into consideration the actual tolerances of the core and diode parameters and of the cycle current.

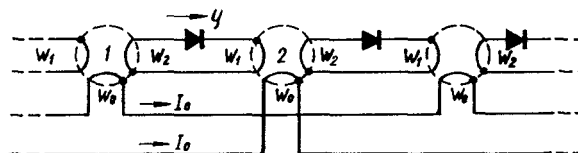


FIGURE 1. Circuit diagram of the shift register.

Figure 1 is the circuit diagram of the shift registers whose parameters are specified with certain tolerances. Suppose that the transient time of the forward diode resistance and the rise time of the cycle current are both negligible (these assumptions are valid if the cycle frequency  $f_0$  does not exceed 150 cps). In this case we may use in our calculations the amplitude value of the cycle current  $I_0$ , and the diode can be simulated by a source  $E_0$  with forward internal resistance  $R$ .

The parameters  $E_0$  and  $R$  are determined from the linearized steady-state current-voltage characteristic of the diode (Figure 2).

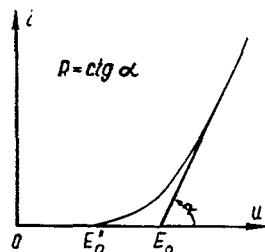


FIGURE 2. The current-voltage characteristic of a silicon diode.

The cycle pulse frequency  $f_0$  is generally known from the start, and we thus know the maximum read time  $\tau_{r\max}$ , which for a two-cycle register is defined by the equality

$$\tau_{r\max} = \frac{1}{k_s 2f_0}, \quad (1)$$

where  $k_w$  is a margin (safety) factor ( $k_w \geq 1$ ).

Let  $\tau_{r\max}$  be known. The aim of the calculation is then to determine the turn numbers  $\omega_1$  and  $\omega_2$  and the rated ampere-turn value  $I_0 \omega_0$  of the winding.

If the circuit parameters are specified exactly and the reverse flow of information is completely suppressed by the diode cutoff voltage  $E'_0$ , which is significant for silicon diodes (Figure 2), the transmission of a ONE signal by the register is described by the set of equation

$$2\Phi_{r1}\omega_2 - 2\Phi_{r2}\omega_1 = q_r R + E'_0 \tau_r; \quad (2)$$

$$I_0 \omega_0 \tau_r = S_{w1} l_1 + H_{01} l_1 \tau_r + q_r \omega_2; \quad (3)$$

$$(\Phi_{r1} + \Phi_1) \omega_2 - 2\Phi_{r2} \omega_1 = q_w R + E'_0 \tau_w; \quad (4)$$

$$q_w \omega_1 = S_{w2} + H_{02} l_2 \tau_w; \quad (5)$$

$$I_0 \omega_0 \tau_w = l_1 Q_{01} (\Phi_1) + H_{01} l_1 \tau_w + q_w \omega_2, \quad (6)$$

where  $\Phi_{r1}$  and  $\Phi_{r2}$  are the residual magnetic fluxes in the first and the second core, respectively;

$q_r$  is the electric charge in the coupling loop during the read cycle of the first core;

$q_w$  is the electric charge in the coupling loop during the write cycle of the second core;

$\tau_r$  is the read access time of the first core;

$\tau_w$  is the write access time of the second core;

- $S_{w1}$  and  $S_{w2}$  are the switching coefficients of the first and the second core, respectively;  
 $H_{01}$  and  $H_{02}$  are the equivalent coercive forces for piecewise-linear approximation of the transient surfaces of the first and the second core, respectively;  
 $\Phi_1$  is the magnetic flux through the first core;  
 $l_1$  and  $l_2$  is the length of the average magnetic lines in the first and the second core, respectively;

$$Q_{t1} = \int_0^t (H_1 - H_{01}) dt;$$

$H_1$  is the magnetic field in the first core;

$t$  is the time.

The function  $l_1 Q_{t1}(\Phi_1)$  is a modification of the transient equation of the first core in integral form [1]. The equations are simple expressions of the fundamental laws of electric and magnetic networks and the transient equation of the core, all integrated over the read time  $\tau_r$  and the write time  $\tau_w$  [1].

The function  $l_1 Q_{t1}(\Phi_1)$  is plotted in Figure 3 by the solid curve. To simplify the analysis, we linearize this function by the expression

$$l_1 Q_{t1} = \frac{S_{w1} l_1}{2} \left( 1 + \frac{\Phi_1}{\Phi_{r1}} \right),$$

which is plotted in Figure 3 by the dashed line.

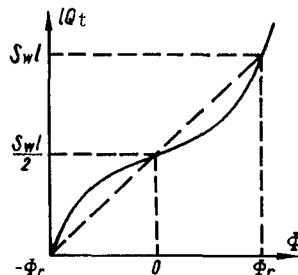


FIGURE 3. Linearized function  $l_1 Q_t(\Phi)$ .

Equation (6) now takes the form

$$I_0 \omega_0 \tau_s = \frac{S_{w1} l_1}{2} \left( 1 + \frac{\Phi_1}{\Phi_{r1}} \right) + H_{01} l_1 \tau_w + q_w \omega_2. \quad (6a)$$

Eliminating  $\Phi_1$  and  $q_w$  between equations (4), (5), and (6a), we find the write time

$$\tau_w = \frac{S_{w2} l_2 (S_{w1} l_1 R + 2 \Phi_{r1} \omega_2^2) + S_{w1} l_1 2 \Phi_{r2} \omega_1^2}{2 \Phi_{r1} \omega_1 \omega_2 (I_0 \omega_0 - H_{01} l_1) - H_{02} l_2 (S_{w1} l_1 R + 2 \Phi_{r1} \omega_2^2) - S_{w1} l_1 E_0 \omega_1}. \quad (7)$$

The read time  $\tau_r$  is found from (2) and (3):

$$\tau_r = \frac{RS_{w1}l_1 + 2\omega_2(\Phi_{r1}\omega_2 - \Phi_{r2}\omega_1)}{R(I_0\omega_0 - H_{01}l_1) + \omega_2E_0}. \quad (8)$$

The register will function if the write time  $\tau_w$  is at most equal to the read time  $\tau_r$ . These times are functions of the core and diode parameters and the corresponding tolerances. The condition  $\tau_w \leq \tau_r$  is always satisfied if we take  $\tau_{w\max} = \tau_{r\min}$ , where  $\tau_{w\max}$  is determined for tolerances with such signs that give the maximum write time, and  $\tau_{r\min}$  corresponds to tolerances with signs which ensure the minimum read time.

This approach, however, will ensure an excessive safety margin, i.e., the inequality  $\tau_w < \tau_r$  will become too pronounced, since the expressions for  $\tau_w$  and  $\tau_r$  will include the same parameters with tolerances of opposite signs, which is clearly ridiculous. Therefore  $\tau_w$  and  $\tau_r$  should be set equal for a combination of tolerances of such signs which ensures a maximum ratio of write-to-read  $\tau_w/\tau_r$ .

Let us find the signs of the tolerances which give a maximum value of the ratio  $\tau_w/\tau_r$ . To this end, we write  $\tau_w/\tau_r$  in the form

$$\frac{\tau_w}{\tau_r} = \frac{S_{w2}l_2(S_{w1}l_1R + 2\Phi_{r1}\omega_2^2) + S_{r1}l_12\Phi_{r2}\omega_1^2}{2\Phi_{r1}\omega_2\omega_2(I_0\omega_0 - H_{01}l_1) - H_{02}l_2(S_{w1}l_1R + 2\Phi_{r1}\omega_2^2) - S_{w1}l_1E_0\omega_1} \times \\ \times \frac{R(I_0\omega_0 - H_{01}l_1) + \omega_2E_0}{RS_{w1}l_1 + 2\omega_2(\Phi_{r1}\omega_2 - \Phi_{r2}\omega_1)}.$$

Analysis of equation (9) shows that  $\tau_w/\tau_r \uparrow$  is

$$\Phi_{r1} \downarrow, \Phi_{r2} \uparrow, H_{01}l_1 \uparrow, H_{02}l_2 \uparrow, I_0\omega_0 \downarrow, S_{w1}l_1 \uparrow, S_{w2}l_2 \uparrow, E_0 \uparrow, R \uparrow,$$

where the upward arrow  $\uparrow$  implies increase and the downward arrow  $\downarrow$  decrease of the particular parameters. All parameters with the upward arrow  $\uparrow$  should be taken with positive tolerances, whereas  $\downarrow$  corresponds to negative tolerances.

The first design relations with allowance for parameter tolerances can thus be obtained by setting the write time equal to the read time, provided that the corresponding relations include the parameters with positive or negative tolerances in accordance with the results from equation (9). This result, however, can also be arrived at by using the starting equations of a circuit which is substantially simplified if the write and read times are taken equal. In this case, the function  $l_1Q_{t1}(\Phi_1)$  does not have to be linearized. The set of starting equations for  $\tau_w = \tau_r$  is

$$2\Phi_{r1}\omega_2 - 2\Phi_{r2}\omega_1 = qR + E_0\tau; \quad (10)$$

$$l_2\omega_0\tau = S_{w1}l_1 + H_{01}l_1\tau + q\omega_2; \quad (11)$$

$$q\omega_1 = S_{w2}l_2 + H_{02}l_2\tau, \quad (12)$$

where  $\tau = \tau_r = \tau_w$  and  $q = q_r = q_w$ .

We rewrite these equations using the parameter tolerances and the tolerance in the cycle current (the cycle ampere-turns). We introduce the

following abbreviated notation:

$$\Phi_{r1} + \Delta\Phi_{r1} = \Phi_{r1}^{\uparrow}; \quad \Phi_{r1} - \Delta\Phi_{r1} = \Phi_{r1}^{\downarrow}; \quad I_0\omega_0 + \Delta I_0\omega_0 = I_0\omega_0^{\uparrow};$$

$$I_0\omega_0 - \Delta I_0\omega_0 = I_0\omega_0^{\downarrow}, \quad \text{etc.},$$

where  $V$  is the deviation of the parameter from its rated value. Seeing that the rated values of the parameters are the same for all the cores, we have in final form

$$2\Phi_{r1}^{\downarrow}\omega_2 - 2\Phi_{r1}^{\uparrow}\omega_1 = qR^{\uparrow} + E_0^{\uparrow}\tau; \quad (13)$$

$$I_0\omega_0^{\downarrow}\tau = S_w l^{\uparrow} + H_0 l^{\uparrow}\tau + q\omega_2; \quad (14)$$

$$q\omega_1 = S_w l^{\uparrow} + H_0 l^{\uparrow}\tau. \quad (15)$$

Eliminating  $q$  and  $\tau$  between these equations, we end up with a single equation:

$$I_0\omega_0^{\downarrow} = \frac{2\Phi_{r1}^{\downarrow}H_0 l^{\uparrow}\omega_2^2 - [2\omega_1 H_0 l^{\uparrow}(\Phi_{r1}^{\uparrow} - \Phi_{r1}^{\downarrow}) - S_w l^{\uparrow}E_0^{\uparrow}]\omega_2 - (2\Phi_{r1}^{\uparrow}\omega_1 H_0 l^{\uparrow} - S_w l^{\uparrow}E_0^{\uparrow}\omega_1)}{2\omega_1\Phi_{r1}^{\downarrow}\omega_2 - 2\omega_1^2\Phi_{r1}^{\uparrow} - S_w l^{\uparrow}R^{\uparrow}}. \quad (16)$$

Let us determine the signs of the tolerances which ensure maximum read time. Analysis of equation (8) shows that

$$\tau_r^{\uparrow}, \quad \text{if } S_w l_1^{\uparrow}, \Phi_{r1}^{\uparrow}, \Phi_{r2}^{\downarrow}, I_0\omega_0^{\downarrow}, H_0 l_1^{\uparrow}, E_0^{\downarrow} \text{ and } R^{\downarrow}.$$

We can now write equation (8) for  $I_0\omega_0^{\downarrow}$  in the form

$$I_0\omega_0^{\downarrow} = \frac{S_w l^{\uparrow}}{\tau_{r \max}} + H_0 l^{\uparrow} + \frac{2\omega_2}{R^{\downarrow}\tau_{r \max}} (\Phi_{r1}^{\uparrow}\omega_2 - \Phi_{r1}^{\downarrow}\omega_1) - \frac{\omega_2 E_0^{\downarrow}}{R^{\downarrow}}. \quad (17)$$

Equations (16) and (17) give the minimum value of the cycle ampere-turns  $I_0\omega_0^{\downarrow}$  and the turn number  $\omega_2$ , if  $\omega_1$  is known. In most cases, however,  $\omega_1$  is not known and should be determined.

The turn number  $\omega_1$  is generally chosen so that  $\omega_{1 \min} < \omega_1 < \omega_{1 \max}$ , where  $\omega_{1 \min}$  corresponds to the condition that the current through the coupling loop is equal to the maximum allowed current through the diode, and  $\omega_{1 \max}$  corresponds to the case when the reverse flow of information (noise) is completely suppressed.

In our case this choice of  $\omega_1$  is not immediate, since all the equations are solved simultaneously. From the energy aspect, it is advantageous to take the maximum permissible turn number  $\omega_1$ . Since the parameter tolerances are taken into consideration, no allowance should be made for a margin of noise resistance of the register, and the calculations can be carried out for the maximum permissible turn number  $\omega_1$ .

The condition of noise suppression is

$$\frac{2\Phi_{r1}\omega_1 k_A}{\tau_r} \leq E_0', \quad (18)$$

where the left-hand side is an expression of the e.m.f. amplitude induced in the winding  $\omega_1$  when ONE is read;  $k_A$  is the amplitude factor ( $k_A = 1.3-1.5$ );  $E_0'$  is the diode cutoff voltage (Figure 2).

Inserting the read time  $\tau$  in (18) from equation (8), we get

$$\frac{2\Phi_{r1} \omega_1 k_A [R(I_0 \omega_0 - H_0 l_1) + \omega_2 E_0]}{R S_{w1} l_1 + 2\omega_2 (\Phi_{r1} \omega_2 - \Phi_{r2} \omega_1)} \leq E_0'. \quad (19)$$

The inequality is played down if we take

$$\Phi_{r1} \downarrow, \Phi_{r2} \uparrow, I_0 \omega_0 \uparrow, H_0 l_1 \downarrow, S_{w1} l_1 \downarrow, E_0 \uparrow, R \uparrow E_0' \downarrow.$$

We take the sign of equality in (19), and this gives the maximum turn number  $\omega_1$ . Using the tolerances, we thus write

$$E_0'^{\downarrow} = 2\Phi_{r1} \omega_1 k_A \frac{R(I_0 \omega_0^{\uparrow} - H_0 l_1^{\downarrow}) + \omega_2 E_0^{\uparrow}}{R^{\uparrow} S_{w1} l_1^{\downarrow} + 2\omega_2 (\Phi_{r1}^{\uparrow} \omega_2 - \Phi_{r2}^{\uparrow} \omega_1)}. \quad (20)$$

We have obtained a set of three equations (16), (17), and (20) for circuit design.

Note that the current in the coupling loop is limited by the maximum allowed diode current, i.e., the following inequalities should be satisfied:

$$I_{av,d} \geq \frac{q_{c,max}}{T_0}; \quad (21)$$

$$I_{a,d} \geq \left( \frac{q_r}{\tau_r} \right)_{max} \cdot k_A, \quad (22)$$

where  $I_{av,d}$  is the maximum permissible average diode current;

$I_{a,d}$  is the maximum permissible amplitude of the diode current;

$q_{r,max}$  is the maximum permissible charge in the coupling loop;

$T_0$  is the period of the cycle pulses.

The charge in the coupling loop during the read cycle is obtained from equations (2) and (3):

$$q_c = \frac{2\Phi_{r1} \omega_2 - 2\Phi_{r2} \omega_1 (I_0 \omega_0 - H_0 l_1) - E_0 S_{w1} l_1}{R(I_0 \omega_0 - H_0 l_1) + \omega_2 E_0}. \quad (23)$$

Analysis of equation (23) shows that  $q_r \uparrow$  if

$$\Phi_{r1} \uparrow, \Phi_{r2} \downarrow, S_{w1} l_1 \downarrow, E_0 \downarrow, R \downarrow, I_0 \omega_0 \uparrow, H_0 l_1 \downarrow, \text{ i. e.,} \\ q_{r,max} = \frac{2(\Phi_{r1}^{\uparrow} \omega_2 - \Phi_{r2}^{\downarrow} \omega_1) (I_0 \omega_0^{\uparrow} - H_0 l_1^{\downarrow}) - E_0^{\downarrow} S_{w1} l_1^{\downarrow}}{R^{\downarrow} (I_0 \omega_0^{\uparrow} - H_0 l_1^{\downarrow}) + \omega_2 E_0^{\downarrow}}. \quad (24)$$

It can be shown that  $q_r/\tau_r = (q_r/\tau_r)_{max}$  for tolerances of the same signs. Inserting  $q_{r,max}$ ,  $q_r$  and  $\tau_r$  with parameter tolerances of appropriate sign in inequalities (21) and (22), we finally obtain

$$I_{av,d} \geq \frac{1}{T_0} \cdot \frac{2(\Phi_{r1}^{\uparrow} \omega_2 - \Phi_{r2}^{\downarrow} \omega_1) (I_0 \omega_0^{\uparrow} - H_0 l_1^{\downarrow}) - E_0^{\downarrow} S_{w1} l_1^{\downarrow}}{R^{\downarrow} (I_0 \omega_0^{\uparrow} - H_0 l_1^{\downarrow}) + \omega_2 E_0^{\downarrow}}; \quad (25)$$

$$I_{a,d} \geq k_A \frac{2(\Phi_{r1}^{\uparrow} \omega_2 - \Phi_{r2}^{\downarrow} \omega_1) (I_0 \omega_0^{\uparrow} - H_0 l_1^{\downarrow}) - E_0^{\downarrow} S_{w1} l_1^{\downarrow}}{R^{\downarrow} S_{w1} l_1^{\downarrow} + 2\omega_2 (\Phi_{r1}^{\uparrow} \omega_2 - \Phi_{r2}^{\downarrow} \omega_1)}. \quad (26)$$

It is readily seen that as the temperature decreases  $\tau_r/\tau_r$ ,  $\tau_{r,max}$ , and  $q_{r,max}$  increase, and inequality (19) becomes more pronounced. Thus, to

allow for the temperature effects in register design, we should insert in equations (26), (17) and inequality (25), (26) the values of the parameters determined for the minimum given temperature and in equation (20) the values of the parameters for the maximum given temperature.

Register design thus reduces to simultaneous solution of equations (16), (17), and (20) and verification of the diode operating conditions using inequalities (25) and (26). If at least one of these inequalities is broken, the coupling loop current should be reduced. This can be accomplished by connecting the bias  $E_b$  in series with the diode (Figure 4). In this case the turn number  $w_1$  increases and the coupling loop current diminishes. The design equations are not affected; the only difference is that  $E_0 + E_b$  is substituted for  $E_0$  and  $E_0' + E_b$  for  $E_0'$ . The sign of the tolerance in  $E_b$  coincides with the sign of the tolerance in  $E_0$  and  $E_0'$ , respectively. In practice, the source is built with a very low internal resistance, which is ignored in calculations.

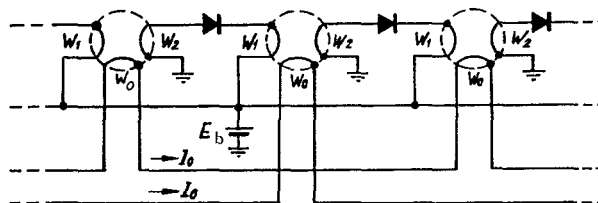


FIGURE 4. A circuit diagram of a shift register with source of bias in the coupling loops.

This design, however, has two shortcomings:

1) the simultaneous solution of equations (16), (17), and (20) involves a solution of a complete equation of higher than fourth degree, i.e., an equation which can be solved in each particular case only by some approximative method;

2) the transient response of the core  $1/\tau = f(H_{av})$  is approximated with a straight line in a wide range of switching times (all equations contain the same values of  $S_w l$  and  $H_0 l$ ), which in some cases may lead to substantial errors.

The first shortcoming is inherent in the design method and thus cannot be avoided.

The second shortcoming is readily eliminated by introducing four read times, which are actually obtained for various sign combinations of the parameter tolerances, and by taking the corresponding  $H_{av}$  values directly from the  $1/\tau = f(H_{av})$  curve.

Seeing that

$$\frac{S_w l}{\tau} + H_0 l = l H_{av}$$

and using the above relations, we obtain instead of (16), (17), (20), (25), and (26), the following set of equations:

$$I_0 w_1^1 = l H_{av}^1 + \frac{2 w_2 (\Phi_r^1 w_2 - \Phi_r^1 w_1)}{R^1 \tau_r^1} - \frac{w_2 E_0^1}{R^1}; \quad (27)$$



$$I_0 \omega_0^{\downarrow} = l H_{av}^{\uparrow} \left( 1 + \frac{\omega_2}{\omega_1} \right); \quad (28)$$

$$E_0^{\downarrow} = \frac{2 \Phi_r^{\uparrow} \omega_1 k_A}{\tau_r''}; \quad (29)$$

$$I_{av, d} \geq \frac{(I_0 \omega_0^{\downarrow} - l H_{av}^{\uparrow}) \tau_r'''}{T_0}; \quad (30)$$

$$I_{av, d} \geq \frac{(I_0 \omega_0^{\downarrow} - l H_{av}^{\uparrow}) k_A}{\omega_2}. \quad (31)$$

where  $\tau_r' = \tau_{r \max}$  and  $H_{av}^{\uparrow}$  the magnetic field corresponding to this read time, with positive tolerance (the scatter of the  $1/\tau = f(H_{av})$  curves is taken into consideration);  $H_{av}^{\uparrow}$  is the magnetic field with positive tolerance, determined for the magnetization reversal time  $\tau$  under conditions of equal read and write times ( $\tau = \tau_w = \tau_r$ ), where  $\tau$  is defined by the relation

$$\tau = \frac{2 \omega_2 (\Phi_r^{\downarrow} \omega_2 - \Phi_r^{\uparrow} \omega_1)}{R^2 (I_0 \omega_0^{\downarrow} - l H_{av}^{\uparrow}) + \omega_2 E_0^{\downarrow}}; \quad (28a)$$

$\tau_r''$  is the minimum read time,

$$\tau_r'' = \tau_{r \min} = \frac{2 \omega_2 (\Phi_r^{\downarrow} \omega_2 - \Phi_r^{\uparrow} \omega_1)}{R^2 (I_0 \omega_0^{\downarrow} - l H_{av}^{\uparrow}) + \omega_2 E_0^{\downarrow}}; \quad (29a)$$

$H_{av}^{\uparrow}$  is the magnetic field corresponding to the read time  $\tau_r''$  with negative tolerance;

$\tau_r'''$  is the read time leading to maximum charge in the coupling loop:

$$\tau_r''' = \frac{2 \omega_2 (\Phi_r^{\downarrow} \omega_2 - \Phi_r^{\uparrow} \omega_1)}{R^2 (I_0 \omega_0^{\downarrow} - l H_{av}^{\uparrow}) + \omega_2 E_0^{\downarrow}}; \quad (30a)$$

$H_{av}^{\uparrow}$  is the magnetic field corresponding to this time, with negative tolerance.

Simultaneous solution of equations (27), (28), and (29) gives

$$\omega_1 = \frac{E_0^{\downarrow} \tau_r''}{2 \Phi_r^{\uparrow} k_A}; \quad (32)$$

$$\omega_2 = \frac{B/2 + \sqrt{(B/2)^2 + AC}}{A}, \quad (33)$$

where

$$A = \frac{2 \Phi_r^{\uparrow}}{R^2 \tau_{r \max}}; \quad B = \frac{2 \Phi_r^{\uparrow} \omega_1}{R^2 \tau_{r \max}} + \frac{E_0^{\downarrow}}{R^2} + \frac{l H_{av}^{\uparrow}}{\omega_1};$$

$$C = l H_{av}^{\uparrow} - l H_{av}^{\uparrow}.$$

$I_0 \omega_0^{\downarrow}$  is determined from equation (27) or (28) after  $\omega_1$  and  $\omega_2$  have been calculated.

The values of the parameters in equations (29a) and (32) are taken for the maximum given temperature, and in all the other equations the values

of the parameters correspond to the minimum working temperature. The bias  $E_b$  is allowed for as described above.

The final result is thus 5 design equations, (32), (29a), (33), (27), or (28), and (28a), and three expressions for checking the diode operating conditions, (30), (30a), and (31).

This design procedure was applied to a digital shift register. Initial specifications:

- 1) Core VT-5 (0.16 VT), measuring  $3 \times 2 \times 1.3$  mm;
- 2) diode D220A;
- 3) maximum read time  $\tau_{r_{\max}} = 4.0 \mu\text{sec}$ ;
- 4) cycle frequency  $f_0 = 100$  kc;
- 5) temperature range from  $-10^\circ\text{C}$  to  $+70^\circ\text{C}$ .

The core parameters were borrowed from /1/ and calculated for  $-10^\circ\text{C}$  using a linear temperature dependence between  $-40^\circ\text{C}$  and  $+20^\circ\text{C}$ ; the diode specifications are from /2/. The diode parameters were assumed to remain constant with variation of temperature: the change in these parameters is negligible compared to the corresponding change in core parameters.

The results are summarized in Table 1. We see that the procedure which makes allowance for tolerances leads to results that markedly differ from those obtained assuming exact values of the parameters (version 1).

TABLE 1.

Design version	$\delta I_0 w_0$ , %	$\delta \Phi_r, \delta I H_{AV}, \delta R, \delta E_0, \delta E_0', \delta E_b$ , %	$I_0 w_0 / a$	$w_1$	$w_2$	$E_b$ , volt
1	0	0	3.1	6	28	0
2	$\pm 20$	$\pm 10$	5.0	9	39	1.3
3	$\pm 40$	$\pm 10$	6.1	14	54	2.6
4	$\pm 60$	$\pm 10$	8.6		94	5.5

For example, a tolerance of  $\pm 40\%$  for the cycle ampere-turns and tolerances of  $\pm 10\%$  for all the other parameters (these are quite realistic figures) roughly doubles the cycle ampere-turns and the turn numbers  $w_1$  and  $w_2$ . Moreover, a bias of 2.6 V is needed. Analysis shows that as the tolerances increase, the range of possible read times is broadened. Thus, if the maximum read time is fixed, the minimum read time decreases. To ensure faster switching we should increase the cycle ampere-turns and the turn number  $w_1$ , which is consistent with the results of our calculations. The increase of bias entails mainly an increase of the ratio  $w_1/\tau_{r_{\min}}$ , so that the e. m. f. induced in the winding  $w_1$  when ONE is read increases.

Although this design procedure does not ensure complete damping of small disturbances — one of the main requirements of stable operation

of the register — it is hoped that its application will greatly simplify the tuning and adjustment stages.

I would like to acknowledge the help of Yu. M. Shamaev in formulating the problem.

#### Bibliography

1. Pirogov, A.I. and Yu. M. Shamaev. Magnitnye serdechniki s pryamougol'noi petlei gisterezisa (Square Hysteresis Cores). — Moskva, Energiya. 1964.
2. Nikol'skii, I. F. Tranzistory i poluprovodnikovye diody (Transistors and Semiconductor Diodes). — Moskva, Svyaz'izdat. 1963.

*A. Ya. Khesin*

## *A TV METHOD FOR AUTOMATIC CONTROL OF TV DISTORTIONS*

The automatic control method for TV distortions considered in this paper uses a TV transducer and an optical coding unit. It is intended for line production control in the manufacture of TV sets and picture tubes. The effect of the resolving power of the transmitting tube on measurement errors is considered.

### INTRODUCTION

Nonlinear (scale) and geometrical distortions of the TV picture have a serious influence on picture quality, since the eye is exceedingly sensitive to any abnormal curvature of straight lines and distention or contraction of the component elements of a pattern. As a result, the permissible nonlinear and geometrical distortions of the TV picture are not more than a few percent, and the linear dimensions of the various elements of the picture should therefore be measured with an accuracy of a few tenths of a percent in order to be able to detect these slight distortions. This high accuracy is not always attainable in photographic and projection measurement techniques [1, 2]. Moreover, these methods are extremely time-consuming and tedious. Therefore, they are inapplicable to complete production control in TV industry and furthermore they do not completely eliminate the danger of subjective errors, as they are based on visual estimates of test table distortions. The photographic method ensures stage-by-stage documentation of the picture distortions, but is it not very efficient in view of the lengthy time needed to process the photographic plates. The projection method does not make provision for any permanent follow-up records, which are absolutely essential for future analysis and further improvement of production.

A complete objective control of TV picture parameters which gives a comprehensive set of documentary records after each test and is nevertheless adaptable to industrial purposes is ensured only by automatic control systems.

### 1. THE APPLICATION OF A TV LOGIC UNIT FOR AUTOMATIC CONTROL OF TV PICTURE PARAMETERS

TV picture distortions can be controlled and analyzed by a TV logic unit with a TV transducer or pickup element mounted in front of the test screen.

The brightness intensity of the Soviet-made picture tube 47LK1B and 59LK1B is not less than 100 nit; the illuminance produced on the photocathode of the transmitting tube is thus of the order of 10 lux, which is quite sufficient for the mass-produced vidicons.

The use of a TV transducer and the application of TV scanning technique makes it possible to convert many-dimensional starting information contained in the analyzed TV picture into a one-dimensional electric signal. In this way, the relevant information for further analysis by the logic unit is isolated fairly easily.

The two-dimensional black-and-white moving picture on a TV screen can be described by a brightness function  $B(x, y, t)$  which depends on three arguments: the two plane coordinates  $x$  and  $y$ , and the time  $t$ . The picture can thus be resolved into a spectrum of frequencies  $\omega = \frac{2\pi}{T}$  and spatial radian frequencies  $\omega_x$  and  $\omega_y$ . The result is a triple Fourier integral

$$B(x, y, t) = \left(\frac{1}{\sqrt{2\pi}}\right)^3 \int_{-\infty}^{\infty} \int_{-\infty}^{\infty} \int_{-\infty}^{\infty} S(\omega_x, \omega_y, \omega) e^{i(\omega_x x + \omega_y y + \omega t)} d\omega_x d\omega_y d\omega, \quad (1)$$

where  $S(\omega_x, \omega_y, \omega)$  is the three-dimensional spectrum of the function  $B(x, y, t)$ .

In automatic control of TV test tables the picture is fixed: this is a black-and-white test table produced on the screen by special test signals. As in (1), it can be resolved into a double Fourier integral

$$B(x, y) = \frac{1}{2\pi} \int_{-\infty}^{\infty} \int_{-\infty}^{\infty} S(\omega_x, \omega_y) e^{i(\omega_x x + \omega_y y)} d\omega_x d\omega_y. \quad (2)$$

The picture is transformed by time scanning in the direction of the axis  $x$  or  $y$ . The electric signal at the output of the TV transducer,  $u=f(t)$ , is therefore only a function of time:

$$f(t) = \frac{1}{\sqrt{2\pi}} \int_{-\infty}^{\infty} S(\omega) e^{i\omega t} d\omega. \quad (3)$$

TV methods are currently used on a fairly wide scale for measurement and monitoring of linear dimensions /4, 5/. According to the type of output information, we distinguish between digital and analog TV measuring units. In the analog unit, the pulse duration  $t_p$  corresponding to the monitored dimension is converted into voltage or current. In a digital system, the time is converted into a digital code (generally binary), i.e., time-pulse coding is employed.

The errors of TV measurement methods are associated with the peculiar design features of the transducers and the TV transmission requirements /4/. The main error sources are the nonlinear and unstable beam deflections, instability of the camera tube parameters, tube misalignment, fluctuation noise, distortion of video signal leading edges, and errors in pulse counting. All these errors, except the limited resolving power of the camera tube and pulse counting errors, can be eliminated by using a digital TV measuring system with optical coding of the monitored picture /5/. This method employs spatial quantization of the picture by means of an optical standard (a coding mask, a fiber-optics coding unit, etc.)

through which the test picture is projected onto the photocathode of the camera TV tube. A digital electric signal is developed in the transducer by scanning the coded projected picture.

Since in this method the message is encoded before it has been distorted in the transducer and the communication channel (by the previously listed sources of errors) and since the optical coding devices are insensitive to electromagnetic noise, the system may ensure high accuracy of measurement.

## 2. THE DESIGN OF THE AUTOMATIC CONTROL SYSTEM

Figure 1 is a block diagram of an automatic TV distortion control system intended for line production control in picture tube and TV set industry. The system uses the principle of optical picture quantization.

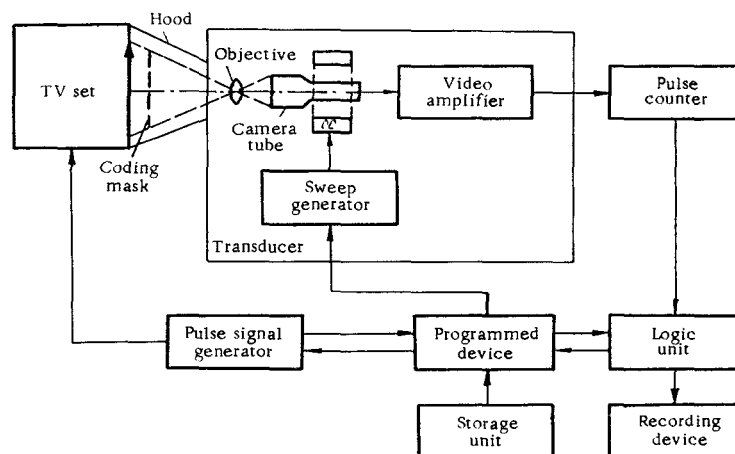


FIGURE 1. Automatic control system for TV picture distortions.

A newly assembled TV set is transported by a start-stop conveyor which stops for 2 or 3 minutes right in front of the TV test transducer. The position of the transducer unit is relative to the TV set to be tested is fixed, as the two are connected by a rigid opaque hood.

The TV transducer should lie on the optical axis of the picture tube. To reduce the hood length, the distance from the transducer to the screen can be made less than five times the screen height, but in this case special corrections must be introduced to allow for screen curvature (the calculation procedure is described in /6/).

The test picture on the screen is produced by a special test pulse generator. This picture is now projected onto the photocathode of the camera tube, after passing through an optical coding mask interposed

between the test screen and the camera tube. The coding mask is a pattern of horizontal or vertical lines (Figure 2a and 2b) strictly parallel to the scan direction; an alternative mask uses a checkered pattern (Figure 2c). When the projected picture is scanned, the video signal at the output of the camera tube is a series of electric pulses which are amplified by the video amplifier and delivered to an electronic pulse counter. The logic unit analyzes the results, which are then recorded by a special recorder. A programmed unit carries out a preset test program in accordance with certain industrial specifications which are stored in the storage unit. The programmed unit also sends control signals which drive the TV sweep generator and the test signal generator.

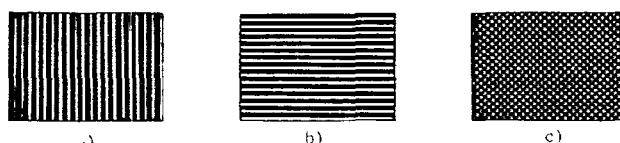


FIGURE 2. Coding masks.

To determine the nonlinear distortions in the horizontal direction, the test pulse generator produces a series of vertical black-and-white strips on the screen (Figure 3a). The width of the strips in different parts of the screen is determined by the nonlinearity of the line scan. In single-line scan along the line  $a-a'$  in the transducer, the transducer output consists of successive pulse trains, and the number of pulses in each train ( $n_1, n_2, n_3, \dots$ ) depends on the width of the corresponding white strip on the screen. The logic unit uses the difference and the sum of the number of pulses corresponding to the widest and the narrowest strip to determine the nonlinear distortion coefficient:

$$K_n = 2 \frac{n_{\max} - n_{\min}}{n_{\max} + n_{\min}} 100\%. \quad (4)$$

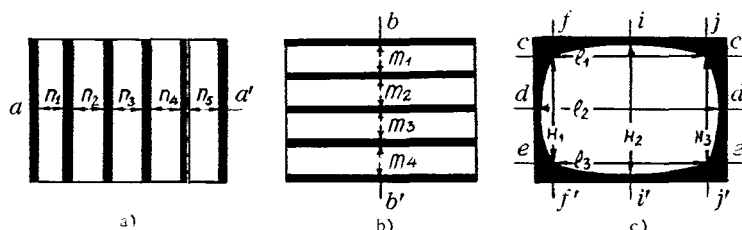


FIGURE 3. Picture of test signals on TV screen.

Vertical nonlinear distortions are similarly determined, but the test signal produces a picture in the form of horizontal strips (Figure 3b), the

single-line scanning in the camera tube is done in the vertical direction along the line  $b-b'$ , and the pulses  $m_1, m_2, m_3, \dots$  are counted.

In vertical scanning, however, care should be taken to avoid interference from lines and quantizing elements of the coding mask. To this end the number of active lines should be a multiple of the number of pairs of vertical quantizing elements.

Geometrical barrel, pincushion, and keystone distortions are determined using a test signal which produces a uniformly white screen. The screen edges are darkened by a "window" test signal (Figure 3c). Geometrical distortions lead to certain deviations from the rectangular shape of the window. Therefore, after scanning along several lines (first horizontally and then vertically), the distortions can be determined from the difference in the number of pulses along parallel segments. The minimum number of scan passes in these measurements is three. These scans give the pulse counts  $l_1, l_2, l_3$  and  $h_1, h_2, h_3$ .

In barrel distortions  $l_2 > l_1, l_1 = l_3$  and the geometrical distortion coefficient in the horizontal direction is calculated from the formula

$$K_{gb} = 2 \frac{l_2 - l_1}{l_2 + l_1} 100\%. \quad (5)$$

For pincushion distortions  $l_2 < l_1, l_1 = l_3$  and

$$K_{gp} = 2 \frac{l_1 - l_2}{l_1 + l_2} 100\%. \quad (6)$$

For keystone distortions

$$K_{gt} = \frac{l_3 - l_1}{l_3 + l_1} 100\% \quad (\text{for } l_3 > l_1). \quad (7)$$

The corresponding distortions in the vertical direction are similarly calculated from the pulse counts  $h_1, h_2, h_3$ .

As the nonlinear and geometric distortions must be measured in two perpendicular directions, the ruled mask should be changed or turned through a right angle when the scan direction is changed. This can be avoided by using a checkered mask, which, however, is not particularly favorable from the viewpoint of parasitic amplitude modulation: to avoid this parasitic modulation, the scanning should be done along a single line of quantizing elements.

### 3. THE EFFECT OF LIMITED RESOLVING POWER OF THE CAMERA TUBE ON MEASUREMENT ACCURACY

The accuracy of linear measurements by the method of optical coding is limited by the resolving power of the camera tube, which determines the minimum size of the quantizing element in the coding mask.

The finite scan beam aperture of the camera tube reduces the depth of modulation of the digital signal (Figure 4). The guiding electrode of the camera tube generally has a circular opening, and the scan aperture



is therefore also nearly circular. If the aperture diameter (the beam cross section diameter)  $d$  is less than the width  $a$  of the mark projected onto the photocathode by the optical coding mark, the quantized signal has 100% mark,  $d > a$ , it simultaneously captures both a black and a white area, and the depth of modulation is naturally reduced. For  $d = 2a$  the beam simultaneously covers one black and one white area, and the signal is converted into a virtually constant voltage (the modulation depth goes to zero).

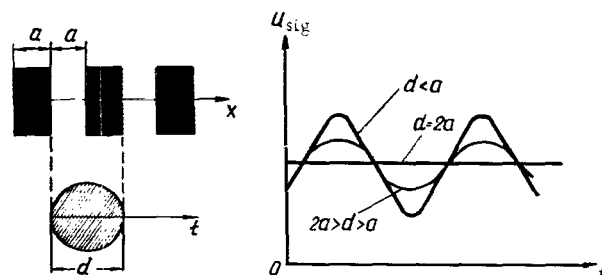


FIGURE 4. The effect of beam aperture of the camera tube on signal shape.

Two quantizing elements are needed to obtain one output pulse, and the maximum number of pulses at the transducer output during a single line scan is therefore equal to half the tube resolving power  $z$ :

$$N_{\max} = \frac{z}{2}. \quad (8)$$

Since the background of the camera tubes is considerably nonuniform and  $z$  markedly drops toward the edges of the photocathode, the resolving power which determines the  $N_{\max}$  of the digital unit should be calculated from the aperture characteristic of the tube assuming a decrease of not more than 50% in modulation depth.

$N_{\max}$  is sometimes called the discreteness of the digital signal,  $D$ . The reciprocal of the discreteness  $D$  determines the maximum relative error in measurements of linear dimensions by the optical coding technique,  $\varepsilon = 1/D$ . This error is associated with pulse counting inaccuracies which are due to the fact that a non-integer number of mark pulses are accommodated within the scanned segment.

$D$  and  $\varepsilon$  determine the quantity of information which is obtained when one linear dimension is measured with a digital TV transducer:

$$I = \log_2 D = \log_2 \frac{1}{\varepsilon}. \quad (9)$$

Thus when the resolving power of the transmitting tube is lowered or the size of the quantizing elements of the coding mask is increased, we lose information.

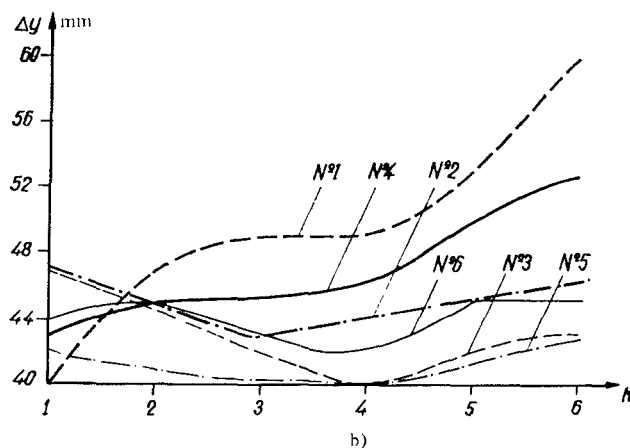
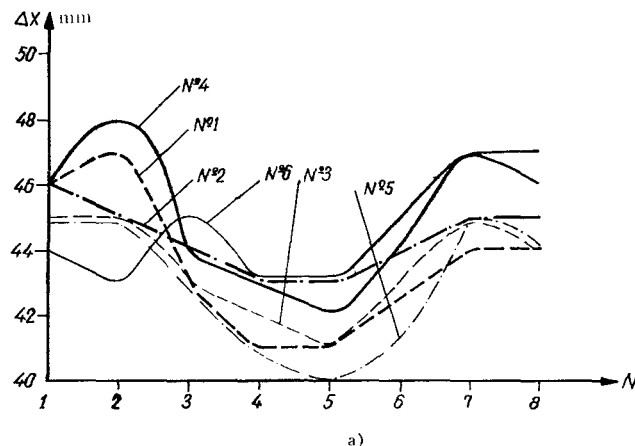


FIGURE 5. Curves of scan nonlinearity for six commercially produced UNT-47 TV sets (Ogonek model):

a — horizontal, b — vertical ( $\Delta x$  and  $\Delta y$  are the dimensions of two adjoining squares of the checkered mask,  $N$  is the number of pairs of squares).

The information concerning the TV image is always transmitted by tubes which inevitably respond after a certain buildup period to the average screen intensity during that period. Instantaneous-action tubes (dissector type) cannot be used for these purposes, since the position of the scanning element on the picture tube screen and the position of the sensing element on the camera tube photocathode do not coincide at any given instant.

Vidicon is the most suitable buildup camera tube for TV transducers used in automatic distortion control.

Figure 5a shows the curves of horizontal scan nonlinearity and Figure 5b of vertical scan nonlinearity for six Ogonek TV sets (UNT-47) from the same line. The two adjoining squares of the checkered field were measured at the end of the assembly line with a "parallex-free" rule. We see from the curves (Figure 5) that the nonlinearity is distinctly nonmonotonic; moreover, it follows different curves, and its variation should therefore be measured both over the entire screen and along small segments. In TV measurements the nonlinear distortions thus should be measured at least in 8–10 vertical and 6–8 horizontal white strips of the test signal. To increase the number of pulses in each series and improve the measurement accuracy, the white strips of the test table should preferably be made wider than the black strips (Figure 3). The permissible geometrical distortion is also fairly low (2–5%). One-inch vidicons (with a diameter of 25 mm) which have a fairly low resolving power therefore cannot ensure the required accuracy (which must be one order of magnitude higher than the measured dimension).

Figure 6a shows an oscillogram of the transducer output signal in a system using a one-inch vidicon. The oscillogram is photographed off the screen of the SI-13 oscilloscope. We see from Figure 6a that for the low signal discreteness ( $D$  of the order of 50) obtained with large coding mask elements ( $d < a$ ) the depth of modulation is fairly large and the signals are readily counted. When the mask elements are made smaller, the depth of modulation decreases and the signal nonuniformity along the line becomes more pronounced. Figure 6b is an oscillogram of the output signal obtained with the same transducer but with a small coding mask element. In this case the resolving power of the transmitting tube is insufficient ( $d > a$ ) to ensure a discreteness of about 200 with a favorable signal/noise ratio. The difficulty can be bypassed however, by using a band filter which isolates the first harmonic of the signal. The filter output (Figure 6c) is a signal with a sufficient amplitude and an adequate signal/noise ratio, which can be delivered to the pulse counter after suitable limiting treatment.

Experimental tests of the application of the TV transducer unit for automatic picture distortion control showed that insufficient resolving power and insufficient field uniformity are not the only shortcomings of the one-inch vidicon, and it is thus not entirely suitable for large-scale plant application. The additional shortcomings include its warming time and adjustment before the actual control is begun, variation of parameters due to voltage and current fluctuations, and others. To reduce the effect of these factors, the vidicon should be connected to a separate control circuit of its own [7] and the voltages and currents should be stabilized.

The currently marketed 1.5-inch vidicon has a resolving power  $z$  of at least 800 lines over the entire picture field. A transducer using this vidicon will therefore give a signal discreteness of at least  $D = \frac{z}{2} = 400$ , i.e., the maximum relative error of linear measurements along the entire line  $\epsilon = \frac{1}{D}$  is at most 0.25%. However, for  $D = 400$  the depth of signal modulation may prove insufficient for further processing (unless a filter is employed). Yet even a somewhat lower discreteness of this vidicon ensures a measurement accuracy which is not less than that of the photographic or projection methods, in which the statistical scatter of distortion measurements in repeated tests is  $\pm 0.5 - 0.75\%$ .

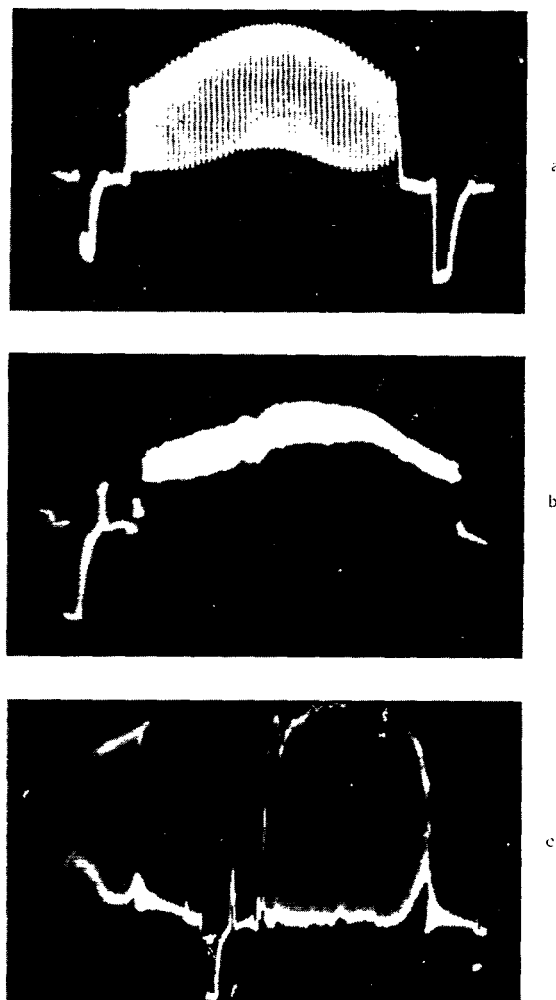


FIGURE 6. Oscillograms of discrete signals at the vidicon output:  
 a — for  $D \approx 50$ , b — for  $D \approx 200$ , c — for  $D \approx 200$  with a band filter.

The measurement accuracy can be considerably improved by using a fiber-optics coding device /8/: here the test line is projected onto one end of the device, where the lightguides are arranged linearly, whereas the lightguides at the other end are spaced out in several lines of a rectangular pattern and the distances between them are greater than the beam aperture of the camera tube. The number of digital pulses at the transducer output

is thus not limited by the resolving power of the camera tube; it is actually determined by the number of lightguides in the fiber-optics device. However, the TV distortions should be measured in two directions, and therefore in order to avoid turning the fiber-optics device mechanically through a right angle, a TV test unit with two separate transducers should be used on the assembly line, one for horizontal distortion measurements and the other for vertical distortion. If a more sophisticated fiber-optics device is used, with the lightguides at the input end arranged in two lines — a horizontal and a vertical one, only one transducer is naturally needed.

## Bibliography

1. GOST 9021-64. Priemniki televizionnye cherno-belogo izobrazheniya (Black- and -White Television Sets: USSR Government Standard 9021-64). — Metody elektricheskikh, opticheskikh i akusticheskikh ispytaniy. Moskva, 1964.
2. Ol'shvang, E. V. Izmerenie geometricheskikh i nelineinykh iskazheniy na ekrane televizora (Measurement of Geometrical and Nonlinear Distortions on a TV Screen). — Tekhnika Kino i Televideniya, 3. 1966.
3. Khesin, A. Ya. Ob avtomatizatsii kontrolya televizionnykh priemnikov (Automatic Control of TV Sets). — Tekhnika Kino i Televideniya, 10. 1964.
4. Polonik, V. S. Televizionnye metody izmereniya razmerov predmetov (TV Methods of Size Measurements). — Tekhnika Kino i Televideniya, 11. 1962.
5. Rabinovich, V. A. — Soviet patent No. 148529, 1 Oct. 1960.
6. Khesin, A. Ya. and A. A. Kurmit. Izmerenie iskazheniy rastra na ekrane kineskopa. — Tekhnika Kino i Televideniya, 4. 1966.
7. Bogdanov, G. M. and S. P. Trifonov. Avtomaticheskaya regulirovka rezhima vidikona (Automatic Control of Vidicon Operation). — Tekhnika Kino i Televideniya, 3. 1966.
8. Rabinovich, V. A. — Soviet patent No. 153126, 29 April 1961.

*A. Ya. Khesin, T. A. Grendze*

# **THE USE OF PHOTOELECTRIC SENSORS FOR AUTOMATIC CONTROL OF GEOMETRICAL TV DISTORTIONS**

Some methods of automatic analysis of the shape and the position of lines on a TV screen using photoelectric elements are considered. The effect of parasitic brightup of the picture tube glass on the accuracy of position measurements is considered.

## **INTRODUCTION**

The TV distortions can be determined by measuring the linear dimensions of different elements of the test table and analyzing the geometry of various patterns on the picture tube screen. The measurements of various test table elements and their comparison, prescribed by the USSR Government Standard GOST 9021-64 /1/, provides the essential information on the magnitude and the kind of nonlinear and geometric distortions. The linear dimensions naturally can be measured and compared automatically /2/. The relevant information can also be obtained by analyzing the shape of lines in different parts of the screen or by measuring the displacement of marker points on the screen.

Geometrical distortions produce a definite curvature of the horizontal and the vertical lines on the screen. The essential information on geometrical distortions is therefore obtained by analyzing the shape of narrow horizontal and vertical strips or by measuring the position of the boundaries between black and white fields in different parts of the test table.

In this article we consider the possibility of automatic analysis of line shapes and positions on a TV screen using photoelectric sensor elements.

## **METHODS OF AUTOMATIC ANALYSIS OF LINE SHAPE AND POSITION ON PICTURE TUBE SCREEN**

The shape and the position of lines need be analyzed only near the very edge of the TV screen, where the geometrical distortions are at their maximum. The shape and the position of a vertical line should be measured near the left- and the right-hand margin of the screen and horizontal distortions are measured near the top and the bottom edges.

To improve the accuracy of this analysis, the thickness of the bright line on the screen should not exceed the size of one element in the picture. Therefore, one of the raster lines if illuminated, can be conveniently used as a horizontal monitor line for distortion measurements. To produce a narrow vertical strip on the screen, a unit step pulse is transmitted whose

duration is equal to one picture element and which is displaced for all the lines by an equal length of time relative to the line synchronizing pulse.

Using the given specifications for the geometrical raster distortion, we can delineate the tolerance field on the screen within which the monitor line should remain on the four sides of the screen (left, right, top, and bottom, Figure 1).

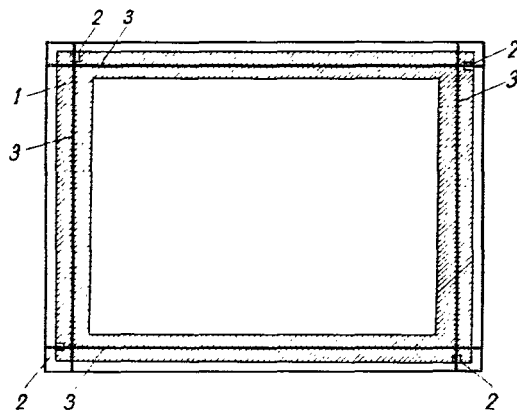


FIGURE 1. Tolerance field (1) along the edges of the picture tube screen and the position of the sensors (2) for centering the monitor lines (3).

The automatic analysis of the line shape is greatly simplified if uniform standards have been established for the resultant geometrical distortions. Thus, if the standard tolerance for the total geometrical distortion is 4% (as in the East German Standard TGL 8838), the allowed line deviations from the mean position on a screen measuring 384 mm in the horizontal direction and 305 mm along the vertical (the Soviet-made 47LK1B picture tube) is  $384 \cdot 0.04 = \pm 15.3$  mm in the horizontal direction and  $305 \cdot 0.04 = \pm 12.2$  mm along the vertical. The tolerance field, i.e., the total allowed deviation of a line on the 47LK1B screen, is 30.6 mm horizontally and 24.4 mm vertically.

If the tolerance field is known, the geometrical distortions are conveniently monitored using a YES—NO photoelectric sensor. This naturally requires a sufficiently sharp change in photodetector signal when the monitor line crosses the boundary of the tolerance field (the photodetector is suddenly illuminated or alternatively obscured).

The main advantage of the automatic analysis of the line position within the tolerance field on the TV screen is that it simultaneously takes account of all the possible distortions which affect the line geometry (for example, the curvature of the vertical line when the TV set is supplied by an asynchronous grid).

The output signal is determined by the inertial properties of the photodetector. If the detector time constant is  $\tau > \frac{1}{f_s}$ , where  $f_s$  is the line scanning frequency, equal to 15,625 Hz, the output signal is independent of

the raster delineation and depends only on the integral brightness intensity of the screen. If, on the other hand,  $\tau < \frac{1}{f_s}$ , the detector output contains a pulsed signal in which the scan frequency is reflected.

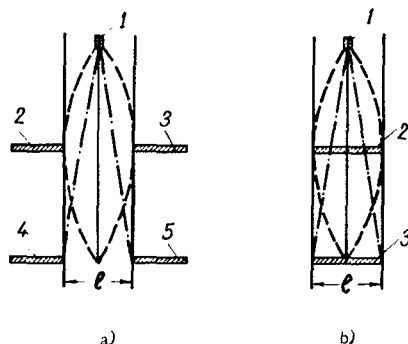


FIGURE 2. Methods of determining the shape of a white line on a TV screen and its position within the tolerance field  $l$ .

Figure 2 illustrates the different photodetector geometries relative to the tolerance field on one of the sides of the picture tube. Detectors 2, 3, 4 and 5 define the limits of the tolerance field  $l$  (see Figure 2a) and detector 1 centers the monitor line. The light-sensitive area of detector 1 is in the shape of a narrow slit parallel to the monitor line. The width of the slit should not exceed its thickness. Automatic line centering is accomplished by gradual displacement of the vertical line in the horizontal direction or successive delineation in the vertical direction until detector 1 delivers a peak signal. After that no further displacement of the line is attempted. A NO (reject) signal is obtained when one of the detectors 2, 3, 4 or 5 is illuminated. The shape and the position of lines on the other sides of the screen is similarly determined. If the readings of the various detectors are received separately, the geometrical distortion can be exactly identified (whether a barrel, a pincushion, a keystone, or other distortion). The sensitive area of detectors 2, 3, 4 and 5 in the longitudinal direction should be large enough to ensure that the detector remains illuminated even in case of maximum displacement of the monitor line. Instead of numerous detectors along the edges of the tolerance field, the four sides of the screen can be fitted with the input ends of fiber-optics lightguides, whose output ends are all connected to a common photoelectric detector, and it is the signal from this detector that is interpreted as a NO signal.

In Figure 2b the light-sensitive surface of detectors 2 and 3 lies inside the tolerance field and their longitudinal dimension is  $l$ . In this case a NO signal is produced when the detectors 2 and 3 are obscured. Line centering, as in the previous case, is done using a maximum signal from detector 1.

Position-sensitive photocells with longitudinal (transverse) photoeffect can be used for automatic line centering and automatic determination of line shift on a TV screen [3/].



## SPECIFIC FEATURES OF PHOTOCELLS USED IN PHOTODETECTORS

Photodetectors use three types of photocells: electron vacuum element (with external photoeffect), photoresistors (with internal photoeffect), and photogalvanic cells — photodiodes and phototransistors /4/.

Since the maximum screen brilliance is fairly low (up to 100 nit), the photocell response is the main parameter which determines its applicability to automatic distortion control.

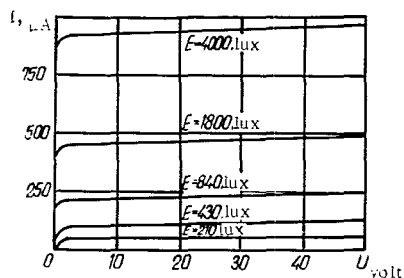


FIGURE 3. Family of current-voltage characteristics of a photodiode.

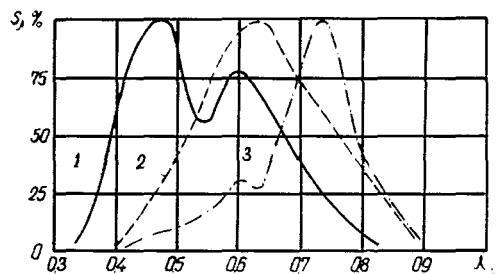


FIGURE 4. Photoresponse curves of the TV screen phosphor (1), a CdS photoresistor (2), and a CdSe photoresistor (3).

For TV screen brilliance of 100 nit, the illumination of a photocell placed touching the screen is at most 200 lux.

Figure 3 shows a family of current-voltage characteristics of a photodiode for various illuminations /4/. For an illumination of 200 lux, the photocurrent is at most 40–50  $\mu\text{A}$ , whereas the dark current of the photodiode is 30  $\mu\text{A}$ , so that the photocurrent is only slightly greater than the dark current. The photocurrent of phototransistors is larger than that of photodiodes, but their dark current reaches 300  $\mu\text{A}$ . The illumination produced by the TV screen is thus insufficient for the use of photodiodes and phototransistors.

An illumination of 200 lux produces a sufficient excess photocurrent (compared to the dark current) in CdS and CdSe photoresistors. The response of the CdSe photoresistors is higher than that of CdS photoresistors, but their photoresponse curve has a narrow maximum at  $\lambda \approx 0.75 \mu$ , whereas the photoresponse of CdS photoresistors occupies a wider region in the visible spectrum, where the glow spectrum of the TV screen phosphor lies (Figure 4). The total response of the CdSe and CdS photoresistors to picture tube glow is therefore virtually the same.

The main advantages of photoresistors are their small size, low cost, and long service life. Any number of photoresistors therefore can be installed for distortion control in different parts of the picture tube screen, ensuring a light-sensitive surface of required size and shape. The shortcomings of photoresistors include their considerable inertia (the time constant  $\tau$  is several tens of milliseconds), substantial scatter of parameters, and variation of the integrated response during the service life /5/.

Maximum response is characteristic of photomultiplier tubes; these are essentially electron-vacuum tubes with external photoeffect and secondary-emission electron multiplication. They have an excellent time resolution and a linear photocurrent characteristic. The photoresponse region of most commercial photomultipliers is fairly wide and in effect coincides with the emission spectrum of the screen phosphor. TV distortions can be conveniently monitored using miniature photomultipliers, not larger than bantam vacuum tubes.

#### THE EFFECT OF PARASITIC PHOSPHORESCENCE ON THE MEASUREMENTS OF LINE POSITION ON A TV SCREEN

The accuracy of the automatic distortion control using photodetectors is determined by the steepness of the characteristic which gives the detector output signal vs. the position of the bright line on the screen.

The steepness of this characteristic depends on the size and shape of the reconstituting aperture and on the parasitic phosphorescence of the screen. The light spot on the receiver screen (the reconstituting aperture) is circular with a normal distribution of electron density in the beam. The circle of confusion in the transmission of a black-white boundary line is approximately equal to the size of the reconstituting aperture, i.e., to the size of one picture element on the receiving screen, which does not exceed 1 mm.

The steepness of the characteristic is thus highly sensitive to parasitic excitation of the screen phosphor.

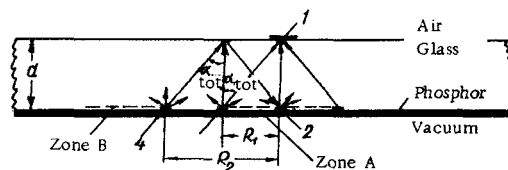


FIGURE 5. The effect of parasitic phosphorescence of the picture tube screen.

Figure 5 shows a cross section through a picture tube screen. Note that the photodetector 1 attached to the outer surface of the glass screen receives not only the direct light from the phosphorescent element 2 directly opposite the detector, but also slanting light from screen elements within a circle of radius  $R_1$  (zone A).

The radius of the parasitic phosphorescence circle  $R_1$  is determined by the thickness of the screen  $d$  and the angle of total reflection  $\alpha_{tot}$ :

$$R_1 = d \operatorname{tg} \alpha_{tot} \quad (1)$$

where

$$\alpha_{tot} = \arcsin \frac{1}{n} \quad (2)$$

For glass  $n = 1.54$  so that  $\alpha_{\text{tot}} = 41^\circ$ .

The screen is thicker along the edges than in the middle. The radius of parasitic phosphorescence is therefore higher at the screen edges.

The useful part of the light flux emitted by the phosphorescent screen element, which does not suffer total reflection and leaves the glass, is

$$\frac{F_n}{F_{\Sigma}} = \frac{2\pi \int_0^{\alpha_{\text{tot}}} I_0 \cos \alpha \sin \alpha d\alpha}{2\pi \int_0^{\frac{\pi}{2}} I_0 \cos \alpha \sin \alpha d\alpha} = \sin^2 \alpha_{\text{tot}} = 0.42, \quad (3)$$

where  $I_0$  is the light intensity along the normal to the screen.

This equation is valid only when the light flux in glass obeys Lambert's law, i.e., when the light intensity emitted by the phosphor is

$$I_{\text{ph}} = I_0 \cos \alpha, \quad (4)$$

where  $\alpha$  is the angle between the normal to the screen and the direction of observation.

For incidence angles  $\alpha < \alpha_{\text{tot}}$  the air - glass interface reflects 4 - 5% of the light flux. Therefore, the main factor influencing the light flux density hitting the photodetector is the loss of luminous energy in the screen glass: in order to enhance the picture contrast, the glass is colored neutral gray and transmits about  $2/3$  of the normally incident light flux.

The attenuation of light in a scattering medium is described by the exponential relation

$$\frac{F''}{F'} = e^{-kd}, \quad (5)$$

where  $k$  is the absorption coefficient;  $d$  is the thickness of glass.

If we take  $\frac{F''}{F'} = e^{-kd} = \frac{1}{2}$ , we find  $kd = 1.1$ , i.e., for  $d = 1$  cm,  $k = 1.1 \text{ cm}^{-1}$ .

Given  $k$  and  $d$ , we can calculate the attenuation of light passing from the outer boundary of the parasitic phosphorescence circle  $A$  to the outer screen surface, compared to the normal light flux:

$$\frac{F_2}{F_1} = e^{-k(d_1 - d)}, \quad (6)$$

where  $F_2$  is the light flux traversing a distance  $d_1$  in glass;  $F_1$  is the normal light flux traversing a distance  $d$  in glass:

$$d_1 = \frac{d}{\cos \alpha_{\text{tot}}}. \quad (7)$$

For  $\alpha_{\text{tot}} = 41^\circ$ ,  $d_1 \approx 1.32 d$ .

Besides the effect of direct parasitic phosphorescence, there is an additional contribution from light suffering total reflection (Figure 5). The radius of the corresponding circle of parasitic phosphorescence  $B$  is

$$R_2 = 2d \operatorname{tg} \alpha_{\text{tot}} = 2 R_1. \quad (8)$$

The light rays hitting the photodetector from element 4 traverse the distance

$$d_2 = \left( 1 + \frac{2}{\cos \alpha_{\text{tot}}} \right) d \quad (9)$$

in glass. For  $\alpha_{\text{tot}} = 41^\circ$ ,  $d_2 \approx 3.65 d$ .

The attenuation of this light component in glass can be calculated from the equality

$$\frac{F_2}{F_1} = e^{-k(d_2 - d)}. \quad (10)$$

The parameters  $d$ ,  $R_1$ ,  $\frac{F_2}{F_1}$  and  $\frac{F_3}{F_1}$  for Soviet-made picture tubes 47LK1B and 59LK1B are listed in Table 1.

TABLE 1.

Parameter	47LK1B		59LK1B	
	center of screen	edge of screen	center of screen	edge of screen
$d$ , mm	6	10	7.5	12.5
$R_1$ , mm	5.2	8.7	6.5	10.9
$\frac{F_2}{F_1}$	0.810	0.705	0.770	0.645
$\frac{F_3}{F_1}$	0.175	0.055	0.113	0.017

We see from the table that the attenuation of the direct parasitic phosphorescence in the screen glass is insignificant compared to the attenuation of the normal light flux, and they therefore make a substantial contribution to the photodetector illumination. The light flux suffering total reflection is attenuation to a much higher degree. Multiple reflections produce a further attenuation of 8–10% compared to the direct light.

Parasitic illumination of the photodetector is also produced by scattered light associated with screen curvature. The scattered light, however, is at most 2% of the principal light flux [6], and it is therefore ignorable.

The parasitic phosphorescence zone can be reduced by several methods. The simplest approach is to use a narrow slit with light-absorbing walls cut through the medium 2 between the photodetector 1 and the outer screen surface (Figure 6a). The direct parasitic phosphorescence zone then shrinks to  $2r$  (instead of  $2R_1$ ).

The illumination from a glowing surface of finite dimensions is

$$E = k \iint \frac{B \cdot dS \cdot f(\alpha) \cdot \cos \alpha}{D^2}, \quad (11)$$

where  $k$  is a coefficient which depends on the system of bright units used;  $B$  is the brightness of a surface element  $dS$ ;  $\alpha$  is the angle between the direction of observation and the normal to the surface;  $f(\alpha)$  is the angular distribution function of the surface brightness;  $D$  is the distance between the luminous surface and the point where the illumination is measured.

When  $D$  is increased, the illumination  $E$  markedly decreases, and may eventually fall below the detector threshold, especially if the screen brightness is fairly low and the slit is narrow.

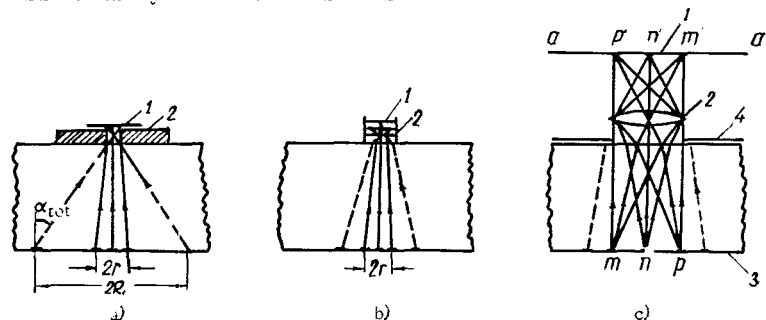


FIGURE 6. Methods for reducing the parasitic phosphorescence.

Better parasitic phosphorescence reduction can be achieved if the slit is replaced by a light chamber 2 with light absorbing walls and adjustable apertures (Figure 6b). The chamber should not be more than a few millimeters deep.

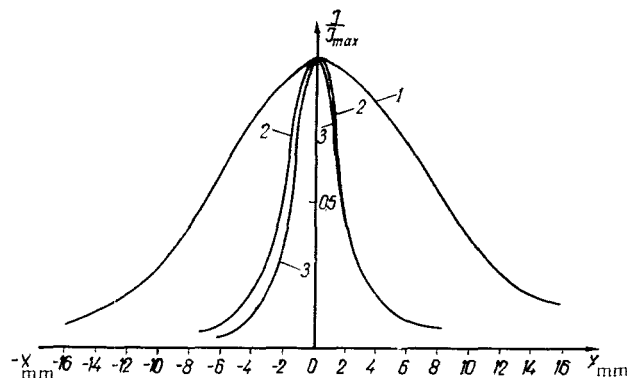


FIGURE 7. Curves of the relative change in photoresistor current vs. the displacement of a bright line on the 47LK18 picture tube.

As we have seen above, the light sensitive area of the photodetector limiting the tolerance field should not exceed 30 mm. A slit of comparable width does not produce a sharp restriction of the parasitic phosphorescence

at the slit edges. The effect of parasitic phosphorescence in this case is reduced with the aid of lens 2, which projects a focused image from the phosphor plane 3 to the plane  $a-a'$  coinciding with the light sensitive area of the detector 1 (Figure 6c). The mask 4 on the picture tube screen blocks off spurious light. In this case, however, the detector illumination is greatly reduced.

Figure 7 shows the experimental curves of the change in photoresistor current as a function of the displacement of a bright line on the picture tube screen (middle of screen). The line thickness is equal to one picture element. If the photoresistor directly touches the picture tube without any slit (curve 1), the parasitic phosphorescence circle is too big to permit exact pinpointing of the line. A 1 mm slit (curve 2) or a short-focus lens ( $f = 4$  mm) with a slit of the same width (curve 3) substantially reduce the parasitic phosphorescence circle, and the line position can be determined to within  $\pm (1-2)$  mm.

We see from Figure 7 that the use of a lens with a narrow slit does not improve the results, since the steepness of curve 3 is almost the same as the steepness of curve 2, whereas the absolute value of the photoresistor current is substantially less than for a slit without a focusing lens.

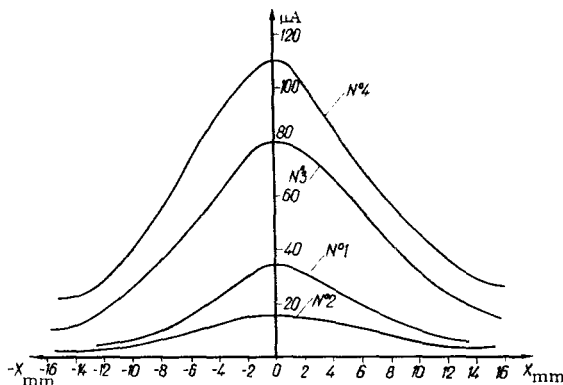


FIGURE 8. Curves of the change in photoresistor current vs. the displacement of the bright line on the 47LK1B picture tube for various photoresistor specimens.

Characteristic 1 does not show any dip between zones A and B, since different parts of the bright line are at different distances from the photoresistor, which after all responds to the total light flux.

Because of the high inertia of the photoresistors, the bright line was moved along the screen at a speed of no more than 1–2 mm/sec. Moreover, comparison of the individual photodetectors mounted in front of the screen revealed a considerable scatter of peak current values and parasitic illumination current (Figure 8).

The application of high-response photomultipliers makes it possible to mount the detector farther from the screen. We can thus choose the optimal distance when the error due to parasitic phosphorescence does not exceed a certain chosen value.

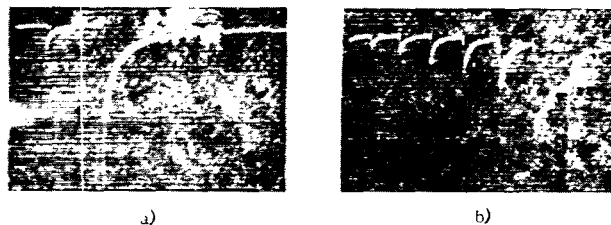


FIGURE 9. Oscillograms of the photomultiplier output signal.

Figure 9 shows oscillograms of photomultiplier output signal obtained with the detector illuminated successively by the lines of a standard raster on the 57LK1B screen through a 1 mm wide slit and a focusing lens with  $f = 35$  mm. If the lens is set at a distance of at least 200 mm from the screen, the photomultiplier output shows one prominent pulse (Figure 9a). The duration of the leading edge does not exceed  $0.1 - 0.2 \mu\text{sec}$ , and the longer trailing edge is determined by screen persistence. If the lens is close to the screen, the parasitic phosphorescence circle is larger and the number of pulses increases (Figure 9b), and it is therefore difficult to decide which of the pulses corresponds to the actual line position.

## CONCLUSIONS

1. Automatic analysis of line shape and position on a picture tube screen with photodetectors provides complete information on total raster distortions associated with geometric distortions and other factors.
2. Photoresistors and photomultipliers are suitable detectors for automatic distortion analysis. Because of the high inertia of photoresistors, however, the analysis can be carried out only if the lines are moved very slowly over the screen.
3. The accuracy of line position measurements can be improved by reducing the parasitic phosphorescence circle.

## Bibliography

1. GOST 9021-64. Priemniki televisionnye cherno-belogo izobrazheniya. Metody elektricheskikh, opticheskikh i akusticheskikh ispytaniy (USSR Government State Standard 9021-64, Black-and-White TV Receivers. Methods of Electrical, Optical, and Acoustic Tests). — Moskva. 1964.
2. Khesin, A. Ya. A TV Method for Automatic Control of TV Distortions. — Present collection.
3. Baker, L. R. Properties and Application of the New Position — Sensitive Photocells. — Control, 5:47. 1962.
4. Korndorf, S. F. Fotoelektricheskie izmeritel'nye ustroystva v mashinostroenii (Photoelectric Measuring Devices in Machine Building). — Moskva, Mashinostroenie. 1965.

5. Soboleva, N.A. et al. Fotoelektronnye pribory (Photoelectronic Devices). — Moskva, Nauka. 1965.
6. Zvorykin, V. and D.A. Morton. Television. [Russian translation. 1956.]



*L. Yu. Veitsman, V. L. Srebnyi*

# **THYRISTOR SWITCHING CIRCUIT FOR A PULSED CONTROL SYSTEM OF D.C. ELECTRIC MOTORS**

A method is developed for the calculation of transients in the thyristor switching circuit of the pulsed control system of d.c. electric traction motors. Results of laboratory tests are given.

The speeds of traction units supplied by a contact line are currently controlled by a pulse-adjustable resistance, which smoothly varies the resistance in the motor circuit between wide limits [1, 2].

In these systems (Figure 1), a power thyristor T1 is connected in parallel to the starting rheostat. The pulse duty cycle of the thyristor current (equal to the pulse duration divided by the period of oscillation) varies from 0 to 1 during the starting or the braking phase of the motor, so that the stage resistance falls from its maximum value to zero.

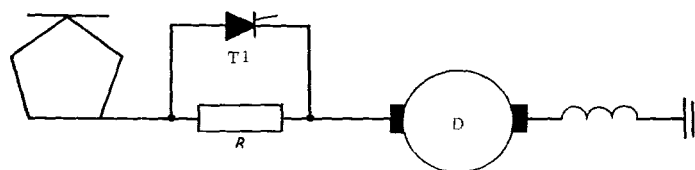


FIGURE 1. Functional diagram of a pulse control system:

$R$  — rheostat stage resistance,  $T1$  — power thyristor,  $D$  — motor.

The main element monitoring the pulse mode of the power thyristor is the switching circuit (Figure 2) comprising an auxiliary thyristor  $T2$  and a quenching capacitor  $C$  ( $r$  is the charging resistance,  $T1$  is the power thyristor,  $T2$  is the auxiliary thyristor,  $R$  is the starting rheostat resistance,  $T3$  is the recharge thyristor,  $L_2$  is the inductance of the leads and the transducer,  $DL$  is the delay unit,  $L_3$  is the inductance of the recharge circuit,  $RT$  is the rectifier,  $D$  is the motor,  $L_e$  is the excitation winding).

The capacitor  $C$  is supplied either from an external source (Figure 2a) or by additional feedback from the traction motors (Figure 2b).

The operating cycle of the switching circuit can be divided into four successive phases.

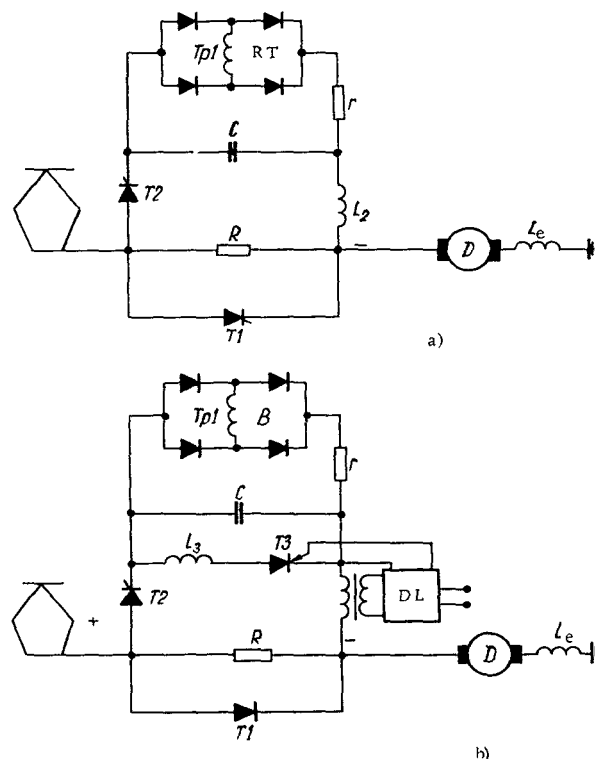


FIGURE 2. Quenching capacitor charging circuit:

(a) using an external source, (b) charging by motor current.

Phase 1 begins when the auxiliary thyristor  $T_2$  is turned on. The capacitor  $C$  charged to a voltage  $U_{cm}$  (the polarity of this voltage is shown in Figure 3a) is discharged through the power thyristor  $T_1$  into the serially connected inductance of the delay unit transducer coil and the lead inductances  $L_2$ . The current through thyristor  $T_1$  falls to zero, and then reverses its direction, again dropping to zero after a time  $t_{T1}$  (Figure 4).

After the recovery time of the thyristor, d. c. bias is applied to  $T_1$ .

In Figure 4  $t_0$  is the time for the thyristor current to fall to zero,  $t_{T2}$  is the recovery time of the auxiliary thyristor;  $i_R$  is the rheostat current;  $i_{T2}$  is the auxiliary thyristor current,  $i_{T1}$  is the power thyristor current,  $U_{T1}$  is the voltage across the power thyristor,  $U_C$  is the voltage across the capacitor.

Phase 2: when the power thyristor  $T_1$  is switched off, the capacitor discharges through the starting rheostat. As a result overvoltage is set up, which is applied to the power thyristor in the back direction. This phase terminates when the voltage on the quenching capacitor drops to zero (Figure 3b).

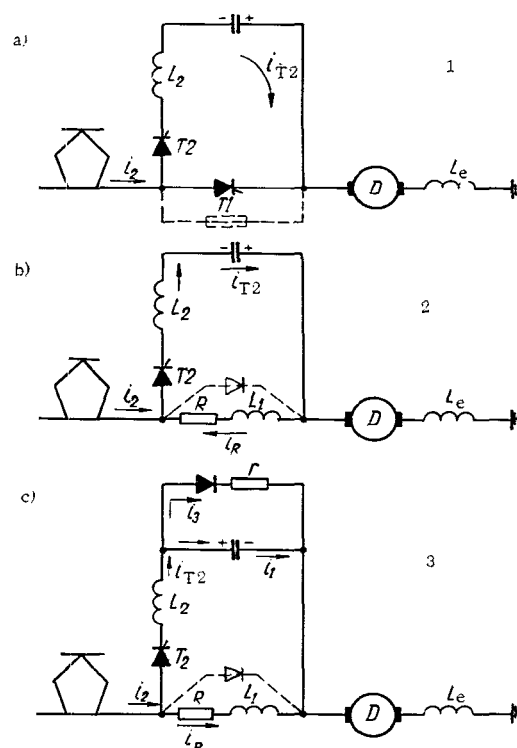


FIGURE 3. Current distribution in the circuit for various phases of the cycle.

Phase 3 begins when the capacitor is recharged by the motor current. Since the polarity of the capacitor voltage is reversed, all the previously cut off diodes of the rectifier bridge are now conducting and the traction motor current flows through these diodes into the charging resistance. Transformer overlapping thus begins, since current flows through all the four diodes of the bridge. The inductance of the rheostat stage produces oscillations in the auxiliary thyristor current, which is necessary to ensure its rapid cutoff. After the recovery time  $t_{T2}$ , the auxiliary thyristor T2 is cut off (Figure 4).

Phase 4. Transformer overlapping may continue. After that, in the circuit shown in Figure 2a, the capacitor is charged by transformer T<sub>11</sub> through the rectifier RT. In the circuit shown in Figure 2b, the transients occur in the following sequence. The signal from the rising edge of the auxiliary thyristor current pulse is differentiated, delayed in the delay unit DL for the duration of the cutoff time of the auxiliary thyristor T2, and is then delivered to the control electrode of the thyristor T3. T3 becomes conducting, recharging the capacitor through the inductance  $L_3$  to a voltage which cuts off the thyristor T1. After that the capacitor charge is built up to the voltage  $U_{cm}$  from the transformer.

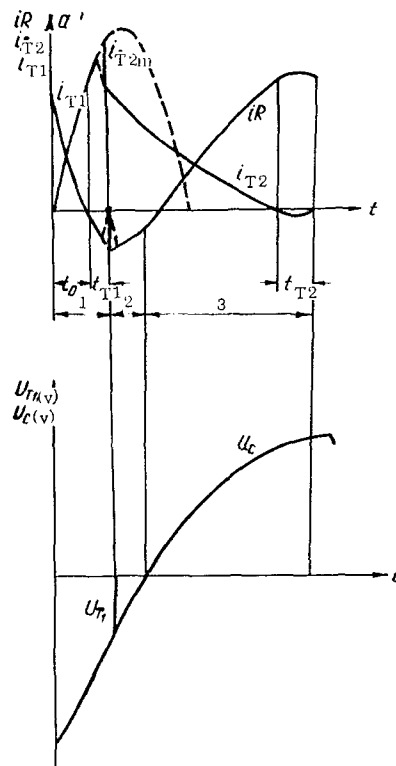


FIGURE 4. Diagram of currents and voltages in the switching circuit.

Our aim is to calculate the transients during the phases 1, 2, and 3 of the cycle.

#### BASIC EQUATIONS OF THE SWITCHING CIRCUIT

The operation of the switching circuit is analyzed under the following assumptions:

- 1) the traction motor current remains constant during the transients;
- 2) the inductance of the starting rheostat and its active resistance are constant;
- 3) the active resistance of the leads is zero;
- 4) the resistance of the cutoff thyristors is infinite, and the resistance of the conducting thyristors is zero;
- 5) the switching-on time of thyristors is ignored;
- 6) back current flows through the thyristor during the whole of the recovery time.

Phase 1. The operatorial Kirchhoff equation of the circuit is

$$i_{T2} + pL_2 i_{T2} - \frac{U_{cm}}{p} = 0, \quad (1)$$

where  $U_{cm}$  is the capacitor voltage at the time when the auxiliary thyristor is switched on;

$i_{T2}$  is the auxiliary thyristor current.

The solution of this equation has the form

$$i_{T2} = \frac{U_{cm}}{\omega_0 L_2} \sin \omega_0 t, \quad (2)$$

where  $\omega_0$  is the radian frequency of the natural oscillations of the circuit;

$L_2$  is the inductance of the leads and the DL transducer (Figure 3).

The thyristor switching off time  $t$  is the sum of the time  $t_0$  the power thyristor current takes to fall to zero plus the recovery time  $t_{T1}$  (Figure 5).

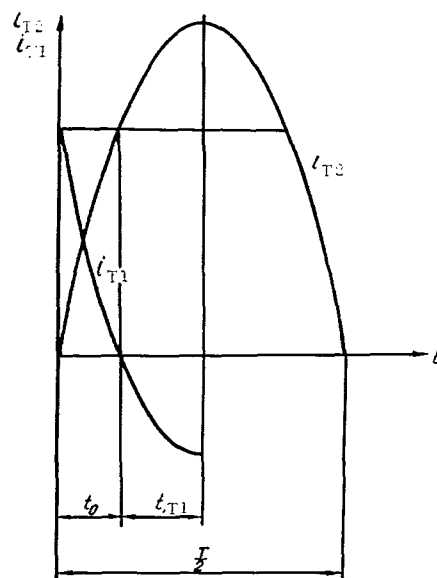


FIGURE 5. Illustrating the power thyristor cutoff conditions.

The time  $t_0$  is obtained from relation (2) by setting  $i_{T2} = i_2$  for  $t = t_0$ , where  $i_2$  is the motor current:

$$t_0 = \frac{1}{\omega_0} \arcsin \frac{i_2 \omega_0 L_2}{U_{cm}}.$$

The switching-off time of the power thyristor is then

$$t = t_{T1} + \frac{1}{\omega_0} \arcsin \frac{i_2 \omega_0 L_2}{U_{cm}}. \quad (3)$$

Inserting (3) in (2), we obtain the maximum current through the auxiliary thyristor (Figure 4):

$$i_{T2m} = i_2 (\cos \omega_0 t_{T1} + \sqrt{a^2 - 1} \cdot \sin \omega_0 t_{T1}), \quad (4)$$

where  $a = \frac{U_{cm}}{i_2 \omega_0 L_2}$ .

The maximum current through the power thyristor at the end of the phase is

$$i_{T1m} = i_2 - i_{T2m} = i_2 (1 - \cos \omega_0 t_{T1} - \sqrt{a^2 - 1} \cdot \sin \omega_0 t_{T1}). \quad (5)$$

We see from this expression that the negative current through the thyristor increases with increasing coefficient  $a$ , i.e., for given  $L_2$  and  $C$ , with increasing initial voltage on the quenching capacitor  $U_{cm}$ . On the other hand, a larger back current pulse increases the switching-off thyristor losses [3], which is highly undesirable. Therefore  $U_{cm}$  should not be made too large and should ensure reliable cutoff of the power thyristor at the largest allowed currents in the motor circuit.

Let us calculate the minimum capacitor voltage needed to ensure reliable thyristor cutoff.

The condition of power thyristor cutoff is written in the form (Figure 5)

$$i_0 + t_{T1} \leq \frac{\pi}{2 \omega_0},$$

or

$$\frac{1}{\omega_0} \arcsin \frac{1}{a} + t_{T1} \leq \frac{\pi}{2 \omega_0}, \quad (6)$$

whence for the capacitor voltage

$$U_{cm} \geq \frac{i_2}{\sqrt{\frac{C}{L_2}} \cos \omega_0 t_{T1}}. \quad (7)$$

The capacitor voltage at the end of Phase 1 is

$$U_{c0} = U_{cm} - \frac{1}{C} \int_0^{t_0 + t_{T1}} i_{T2} dt = U_{cm} - \frac{i_2}{\omega_0 C} (a - \sqrt{a^2 - 1} \cdot \cos \omega_0 t_{T1} + \sin \omega_0 t_{T1}). \quad (8)$$

Phase 2. The equations of currents and voltages in operational form are now

$$\begin{aligned} \frac{i_2}{p} &= i_R + i_{T2}; \\ i_R(R + pL_1) - i_{R0}L_1 &= pL_2 i_{T2} - i_{T20}L_2 - \frac{U_{c0}}{p} + \frac{i_{T2}}{pC}, \end{aligned} \quad (9)$$

where  $R$  is the stage resistance;

$i_R$  is the stage current;

$L_1$  is the stage inductance.

Taking  $i_R = 0$  and  $i_{T20} = i_2$ , we obtain the solution of the set of equations for the current through the auxiliary thyristor:

$$i_{T2} = \frac{U_{c0} + i_2 R}{\omega L} e^{-\alpha t} \sin \omega t + i_2 e^{-\alpha t} \left( \cos \omega t - \frac{\alpha}{\omega} \sin \omega t \right). \quad (10)$$

where  $\alpha = \frac{R}{2L}$ ;  $\omega = \sqrt{\alpha^2 - \frac{1}{LC}}$  for  $\frac{1}{LC} > \alpha^2$  and

$$L = L_1 + L_2.$$

Since usually  $L_2 \ll L_1$ ,

$$\alpha = \frac{R}{2L_1}, \quad \omega = \sqrt{\frac{1}{L_1 C} - \alpha^2}.$$

The auxiliary thyristor current is thus

$$i_{T2} = e^{-\alpha t} \left\{ \frac{U_{c0}}{\omega L_1} \sin \omega t + i_2 \left[ \frac{0.5R \sin \omega t}{\omega L_1} + \cos \omega t \right] \right\}. \quad (11)$$

The current through the starting resistance is

$$i_R = i_2 - i_{T2} = -\frac{U_{c0}}{\omega L_1} e^{-\alpha t} \sin \omega t - i_2 \left\{ \left[ \frac{0.5R \sin \omega t}{\omega L_1} + \cos \omega t \right] e^{-\alpha t} + 1 \right\}. \quad (12)$$

To choose the power thyristor parameters, we require the maximum back voltage applied to the cutoff diode. This voltage can be obtained from equation (8) if we ignore the drop of voltage across the inductance  $L_2$ , i.e., take

$$U_{cm} = U_{c0}. \quad (13)$$

Phase 3. The equations of currents and voltages in this phase in operatorial form are

$$\left. \begin{aligned} \frac{i_2}{p} &= i_{T2} + i_R; \\ i_{T2} &= i_1 + i_3; \\ i_R(R + pL_1) - i_{R0}L_1 &= \frac{i_1}{pC} - i_{T20}L_2 + pi_{T2}L_2; \\ \frac{i_1}{pC} &= i_3r, \end{aligned} \right\} \quad (14)$$

where  $i_{T20}$  is the initial current through the auxiliary thyristor, determined by equation (11) at the end of phase 2;

$i_1$  is the capacitor current;

$i_3$  is the resistor current.

The solution of equations (14) for the transform of the capacitor current, taking  $i_{R0}=0$  and ignoring the inductance  $L_2$ , takes the form

$$i_1 = \frac{i_2}{L_1} \frac{R}{p^2 + p \left( \frac{1}{rC} + \frac{R}{L_1} \right) + \frac{1}{L_1 C}} + \frac{i_{T20} L_2 + i_2 L_1}{L_1} \cdot \frac{p}{p^2 + p \left( \frac{1}{rC} + \frac{R}{L_1} \right) + \frac{1}{L_1 C}}.$$

The roots of the characteristic equation are

$$p_{1,2} = - \left( \frac{1}{2rC} + \frac{R}{2L_1} \right) \pm \sqrt{\left( \frac{1}{2rC} + \frac{R}{2L_1} \right)^2 - \frac{R+r}{r} \cdot \frac{1}{CL_1}}.$$

For

$$\left( \frac{1}{2rC} + \frac{R}{2L_1} \right)^2 < \frac{R+r}{r} \cdot \frac{1}{CL_1}$$

we have an oscillatory process; otherwise the process is aperiodic.

To quench the auxiliary thyristor, the first condition must be satisfied. Therefore, in what follows we will only consider the oscillatory mode of the circuit.

We set

$$\beta = \frac{1}{2rC} + \frac{R}{2L_1};$$

$$\omega_1 = \sqrt{\frac{1}{L_1 C} \cdot \frac{R+r}{r} - \beta^2}.$$

Let us find the critical value of the charging resistance  $r_k$  which just allows the oscillatory mode. This critical resistance is obtained from the equality

$$\frac{1}{L_1 C} \cdot \frac{R+r}{r} - \beta^2 = 0,$$

and we should have  $r_k > r$ , so that

$$r_k > r = \frac{2r_B^3 - r_B^2 R}{4r_B^2 - R^2}, \quad (15)$$

where  $r_B = \sqrt{\frac{L_1}{C}}$ .

Figure 6 plots the lines  $r_1 = f(R)$  for  $r_B = 3-15$  ohm which correspond to the actual values of parameters in such circuits. We see from these lines that the charging resistance ensuring oscillatory operating conditions is of the same order of magnitude as the total stage resistance, and lower resistances have little effect on the transients.

The expression for the capacitor current is

$$i_1 = i_2 \frac{R}{\omega_1 L_1} e^{-\beta t} \sin \omega_1 t + \frac{i_{T20} L_2 + i_2 L_1}{L_1} e^{-\beta t} \times$$

$$\times \left[ \cos \omega_1 t - \frac{\beta}{\omega_1} \sin \omega_1 t \right].$$



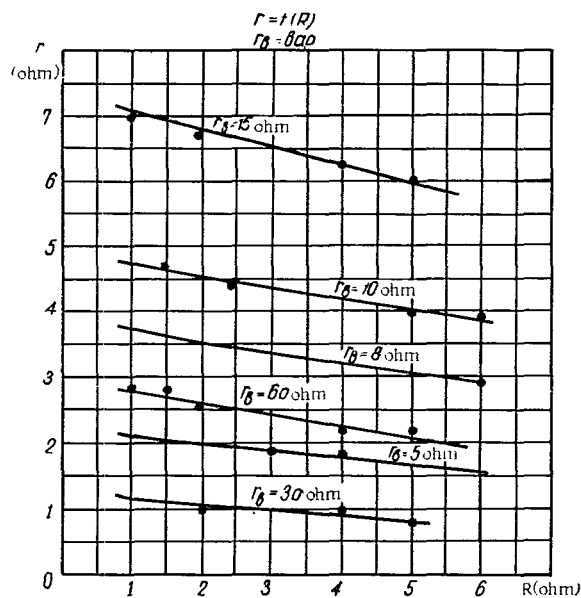


FIGURE 6. The plot of  $r = f(R)$  with  $r_0$  as the parameter.

Since  $i_{T20} L_2 \ll i_2 L_1$ , we have

$$i_1 = i_2 e^{-\beta t} \left[ \left( \frac{R}{\omega_1 L_1} - \frac{\beta}{\omega_1} \right) \sin \omega_1 t + \cos \omega_1 t \right]. \quad (16)$$

The charging circuit resistance is

$$i_3 = \frac{i_2}{cr(\beta^2 + \omega_1^2)} \{ (\omega_1 - \beta D) e^{-\beta t} \sin \omega_1 t - (D \omega_1 + \beta) \cos \omega_1 t + D \omega_1 + \beta \}, \quad (17)$$

where  $D = \frac{R}{\omega_1 L_1} - \frac{\beta}{\omega_1}$ .

The auxiliary thyristor current is

$$i_{T2} = i_1 + i_3 = i_2 \left\{ \sin \omega_1 t \cdot e^{-\beta t} \left[ D + \frac{\omega_1 - D\beta}{cr(\omega_1^2 + \beta^2)} \right] + \frac{r}{R+r} \cos \omega_1 t \cdot e^{-\beta t} + \frac{R}{R+r} \right\}. \quad (18)$$

The starting rheostat current is

$$i_4 = i_2 - i_{T2} = i_2 \left\{ 1 - \sin \omega_1 t \left[ D + \frac{\omega_1 - D\beta}{cr(\omega_1^2 + \beta^2)} \right] - \frac{r}{R+r} \cos \omega_1 t \cdot e^{-\beta t} - \frac{R}{R+r} \right\}. \quad (19)$$

The capacitor voltage at the end of phase 3 is

$$U_{c1} = \frac{1}{C} \int_0^\delta i_4 dt = \frac{i_2}{C} \frac{1}{\beta^2 + \omega_1^2} \{ e^{-\beta\delta} (\omega_1 - D\beta) \sin \omega_1 \delta - e^{-\beta\delta} (\beta + D \omega_1) \cos \omega_1 \delta + \beta + D \omega_1 \}, \quad (20)$$

where  $\delta$  is the duration of the "on" state of the auxiliary thyristor.

To choose the thyristor switching frequency in pulsed control systems, we require the parameter  $\delta$ , since it limits the capacitor charging time to the polarity which is needed to cut off the power thyristor.

Ignoring the recovery time  $t_{T2}$  of the auxiliary thyristor, which is immeasurably small that the duration of the "on" state, and neglecting the effect of the charging circuit and the duration of phase 1, we obtain under our assumptions for the duration of the "on" state of the auxiliary thyristor

$$\delta = \frac{T}{2} - t_2, \quad (21)$$

where  $t_2$  is a time which depends on the initial circuit conditions;

$$T = \frac{2\pi}{\omega}.$$

The time  $t_2$  is found from (11) for  $i_{T2} = 0$ :

$$t_2 = \frac{1}{\omega} \arcsin \frac{i_2}{\sqrt{\left(\frac{U_{c0}}{\omega L_1} + i_2 \frac{0.5R}{\omega L_1}\right)^2 + i_2^2}}. \quad (22)$$

Inserting  $t$  from (22) and  $T$  from (21), we thus get

$$\delta = \frac{1}{\omega} \left[ \pi - \arcsin \frac{i_2}{\sqrt{\left(\frac{U_{c0}}{\omega L_1} + i_2 \frac{0.5R}{\omega L_1}\right)^2 + i_2^2}} \right]. \quad (23)$$

Analysis of this expression shows that the duration of the "on" state of the auxiliary thyristor decreases as the traction motor current increases for low loads and is almost independent of the motor current in the limiting mode, when the amplitude of the auxiliary thyristor current is only slightly greater than the motor current.

## RESULTS OF TESTS

The pulsed control system was tested using a 200 kW URT-100 traction motor, a braking unit, a thyristor unit with VKDU-100-4B and UPVK-5-3B thyristors, a transformer supplying the switching circuit and control circuits.

Experimental tests were carried out at frequencies of 100 and 400 kHz. Both the switching circuit parameters (the quenching capacitance, the inductances  $L_1$  and  $L_2$ , the starting rheostat resistance  $R$ ) and the traction motor current were changed. The traction motor current varied from 0 to 240 amp.

Current and voltage oscillograms were taken for the various component elements of the switching circuits, and the minimum permissible capacitor voltage was determined needed to ensure reliable cutoff of the power thyristor.

Figure 7 is an oscillogram of the current through the auxiliary thyristor of the switching circuit. The tests essentially confirm the principal theoretical conclusions of the study.

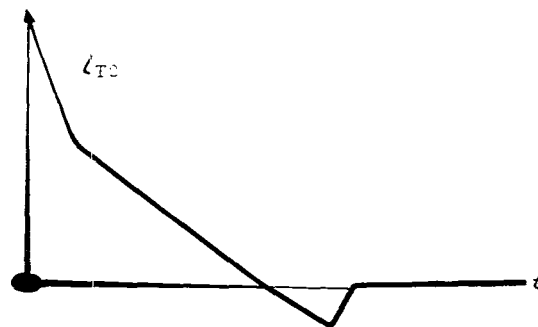


FIGURE 7. Oscillogram of the current through the auxiliary thyristor.

## CONCLUSIONS

The theoretical analysis of the switching circuit of a pulsed control system d.c. traction motors led to a procedure for the calculation of the transients, which gives the instantaneous and the amplitude values of the currents and voltages in the circuit. These values can be used to design and select the various component elements of the unit.

Experimental tests bear out the principal results of the work.

## Bibliography

1. Giessow, G. and S. Kulka. Die Anwendung von pulsgesteuerten Widerständen bei Gleichstrom-Reihenschlussmotoren und Drehstrom-Schleifringläufermotoren. — AEG-Mitt., 55(2):123, 1965.
2. Veitsman, L. Yu. Avtomaticheskaya sistema impul'snogo regulirovaniya puskа tyagovykh dvigatelei elektropodvizhnogo sostava postoyannogo toka (An Automatic System for Pulsed Control of D. C. Traction Motor Starting). — In: "Avtomatika i vychislitel'naya tekhnika," p. 9. Riga, Zinatne. 1965.
3. Meyer, M. Beanspruchung von Thyristoren in selbstgeführten Stromrichtern. — Siemens-Z., 39(5):495. 1965.

*E. Kh. Khermanis, Yu. Ya. Koki, V. A. Zalitis,  
V. G. Karklin'sh, G. P. Tarasov*

# ***AUTOMATIC COMPENSATION CIRCUIT FOR SLOW- SWEEP CONTROL OF A STROBOSCOPIC OSCILLOGRAPH***

This article deals with the operating principle and functional circuit of the device. The advantages of two-way monitoring of the input signal and its use for slow-sweep control of a stroboscopic oscillograph in order to reduce the time required to analyze the signal are explained.

The use of an automatic compensation circuit in a stroboscopic converter considerably improves the performance of a stroboscopic oscillograph: it broadens the pass band, eliminates nonlinear distortion and increases the sensitivity.

The lack of an automatic compensation circuit results in an increase in the analysis time. In automatic compensation circuits with discharge and one-way monitoring of the input signal the number of strobe pulses in the pulse train is determined by the charge of the storage capacitor starting from some initial level until breakdown, corresponding to the compensation of the input signal at a given readoff point. Particularly ineffective is the use of strobe pulses in the form of a pulse train with regard to the readoff points of the flat portions of the signal. If instead of a breakdown in the voltage of the storage capacitor after each reading in one-way monitoring circuits we use a steady, slow discharge of the capacitor, the analysis time for reading off the points of the trailing edge is sharply increased, since the compensation level is reached in accordance with an exponential law, whereby the time constant of the storage capacitor discharge is large. The latter cannot be substantially reduced, because the adjustment error is increased and the discharge of the storage capacitor is inhibited upon reading off the leading edge and the flat portions of the signals.

Below we shall discuss how an automatic compensation circuit is effected by employing two-way monitoring of the signal in question. This type of voltage control at the converter output enables us to read both the decay and the rise of the observed transient process, considerably reducing the time of analysis. Reduction of the analysis time is achieved by reducing the number of strobe pulses in the pulse train with respect to a given readoff point. The required number of strobe pulses in the pulse train is determined by the difference between the voltage at a given readoff point and preceeding readoff points. If by means of a compensating voltage a level is attained, corresponding to the voltage at a given readoff point, the automatic compensation circuit generates a slow-sweep control signal, effecting a shift in the strobe pulse along the readoff interval, i.e., a jump to the next readoff point.

Figure 1 gives the block diagram of the automatic compensation device for the slow-sweep control of a stroboscopic oscillograph: 1 — converter; 2 — strobe-pulse generator (SPG); 3 — storage capacitor with repeater; 4 — amplifier-expander; 5 and 6 — charging and discharge switches of the capacitor; 7 and 8 — driven relaxation oscillators; 9 — logic circuit; 10 — circuit controlled by electronic switches 5 and 6; 11 — monitoring amplifier; 12 — slow-sweep generator.

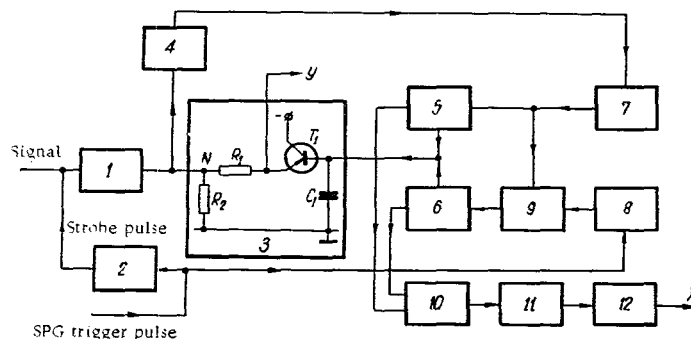


FIGURE 1. Block diagram of an automatic compensator for the slow-sweep control of a stroboscopic oscillograph.

The test version of the functional circuit, corresponding to the block diagram in Figure 1, is given in Figure 2.

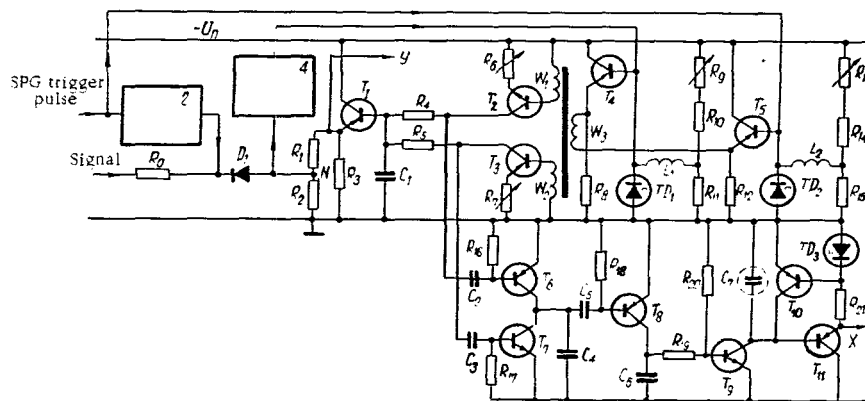


FIGURE 2. Functional circuit.

The stroboscopic converter consists of a widely known circuit in which the strobe pulses are triggered at the right time by actuating a semiconductor diode. If the circuit does not effect compensation, then diode  $D_1$

opens upon each strobe pulse. In a compensating circuit (as is the case here) diode  $D_1$  triggers strobe pulses only when the sum of the signal voltage at a given readoff point and the voltage of the strobe pulses exceeds the voltage at  $N$ . The relaxation oscillators correspond to a delayed multivibrator circuit consisting of a tunnel diode and an inductance. Relaxation oscillator 7 triggers a discharge by means of the strobe pulse when the diode  $D_1$  is open. Relaxation oscillator 8 triggers a discharge for each cycle of the strobe pulses from the strobe-pulse generator. The duration of the pulse, shaped by relaxation operator 7, is twice as long as that of the output pulse of relaxation oscillator 8. The square pulses shaped by relaxation oscillators 7 and 8 are intensified via the current by the repeaters at transistors  $T_4$  and  $T_5$ , respectively. The emitters of  $T_4$  and  $T_5$  are both connected to the winding  $W_3$  of the transformer  $T_p$ . Thus, we must consider the two possible cases for which the relaxation oscillators are triggered:

- 1) the strobe pulse triggers relaxation oscillator 8, but not relaxation oscillator 7;

- 2) the strobe pulse triggers both relaxation oscillators.

In the first case a current flows through the winding  $W_3$  from the output of the repeater at  $T_4$  to the emitter of  $T_5$ . The duration of the current pulse is equal to that of the output pulse of relaxation oscillator 8. In the second case, when a negative voltage drop occurs at the emitters of  $T_4$  and  $T_5$ , no current flows through  $W_3$ . The current pulse is generated after completion of the output pulse of relaxation oscillator 8, since the duration of the pulse of relaxation oscillator 7 was selected twice as large as that of relaxation oscillator 8. The current pulse in the second case possesses an opposite polarity of the same duration as the trigger pulse of the relaxation oscillators in the first case.

This suffices to actuate respectively switches 5 and 6 by means of windings  $W_1$  and  $W_2$  of the transformer  $T_p$ , since in the case of an inadequate compensation voltage at  $N$  charging of capacitor  $C_1$  takes place, while in the case of overcompensation a discharge occurs. Resistors  $R_6$  and  $R_7$  are monitored. The monitor charge (or discharge) of the storage capacitor  $C_1$  determines the quality of control. An increase in the monitor charge enhances the circuit response speed, but causes larger errors in the control.

The quality of the test of the follow-up system is characterized by the order in which switches 5 and 6 are actuated: if the automatic compensation system does to succeed to follow the variations of the studied signal, then only one of the switches (5 or 6) is actuated; when the monitoring is good, switches 5 and 6 are successively actuated. Circuit 10, consisting of transistors  $T_6$  and  $T_7$ , charges and discharges capacitor  $C_4$  upon the arrival of pulses from the collectors of  $T_2$  and  $T_3$  (switches 5 and 6). The output signals of block 10 are subsequently differentiated and arrive at the input of the monitoring amplifier, consisting of transistor  $T_8$ . The slow-sweep generator, consisting of transistors  $T_9$ ,  $T_{10}$  and  $T_{11}$ , and the tunnel diode  $TD_3$ , was adjusted to an extremely low sweep frequency when no signals arrived at the base of  $T_9$  from 11. If the follow-up system succeeds in monitoring the studied signal, then switches 5 and 6 are successively actuated and signals from the monitoring amplifier 11 arrive at the base of  $T_9$ , leading to an increase in the flow of charge in capacitor  $C_7$  of the

slow-sweep generator; a step voltage at  $C_7$ , generated by the signal from block 11, corresponds to a jump to the next readoff point.

The above version of the functional circuit indicates the possibility of employing two-way monitoring for the slow-sweep control of a stroboscopic oscillograph with the aim of reducing the signal analysis time. This type of control is effected by alternating the order of charging and discharging the storage capacitor of the automatic compensation circuit which is determined by the speed with which the studied signal varies.

*D. K. Zibin'*

### *SYNTHESIS OF MULTISTAGE TRIGGERS*

The synthesis of multistable triggers from simpler components using the multistage approach is described. Examples of functional and circuit diagrams are shown.

Triggers are the commonest component units in digital computers and sampled-data control systems. The recent advances in solid-state electronics led to the introduction of highly effective multistable triggers, which are gradually replacing the usual flip-flops. The general theory of design of multistable triggers is presented in /1/. We applied this theory to the synthesis of multistable triggers from simpler components by the multistage approach.

### PROCEDURE

Each stage of a normal solid-state trigger contains an inverter amplifier, whose collector circuit is the output of the stage and whose base circuit is the input. Under certain conditions, these stages will form a trigger, provided that their inputs and outputs are cross-linked. The "amplifier" concept in these devices is to be considered with some reservation. This stage alternately functions as a made switch, an amplifier, and a broken switch during one complete cycle. The amplifying properties of this component are not manifested during the first and the third phase of the cycle, so that the multistable trigger can use some different components capable of performing the same three functions, e.g., triggers. In this case the various outputs of the trigger should be connected through an OR circuit with the common output of the stage, and the common input of the entire stage should be connected to substage inputs (Figure 1). Thus, if the transistor  $T_1$  is cut off, the transistors  $T_2$ ,  $T_3$ , and  $T_4$  are conducting, since they receive the base current from the collector circuit of the cutoff transistor  $T_1$ . The output voltages of this trigger are shown in Figure 2.

The four transistors can of course be analogously replaced with bistable triggers, etc. (Figure 3). Therefore the resulting multistable triggers can be classified as multistage circuits. In accordance with the general theory of multistable triggers /1/, multistage triggers can be used to simulate three-, four-, five-bit and even more complex configurations (Figure 4).



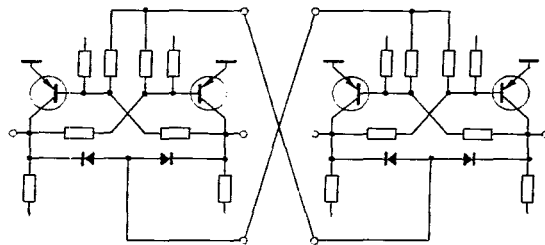


FIGURE 1. A two-stage trigger.

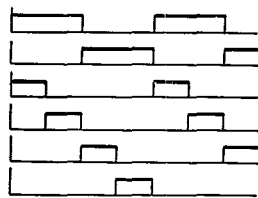


FIGURE 2. The output voltages of a two-stage trigger.

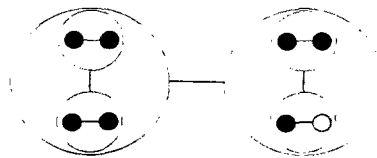


FIGURE 3. Functional diagram of a three-stage trigger.

However, as the number of bits is increased, the stability parameters deteriorate (the output voltage and the permissible load current decrease). In ordinary multistable triggers this shortcoming is eliminated by introducing a second backup transistor in each bit stage. In multistage triggers fewer amplifying transistors are required. For example, the trigger shown in Figure 4a requires only two amplifying transistors, the circuit in Figure 4b only three, and so on.

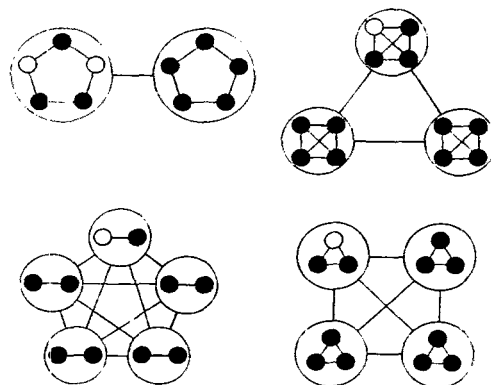


FIGURE 4. Functional diagrams of some two-stage triggers.

The multistage triggers considered above are regarded as elementary devices in Pavlenko's classification /2/, since they cannot be split into constituent components without breaking at least several base-collector linkages. It is nevertheless highly important to understand their building blocks. Clearly, any multistable trigger can be built up from bi- or tristable triggers. In this case, the maximum possible number of states will be greater than in an analogous conventional trigger. This is so because the operating conditions of the base circuit of the cutoff transistors are improved in the multistage trigger: there are fewer base-collector linkage elements connected to the transistor base. Particularly simple and attractive for many-bit configurations are triggers with diode base-collector linkages.

### Bibliography

1. Zibin', D.K. Simmetrichnye mnogostabil'nye triggery (Symmetric Multistable Triggers).— In: "Avtomatika i vychislitel'naya tekhnika," p.15. Riga, Zinatne. 1966.
2. Pavlenko, P.I. Schetno-impul'snyi khronometr (Pulse-Counting Chronometer).— Moskva, Fizmatgiz. 1963.

*G.S. Goltvinskaya, D.K. Zibin'*

# **AN ASSEMBLY OF TRANSISTORIZED MULTIVIBRATOR CIRCUITS**

The design of astable, monostable, and bistable multivibrator circuits using p-type and n-type planar transistors is described. The advantages and characteristic features of these devices are discussed. Various applications are considered.

Multivibrators using two planar transistors are widely known. In a certain sense these devices are direct analogs of the corresponding vacuum tube circuits. The application of transistors does not introduce any new element into their functional properties, so that the peculiar advantages and features of transistors are not always fully utilized. In a number of cases, better performance can be achieved by redesigning the circuit so as to make full use of the specific transistor characteristics. In this respect, so-called complementary circuits using p-type and n-type transistors are of certain interest [1]. Certain devices of this type have been described in the literature, but these descriptions unfortunately do not link up with the common circuit components. The ever growing number of individual devices and lack of generalizing analysis of the entire class creates a quite misleading and unnecessary impression of extreme complexity and obstructs the selection of optimum alternatives for new equipment.

In this paper we will try to describe the general procedure for circuit design using p-type and n-type transistors. Following this procedure, the authors built and tested a number of basic devices (an astable multivibrator, a delayed multivibrator, univibrator, multivibrator with capacitive emitter coupling, multivibrator with emitter timing capacitor, symmetric trigger, and trigger with emitter coupling), for most of which this approach was entirely without precedent. Space limitations, however, do not permit discussing the circuit diagrams of these individual devices.

## **PROCEDURE**

Simple change in each basic circuit will permit replacing a p-type transistor with an n-type one and vice versa (Figure 1). In the modified circuit, as in the original device, the transistors are connected in parallel to the source. The main difference between these complementary circuits is that in the modified circuit both transistors are cut off or made conducting always simultaneously. Because of this curious property, we

can proceed to design a number of standard circuits using transistors connected in series. For example, if we connect the collector resistances in series, the result is the circuit shown in Figure 2a. Figure 2b shows the emitters connected in series.

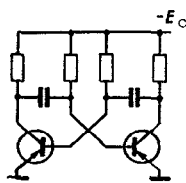
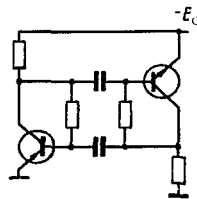


FIGURE 1. The multivibrator circuit.



Another possibility is to connect the power source in an asymmetric fashion, which again gives a different circuit (Figure 2c). In other words, the transistors, the collector resistances, and the source give a closed series circuit. The source can be positioned anywhere in this circuit. The control circuits of the individual transistors were not changed, and the different

circuits therefore function in the usual manner.

All the circuits shown in Figure 2 are thus modifications of the original circuit, although they look quite different. They are all symmetric about the contact points of the emitters or the collector resistances. The output voltage, however, is collected asymmetrically relative to the common lead (see Figure 2c, for instance), and this accounts for the superficial differences between the different circuits. The functional analogy remains valid, however, since the internal processes in a system are independent of the particular frame of reference used.

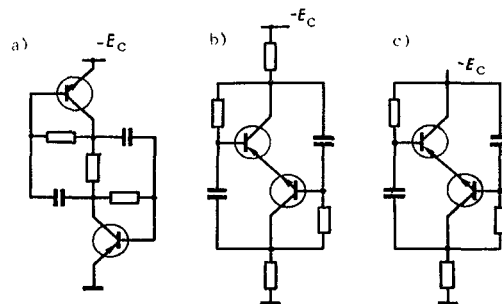


FIGURE 2. Multivibrator with transistors in a series.

In the above circuits both transistors have common-emitter circuits. They are free from any (a.c.) emitter coupling. For example, in the circuit of Figure 2b the emitters can be connected to the midpoint of the power source. This will not make any substantial difference to circuit operation. The absence of emitter coupling permits designing a number of circuits with several sources, i.e., separate source for each transistor.

Modifications of other circuits can be obtained along the same lines. For example, Figure 3a shows a circuit with a single capacitive and a single resistive base-collector coupling, developed from an ordinary delayed

multivibrator. Connecting the emitters (2-3) or the collectors (1-4) in series, we obtain the modifications b and c. Circuit b can be further modified by omitting one of the collector resistances, as in Figures 2b and 2c.

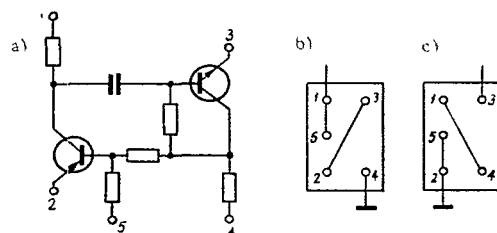


FIGURE 3. Multivibrator with capacitive and resistive base-collector coupling.

Unlike the ordinary delayed multivibrator, this circuit develops sustained oscillations. If the timing resistance is disconnected from the collector and connected to the source, a waiting mode is generated.

Figure 4 shows a trigger circuit and its modifications.

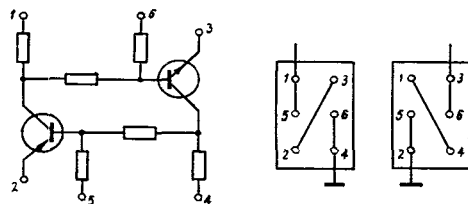


FIGURE 4. Trigger.

Comparison of the circuits from different groups clearly brings out both the common and the distinctive features. For example, the atable multivibrators (Figures 1, 2) are characterized by two capacitive base-collector couplings. In delayed multivibrators, one of the capacitive couplings has been exchanged for a resistive coupling. Introduction of direct emitter coupling will eliminate one of the base-collector couplings altogether.

Thus, knowing the basic circuits and having understood the method whereby the different modifications are generated, we can easily find our way through the entire maze of modified multivibrator circuits.

#### ADVANTAGES AND CHARACTERISTIC FEATURES

Pulsed devices using p-type and n-type transistors have a number of distinct advantages. Their power requirements are minimum, a

great advantage in equipment which is in waiting mode for most of the time and functions only briefly.

Multivibrators of this type will generate pulses of very high duty factor. In some cases they will replace blocking oscillators, which are much more difficult to manufacture technologically. These circuits are moreover free from any spurious oscillations and pulse distortion.

Series arrangement of transistors in a symmetric circuit halves the voltage across each transistor. This is highly advantageous for increasing the source voltage.

In many cases only one of the outputs of a conventional symmetric circuit is actually used. If this is the case, a better policy is to use a modified circuit with an asymmetric source. The device then is markedly simplified, for example, one of the RC circuits is eliminated.

The complementary circuits also have a number of distinctive features.

Hard self-excitation may arise in conventional multivibrators with negative bias (Figure 1a, for example). This is so because the base resistance leads to saturation, and the transistor then behaves as a passive element. The corresponding equilibrium is therefore stable. Once triggered from the outside, however, the multivibrator will function normally.

The situation is different in complementary circuits. During each pulse, both transistors conduct. The multivibrator therefore cannot develop sustained oscillations, if the transistors are saturated. This shortcoming is readily eliminated, however. It suffices to connect the timing base resistors to the collector of the same transistor. Then, as soon as the capacitor discharges, the transistor is inevitably desaturated, and the multivibrator ensures reliable pulse generation (Figure 1b).

Rapid discharge of the timing capacitors through conducting transistors generates very short pulses. In these cases the discharge current should be limited to permissible level by special additional resistors.

The significance of the complementary circuits is not restricted to their immediate benefits. They apparently will be used in the development of a number of new pulse devices.

## Bibliography

1. Nicolet, M. A. Complementary Transistor Flip-Flop Circuits.—  
IEEE Transactions on Circuit Theory, Dec. 1963.

*E. M. Andrianov*

## *A UNIVERSAL MULTISTABLE DEVICE*

A new transistor multistable trigger circuit is described. Its functional diagram is shown to cover a wide range of particular multistable devices. The general functional diagram, called a universal multistable device, is analyzed.

In some transistor multistable triggers the stable state is fixed by potential coupling using resistors and diodes between the transistors. Such circuits are described in the literature [1-6]. Their application in complex circuits reduces the number of transistors and lowers the power requirements compared to those in analogous circuits using conventional triggers.

However, the existing multistable triggers have a number of shortcomings which limit their large-scale use. The main advantages are the following:

- 1) the external load can be controlled between narrow limits only, since each transistor has only one collector output. In other words, multistable triggers are not versatile enough as far as the logic of complex circuits is concerned;
- 2) the parameters of the constituent elements are expected to meet exacting requirements, so that hand-picked transistors are needed and the circuit demands painstaking tuning;
- 3) the operating conditions of the transistors are set with an eye to the ultimate aim, i.e., attaining a stable state, but on account of the exacting requirements the conditions cannot be freely adjusted in order to achieve optimum reliability of circuit operation;
- 4) the number of stages cannot exceed five (see [2], p. 142), which is too few to fully utilize the load potential of the transistors.

We will describe a multistable trigger in which these shortcomings have been largely eliminated (Figure 1). We will briefly consider the essential features of the circuit, and also generalize the trigger design to a whole range of multistable triggers which differ in one of two individual features.

The corresponding generalized functional diagram (Figure 2) will be called a universal multistable device (UMD). We will analyze the UMD in order to establish the common properties of the entire class of multistable devices.

# 1. CHARACTERISTIC FEATURES OF THE MULTISTABLE TRIGGER CIRCUIT

Consider the circuit in Figure 1, which represents a transistor multistable circuit. Each stage contains one switched transistor and has two outputs to which load can be connected.

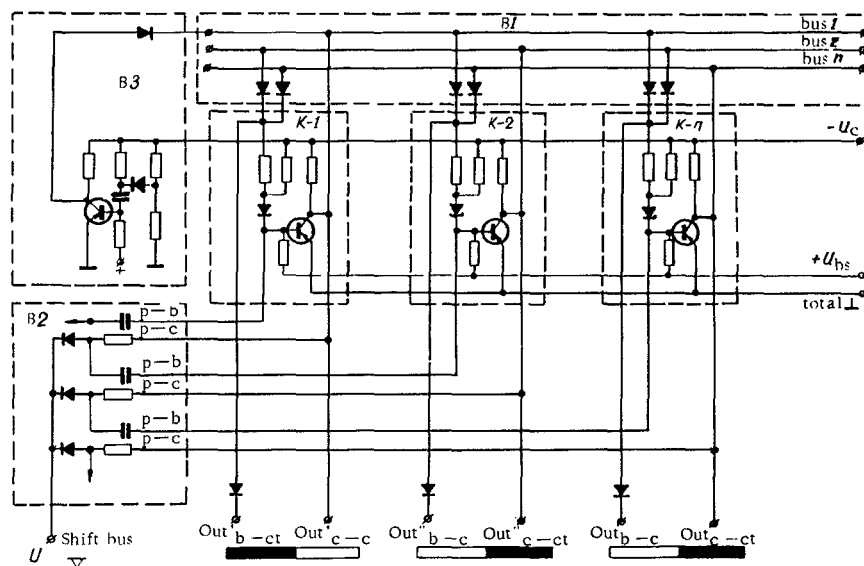


FIGURE 1. Circuit diagram of a multistable transistor.

The output  $Out_c$  is connected to the collector, and the second output  $Out_b$  to the base circuit.

A stabilatron is inserted between the transistor base and  $Out_b$ . The stabilatron threshold voltage is chosen so that it firmly cuts off the diode in the load circuit. If the stabilatron is conducting, base current flows and the transistor conducts. The resulting drop of voltage across the stabilatron cuts off  $Out_b$ .

If the stabilatron is cut off, the transistor is cut off by the bias  $U_{bs}$ . Then  $Out_c$  is cut off, and the load current from  $Out_b$  flows through the potential coupling diode to a bus which is momentarily earthed by the transistor conducting at that instant. The two outputs  $Out_c$  and  $Out_b$  of each stage are thus always in opposite states: when one conducts load current, the other is cut off, and vice versa.

The introduction of a threshold element (stabilatron) is a distinctive feature of the circuit being considered: it expanded the logic potential of the multistable trigger by providing additional outputs.

The potential coupling between the transistors (Figure 1) is effected by means of diodes and common bars 1, 2,  $n$  so that when one of the transistors



conducts, all the other transistors remain cut off. The pulse coupling between the stages in the circuit is sequential, i.e., the output of the first stage  $1_{p-b}$  is connected with  $2_{p-b}$ , and so on. This arrangement can be described as a multistable trigger with sequential shift of the conducting state.

Let us build up the functional diagram of the trigger following the principal units outlined in Figure 1.

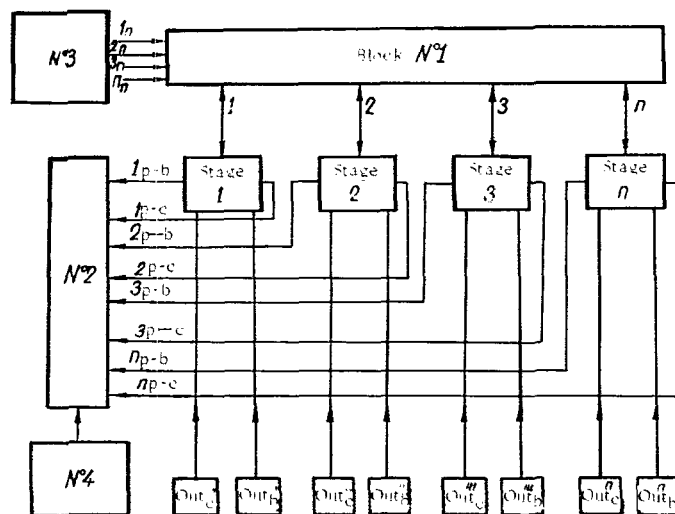


FIGURE 2. A general functional diagram of a universal multistable device.

The functional diagram is shown in Figure 2. The stage outputs  $1_{p-b}$ ,  $1_{p-c}$ , ...,  $n_{p-b}$ ,  $n_{p-c}$  can be connected in any other order different from that shown in Figure 1. The potential coupling diodes can also be linked by a different configuration. The functional diagram in Figure 2 is therefore a general prototype of multistable circuits, and we will call it a universal multistable device (UMD). The circuit diagram in Figure 1 is one of the possible versions of a UMD.

## II. ANALYSIS OF THE UMD FUNCTIONAL DIAGRAM

The UMD (Figure 2) is made up of stages 1, 2, 3, ...,  $n$  with two kinds of coupling between them:

- a) potential coupling (block 1);
- b) pulse coupling (block 2).

Each stage comprises one transistor, one resistor, a diode, and a stabilatron; it has two outputs to which load is connected:

$Out_c'$  and  $Out_b'$ ,  $Out_c''$  and  $Out_b''$ , ...,  $Out_c'n$  and  $Out_b'n$ .

The two inputs  $Out_c$  and  $Out_b$  are always maintained in opposite states.

Block 1 comprises one or several connected diode matrices, which determine the stable state of the UMD. Block 2 includes capacitors and resistors responsible for the pulse coupling of the stages. Block 3 is a transistor circuit which controls the UMD using the potential coupling lines.

In what follows we will only consider the state of  $Out_c$ . With regard to  $Out_b$ , the entire reasoning is simply reversed, since  $Out_c$  and  $Out_b$  are always of opposite polarities.

We introduce the following notation:

$Out_{c-c}$  and  $Out_{b-c}$  — the stage outputs which conduct the load current are assigned the code 0;

$Out_{c-cr}$  and  $Out_{b-cr}$  — the stage outputs which are cut off to load current are assigned the code 1.

We can consider various UMD versions with different combinations of conducting and cutoff outputs  $Out_c$  (Table 1).

TABLE 1.

UMD version	UMD stage					
	1	2	3	...	$n-1$	$n$
1	0	1	1	...	1	1
2	0	0	1	...	1	1
...	...	...	...	...	...	...
K	0	0	0	...	0	1

Rearranging the ones and the zeros in the intermediate rows of the table, except the 1st and the K-th row, may produce further UMD versions (e.g., the 2nd row can be taken from Table 2).

TABLE 2.

UMD version	UMD stage							
	1	2	3	4	5	...	$n-1$	$n$
1	0	1	0	1	1	...	1	1
2	0	1	1	0	1	...	1	1
...	...	...	...	...	...	...	...	...
K	0	1	1	1	1	...	1	0

Note that not all the combinations are feasible for a given number  $n$  of stages 2, 4, ...

The transition of the multistable device from one stable state to another involves changes in the state of the output stages.

Table 3 illustrates the transition for the UMD version corresponding to the 2nd row of Table 1.

TABLE 3.

No. of stable state of UMD	State of $Out_c$ of the UMD stages							
	1	2	3	4	...	$n-2$	$n-1$	$n$
1	0	0	1	1	...	1	1	1
2	1	0	0	1	...	1	1	1
3	1	1	0	0	...	1	1	1
...	...	...	...	...	...	...	...	...
$q-1$	1	1	1	1	...	0	0	1
$q$	1	1	1	1	...	1	0	0
1	0	0	1	1	...	1	1	1

This transition involves a shift of a two-zero combination, which was preserved in all the stable states of the circuit. This combination is interpreted as a code combination of the UMD.

The code combination of UMD is thus a certain combination of  $Out_{c-c}$  and  $Out_{c-c}$  which is limited and includes  $Out_{c-c}$  and which is not broken by transition to any stable state of the UMD. The number of stages forming the code combination is taken equal to  $m$ .

From Tables 1 and 2 we see that  $m$  ranges between the limits

$$m = 1 \text{ to } (n-1).$$

The minimum value of  $m$  is equal to 1, which corresponds to a code combination comprising  $Out_{c-c}$  only. A special case is obtained when  $m=n$ . Then by definition no shift is possible. Irrespective of the external disturbances, the circuit is restored to the initial state. The sequence of changes in the state of this circuit is shown in Table 4.

UMD with  $m=n$  is called a multistage univibrator in our terminology.

The component stages of the UMD can be linked into an open or a closed-ring configuration. In the case under consideration, transmission of shift pulses down the open line will not shift the code combination beyond the  $n$ -th stage. The right-hand limit of the terminal position of the code combination is the  $n$ -th stage, or more precisely the output  $Out_{c-cn}$ .

TABLE 4.

Disturbance	Sequence of UMD states for $m=n$		
	initial	during disturbance and transients	terminal
Pulse making the 2nd transistor conducting	011110	101110	011110
Pulse making the 3rd transistor conducting	011110	010111	011110

Let the initial state of the UMD be such that the beginning of the code combination coincides with the 1st stage, i.e., we have  $\text{Out}'_{c-c}$ . In Tables 1 and 2 all the code combinations are shown in the initial position so as to simplify comparison.

The ring configuration in this case is ensured by means of pulse or potential coupling so that the code combinations are shifted unaltered from the terminal to the initial position by a single pulse. This property of the UMD defines the boundary of the 1st and the  $n$ -th stage in a ring configuration, provided that the 1st stage has been identified.

Under this definition, all the conclusions for an open-configuration UMD are applicable to a ring-configuration UMD. Table 4 illustrates the transition of the code combination from the terminal to the initial position in a ring configuration.

Pulse coupling of stages permits obtaining any sequence of shifts of the code combination. The desired shift sequence is selected in block 2 (Figure 2) by linking the outputs of the corresponding stages

$$1_{p-b}, 1_{p-c}, \dots, n_{p-b}, n_{p-c}.$$

To obtain a directional shift, we have to link the  $p-c$  outputs of one stage with the  $p-b$  outputs of another stage.

Consider a particular example. Suppose we wish to generate a shift sequence of the code combination  $\text{Out}_{c-c}$  as shown in Table 5.

TABLE 5.

Pulse no.	State of $\text{Out}_c$ of the UMD stages				
	1	2	3	4	5
1	0	1	1	1	1
2	1	1	1	0	1
3	1	0	1	1	1
4	1	1	1	1	0
5	1	1	0	1	1
6	0	1	1	1	1

The pulse outputs in this case should be connected as shown in Table 6.

TABLE 6.

Stage outputs	$1p-c$	$2p-c$	$3p-c$	$4p-c$	$5p-c$
$1p-b$					
$2p-b$					
$3p-b$					
$4p-b$					
$5p-b$					

We see that any given position of the code combination is entirely determined by the preceding position. When a shift pulse is transmitted down a common bus, the code combination is shifted in each UMD version into a position determined by the pulse coupling configuration of the stages.

The potential coupling circuits provide a means for independent shift of the code combination. By connecting an auxiliary circuit to the outputs  $1p, 2p, \dots, n_p$  (block 3, Figure 2), the code combination can be moved to any desired position regardless of its original position. This option can be used, in particular, for restoring the UMD to its initial state.

The UMD is thus controlled in two ways:

- sequentially, when each new position of the code combination depends on the previous position. The UMD is controlled by pulses transmitted through a common bar;
- in parallel, when the potential coupling circuit moves the code combination to any desired position irrespective of the previous position.

A combination of both methods provides for a flexible control of the UMD. Consider an example when combined application of the two control techniques makes it possible to achieve the desired shift sequence with minimum effort.

The sequence is defined by Table 7.

We see from Table 7 that the code combinations are expected to return repeatedly (after the 3rd, 5th, 7th, and 9th pulses) to the starting position, thereafter moving to 2nd, 3rd, 4th, and 5th position.

Pulse coupling from 1st stage to 2nd, 3rd, 4th, and 5th stages fails to ensure time resolution (differentiation between pulses), since the shift pulses acts simultaneously on all these stages. We will therefore provide pulse coupling between stages 1, 2, 1; 3 and 1; 4 and 1; 5 and 1. To generate the desired shift sequence, the code combination should be shifted from position 1 to 3, from 1 to 4, and from 1 to 5 using the circuits 4, 4, and 5 of the potential coupling lines and the auxiliary circuit of block 3.

TABLE 7.

Pulse no.	State of Out <sub>c</sub> of UMD stages				
	1	2	3	4	5
1	0	1	1	1	1
2	1	0	1	1	1
3	0	1	1	1	1
4	1	1	0	1	1
5	0	1	1	1	1
6	1	1	1	0	1
7	0	1	1	1	1
8	1	1	1	1	0
9	0	1	1	1	1

The circuit diagram (Figure 1) shows one of the possible realizations of block 3, which restores the UMD to the initial state by transmitting a pulse along the 1st bus of the potential coupling network. Here, when the source is turned on, the transistor is made conducting by the capacitor discharge current. Bus 1 is thus earthed, and the first transistor of the multistable trigger is stabilized in conducting state.

### III. PARTICULAR CASES OF UMD

The UMD can be classified into several distinct functional groups.

1. **Multistable triggers.** Structurally they are identical to the circuit shown in Figure 2. They are controlled both by potential coupling and common-bus pulse coupling.

2. **Multistage switch.** The structure fits that shown in Figure 2, with the pulse coupling unit (block 2) omitted. Readily controlled by potential coupling lines.

3. **Multivibrator circuit.** The structure is analogous to that shown in Figure 2 with the potential coupling (block 1) omitted. Exclusively controlled by pulses. The initial state is the only stable one.

4. **Multistage univibrator.** The structure is that of Figure 2. Code combination  $m=n$ . When control pulses are sensed, the corresponding stage changes the state of its outputs only for the pulse duration plus the time constant of the transients in the circuit.

## CONCLUSIONS

1. The generalized structure circuit of the UMD covers a number of individual multistable devices and provides a general framework for their theoretical treatment.
2. Analysis of the UMD structure reveals flexibility of control and points to ways for the design of new multistable devices.
3. The electric circuit of a multistable trigger (Figure 1) is one of the possible UMD versions. It illustrates the greater logic potential of these circuits, since each one-transistor stage has two outputs of opposite polarity.

## Bibliography

1. Belen'kii, Ya. E. and A. N. Svenson. Mnogofaznyi mul'tivibrator (Multiphase Multivibrator).— Radiotekhnika, 7. 1956.
2. Pavlenko, P. I. Schetno-impul'snyi khronometr (Pulse Counting Chronometer).— Moskva, Fizmatgiz. 1963.
3. Chirkov, M. K. O nekotorykh pereklyuchayushchikh skhemakh (Switching Circuits).— In: "Vychislitel'naya tekhnika i voprosy programirovaniya," No. 2. Leningrad, LGU. 1963.
4. Sirotin, A. A. and V. V. Kireev. Unifitsirovannye tranzistornye raspredeliteli impul'sov dlya upravleniya shagovymi elektrodvigatelyami (Unified Transistor Pulse Distributors for Electric Motor Control).— Elektrichestvo, 2. 1965.
5. Carlson, A. A Seven-Bit Ring Counter. [Russian translation. 1962.]
6. Val'fe. Desyatchnyi schetchik na diodnoi matritse (A Diode-Matrix Decade Counter).— Elektronik, 13. 1962.

National Aeronautics and Space Administration

WASHINGTON, D. C. 20546

OFFICIAL BUSINESS

POSTAGE AND FEES PAID  
NATIONAL AERONAUTICS AND  
SPACE ADMINISTRATION

060 001 33 51 3DS 70089 00903  
AIR FORCE WEAPONS LABORATORY /WLOL/  
KIRTLAND AFB, NEW MEXICO 87117

ATT E. LOU BOWMAN, CHIEF, TECH. LIBRARY